PERFORMANCE ENHANCEMENT OF WIRELESS OFDM SYSTEM FOR MOBILE COMMUNICATION NETWORKS

SAIYAN SAIYOD

A THESIS SUBMITTED IN PARTIAL FULFILLMENT
OF THE REQUIREMENT FOR THE DEGREE OF
DOCTOR OF ENGINEERING IN ELECTRICAL ENGINEERING
FACULTY OF ENGINEERING
KING MONGKUT'S INSTITUTE OF TECHNOLOGY LADKRABANG
2011

KMITL 2011-EN-D-018-054

หัวข้อวิทยานิพนธ์	การเพิ่มประสิทธิภาพของระบบโอเอฟดีเอ็มแบบไร้สายสำหรับเครือข่ายสื่อสารเคลื่อนที่
นักศึกษา	นายสายยัญ สายยศ
รหัสนักศึกษา	48060055
ปริญญา	วิศวกรรมศาสตรดุษฎีบัณฑิต
สาขาวิชา	วิศวกรรมไฟฟ้า
พ.ศ.	2554
อาจารย์ที่ปรึกษาวิทยานิพนธ์	ผศ.ดร. ศักดิ์ชัย ทิพย์จักษุรัตน์
อาจารย์ที่ปรึกษาวิทยานิพนธ์ร่วม	รศ.ดร. รัตติกร วรากูลศิริพันธุ์

บทคัดย่อ

ระบบโอเอฟดีเอ็มแบบไร้สายแบบดั้งเดิม ใช้ความยาวไซคลิกพรีฟิกแบบคงที่ เพื่อป้องกันการเกิดการแทรกสอดกันระหว่างซิมโบลที่เกิดจากมัลติพาทเฟดดิง อย่างไรก็ตามในการสื่อสารเคลื่อนที่ มัลติพาทเฟดดิงจะเปลี่ยนแปลงตามสภาพแวดล้อม ดังนั้นการใช้ความยาวไซคลิกพรีฟิกแบบคงที่อาจจะไม่เหมาะสม ก่อให้เกิดการสูญเสียพื้นที่ใช้งานโดยเปล่าประโยชน์ อย่างไรก็ตามประสิทธิภาพของระบบโอเอฟดีเอ็มแบบไร้สายจะได้รับผลกระทบอย่างมากจากปัญหาออฟเซ็ตความถี่และออฟเซ็ตเวลาซิโบล ที่เกิดจากผลกระทบดอปเปลอร์จากการเคลื่อนที่ของอุปกรณ์สื่อสารเคลื่อนที่ ซึ่งการใช้การแปลงฟูเรียร์แบบไม่ต่อเนื่องและการแปลงผกผันฟูเรียร์แบบไม่ต่อเนื่องสำหรับการแปลงสัญญาณจากโดเมนเวลาเป็นโดเมนความถี่และโดเมนความถี่เป็นโดเมนเวลานั้นอาจจะทำให้ประสิทธิภาพของระบบลดลงอย่างมากในสภาวะแบบนี้ จากที่กล่าวมาข้างต้นนี้ เราได้พิจารณาว่า ความยาวของไซคลิกพรีฟิกควรปรับค่าได้ตามสภาวะของการเกิดมัลติพาทเฟดดิงที่เปลี่ยนไปตามสภาพแวดล้อม ซึ่งจะทำให้ได้ค่าทรูพุตที่ดีที่สุด อย่างไรก็ตาม การแปลงและการประมาณค่าช่องสัญญาณที่เหมาะสมสำหรับการทำงานในสภาวะการเคลื่อนที่ ควรพิจารณาด้วยเช่นกัน ดังนั้นเพื่อเพิ่มประสิทธิภาพของระบบโอเอฟดีเอ็มแบบไร้สายสำหรับเครือข่ายสื่อสารเคลื่อนที่ เราได้เสนอวิธีการปรับปรุงประสิทธิภาพในสองประเด็นดังนี้

ประเด็นที่หนึ่ง เราเสนอวิธีการปรับค่าไซคลิกพรีฟิกให้เหมาะสมกับสภาวะแวดล้อมของการส่งสัญญาณ ภายใต้สภาพแวดล้อมที่มีมัลติพาทเฟดดิง เพื่อปรับปรุงประสิทธิภาพทรูพุต ซึ่งความยาวของไซคลิกพรีฟิกจะถูกปรับขนาดให้เหมาะสมกับค่าการประวิงเวลาที่มากที่สุด ซึ่งจะพิจาณาจากกรณีดังนี้ เมื่อเครื่องส่งหรือเครื่องรับมีการเปลี่ยนตำแหน่ง หรือเมื่อเครื่องรับตรวจพบการซ้อนทับกันของซิมโบล เมื่อเกิดกรณีดังกล่าว ระบบจะทำการคำนวณค่าไซคลิกพรีฟิกที่

เหมาะสมและนำค่าดังกล่าวไปปรับเป็นค่าไซคลิกพรีฟิกใหม่ จากผลการจำลองการทำงานแสดงให้เห็นว่า วิธีการที่นำเสนอ ให้ค่าทรูพุตที่ดีกว่าระบบโอเอฟดีเอ็มแบบดั้งเดิม

ประเด็นที่สอง เราพิจารณาในส่วนของการแปลงสัญญาณในระบบโอเอฟดีเอ็มแบบดั้งเดิมที่ใช้การแปลงฟูเรียร์แบบไม่ต่อเนื่อง โดยการแทนที่ด้วยการแปลงฮาร์โมนิคแบบไม่ต่อเนื่องที่เราทำการปรับปรุง ให้มีความเหมาะสมกับการใช้งานในเครือข่ายสื่อสารเคลื่อนที่ เราเรียกวิธีการที่เรานำเสนอว่า การปรับปรุงการแปลงฮาร์โมนิคโอเอฟดีเอ็มแบบไม่ต่อเนื่อง (เอ็มดีเอชที-โอเอฟดีเอ็ม) เอ็มดีเอชที-โอเอฟดีเอ็มประกอบไปด้วยการแปลงและการประมาณค่าช่องสัญญาณที่นำเสนอ เราทำการรวมคุณลักษณะของการแปลงฮาร์โมนิคและความถี่ชั่วขณะเข้าด้วยกัน เพื่อเสนอเป็นการแปลงแบบใหม่ ที่สามารถปรับค่าการทำงานให้เหมาะสมกับสภาวะแวดล้อมได้ นอกจากนี้เรานำเสนอการประมาณค่าช่องสัญญาณที่ทำงานร่วมกับเอ็มดีเอชที-โอเอฟดีเอ็ม ซึ่งสามารถทำงานได้ทั้งในโดเมนเวลาและโดเมนความถี่ วิธีการที่นำเสนอ สามารถทำให้ระบบโอเอฟดีเอ็มแบบไร้สายสามารถทนทานต่อดอปเปลอร์สเปรดและสัญญาณรบกวนได้มากกว่าวิธีการแบบดั้งเดิม ประสิทธิภาพของวิธีการเอ็มดีเอชที-โอเอฟดีเอ็ม ถูกประเมินค่าโดยการจำลองการทำงาน เราเปรียบเทียบประสิทธิภาพของวิธีการเอ็มดีเอชที-โอเอฟดีเอ็มกับวิธีการแบบดั้งเดิม ดีเอฟที-โอเอฟดีเอ็มโดยการวัดอัตราความผิดพลาดของซิมโบล (เอสอีอาร์) จากผลการจำลองการทำงานแสดงให้เห็นว่า เอ็มดีเอชที-โอเอฟดีเอ็ม มีประสิทธิภาพในการทนทานต่อดอปเปลอร์สเปรดได้ที่ดีกว่าวิธีการดั้งเดิม ดีเอฟที-โอเอฟดีเอ็ม

Thesis Title	Performance Enhancement of Wireless OFDM System for Mobile Communication Networks
Student	Mr.Saiyan Saiyod
Student ID.	48060055
Degree	Doctor of Engineering
Program	Electrical Engineering
Year	2011
Thesis Advisor	Asst. Prof. Dr. Sakchai Thipchaksurat
Thesis Co-Advisor	Assoc. Prof. Dr. Ruttikorn Varakulsiripunth

ABSTRACT

Conventional wireless OFDM systems, a cyclic prefix length is fixed as constant in order to avoid inter-symbol interference cause by multi-path fading. In mobile communications, however, the multi-path fading occurs depending on the environments. Therefore, using the fixed cyclic prefix length may be not suitable thereby losing the useful data portion. However, the system performance of wireless OFDM systems is suffered from frequency offset and symbol timing offset due to the Doppler effect caused by mobile unit movement. Using the discrete Fourier transform (DFT) and inverse discrete Fourier transform (IDFT) for traditional signal transformation from the time-domain into frequency-domain, and vice versa, the system performance may be severely degraded. The problems mention above, we have considered that the cyclic prefix length should be adaptively adjusted according to the multi-path fading on the current environment. Thus, the throughput performance will be optimized. However, the suitable transformation and channel estimation performing in mobile environments are considered as well. Therefore, to enhance the system performances of wireless OFDM systems for mobile communication networks, we have proposed the performance improvement in two issues separately as follows.

In the first issue, we have proposed an adaptive cyclic prefix for signal transmission under multi-path fading environments in order to improve the throughput performance. The length of cyclic prefix is adjusted as fit as the maximum delay spread in which consider as following conditions. When, the transmitter or receiver changed its location, or when the inter-symbol interference is detected by the receiver, then the proposed algorithm will be introduced to

calculate new appropriate cyclic prefix and use it for adjusting the new cyclic prefix. The simulation results have shown that the proposed algorithm achieved better throughput performance than the conventional OFDM.

For the second issue, we consider the signal transformation in the conventional OFDM which uses the discrete Fourier transform (DFT) for signal transformation. We propose the discrete harmonic transform as the signal transformation in OFDM instead of DFT. In order to do that we have to derive the new equation of the discrete harmonic transform which is suitable for mobile communications. We call our proposed scheme as he modified discrete harmonic transform OFDM (MDHT-OFDM) scheme. MDHT-OFDM consists of the proposed transformation and proposed channel estimation. We combine the good characteristics of harmonic transform and instantaneous frequency to be a novel transformation which can be performed adaptively. We also propose the new channel estimation that can be used with MDHT-OFDM. The proposed channel estimation can be performed in both time-domain and frequency-domain. MDHT-OFDM scheme provide the wireless OFDM systems can mitigate the Doppler spread and robust to noise more than the conventional DFT-OFDM scheme. The performance of a MDHT-OFDM scheme is evaluated by means of a simulation. We compare the performance of a MDHT-OFDM scheme with the one of the conventional DFT-OFDM scheme in the term of symbol error rate (SER). The simulation results have shown that MDHT-OFDM scheme can achieve the better performance comparing with those of the conventional DFT-OFDM scheme in mitigating the Doppler spread.

ACKNOWLEDGEMENTS

Firstly, I would like to express my great gratitude towards my thesis advisor, Asst.Prof.Dr. Sakchai Thipchaksurat who has given me much suggestion, support, advice from the very early stage of this research as well as giving me extraordinary experiences throughout the work. I would also like to express my great gratitude towards my thesis Co-Advisor, Assoc.Prof.Dr. Ruttikorn Varakulsiripunth who provided valuable guidance and support throughout my study. I am also indebted to Prof.Dr. Yoshikuni Onozato, Prof.Dr. Yasushi Kato, Prof.Dr. Susumu Yoshida, and Asst.Prof.Dr. Kuntpong Woraratpanya for their advises, challenging instruction and support. I would like to thank Miss Patcharin Chinnawan, Mr.Tawatchai Chontong, Mr.Wayan Mustika, and all members in Communication Networks Laboratory for their cheerfulness, spiritual and support. Many thank to Mr.Jumnean Kaprakon for proof reading of my Journal paper.

I would like to acknowledge the support from National Institute of Information and Communications Technology, Japan (*NICT*) for their financial supports and chances to internship at Japan. I would also like to express my sincere gratitude to Dr.Hiroshi Harada, Dr.Ryuhei Funada, and all members in Ubiquitous Mobile Communications Group for their comments, suggestions and discussions in this research.

I would also like to acknowledge the support from Office of the Higher Education Commission, Ministry of Education, and Department of Computer Science, Faculty of Science, Khonkaen University for the scholarship with the financial support.

Finally, I would mostly like to thank my parents, my brothers and my sisters, whose constant and limitless support, motivation, and unwavering belief in me had a great part in nurturing my dream and bringing his work to completion.

Saiyan Saiyod

TABLE OF CONTENTS

TABLE OF CONTENTS (CONT)

TABLE OF CONTENTS (CONT)

Page

LIST OF FIGURES

Figure **Page**

LIST OF FIGURES (CONT)

Figure **Page**

LIST OF FIGURES (CONT)

LIST OF FIGURES (CONT)

Figure **Page**

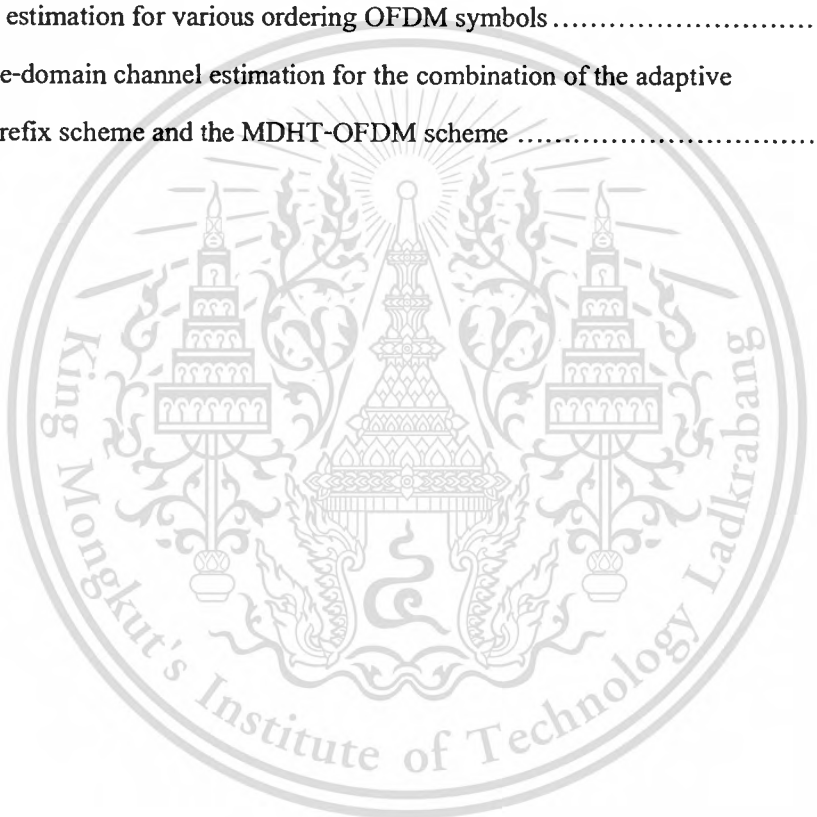

LIST OF TABLES

Chapter 1

Introductions

1.1 Statement and Significant of the Problems

The ability to communicate with anyone from anywhere and anytime has been mankind's dream for a long time. Wireless is the only medium that can enable such kind of communications. However, mobile communications are ones kind of wireless communication that enable user to communicate anytime and anywhere. They have gained an increased interest over recent decades. This has been fuelled by a large demand on high frequency utilization as well as a large number of users requiring simultaneous high data rate access for the applications of wireless mobile Internet and e-commerce. The convergence of wireless mobile and access will be the next storm in the mobile communications.

In mobile communications, the emitted electromagnetic waves often do not reach the receiving antenna directly due to obstacles blocking the line-of-sight (LOS) path. The received waves are a superposition of waves coming from all directions due to reflection, diffraction, and scattering caused by buildings, trees, and other obstacles. This effect is known as multi-path fading. A typical scenario for the terrestrial mobile radio channel is shown in Figure.1.1. Besides the multi-path fading, also the Doppler effect has a negative influence on the transmission characteristics of the mobile radio channel. Due to the movement of the mobile unit, the Doppler effect is occurred.

At recent major international conferences on wireless communications, there have been several sections on beyond third generation (3G) or fourth generation (4G) mobile communication systems, where modulation/demodulation and multiplexing/multiple access schemes related to multi-carrier techniques have been drawn a lot of attention. Orthogonal Frequency Division Multiplexing (OFDM) is a special form of multi-carrier techniques, where a single data stream is transmitted over a number of lower rate sub-carriers. It is worth mentioning here that OFDM can be seen as either a modulation technique or a multiplexing technique.

OFDM has been adopted by various standards in recent years including IEEE 802.11a wireless LAN standards. OFDM is a multi-carrier system where data bits are encoded to multiple sub-carriers, while being sent simultaneously to optimize usage of bandwidth. A set of orthogonal sub-carriers together forms an OFDM symbol. To avoid inter-symbol interference (ISI) due to multi-path fading, successive OFDM symbols are separated by guard interval (GI).

This makes the OFDM system resistant to multi-path fading effects. This GI is required to be at least equal to or longer than the maximum delay spread (τ_{max}) of the system. Using a cyclic prefix (CP) as the guard interval is a simple way to combat the ISI, however also reduces the transmission efficiency of the system. Moreover, the CP length is assigned as a constant value. For example, in 802.11a wireless LAN, a fix proportion of 1/5 of the energy and time is spent on CPs. Conventional OFDM system usually chooses a fixed CP length based on the average or even maximum delay spread the mobile terminal may experience. For example, if the receiver is designed based on the measurement in the office, it will undergo severed ISI when the user moves to a factory. On the other hand, if the receiver is designed according to the measurement in the factory, some of the guard interval is unnecessary which will consume the scare spectral and power resources but achieve no extra gain. However, the multi-path fading is varied depending on the environments. Thus, the throughput performance is not optimized due to the constant value of CP length.

For these reasons, so it is natural to think that if we can estimate the maximum delay spread τ_{max} and change the length of CP accordingly, the overhead of CPs will be reduced when delay spread is small and the ISI will still be eliminated when delay spread becomes large. The appropriate CP (ACP) length is a system parameter which is assigned by the transmitter. However, the ACP length depends on the transmission environments. So, when the receiver moves from one transmission environment to another, the ACP must be changed. As a result, CPs overhead reducing introduces the improving of the throughput performances. Thus, the system performance will be improved according to the multi-path fading environments.

However, a major disadvantage of the OFDM system is its sensitivity to frequency offset errors due to Doppler effect of the mobile movement. The deviation in the carrier frequency will damage the orthogonality among sub-carriers and hence give rise inter-carrier interference (ICI) which degrades the system performance severely. However, the widespread use of OFDM in several communication standards and the increasing request for communication capabilities in high-mobility environments have recently renewed the interest in wireless OFDM systems that are able to cape with significant Doppler effect. Moreover, the conventional channel estimation of the conventional OFDM systems performs in the frequency-domain in which its accuracy will decrease due to the affected signal-to-noise ratio (SNR).

The aforementioned reasons motivated the use of adaptive techniques for wireless OFDM systems in mobile communications. Adaptation aims to improve the throughput performance and enhance its symbol error rate (SER) performance. However, adaptation

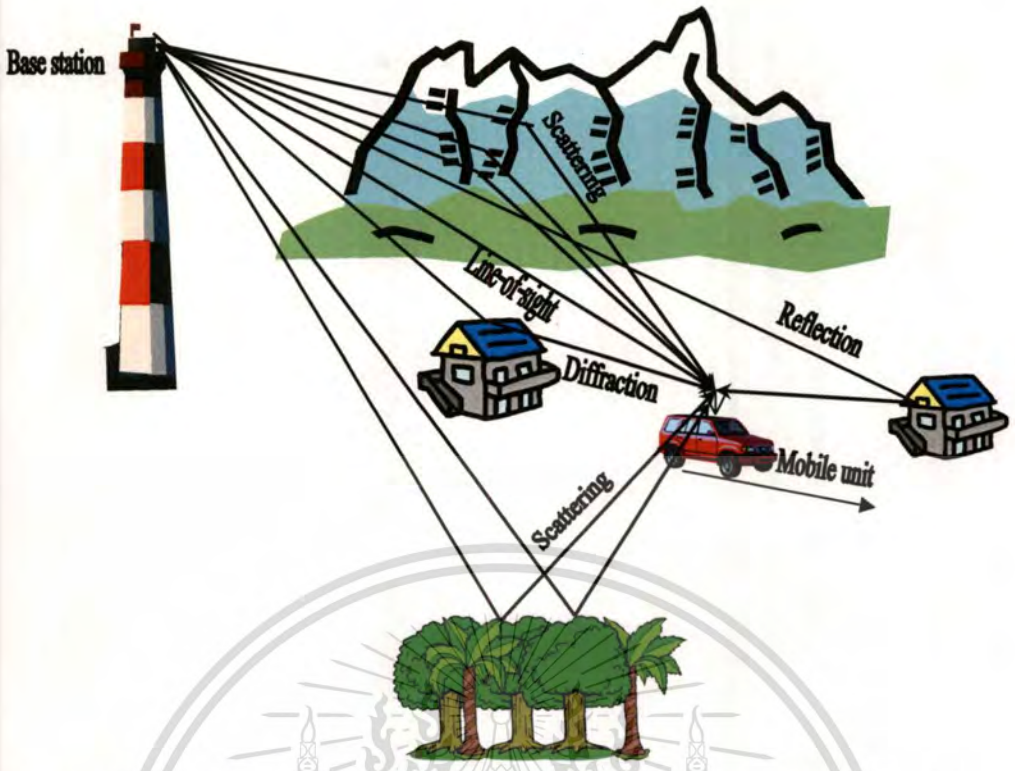

Figure 1.1 Typical mobile communication illustrating multi-path and Doppler effect

requires a form of accurate parameter measurements which are the maximum delay spread and Doppler spread information. The novel channel estimation will be proposed, it will used to determine the suited parameters for the wireless OFDM systems and hence the overall system performance will be improved.

1.2 Goal and Objective

Over the last few years, many methods that propose for wireless OFDM systems have been proposed and enhanced to efficiently mitigate the Doppler effect.

The objective of this thesis are 1) to improve the throughput performance under multi-path environments, 2) to mitigate the Doppler spread due to mobile movements 3) to simulate and analyze proposed schemes, 4) to evaluate the proposed schemes on its performance. These evaluations will be done through simulation.

The goal of this thesis was to:

- Get a general understanding of mobile wireless OFDM systems, mobile communications, and the problem issues in wireless mobile communications.
- Solve the problem to support the wireless OFDM systems in mobile communications.
- Compare the performance of the proposed scheme with the conventional OFDM systems in mobile communications.

1.3 Related Theory

Orthogonal frequency division multiplexing (OFDM) is a special class of multi-carrier modulation (MCM) in which the data information is carried over many lower rate sub-carriers. Another way to view the orthogonality property of OFDM signals is to look at its spectrum. In the frequency domain each OFDM subcarrier has a *sinc*, $\sin(x)/x$, frequency response, as shown in Figure 1.2. This is a result of the symbol time corresponding to the inverse of the carrier spacing. As far as the receiver is concerned each OFDM symbol transmitted for a fixed time (T_{FFT}) with no tapering at the ends of the symbol. This symbol time corresponds to the inverse of the subcarrier spacing of $1/T_{FFT}$ Hz. This rectangular, boxcar, waveform in the time-domain results in a *sinc* frequency response in the frequency domain. The *sinc* shape has a narrow main lobe, with many side-lobes that decay slowly with the magnitude of the frequency difference away from the centre. Each carrier has a peak at the centre frequency and nulls evenly spaced with a frequency gap equal to the carrier spacing. The orthogonal nature of the transmission is a result of the peak of each subcarrier corresponding to the nulls of all other subcarriers. When this signal is detected using a discrete Fourier transform (DFT) the spectrum is not continuous as shown in Figure 1.2, but has discrete samples. The sampled spectrums are shown as 'o's in the figure. If the DFT is time synchronized, the frequency samples of the DFT correspond to just the peaks of the subcarriers, thus the overlapping frequency region between subcarriers does not affect the receiver. The measured peaks correspond to the nulls for all other subcarriers, resulting in orthogonality between the subcarriers.

OFDM signals are typically generated digitally due to the difficulty in creating large banks of phase lock oscillators and receivers in the analog domain. The transmitter section converts digital data to be transmitted, into a mapping of sub-carrier amplitude and phase. It then transforms this spectral representation of the data into the time-domain using an inverse discrete Fourier transform (IDFT). The inverse fast Fourier transform (IFFT) performs the same operations as an IDFT, except that it is much more computationally efficiency, and so is used in all practical systems. In order to transmit the OFDM signal the calculated time-domain signal is then mixed up to the required frequency.

The receiver performs the reverse operation of the transmitter, mixing the radio frequency to base band for processing, then using a fast Fourier transform (FFT) to analyze the signal in the frequency-domain. The amplitude and phase of the sub-carriers is then picked out and converted back to digital data.

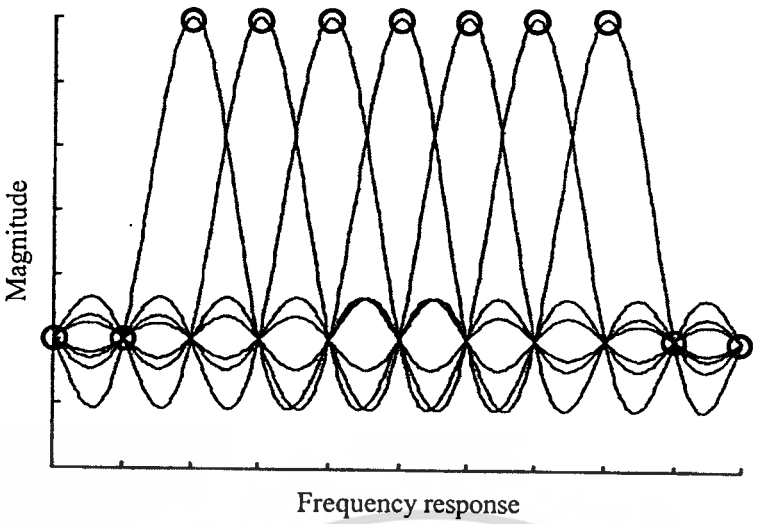

Figure 1.2 Frequency response of the sub-carrier in OFDM signals

The IFFT and the FFT are complementary function and the most appropriate term depends on whether the signal is being received or generated. In cases where the signal is independent of this distinction then the term FFT and IFFT is used interchangeably.

1.4 Process of the Study

The research was begun with the comprehensive review of the concept mobile communications, review of the conventional wireless OFDM systems, review of the wireless OFDM system problem in mobile communications. Then, we observe the performance evaluation issues and challenge in mobile communications which concern with the problem in multi-path fading and Doppler spread environments. Finally, we proposed the method to deal with the wireless OFDM systems as two parts. Firstly, we have proposed an adaptive cyclic prefix for OFDM signal transmission under multi-path environment to improve the throughput performance. Secondly, we have proposed the Doppler spread mitigation using Harmonic transform for wireless OFDM systems in mobile communications. Our proposed schemes are done by improving the processes of the conventional wireless OFDM systems. We conducted the simulation by coding in MATLAB software. The results of simulations are analyzed the improved performance by comparing with the conventional ones.

1.5 Scope and Organization of this Thesis

In the second chapter, we provide some fundamental background relate to this thesis. It covers the basic OFDM systems, transformation, channel models, and channel estimation.

In the third chapter, we will describe the detail of our proposed method, called adaptive cyclic prefix for OFDM signal transmission under multi-path fading environments. The numerical analysis is also described in this chapter.

In the fourth chapter, we will describe the detail of our proposed scheme, called Doppler spread mitigation using Harmonic transform for wireless OFDM system in mobile communications.

In the fifth chapter, we evaluated and compared the performance of our proposed scheme. We separate the performance evaluations as two parts. Firstly, we compare the performance evaluations between the proposed adaptive cyclic prefix for OFDM transmission under multi-path fading environments and the conventional one within two conditions which are none-cooperative and cooperative with movement detector. Secondly, we compared the performance evaluation between the proposed MDHT-OFDM scheme and the conventional DFT-OFDM scheme in several conditions such as the performance comparisons for the Doppler spread of each modulation mapping scheme, the performance comparisons of channel estimation for the Doppler spread, the performance comparisons of the Doppler Spread Variation, and the performance comparisons for the ordering of the OFDM symbol in the frame, respectively. The performance analyses of our proposed schemes are done using the simulation software. As for the simulation software, we used MATLAB under Windows XP platform.

Finally, in the sixth chapter, we summarized the results obtained in chapter five into conclusions.

Chapter 2

Literature Review and Preliminaries

2.1 Literature Review

Orthogonal Frequency Division Multiplexing (OFDM) belongs to a broader class of multi-carrier modulation (MCM) in which the data information is carried over many lower rate sub-carriers. The concept of OFDM was first introduced by Chang in a seminal paper in 1966 [1]. Actual use of OFDM was limited and the practicability of the concept was questioned. The term "OFDM" in fact first appeared in a separate patent of his in 1972 [2]. The field of OFDM had long been developed as a peripheral interest in military applications because there was a lack of broadband applications for OFDM and powerful integrated electronic circuits to support the complex computation required by OFDM.

However, the arrival of broadband digital applications and maturing of very large-scale integrated (VLSI) CMOS chips in the 1990s brought OFDM into the spotlight. In 1995, OFDM was adopted as the European digital audio broadcasting (DAB) standard, ensuring its significance as an important modulation technology and heralding a new era of OFDM success in a broad range of applications [3]. Among the important standards that incorporate OFDM modulation technology are the European digital video broadcasting (DVB), wireless local area networks (Wi-Fi; IEEE 802.11a/g), wireless metropolitan area networks (WiMAX;802.16e),asymmetric digital subscriber line (ADSL; ITU G.992.1), and long-term evolution (LTE) the fourth-generation mobile communications technology.

A fundamental challenge with OFDM is that a large number of sub-carriers are needed so that the transmission channel affects each sub-carrier as a flat channel. This leads to an extremely complex architecture involving many oscillators and filters at both transmitter and receiver. The proposal in [4] first revealed that OFDM modulation/demodulation can be implemented by using IDFT and DFT.

One of the enabling techniques for OFDM is the insertion of cyclic prefix (CP). CP was proposed to resolve the channel dispersion-induced ISI and ICI. CP has been proposed by [5] in 1980. However, in 1995, the DAB has been proposed by [6] in which the cyclic prefix can be selected the level of CP length by considering the multi-path fading environments. But, the CP length levels can be selected only a few values. However, the proposal in [7] has proposed the adaptive cyclic prefix in which the CP length can be adapted depending on the environments.

However, the wireless OFDM systems vary their sensitive to frequency offset and symbol timing offset due to the Doppler effect of the mobile communications [8]. Therefore, the Doppler spread (f_D) is a measure of the spectral broadening caused by the Doppler effect. Thus, the orthogonal among sub-carriers is destroyed, which results in ICI thereby degrading the systems performance severely. Moreover, in mobile communications, the channel is time-variant during one OFDM symbol period.

The conventional OFDM systems employ the inverse discrete Fourier transform (IDFT) and discrete Fourier transform (DFT). However, the practical implementation involves the inverse fast Fourier transform (IFFT) and the fast Fourier transform (FFT) at the transmitter and receiver respectively using the fast algorithms of the IDFT and DFT. Therefore, we agree with [8] that the occurrence of the ICI is due to the use of the DFT for transformation from time-domain into frequency-domain, when the channel is the time-varying channel. Therefore, the time scales of the received signals change the wavelength. This result induces the loss of orthogonal among OFDM sub-carriers due to the DFT performance.

However, in order to cope with the Doppler spread in the conventional DFT-OFDM scheme, compensation and equalization techniques are needed. The channel estimation (CE) and pilot-aided, are used for those techniques. The accuracy of the system depends on the performance of the channel estimation, amount and pattern of pilot-aided. The pilot-aided are inserted in the OFDM symbol in order to put the reference data in the OFDM symbol. Thus, the use of pilot-aided lowers the achievable data rate. Moreover, the channel estimation of conventional OFDM is performed after transformation. Thereby, the accuracy of the estimated values is affected by additive white Gaussian noise (AWGN).

Most of the previous algorithms to mitigate the Doppler spread are to deal with ICI cancellation, and simply focus on mitigating the irreducible error floor [10]. However, many approaches estimate the frequency offset first then correct it, but usually required considerable computational complexity [11]. Another common approach is to apply various signal processing techniques to reduce the sensitivity of the OFDM system to the frequency offset; hence many windowing methods have been presented.

In this research, we have considered that the transformation of wireless OFDM systems should be improved. A solution to avoid deterioration of DFT is the warped Fourier transform [12]–[14], in which the signal is warped in time before the calculation of the spectrum. The harmonic transform is a good alternative way. The harmonic transform has been proposed in [12], but it has been proposed for signal analysis, especially speech signals. Moreover, the

proposal in [15] is a good attractive choice for OFDM systems. The main idea of the proposal is to improve the efficiency of the transformation for the OFDM systems using a harmonic transform. We have found that the harmonic transform has good properties for signals that contain a time-varying signal. Unfortunately, the discrete form of harmonic transform was proposed in [12], is not suitable for wireless OFDM systems. Because the traditional harmonic transform is designed for speech signal analysis, the unit phase function ($\phi_u(t)$) of its depends on the scaling property which is determined by the relation between $\phi_u(t)$ and $\phi_u(t/a)$, where a is a constant. Scaling and phase shifting operation are defined before calculation in order that the suitable parameters are set as constant. Moreover, only real numbers are required by speech signal analysis. In contrast, the transformations of wireless OFDM systems require the complex numbers. In mobile communications, the mobile station may often change its position during the communication as we call the mobility of mobile station. In this situation, the constant parameter may be not suitable. This means that it should be varied according to the mobility of mobile station. Therefore, the traditional harmonic transform may be not suitable for the mobile communications. For this reason, the traditional harmonic transform should be modified. In this paper, we derive the appropriate equations that more suitable for the mobility situation in the mobile communication systems which is the one of our contribution.

However, in order to apply the harmonic transform for wireless OFDM systems, a modification of the discrete harmonic transform is needed. We combine the good characteristics of the harmonic transform and the concept of instantaneous frequency [16]–[20] together. The proposed transformation is called modified discrete harmonic transform (MDHT) [21]. Moreover, the proposed scheme is called the MDHT-OFDM scheme. Furthermore, the MDHT is performed as an adaptive transformation which cooperates with the parameters. Thus, adaptation requires a form of accurate parameter measurement. One key parameter in adaptation of mobile communications is f_D. Therefore, we propose a novel channel estimation technique that can cooperate to provide the suitable parameters for the MDHT-OFDM scheme. The proposed channel estimation is performed in both the time-domain and the frequency-domain. In the time-domain estimation, the self-correlation function is performed to get the OFDM Framing Duration ($T_{estimated}$) in order to calculate the Doppler scaling factor ($\alpha_{estimated}$) and the symbol timing offset ($\varepsilon_{estimated}$). We use $\alpha_{estimated}$ by means of f_D. On the other hand, the frequency-domain estimation is performed in order to get the root mean square error of the preamble symbol (θ_{RMSE}) in order to select a suitable modulation mapping scheme.

2.2 Mobile Communications

For several years, the mobile communications sector has definitely been the fastest growing market segment in telecommunications. Experts agree that today we are just at the beginning of the global development, which will increase considerably during the next years [22]. Trying to find the factors responsible for this development, one immediately discovers a broad range of reasons. Certainly, the liberalization of the telecommunication services, the opening and deregulation of the European and Asia markets, the topping of frequency ranges around and over 1 GHz, improved modulation and coding techniques, as well as impressive progress in the semiconductor technology, and, last but not least, a better knowledge of the propagation processes of electromagnetic wave in an extraordinary complex environment have made their contribution to this success.

2.2.1 Introduction

The beginning of this turbulent development now can be traced to more than 40 years ago. The first-generation mobile radio systems developed at that time ere entirely based on analog technique. They were strictly limited in their capacity of subscribers and their accessibility.

Second-generation mobile radio systems are characterized by digitalization of the networks. It operates at a frequency rang of 900 MHz and offers all subscribers. In addition to this, the DCS 1800 (Digital Cellular system 1800) has been running parallel to the D-Net since 1994, operating at a frequency range of 1800 MHz. Mainly, these two networks only differ in their respective frequency range.

In Europe, third-generation mobile radio systems is expect to be practically ready for use at the beginning of the twenty-first century with the introduction of the Universal Mobile Telecommunications System (UMTS) and the Mobile Broadband System (MBS). With UMTS, in Europe one is aiming at inheriting the various services offered by second generation mobile radio systems into one universal system. An individual subscriber can then be called at any time, from any place (car, train, aircraft, etc.) and will be able to use all services via a universal terminal. With the same aim, the system IMT 2000 (International Mobile Telecommunications 2000) is being worked on worldwide. Apart form that, UMTS/IMT 2000 will also provide multimedia services and other broadband services with maximum data rates up to 2 Mbit/s at a frequency range of 2 GHz. MBS plans mobile broadband services up to a data rate of 155 Mbit/s at a frequency range between 60 and 70 GHz. This concept is aimed to cover the whole

area with mobile terminals; form fixed optical fibre networks over optical fibre connected base stations to the indoor area. For UMTS/IMT 2000 as for MBS, communication by satellites will be of vital importance [22].

At the end of this technical evolution from today's point of view is the development of the fourth generation mobile radio systems. The aim of this is integration of broadband mobile services, which will make it necessary to extend the mobile communication to frequency ranges up to 100 GHz [23].

2.2.2 Channel Models

In mobile radio communications, the emitted electromagnetic waves often do not reach the receiving antenna directly due to obstacles blocking the line-of-sight (LOS) path. In fact, the received waves are a superposition of waves coming from all directions due to reflection, diffraction, and scattering caused by building, tree, and other obstacles. This effect is known as multi-path propagation. A typical scenario for the terrestrial mobile radio channel is shown in Figure 2.1. Due to the multi-path propagation, the received signal consists of an infinite sum of attenuated, delayed and phase-shifted replicas of the transmitted signal, each influencing each other. Depending on the phase of each partial wave, the superposition can be constructive or

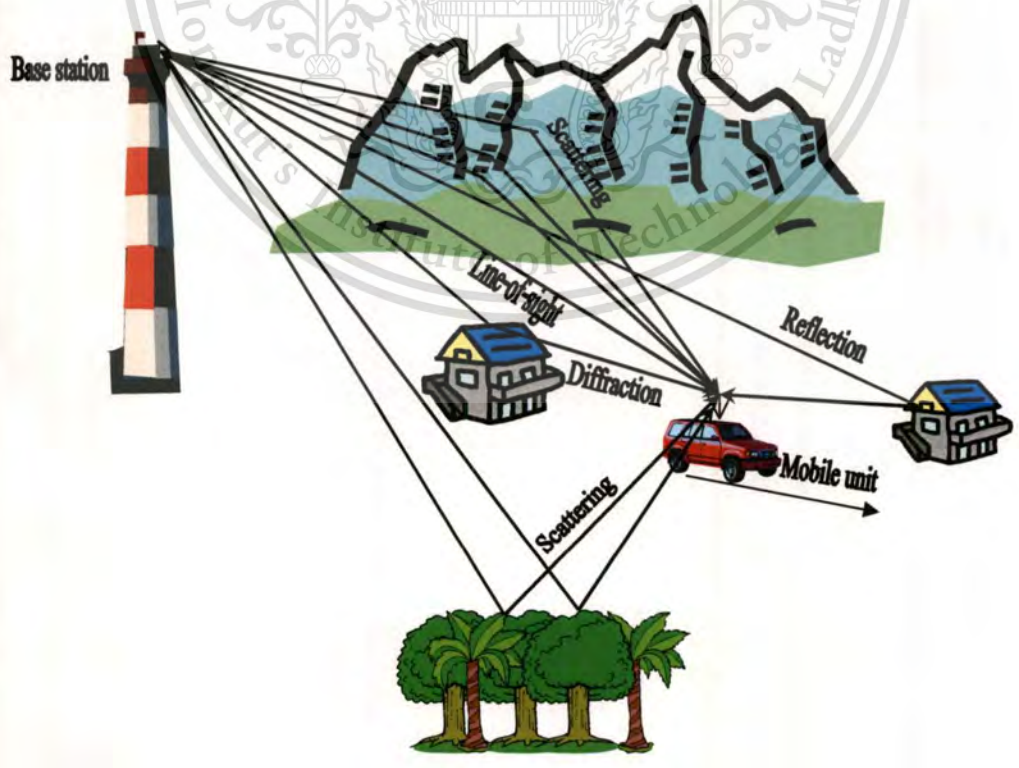

Figure 2.1 Typical mobile radio scenarios illustrating multipath propagation in a terrestrial mobile radio environment

destructive. Apart from that, when transmitting digital signals, the form of the transmitted impulse can be distorted during transmission and often several individually distinguishable impulses occur at the receiver due to multipath propagation. This effect is called the *impulse dispersion*. The value of the impulse dispersion depends on the propagation delay differences and the amplitude relations of the partial waves. The distortions caused by multipath propagation are linear and have to be compensated for on the receiver side, for example, by an equalizer.

Beside the multi-path propagation, also the Doppler effect has a negative influence on the transmission characteristics of the mobile radio channel. Due to the movement of the mobile unit, the Doppler effect causes a frequency shift of each of the partial waves. The *angle of arrival* α_n, which is defined by the direction of arrival of the *n*th incident wave and direction of motion of the mobile unit as shown in Figure 2.2, determines the Doppler frequency (frequency shift) of the *n*th incident wave according to the relation

$$f_n = f_{\max} \cos\alpha_n . \tag{2.1}$$

In this case, $f_{\max}$ is the *maximum Doppler frequency* related to the speed of the mobile unit v, the speed of light c_0, and the carrier frequency f_0 by the equation

$$f_{\max} = \frac{v}{c_0} f_0 . \tag{2.2}$$

The maximum (minimum) Doppler frequency, i.e., $f_n = f_{\max}\,(f_n = -f_{\max})$, is reached for $\alpha_n = 0\ (\alpha_n = \pi)$. In comparison, though, $f_n = 0$ for $\alpha_n = \pi/2$ and $\alpha_n = 3\pi/2$. Due to the

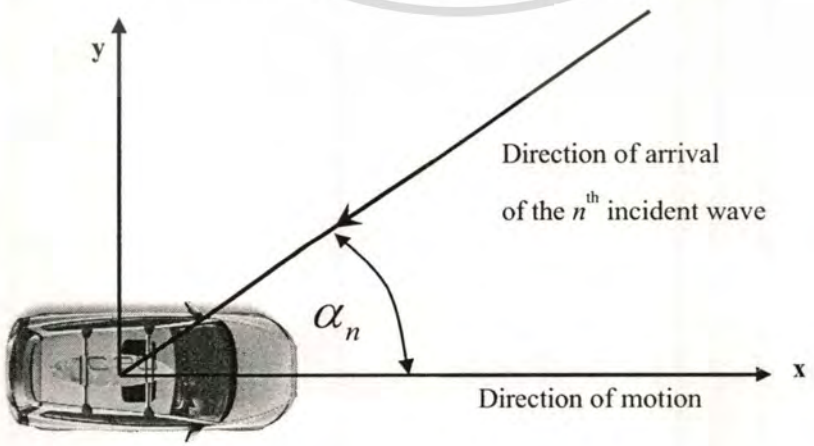

Figure 2.2 Angle of arrival α_n of the *n*th incident wave illustrating the Doppler effect

Doppler effect, the spectrum of the transmitted signal undergoes a frequency expansion during transmission. This effect is called the *frequency dispersion*. The value of the frequency dispersion mainly depends on the maximum Doppler frequency and the amplitudes of the received partial waves. In the time-domain, the Doppler effect implicates that the impulse response of the channel becomes time-variant. One can easily show that mobile radio channels fulfill the principle of superposition and therefore are linear systems. Due to the time-variant behavior of the impulse response, mobile radio channels therefore generally belong to the class of linear time-variant systems.

In digital data transmission, the momentary fading of the received signal causes ***burst errors***, i.e., errors with strong statistical connections to each other. Modern methods of modeling mobile radio channels are especially useful, for they not only can model the statistical properties of real-world (measured) channels regarding the probability density function (first order statistics) of the channel amplitude sufficiently enough, but also regarding the level-crossing rate (second order statistics) and average duration of fades (second order statistics)

2.2.2.1 Introduction to the theory of deterministic process

In this section, we will introduce a fundamental method which is based on a superposition of a finite number of harmonic functions. The principle of this procedure is based on an approach of Rice [22]. In subsection, we will first explain the principle of deterministic channel modeling. The following next subsection deals with elementary properties of deterministic processes.

In the literature, one essentially finds two fundamental methods for the modeling colored Gaussian random processes: the *filter method* and *the Rice method*.

When using the filter method, as shown in Figure 2.3, white Gaussian noise (WGN) $v_i(t)$ is given to the input of a linear time-invariant filter, whose transfer function is denoted by $H_i(f)$. In the following, we assume that the filter is ideal, i.e., the transfer function $H_i(f)$ can be fitted to any given frequency response with arbitrary precision. If $v_i(t) \sim N(0,1)$, then we have a zero-mean stochastic Gaussian random process $\mu_i(t)$ at the filter output, where according the power spectral density $S_{\mu_i\mu_i}(f)$ of $\mu_i(t)$ matches the square of the absolute value of the transfer function, i.e., $S_{\mu_i\mu_i}(f) = |H_i(f)|^2$. Hence, by filtering of white Gaussian noise $v_i(t)$, we obtain colored Gaussian random process $\mu_i(t)$.

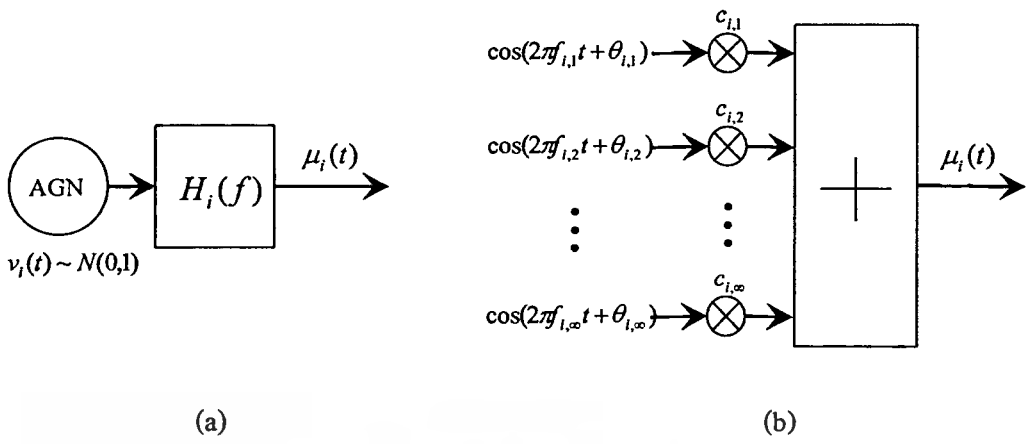

Figure 2.3 Stochastic reference models for colored Gaussian random processes $\mu_i(t)$: (a) Filter method and (b) Rice method

The principle of the Rice method [22] is illustrated in Figure 2.3. It is based on a superposition of an infinite number of weighted harmonic functions with equidistant frequencies and random phases. According to this principle, a stochastic Gaussian process $\mu_i(t)$ can be described mathematically as

$$\mu_i(t) = \lim_{N_i \to \infty} \sum_{n=1}^{N_i} c_{i,n} \cos(2\pi f_{i,n} t + \theta_{i,n}), \tag{2.3}$$

where

$$c_{i,n} = 2\sqrt{\Delta f_i S_{\mu_i \mu_i}(f_{i,n})}, \tag{2.4}$$

$$f_{i,n} = n \cdot \Delta f_i . \tag{2.5}$$

The phase $\theta_{i,n}$ (n=1,2,…,N_i) are random variables, which are uniform distributed in the interval $(0,2\pi]$, and the quantity Δf_i is here chosen in such a way that Eq.(2.5) covers the whole relevant frequency range, where it is furthermore assumed that the following property holds: $\Delta f_i \to 0$ as $N_i \to \infty$.

As we know, a Gaussian random process is completely characterized by its mean value and its color, which can be described either by the power spectral density or, alternatively, by the autocorrelation function. However, we will first present a detailed analysis of the Rice method. It should be noted that many of the results found for the Rice method can be applied directly to the filter method.

If the Rice method is applied by using only a finite number of harmonic function N_i, then we obtain a further stochastic process denoted by

$$\hat{\mu}_i(t) = \sum_{n=1}^{N_i} c_{i,n} \cos(2\pi f_{i,n} t + \theta_{i,n}), \tag{2.6}$$

where we assume for the moment that the parameters $c_{i,n}$ and $f_{i,n}$ are still given by Eq.(2.4) and Eq.(2.5), respectively, and $\theta_{i,n}$ are again uniformly distributed random variables. Now, this method can be applied to the realization of a simulation model whose general structure is shown in Figure 2.4. It is obvious that $\hat{\mu}_i(t) \to \mu_i(t)$ holds as $N_i \to \infty$. At this point, it should be emphasized that the simulation model is still stochastic nature, since the phases $\theta_{i,n}$ are uniformly distributed random variables for all $n = 1,2,...,N_i$.

Only after the phases $\theta_{i,n}$ $(n = 1,2,...,N_i)$ are taken out of a random generator with a uniform distribution in the interval $(0,2\pi]$, the phase $\theta_{i,n}$ is no longer represent random variables but constant quantities, since they are now realizations (outcomes) random variable. Thus, in connection with Eq.(2.4), Eq.(2.5) and Eq.(2.6), it becomes obvious that

$$\tilde{\mu}_i(t) = \sum_{n=1}^{N_i} c_{i,n} \cos(2\pi f_{i,n} t + \theta_{i,n}), \tag{2.7}$$

is a *deterministic process* or *deterministic function*. Hence, from the stochastic simulation model shown in Figure 2.4(a), a deterministic simulation model follows, whose structure is presented in Figure 2.4(b), in its continuous-time form of representation. Note that in the limit $N_i \to \infty$, the deterministic process $\tilde{\mu}_i(t)$ tends to a sample function of the stochastic process $\mu_i(t)$.

This section will be shown that by choosing the parameters describing the deterministic process Eq.(2.7) appropriately, a very good approximation can be achieved in such a way that the statistical properties of $\tilde{\mu}_i(t)$ are very close to those of the underlying zero-mean colored Gaussian random process $\mu_i(t)$. For this reason, $\tilde{\mu}_i(t)$ will be called *real deterministic Gaussian process* and

$$\tilde{\mu}_i(t) = \tilde{\mu}_1(t) + j\tilde{\mu}_2(t), \tag{2.8}$$

will be named *complex deterministic Gaussian process*. With reference to Rayleigh process, a so-called deterministic Rayleigh process

$$\tilde{\zeta}(t) = |\tilde{\mu}(t)| = |\tilde{\mu}_1(t) + j\tilde{\mu}_2(t)|. \tag{2.9}$$

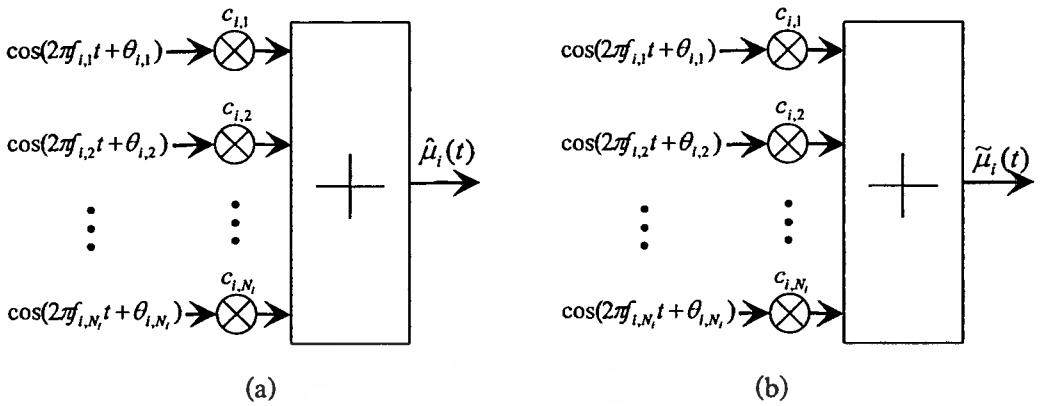

Figure 2.4 Simulation model for colored Gaussian random process

(a) Stochastic simulation model (random phases $\theta_{i,n}$) and

(b) Deterministic simulation model (constant phases $\theta_{i,n}$)

The deterministic processes are exclusively used for the modeling of the time-variant fading behavior caused by the Doppler effect, we will in the following call the parameters $c_{i,n}$, $f_{i,n}$, and $\theta_{i,n}$ describing the deterministic process Eq.(2.7) the Doppler coefficients, discrete Doppler frequencies, and Doppler phases, respectively.

2.2.2.2 Methods for the computation of the model parameters of deterministic processes

By now there is multitude of various methods for the computation of the primary parameters of the simulation model. Exactly like the original Rice method, the methods of equal distances as well as the mean-square-error method are characterized by the fact that the distances between neighboring discrete Doppler frequencies are equidistant.

Methods for the computation of the discrete Doppler frequencies and Doppler coefficients

2.2.2.3 Method of equal distances (MED)

One of the main characteristics of the methods of equal distances (MED) is that discrete Doppler frequencies, which are found in neighboring pairs, have the same distance. This property is achieved by defining the discrete Doppler frequencies $f_{i,n}$ as

$$f_{i,n} := \frac{\Delta f_i}{2}(2n-1), \quad n = 1,2,...,N_i, \tag{2.10}$$

where $\Delta f_i = f_{i,n} - f_{i,n-1}$, $n = 2,3,...,N_i$, denotes the distance between two neighboring discrete Doppler frequencies of the *i*th deterministic process $\tilde{\mu}_i(t)$ $(i = 1,2)$.

In order to compute the Doppler coefficients $c_{i,n}$, we take a look at the frequency interval

$$I_{i,n} := \left[f_{i,n} - \frac{\Delta f_i}{2}, f_{i,n} + \frac{\Delta f_i}{2} \right), \quad n = 1,2,...,N_i, \tag{2.11}$$

and demand that within this interval, the mean power of the power spectral density $S_{\mu_i\mu_i}(f)$ of the stochastic reference model is identical to that of the power spectral density $\tilde{S}_{\mu_i\mu_i}(f)$ of the deterministic simulation model, i.e.,

$$\int_{f \in I_{i,n}} S_{\mu_i\mu_i}(f) df = \int_{f \in I_{i,n}} \tilde{S}_{\mu_i\mu_i}(f) df, \tag{2.12}$$

for all $n = 1,2,...,N_i$ and $i = 1,2$. Thus, the Doppler coefficients $c_{i,n}$ are determined by the expression

$$c_{i,n} = 2\sqrt{\int_{f \in I_{i,n}} S_{\mu_i\mu_i}(f) df}. \tag{2.13}$$

Thus, for an infinite number of harmonic functions, the deterministic processes designed according to the method of equal distances can be interpreted as sample functions of the underlying ideal Gaussian random process.

The greatest common divisor of the discrete Doppler frequencies is

$$F_i = \gcd\{f_{i,n}\}_{n=1}^{N_i} = \frac{\Delta f_i}{2}. \tag{2.14}$$

Consequently, $\tilde{\mu}_i(t)$ is periodical with the period $T_i = 1/F_i = 2/\Delta f_i$. To obtain a large value for T_i, a small value for Δf_i is required, which is in general involved with a high realization amount.

2.2.2.4 Jakes power spectral density

The frequency range of the Jakes power spectral density is limited to the range $|f| \le f_{\max}$, so that for a given number of harmonic functions N_i, a reasonable value for the difference between two neighboring discrete Doppler frequencies $\Delta f_i = f_{\max}/N_i$. Consequently, form Eq.(2.10) we obtain the following relation for the discrete Doppler frequencies $f_{i,n}$

$$f_{i,n} = \frac{f_{\max}}{2N_i}(2n-1). \tag{2.15}$$

for all $n = 1,2,...,N_i$ and $i = 1,2$. The corresponding Doppler coefficients $c_{i,n}$ can now easily be computed with Eq.(2.11), Eq.(2.13) and Eq.(2.15). After an elementary computation, we find the expression

$$c_{i,n} = \frac{2\sigma_0}{\sqrt{\pi}}\left[\arcsin\left(\frac{n}{N_i}\right) - \arcsin\left(\frac{n-1}{N_i}\right)\right]^{1/2}, \tag{2.16}$$

for all $n = 1,2,...,N_i$ and $i = 1,2$.

The deterministic processes $\tilde{\mu}_i(t)$ designed with Eq.(2.15) and Eq.(2.16) obviously have the mean value $\tilde{m}_{\mu_i}(t) = 0$ and the mean power

$$\tilde{\sigma}^2_{\mu_i} = \tilde{r}_{\mu_i\mu_i}(0) = \sum_{n=1}^{N_i} \frac{c_{i,n}^2}{2} = \sigma_0^2. \tag{2.17}$$

Hence, both the mean value and the mean power of the deterministic process $\tilde{\mu}_i(t)$ exactly match the corresponding quantities of the stochastic process $\mu_i(t)$, i.e., the expected value and the variance. As an example, the power spectral density $\tilde{S}_{\mu_i\mu_i}(f)$ is depicted in Figure 2.5.

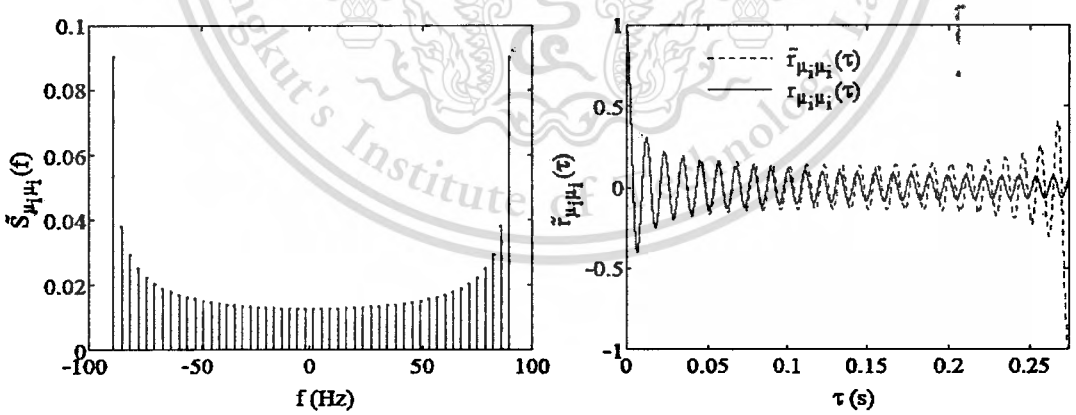

(a) (b)

Figure 2.5 (a) Power spectral density $\tilde{S}_{\mu_i\mu_i}(f)$ and (b) autocorrelation function $\tilde{r}_{\mu_i\mu_i}(\tau)$ for N_i=25 (MED, Jakes PSD, $f_{\max}$=91 Hz, σ_0^2=1)

2.2.2.5 Frequency-selective stochastic and deterministic channel models

The frequency-nonselective mobile radio channels are characterized by the fact that the differences between the propagation delays of the received electromagnetic waves can be ignored compared to the symbol interval. Obviously, this assumption is less and less justified the shorter the symbol interval or the higher the data rate becomes. Channels for which the propagation delay differences cannot be ignored in comparison with the symbol interval, therefore, represent a further important class of channels, namely the class of *frequency-selective channels*.

2.2.3 COST 207 Channel Model

In 1984, the European working group COST 207 (COST: European Cooperation in the Field of Scientific and Technical Research) was established by CEPT (Conference of European Posts and Telecommunications Administrations). At that time, this working group developed suitable channel models for typical propagation environments, in view of the planned pan-European mobile communication system GSM. The typical propagation environments are classifiable into areas with rural character (RA, Rural Area), areas typical for cities and suburbs (TU, Typical Urban), densely built urban areas with bad propagation conditions (BU, Bad Urban), and hilly terrains (HT, Hill Terrain). Basing on the WSSUS assumption, the working group COST 207 developed specifications for the delay power spectral density and the Doppler power spectral density for these four classes of propagation environments [20].

The specification of typical delay power spectral densities $S_{\tau'\tau'}(\tau')$ is based on the assumption that the corresponding probability density function $p_{\tau'}(\tau')$, which is proportional to $S_{\tau'\tau'}(\tau')$, can be represented by one or more negative exponential functions. The delay power spectral density function $S_{\tau'\tau'}(\tau')$ of the channel models according to COST 207 are shown in Figure 2.6. The four types of Doppler power spectral densities $S_{\mu\mu}(f)$ specified by COST 207 is shown in Figure 2.7.

Regarding the design of hardware or software simulation models for frequency-selective channels, a discrimination of the delay power spectral density $S_{\tau'\tau'}(\tau')$ has to be performed. In particular, the propagation delays τ' have to be made discrete and adapted to the sampling interval. This is the reason why discrete L-path channel models have been specified in [22] for the four propagation areas. Some of these specified L-path channel models are listed in Table 2.1. In [22], moreover, alternative 6-path channel models as well as more complex, but therefore more exact.

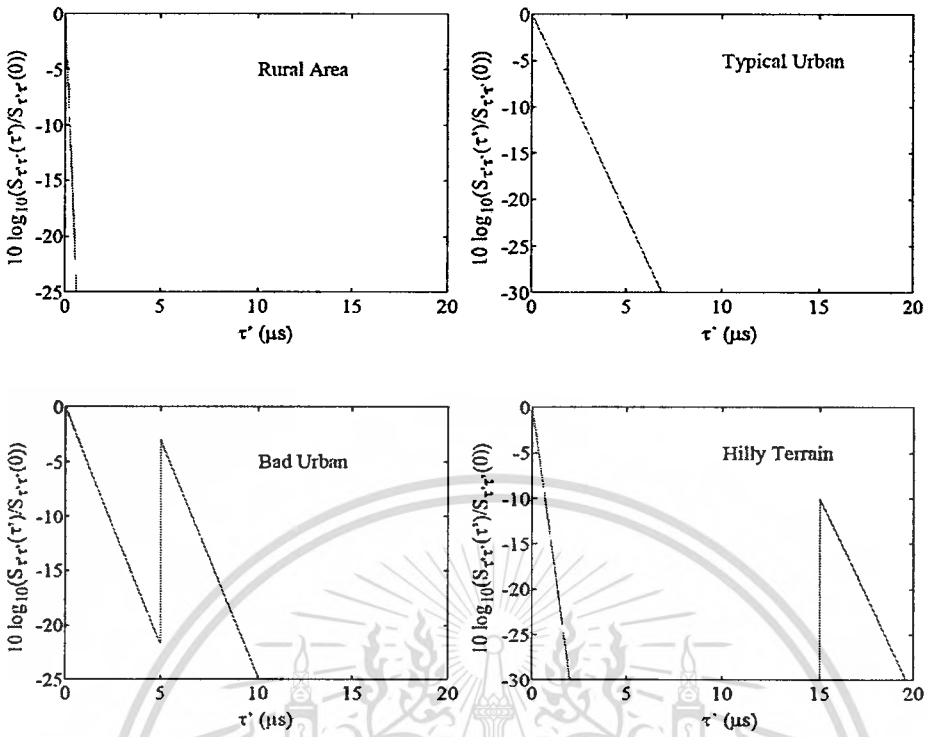

Figure 2.6 Delay power spectral densities $S_{\tau'\tau'}(\tau')$ of the channel models according to COST 207

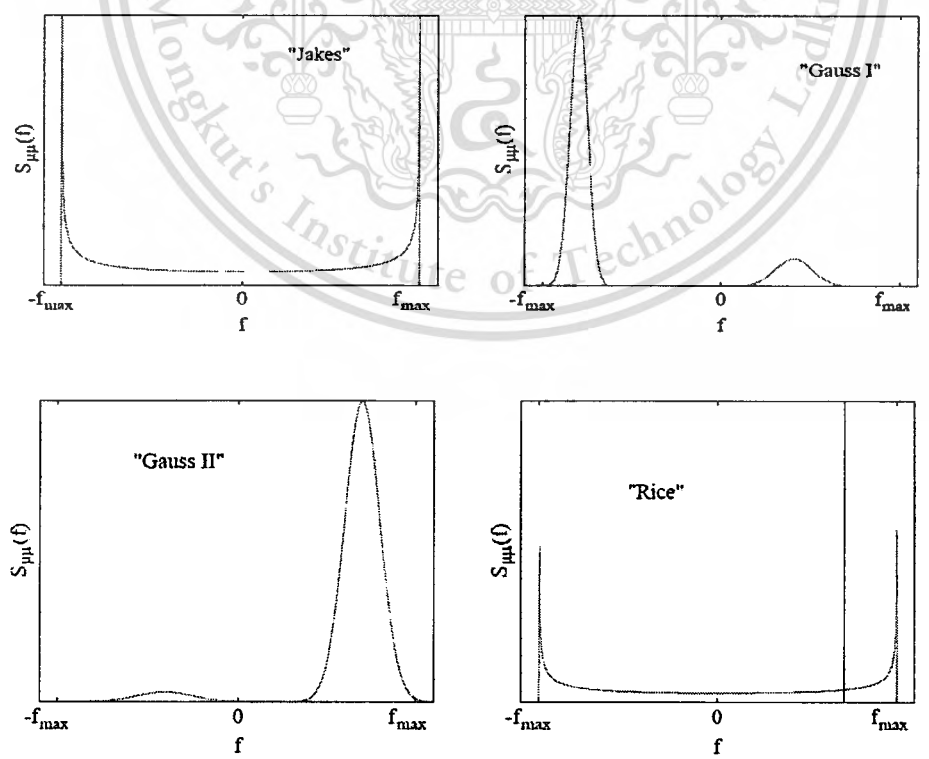

Figure 2.7 Doppler power spectral densities $S_{\mu\mu}(f)$ of the channel models according to COST 207

Table 2.1 Specification of the 6-path channel models according to COST 207

Path #	Rural area (RA)		Type urban (TU)	
	Delay (μs))	Power (dB)	Delay (μs))	Power (dB)
1	0	0	0	-3
2	0.1	-4	0.2	0
3	0.2	-8	0.5	-2
4	03	-12	1.6	-6
5	0.4	-16	2.3	-8
6	0.5	-20	5.0	-10
	Bad urban (BU)		Hilly terrain (HT)	
1	0	-2.5	0	0
2	0.3	0	0.1	-1.5
3	1	-3	0.3	-4.5
4	1.6	-5	0.5	-7.5
5	5	-2	15	-8
6	6.6	-4	17.2	-17.7

2.2.3.1 Frequency-Selective Deterministic Channel Models

In this section, we will deal with the derivation and the analysis of the frequency-selective deterministic channel models. Starting point of the derivation of the system function of frequency-selective deterministic channel models is the time-variant impulse response consisting of a sum of L discrete propagation paths

$$\tilde{h}(\tau',t)=\sum_{\ell=0}^{L-1}\tilde{a}_\ell\tilde{\mu}_\ell(t)\delta(\tau'-\tilde{\tau}'_\ell)\,. \tag{2.18}$$

The quantities $\tilde{a}_\ell$ in Eq.(2.18) are real-valued and they are called the *delay coefficients*. As we will see later on, both the delay coefficients $\tilde{a}_\ell$ and the discrete propagation delays $\tilde{\tau}'_\ell$ determine the power spectral density of frequency-selective deterministic channel models.

Strictly speaking, the delay coefficient $\tilde{a}_\ell$ is a measure of the square root of the average delay power which is assigned to the ℓth discrete propagation path. In general, one can say that the delay coefficients $\tilde{a}_\ell$ and the discrete propagation delays $\tilde{\tau}'_\ell$ determine the frequency-selective behavior of the channel, which can be attributed to the effect of multipath propagation. In present case, it is assumed that elliptical scattering zone with different discrete axes are the reason for multipath propagation. The disturbances of the channel caused by the Doppler effect, i.e., the disturbances caused by the motion of the receiver (transmitter), are modeled in Eq.(2.18), according to the principle of deterministic channel modeling, by complex deterministic Gaussian processes

$$\tilde{\mu}_\ell(t) = \tilde{\mu}_{1,\ell}(t) + j\tilde{\mu}_{2,\ell}(t), \quad \ell = 0,1,...,L-1, \tag{2.19}$$

where

$$\tilde{\mu}_{i,\ell}(t) = \sum_{n=1}^{N_{i,\ell}} c_{i,n,\ell} \cos(2\pi f_{i,n,\ell} t + \theta_{i,n,\ell}), \; i = 1,2. \tag{2.20}$$

Here, $N_{i,\ell}$ denotes the number of harmonic functions belonging to the real part ($i=1$) or the imaginary part ($i=2$) of the ℓ th propagation path. In Eq.(2.19), $c_{i,n,\ell}$ is the Doppler coefficient of the nth component of the ℓ th propagation path, and the remaining model parameters $f_{i,n,\ell}$ and $\theta_{i,n,\ell}$ are, as stated before, called the Doppler frequencies and the Doppler phases, respectively.

2.2.3.2 System Function of Frequency-Selective Deterministic Channel Models

Figure 2.8 shows the structure of the complex Gaussian random process $\tilde{\mu}_\ell(t)$ in the continuous-time representation. To ensure that the simulation model derived below has the same striking properties as a US model, the complex deterministic Gaussian process $\tilde{\mu}_\ell(t)$ must be uncorrelated for different propagation paths. Therefore, it is inevitable that the deterministic Gaussian processes $\tilde{\mu}_\ell(t)$ and $\tilde{\mu}_\lambda(t)$ are designed in such a way that they are uncorrelated for $\ell \neq \lambda$, where ℓ, λ=0, 1, ..., L-1. This demand can easily be fulfilled. One merely has to ensure that the discrete Doppler frequencies $f_{i,n,\ell}$ are designed so that the resulting sets $\{f_{i,n,\ell}\}$ are disjoint (mutually exclusive) for different propagation paths. For the simulation model, the demand for uncorrelated scattering (US) propagation can therefore be formulated as follows:

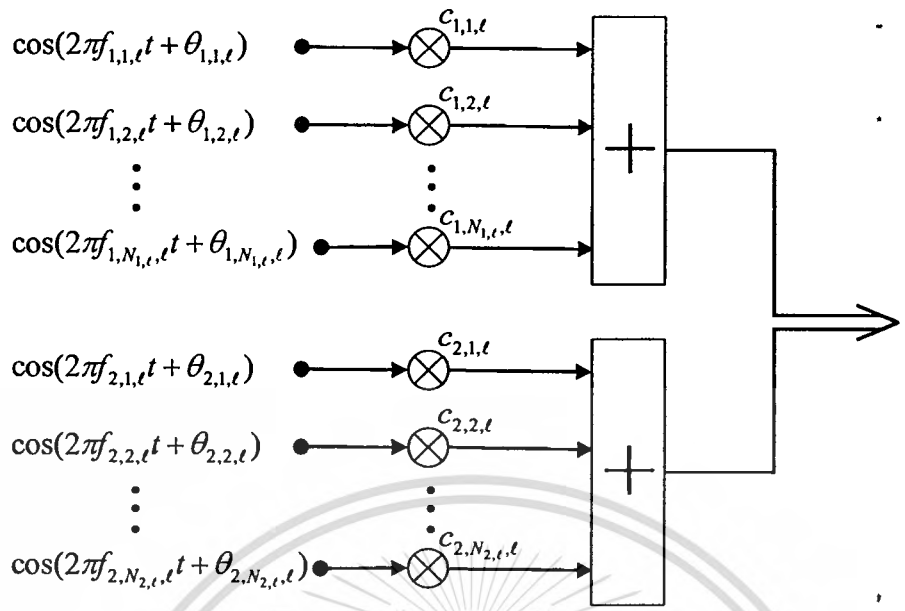

Figure 2.8 Simulation model for complex deterministic Gaussian process $\widetilde{\mu}_\ell(t)$

$$\text{US} \Leftrightarrow f_{i,n,\ell} \neq f_{j,m,\lambda} \quad \text{for } i=1,2. \tag{2.21}$$

where $i, j = 1, 2$, n=1, 2, ..., $N_{i,\ell}$, m= 1, 2, ..., $N_{i,\lambda}$, and $\ell, \lambda = 0, 1, \ldots, L$-1

At this stage, it should be mentioned that all parameters determining the statistical behavior of the time-variant impulse response $\widetilde{h}(\tau',t)$ can be calculated in such a way that the scattering function. We may therefore assume that the parameters mentions above are not only know, but also constant quantities, which will not be changed during the channel simulation run. In this case, the time-variant impulse response $\widetilde{h}(\tau',t)$ is a deterministic function which will consequently be called the *time-variant deterministic impulse response*. It defines a further important class of channel models. In the following, channel model with an impulse response according to Eq.(2.18) will be called DGUS models.

Since the discrete propagation delays $\widetilde{\tau}'_\ell$ in Eq.(2.18) cannot become negative, $\widetilde{h}(\tau',t)$ fulfils the causality condition, i.e., it holds

$$\widetilde{h}(\tau',t) = 0 \quad \text{for } \tau' < 0. \tag{2.22}$$

By analogy, we can compute the output signal $y(t)$ for any given input signal $x(t)$ by applying

$$y(t) = \int_0^\infty x(t-\tau')\tilde{h}(\tau',t)d\tau' . \tag{2.23}$$

If we now employ the expression Eq.(2.18) for the time-variant deterministic impulse response $\tilde{h}(\tau',t)$, we obtain

$$y(t) = \sum_{\ell=0}^{L-1} \tilde{a}_\ell \tilde{\mu}_\ell(t) x(t-\tilde{\tau}'_\ell) . \tag{2.24}$$

Hence, the output signal $y(t)$ of the channel can be interpreted as a superposition of L delayed versions of the input signal $x(t-\tilde{\tau}_\ell)$, where each of the delayed versions is weighted by a constant delay coefficient $\tilde{a}_\ell$ and a time-variant complex deterministic Gaussian process $\tilde{\mu}_\ell(t)$. Without restriction of generality, we may ignore the propagation delay of the line-of-sight component in this model. To simplify matters, we define $\tilde{\tau}'_0 = 0$. This does not cause any problem, because only the propagation delay differences $\Delta\tilde{\tau}'_\ell = \tilde{\tau}'_\ell - \tilde{\tau}'_{\ell-1}$ $(\ell = 1,2,...,L-1)$ are relevant for the system behavior. From Eq.(2.24) follows the tapped-delay-line structure show in Figure 2.9 of the deterministic simulation model for a frequency-selective mobile radio channel in the continuous-time representation.

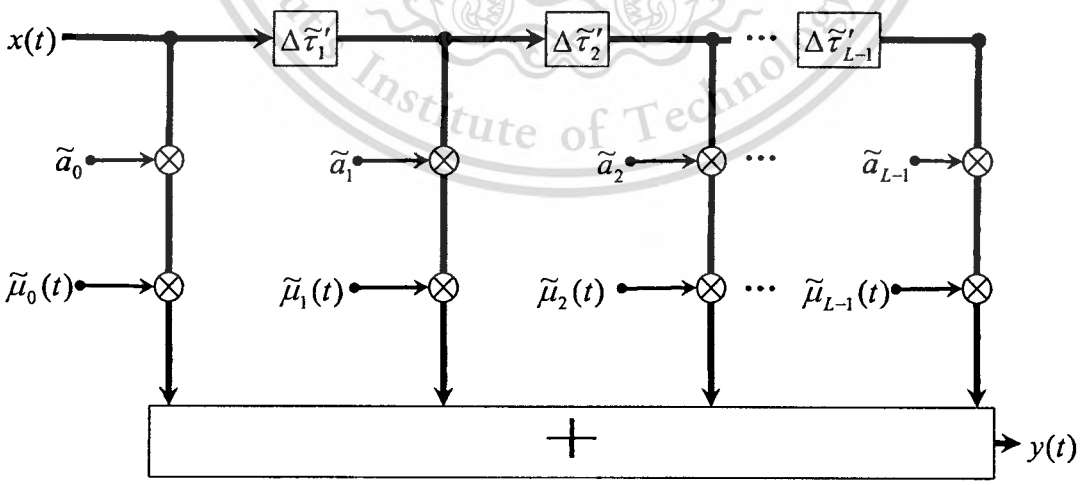

Figure 2.9 Deterministic simulation model for a frequency-selective mobile radio channel in the equivalent complex baseband

The discrete-time simulation model, required for computer simulations, can be obtained from the continuous-time structure, e.g., by substituting $\tilde{\tau}'_\ell \to \ell T'_s$, $x(t) \to x(kT'_s)$, $y(t) \to y(kT'_s)$ and $\tilde{\mu}_\ell(t) \to \tilde{\mu}_\ell(kT'_s)$, where T_s and T'_s denote sampling intervals, k is an integer, and ℓ refers to the ℓ th propagation path (ℓ =0, 1,..., L-1). For the propagation delay differences $\Delta\tilde{\tau}'_\ell = \tilde{\tau}'_\ell - \tilde{\tau}'_{\ell-1}$, we in this case obtain $\Delta\tilde{\tau}'_\ell = T'_s$ for all ℓ =0, 1,..., L-1. The sampling intervals T_s and T'_s have to be sufficiently small, but must not necessarily be identical. Between T_s and T'_s, we can therefore establish the general relation $T_s = m'_s T'_s$, where $m'_s \in \mathrm{N}$ is in the following called the *sampling rate ratio*. The larger (smaller) the sampling rate ratio m'_s is chosen, the higher (lower) the simulation speed of the channel simulator is and the larger (smaller) the error occurring due to the discretization of $\tilde{\mu}_\ell(t)$ is. The sampling rate ratio m'_s enables the user to find a good compromise between simulation speed and the precision of the channel model. As a guideline, m'_s should be chosen so that the sampling interval T_s satisfies the condition $T'_s \le T_s \le T_{sym}$ for any given symbol interval T_{sym}. The upper limit $T_s = T_{sym}$ corresponds to the often made assumption that the impulse response is constant for the duration of one data symbol. However, this assumption is only justified if the product $f_{\max} T_{sym}$ is very small.

2.2.4 Characteristics of Multi-path Fading Channel

In mobile radio communications, is severely affected by multi-path propagation; the electromagnetic wave is scattered, diffracted an reflected, and reaches the antenna via various ways a an incoherent superposition of many signals with different delay times that are caused by the different path lengths of these signals [23]. This leads to an interference pattern that depends on the frequency and the location. Mobile receiver moves through an interference pattern that may change within milliseconds and that varies over the transmission bandwidth. One says that the mobile radio channel is characterized by time variance and frequency selectivity. The time variant is determined by the relative speed v between receiver and transmitter.

The frequency selectivity of the channel is determined by the different delay time of the signals. They can be calculated as the ratio between the traveling distances and the velocity of light. 1 μs delay time difference corresponds to 300 meters. of path difference [23]. Longer echoes correspond to more fade within the transmission bandwidth. In time-domain, ISI disturbs the transmission if the delay time differences are not much smaller than the symbol duration. We can define a correlation frequency as follows

$$f_{corr} = \Delta\tau^{-1}, \tag{2.25}$$

where $\Delta\tau$ is the square root of the variance of the power distribution of the echoes, which we call the delay spread. f_{corr} is often called coherence (or coherency) bandwidth because channel can be regarded as frequency-nonselective.

We now assume tat both transmitter and receiver are at rest (or the time variance is so slow that it can neglected for the time period under consideration) and we can ignore any Doppler shift. We do not ignore the delays $\tau_k = l_k / c_0$ of the complex baseband signal $s(t) \mapsto s(t-\tau_k)$ for the different propagation paths of length l_k. We can get for the receiver signal

$$\tilde{r}(t) = \sqrt{2}\sum \Re\left\{a_k e^{j\theta_k} s(t-\tau_k) e^{j2\pi f_0 t}\right\}. \tag{2.26}$$

The delays of the carrier are already included in the phases θ_k, The complex baseband transmit and receive signals $s(t)$ and $r(t)$ are related by

$$r(t) = h(t) * s(t), \tag{2.27}$$

where

$$h(t) = \sum_{k=1}^{N} a_k e^{j\theta_k} \delta(t-\tau_k), \tag{2.28}$$

is the impulse response of the channel. The corresponding channel transfer function is given by

$$H(f) = \sum_{k=1}^{N} a_k e^{j\theta_k} e^{-j2\pi f\tau_k}. \tag{2.29}$$

Since, the variable for this process is a frequency, there is a power density distribution a function of a time variable τ that can be indentified as the delay time. Figure 2.10(a) illustrates such a delay power spectrum corresponding to the process given by the Eq.(2.28) and Eq.(2.29). However, in most real situations, the received signal is a continuous rather than a discrete superposition of delay signal components, resulting in a continuous delay power spectrum as shown in Figure 2.10(b)

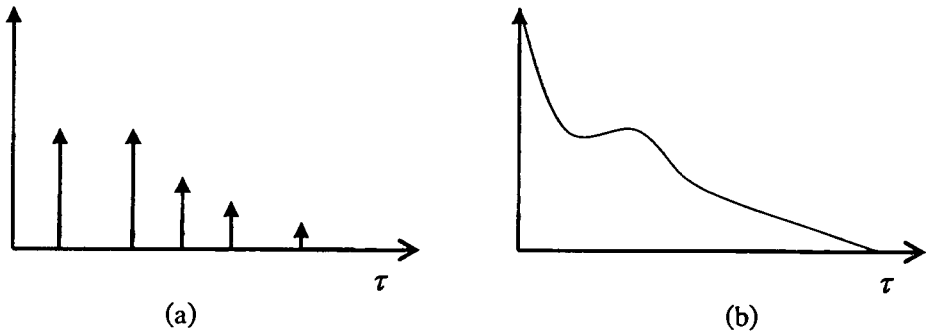

Figure 2.10 Example of a discrete (a) and continuous (b) delay power spectrum

2.2.5 The AWGN Channel

In reality, transmission is always corrupted by noise. The usual mathematical model is the AWGN (Additive White Gaussian Noise) channel. It is a very good model for the physical reality as long as the thermal noise at the receiver is the only source of disturbance. Nevertheless, because of its simplicity, it is often used to model man-made noise or multi-user interference. The AWGN channel model can be characterized as follows [23]:

- The noise is an additive random disturbance of the useful signal $s(t)$, that is , the receive signal is given by

$$r(t) = s(t) + w(t) \tag{2.30}$$

- The noise is *white*, that is, it has a constant power spectral density (PSD). The one-side PSD is usually denoted by N_0, so $N_0/2$ is the two-side PSD, and BN_0 is the noise inside the (noise) bandwidth *B*. For thermal resistor noise, $N_0 = kT_0$, where k is the Boltzmann constant and T_0 is the absolute temperature. The unit of N_0 is [W/Hz].
- The noise is a stationary and zero mean *Gaussian* random process. This means that the output of every (linear) noise measurement is a zero mean Gaussian random variable that does not depend on the time instant when the measurement is done.

One must keep in mind that the AWGN model is a mathematical fiction, because it implies that the total power is infinite. Thus, a time sample of the white noise has infinite average power, which is certainly not a physically reasonable property. It is known from statistical physics that the thermal noise density decreases exponentially at high frequencies.

2.3 Basic Principles of OFDM Systems

In this section, we present a brief discussion on the basic principles of OFDM systems. We would like to introduce the orthogonality theory, OFDM generation and reception, modulation mapping scheme, transformation for OFDM systems, guard interval, and channel estimation. The details will be presented as follows.

2.3.1 Introduction

Orthogonal Frequency Division Multiplexing (OFDM) is very similar to the well known and used technique of Frequency Division Multiplexing (FDM). OFDM uses the principles of FDM to allow multiple messages to be sent over a single radio channel. It is however in a much more controlled manner, allowing an improved spectral efficiency.

OFDM is different from FDM in several ways. In conventional broadcasting each radio station transmits on a different frequency, effectively using FDM to maintain a separation between the stations. However, there is no coordination or synchronization between each of these stations. With an OFDM transmission such as DAB, the information signals from multiple stations are combined into a single multiplexed stream of data. This data is then transmitted using an OFDM ensemble that is made up from a dense packing of many sub-carriers. All the sub-carriers within the OFDM signal are time and frequency synchronized to each other, allowing the interference between sub-carriers to be carefully controlled. These multiple sub-carriers overlap in the frequency-domain, but do not cause ICI due to the orthogonal nature of the modulation. Typically with FDM the transmission signals need to have a large frequency guard-band between channels to prevent interference. This lowers the overall spectral efficiency. However with OFDM the orthogonal packing of the sub-carriers greatly reduces this guard band, improving the spectral efficiency.

OFDM is based on parallel transmission scheme that reduce the effects of multi-path fading. In the multi-path environment, the receiver receives the signals not only the direct transmission signal but also the several reflected signals arrive. Those signals arrive to the receiver at the different time. From time-domain point of view, several signals with different arrival times, signal power, and phases are received at the receiver. The multi-path fading environment is characterized by a channel impulse response. On the other hand, from frequency-domain point of view, the multi-path fading environment is characterized by the enhancement of some frequencies and the attenuation of others. Because the symbol duration

increases for the lower rate parallel subcarriers, the relative amount of dispersion in time caused by multi-path is decreased.

2.3.2 Orthogonality

Signals are orthogonal if they are mutually independent of each other. Orthogonality is a property that allows multiple information signals to be transmitted perfectly over a common channel and detected, without interference. Loss of orthogonality results in blurring between these information signals and degradation in communications. Many common multiplexing schemes are inherently orthogonal. Time Division Multiplexing (TDM) allows transmission of multiple information signals over a single channel by assigning unique time slots to each separate information signal. During each time slot only the signal from a single source is transmitted preventing any interference between the multiple information sources. Because of this TDM is orthogonal in nature. In the frequency-domain most FDM systems are orthogonal as each of the separate transmission signals are well spaced out in frequency preventing interference.

Although these methods are orthogonal the term OFDM has been reserved for a special form of FDM. The sub-carriers in an OFDM signal are spaced as close as is theoretically possible while maintain orthogonality between them. OFDM achieves orthogonality in the frequency domain by allocating each of the separate information signals onto different sub-carriers. OFDM signals are made up from a sum of sinusoids, with each corresponding to a sub-carrier. The baseband frequency of each sub-carrier is chosen to be an integer multiple of the inverse of the symbol time, resulting in all sub-carriers having an integer number of cycles per

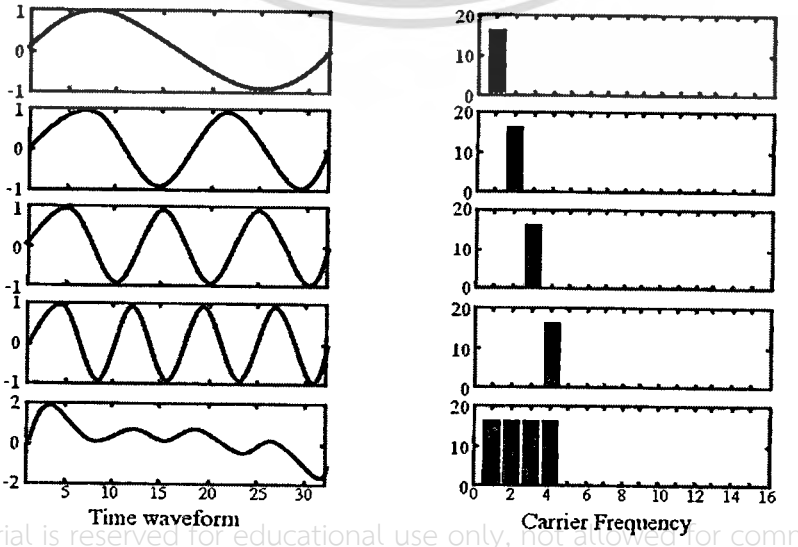

Figure 2.11 Time-domain construction of OFDM signal

symbol. As a consequence the sub-carriers are orthogonal to each other. Figure 2.11 shows the construction of an OFDM signal with four sub-carriers.

Sets of functions are orthogonal to each other if they match the conditions in Eq.(2.31). If any two different functions within the set are multiplied, and integrated over a symbol period, the result is zero, for orthogonal functions. Another way of thinking of this is that if we look at a matched receiver for one of the orthogonal functions, a sub-carrier in the case of OFDM, then the receiver will only see the result for that function. The results from all other functions in the set integrate to zero, and thus have no effect.

$$\int_0^T s_i(t)s_j(t)dt = \begin{cases} C & i=j \\ 0 & i \neq j \end{cases}. \tag{2.31}$$

Equation (2.32) shows a set of orthogonal sinusoids, which represent the sub-carriers for an un-modulated real OFDM signal.

$$s_k(t) = \begin{cases} \sin(2\pi k f_0 t) & 0 < t < T_{symbol} \quad k = 1,2,...,N \\ 0 & otherwise \end{cases}, \tag{2.32}$$

where f_0 is the carrier frequency, N is the number of carriers, T_{symbol} is the symbol period. Since the highest frequency component is Nf_0 the transmission bandwidth is also Nf_0.

These sub-carriers are orthogonal to each other because when we multiply the waveforms of any two sub-carriers and integrate over the symbol period the result is zero. Multiplying the two sine waves together is the same as mixing these sub-carriers. This results in sum and difference frequency components, which will always be integer sub-carrier frequencies, as the frequency of the two mixing sub-carriers has integer number of cycles. Since the system is linear we can integrate the result by taking the integral of each frequency component separately then combining the results by adding the two sub-integrals. The two frequency components after the mixing have an integer number of cycles over the period and so the sub-integral of each component will be zero, as the integral of a sinusoid over an entire period is zero. Both the sub-integrals are zeros and so the resulting addition of the two will also be zero, thus we have established that the frequency components are orthogonal to each other.

Another way to view the orthogonality property of OFDM signals is to look at its spectrum. In the frequency-domain each OFDM sub-carrier has a *sinc*, $\sin(x)/x$, frequency response, as shown in Figure 1.2. This is a result of the symbol time corresponding to the inverse of the carrier spacing. As far as the receiver is concerned each OFDM symbol

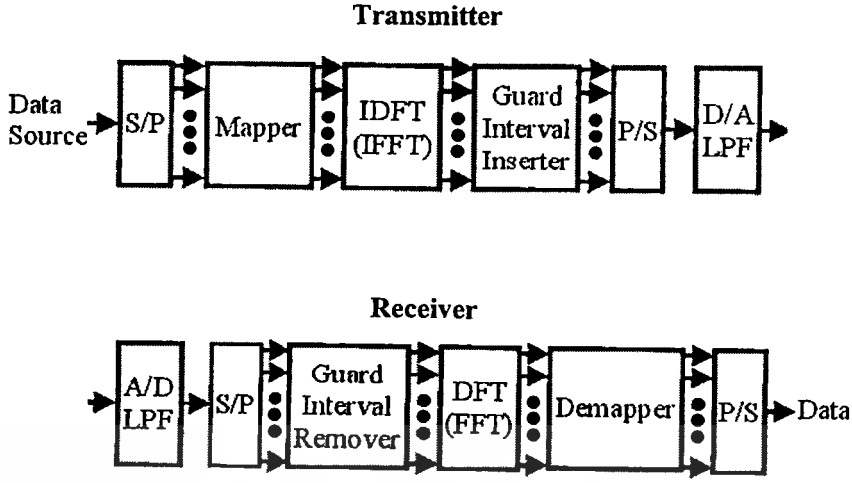

Figure 2.12 Block diagram of a conventional OFDM transceiver

transmitted for a fixed time (T_{FFT}) with no tapering at the ends of the symbol. This symbol time corresponds to the inverse of the sub-carrier spacing of $1/T_{FFT}$ Hz.

2.3.3 OFDM Generation and Reception

To generate OFDM successfully the relationship between all the carriers must be carefully controlled to maintain the orthogonality of the carriers. For this reason, OFDM is generated by firstly choosing the spectrum required, based on the input data, and modulation mapping scheme used. Each carrier to be produced is assigned some data to transmit. The required amplitude and phase of the carrier is then calculated based on the modulation scheme (typically differential BPSK, QPSK, or QAM). The required spectrum is then converted back to its time domain signal using an inverse discrete Fourier transform (IDFT). The inverse fast Fourier transform (IFFT) performs the same operations as an IDFT, except that it is much more computationally efficiency, and so is used in all practical systems. The IFFT performs the transformation very efficiently, and provides a simple way of ensuring the carrier signals produced are orthogonal.

The receiver performs the reverse operation of the transmitter, mixing the RF signal to base band for processing, then using a discrete Fourier transform (DFT) or fast Fourier transform (FFT) to analyze the signal in the frequency domain. The amplitude and phase of the sub-carriers is then picked out and converted back to digital data. The IFFT and the FFT are complementary function and the most appropriate term depends on whether the signal is being received or generated. In cases where the signal is independent of this distinction then the term

FFT and IFFT is used interchangeably. The block diagram of a basic OFDM transceiver is shown in Figure 2.12.

The fast Fourier transform (FFT) transforms a cyclic time-domain signal into its equivalent frequency spectrum. This is done by finding the equivalent waveform, generated by a sum of orthogonal sinusoidal components. The amplitude and phase of the sinusoidal components represent the frequency spectrum of the time-domain signal. The IFFT performs the reverse process, transforming a spectrum (amplitude and phase of each component) into a time-domain signal. An IFFT converts a number of complex data points, of length that is a power of 2, into the time-domain signal of the same number of points. Each data point in frequency spectrum used for an FFT or IFFT is called a bin.

The orthogonal carriers required for the OFDM signal can be easily generated by setting the amplitude and phase of each frequency bin, then performing the IFFT. Since each bin of an IFFT corresponds to the amplitude and phase of a set of orthogonal sinusoids, the reverse process guarantees that the carriers generated are orthogonal.

2.3.4 Modulation Mapping Scheme

Consider some digital information that is given by a finite bit sequence. To transmit this information over a physical channel by a passband signal $\tilde{s}(t) = \Re\{s(t)e^{j2\pi f_0 t}\}$, we need a mapping rule between the set of bit sequences and the set of possible signals. We call such mapping rule a modulation mapping scheme. A linear digital modulation scheme is characterized by the complex baseband signal [23]

$$s(t) = \sum_{k=1}^{K} s_k g_k(t), \tag{2.33}$$

where the information is carried by the complex transmit symbols s_k. This is linear mapping from the vector $s = (s1,...,s_k)^T$ of transmit symbols to the continuous transmit signal $s(t)$. In this section, the most popular signal constellations for the modulation symbols s_k will be explained. s_k are used to transmit information by choosing one of M possible points of that constellation. We assume that M is a power of two, so each complex symbol s_k carries $\log_2(M)$ bits of the information. Although it is possible to combine several symbols to a higher-dimensional constellation, we can restrict ourselves to a discrete-time transmission setup where the complex modulation symbols

$$s_k = x_k + jy_k. \tag{2.34}$$

When we transmit digital data like +1 or -1 by using radio waves, the best way is to modulate carrier signals with frequency f_c in accordance with the information of digital information. The meaning of "modulate" is to vary the peculiar component that is included in the carrier signal wave. The waveform of the carrier signal is written as follows [24]:

$$S(t) = A\cos\{2\pi f_c t + \theta(t)\}, \tag{2.35}$$

where A, f_c, and $\theta(t)$ are the amplitude, center frequency, and time-variant phase of the carrier wave signal, respectively. In Eq.(2.35), we have three peculiar components by which users can change the value. There three are amplitude, frequency, and phase, and if we change the amplitude of Eq.(2.35) in accordance with the digital information data, we call the modulation scheme AM. Moreover, if we change the frequency of Eq.(2.35) with information digital data, then we call the modulation scheme FM. Finally, if we change the phase of Eq.(2.35) in accordance with the digital information data, we call the modulation scheme PM or PSK [24].

The IQ plot for a modulation mapping scheme shows the transmitted vector for all data word combinations. Each data word combination must be allocated a unique IQ vector. Gray coding is a method for this allocation so that neighboring points in the constellation only differ by a single bit. This coding helps to minimize the overall bit error rate as it reduces the chance of multiple bit errors occurring from a single symbol error. Table 2.2 shows the sequencing for gray coding in decimal format.

Table 2.2 4 bit Gray coding in binary

Decimal	Gray Coding	Decimal	Gray Coding
0	0, 0, 0, 0	8	1, 1, 0, 0
1	0, 0, 0, 1	9	1, 1, 0, 1
2	0, 0, 1, 1	10	1, 1, 1, 1
3	0, 0, 1, 0	11	1, 1, 1, 0
4	0, 1, 1, 0	12	1, 0, 1, 0
5	0, 1, 1, 1	12	1, 0, 1, 1
6	0, 1, 0, 1	14	1, 0, 0, 1
7	0, 1, 0, 0	15	1, 0, 0, 0

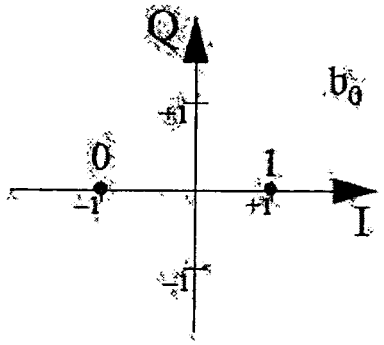

Figure 2.13 *IQ* diagram for BPSK modulation mapping scheme

2.3.4.1 BPSK

For *M*-PSK (phase-shift keying), the modulation symbols s_k can be written as [23]

$$s_k = \sqrt{E_S} e^{j\phi_k}. \tag{2.36}$$

That is, all the information is contained in the *M* position phase value ϕ_k of the symbol. Two adjacent points of the constellation have the phase difference $2\pi/M$. It is a matter of convenience whether $\phi = 0$ is a point of the constellation or not. For 2-PSK, often called BPSK (binary PSK) the phase may take the two values $\phi_k \in \{0, \pi\}$ and thus 2-PSK is just the same as 2-ASK. For 4-PSK, often called QPSK (quaternary PSK) the phase may take the four values $\phi_k \in \{\pm\pi/4, \pm 3\pi/4\}$ [24].

In the BPSK modulation scheme, the input digital data 0 or 1 is directly converted to the phase of 0 or π, respectively. Therefore, the waveform is shown as follows

$$s(t) = A\cos\{2\pi f_c t + \pi \cdot d_k\}, \tag{2.37}$$

where d_k is the information data sequence.

The phase of a constant amplitude carrier signal moves between zero and 180 degrees. On an *I* and *Q* diagram, the *I* state has two different values as shown in Figure 2.13. There are two possible locations in the state diagram, so a binary one or zero can be sent. The symbol rate is one bit per symbol.

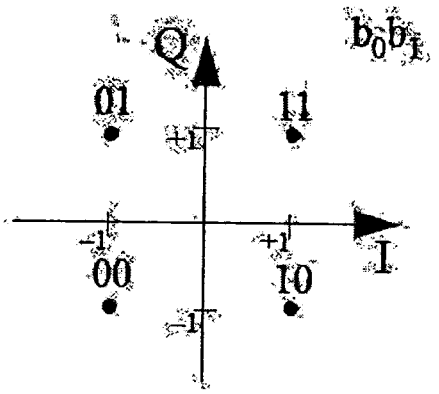

Figure 2.14 *IQ* diagram for QPSK modulation mapping scheme

2.3.4.2 QPSK

A QPSK signal is generated by two BPSK signals. To distinguish the two signals, we use tow orthogonal carrier signals. One is given by $\cos(2\pi f_c t)$, and the other is given by $\sin(2\pi f_c t)$. The two carrier signals remain orthogonal in the area of a period

$$\int_0^{T_c} \cos 2\pi f_c t \times \sin 2\pi f_c t = 0, \tag{2.38}$$

where T_c is the period of the carrier signals and

$$f_c = \frac{1}{T_c}. \tag{2.39}$$

By using $\cos(2\pi f_c t)$ and $\sin(2\pi f_c t)$, we can represent QPSK signals by

$$s(t) = \frac{1}{\sqrt{2}} d_I(t)\cos(2\pi f_c t) + \frac{1}{\sqrt{2}} d_Q(t)\sin(2\pi f_c t). \tag{2.40}$$

A channel in which $\cos(2\pi f_c t)$ is used as a carrier signal is generally called a phase channel, or *I*, and a channel in which $\sin(2\pi f_c t)$ is used as a carrier signal is generally called a quadrature-phase channel, or *Q*. Therefore, $d_I(t)$ and $d_Q(t)$ are the data in *I* and *Q*, respectively. Modulation schemes that use *I* and *Q* are called quadrature modulation schemes. The *IQ* diagram is shown in Figure 2.14.

2.3.4.3 16QAM

For *M*-ASK (amplitude-shift keying), a tuple of $M = \log_2(M)$ bits will be mapped only on the real part x_k of s_k, while the imaginary part y_k will be set to zero. The M points will be placed equidistant and symmetrically about zero. Denoting the distance between two points by $2d$, the signal constellation for 2-ASK is given by $x_1 \in \{\pm d\}$, for 4-ASK by $x_1 \in \{\pm d, \pm 3d\}$ and for 8-ASK by $x_1 \in \{\pm d, \pm 3d, \pm 5d, \pm 7d\}$. We consider Gray mapping, that is, two neighboring points differ only in one bit. In Figure 2.15, the *M*-ASK signal constellations are depicted for *M*=2, 4, 8 [23].

For ASK constellations, only the *I*-component, corresponding to the cosine wave, will be modulated, while the sine wave will not be present in the passband signal. Since, in general, every passband signal of a certain bandwidth may have both components, 50% of the bandwidth resources remain unused. A simple way to use these resources is to apply the same ASK modulation for the *Q*-component too. We thus have complex modulation symbols $s_k = x_k + jy_k$, where both x_k and y_k are taken from an *M*-ASK constellation. The result is square constellation of M^2 signal points in the complex plane, as depicted in Figure 2.16 and Figure 2.17 for $M^2 = 16$ and $M^2 = 64$, respectively. We can these $M^2 - \text{QAM}$ (quadrature amplitude modulation) [23].

In the QAM, the amplitude of *I* and *Q* are determined using more bits. Figure 2.16 shows the constellations of 16QAM. In this scheme, we transmit 2^{2n} bits during each symbol time. A key factor when doing this is how to assign the transmission bit to the amplitude. In this section, we introduce the Gray encoding method for 2^{2n} QAM (n=1, 2, 3, 4) [24].

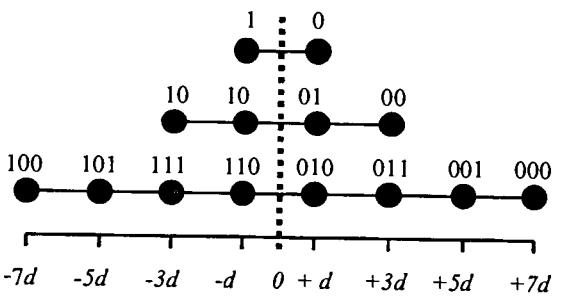

Figure 2.15 *M*-ASK Constellation for M=2, 4, 8

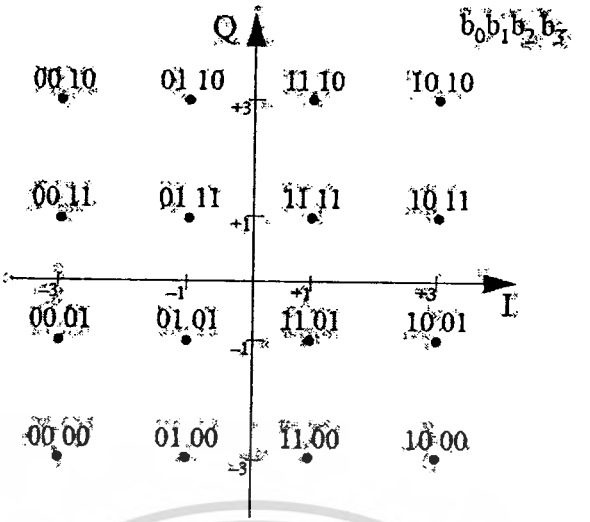

Figure 2.16 *IQ* plot of 16QAM modulation mapping scheme

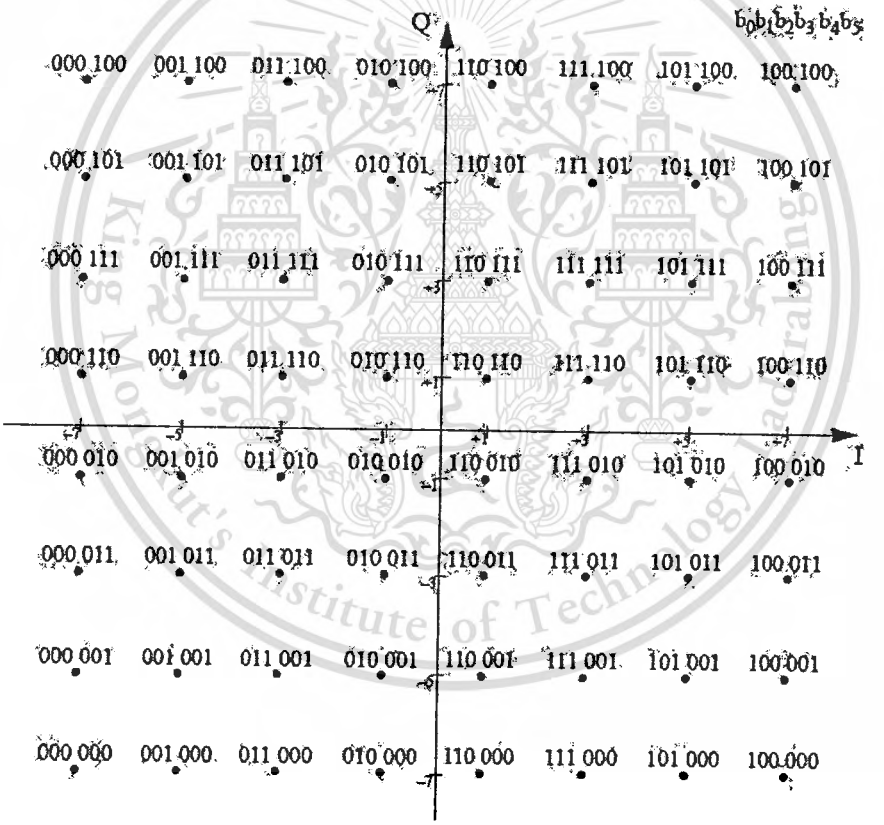

Figure 2.17 *IQ* plot of 64QAM modulation mapping scheme

2.3.4.4 64QAM

64QAM modulation mapping scheme technique is the same as 16QAM modulation mapping scheme except that it has higher level of constellations than 16QAM. In 64-state Quadrature Amplitude Modulation (64QAM), there are eight *I* values and eight *Q* values. This results in a total of 64 possible states for the signal. It can transition from any state to any other

state at every symbol time. Since $64 = 2^6$, six bits per symbol can be sent. This consists of three bits for I and three bits for Q. The symbol rate is one six of the bit rate. So this modulation format produces a more spectrally efficient transmission. It is more efficient than BPSK, QPSK, and 16QAM. The IQ diagram is shown in Figure 2.17.

2.3.5 Transformation for OFDM systems

Although multi-carrier modulation was invented in the 1950s, its requirement for separate modulators and demodulators on each sub-channel was too complex for most system implementations at the time. However, the development of simple and cheap implementations of the DFT and the IDFT twenty years later combined with the realization that multi-carrier modulation could be implemented with these algorithms [25].

The idea of using the DFT revived the OFDM employing time-limited orthogonal signals. Sampling $s(t)$ $(iT_s < t \le (i+1)T_s)$ with sampling rate of $t_{spl}(=T_s/N_{SC})$, the transmitted signal is written in a column vector form as [27]

$$\begin{aligned} S &= \left[s(iT_s + t_{spl}), \ldots, s(iT_s + qt_{spl}), \ldots, s(iT_s + N_{SC}t_{spl})\right]^T \\ &= W^{-1}(N_{NC})C_i, \end{aligned} \tag{2.41}$$

where $*^T$ denotes the transpose of $*$, and $W^{-1}(N_{SC})$ and C_i are the N_{SC} point IDFT matrix and the ith symbol (column) vector, respectively

$$W^{-1}(N_{SC}) = \{w_{qk}^{-1}\}$$

$$w_{qk}^{-1} = e^{j2\pi\frac{q(k-1)}{N_{SC}}}, \tag{2.42}$$

$$C_i = \left[c_{1i}, c_{2i}, \ldots, c_{N_{SC}i}\right]^T. \tag{2.43}$$

Equation 2.41 clearly shows that the transmitted symbol vector is recovered at the receiver by means of the DFT

$$C_i = W(N_{SC})S, \tag{2.44}$$

where $W(N_{SC})$ is the N_{SC}-point DFT matrix given by

$$W(N_{SC}) = \{w_{qk}\}$$

$$w_{qk} = e^{-j2\pi\frac{q(k-1)}{N_{SC}}}. \tag{2.45}$$

When employing rectangular DFT window at the receiver, inter-carrier interference can be perfectly eliminated.

The use of IDFT/DFT totally eliminates bank of sub-carrier oscillators at the transmitter/receiver, and furthermore, if selecting the number of sub-carriers as the power of two, we can replace the DFT by the FFT. The advantage of OFDM in mobile communications was first suggested in [27].

However, the detail of IDFT/DFT will be presented here. The representation of a signal in the form of a linear combination of complex sinusoids is called the Fourier series in honor of Jean Baptiste Joseph Fourier, a French mathematician of the late eighteenth and early nineteenth centuries [28].

In a Fourier series representation of a signal, the higher-frequency sine and cosine have frequencies that are integer multiples of the fundamental frequency. The multiple is called the *harmonic number* and will be designated by k. So, for example, the function $\cos(2\pi(kf_F)t)$ is *k*th-harmonic cosine, and its frequency is kf_F. If the signal to be represented is $x(t)$, then the amplitude of the *k*th-harmonic sine will be designated $X_s[k]$ and the amplitude of the *k*th-harmonic cosine will be designated $X_c[k]$. So the amplitudes of the sines and cosines are both functions of a discrete independent variable, not discrete time n, but rather discrete harmonic number k. The function $X_s[k]$ and $X_c[k]$, together with the constant term, will be called the harmonic function of the Fourier series of the original signal, in this case the trigonometric Fourier series [28].

Consider a finite duration discrete-time signal $x(n)$, $0 \le n \le N-1$. The *N*-point DFT of $x(n)$ is defined as

$$X(k) = \sum_{n=0}^{N-1} x(n) W_N^{nk}, \tag{2.46}$$

for $0 \le k \le N-1$, where $W_N = e^{-j2\pi/N}$. The original signal $x(n)$ can be exactly recovered from $X(k)$ by the inverse DFT (IDFT)

$$X(k) = \sum_{n=0}^{N-1} x(n) W_N^{nk}, \tag{2.47}$$

for $0 \le n \le N-1$.

Since the DFT and IDFT basically require the same type of computation, we will mainly focus on the fast algorithms for the computation of the DFT. The same algorithm can be easily applied to the computation of the IDFT. A direct computation of Eq.(2.46) requires N^2

complex multiplications and $N(N-1)$ complex additions [29]. When N is large, the computational complexity becomes prohibitive. The computational complexity can be significantly reduced if the symmetry property

$$W_N^{k+N/2} = -W_N^k, \tag{2.48}$$

and the periodicity property

$$W_N^{k+N} = W_N^k, \tag{2.49}$$

are utilized in the DFT computation. Numerous efficient algorithms based on these properties have been reported in the several papers and they are generally known as the fast Fourier transform (FFT) algorithms. In the rest of this subsection, we will give the example of the radix-2 algorithm by using of the symmetric and periodic properties in deriving fast algorithms.

Let us assume that the sequence length N is even. By using the relationship $W_N^2 = W_{N/2}$, the DFT in Eq.(2.46) can be expressed as

$$\begin{aligned} X(k) &= \sum_{n=0}^{N-1} x(n) W_N^{nk} \\ &= \sum_{n=0}^{N/2-1} x(2n) W_N^{2nk} + \sum_{n=0}^{N/2-1} x(2n+1) W_N^{(2n+1)nk} \\ &= \sum_{n=0}^{N/2-1} x(2n) W_{N/2}^{nk} + W_N^k \sum_{n=0}^{N/2-1} x(2n+1) W_{N/2}^{nk} \\ &= F(k) = W_N^k G(k), \end{aligned} \tag{2.50}$$

where

$$F(k) = \sum_{n=0}^{N/2-1} x(2n) W_{N/2}^{nk}, \; k = 0,1,\ldots,\frac{N}{2}-1, \tag{2.51}$$

$$G(k) = \sum_{n=0}^{N/2-1} x(2n+1) W_{N/2}^{nk}, \; n = 0,1,\ldots,\frac{N}{2}-1. \tag{2.52}$$

Both $F(k)$ and $G(k)$ are the length $N/2$ DFT of subsequences $x(2n)$ and $x(2n+1)$, respectively. When the periodicity property is applied, it can easily verify that $F(k+N/2) = F(k)$, $G(k+N/2) = G(k)$ and $W_N^{k+N/2} = -W_N^k$, which leads to

$$X\left(k+\frac{N}{2}\right) = F(k) - W_N^k G(k). \tag{2.53}$$

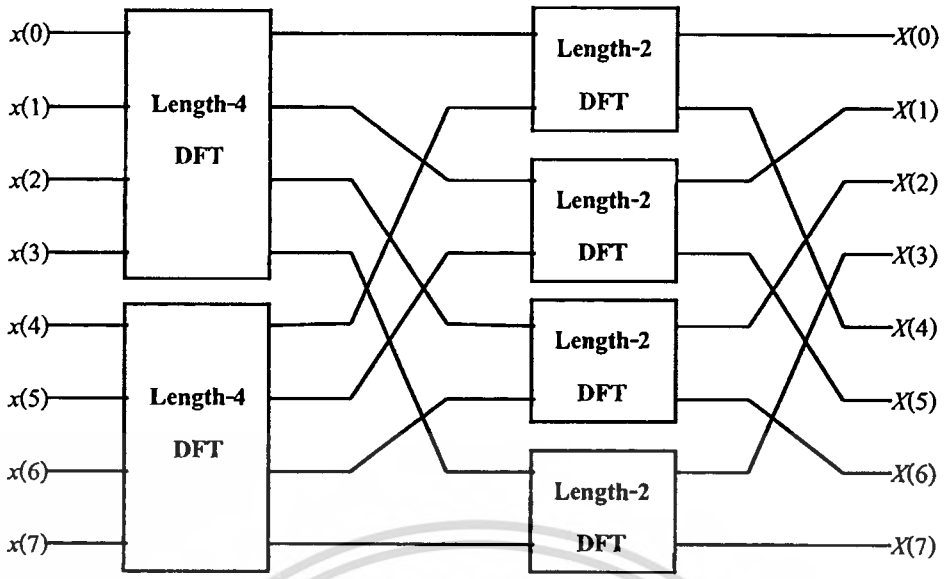

Figure 2.18 Signal flow graph of the decimation-in-time radix-2 algorithm for N=8

Therefore, the length N DFT can be computed by

$$X(k)=F(k)+W_N^k G(k),\ k=0,1,\ldots,\frac{N}{2}-1, \tag{2.54}$$

$$X\left(k+\frac{N}{2}\right)=F(k)-W_N^k G(k)\ ,\ k=0,1,\ldots,\frac{N}{2}-1. \tag{2.55}$$

Figure 2.18 shows the signal flow graph for a length 8 DFT. The length $N/2$ DFT given in Eq.(2.51) and Eq.(2.52) can be decomposed further in the same way as long as the length of subsequences is even.

2.3.6 Guard Interval

We will now describe the guard interval. The orthogonality of sub-carriers in OFDM can be maintained, and individual sub-carriers can be completely separated by using FFT circuit at the receiver when there are no ISI and ICI introduced by transmission channel distortion. In practice, however, these conditions cannot be obtained. Because the spectra of an OFDM signal are not strictly band-limited, the distortion, due to multi-path fading, causes each sub-carrier to spread the power into the adjacent channels [24].

One way to eliminate ISI is to create a cyclically extended guard interval, where each OFDM symbol is preceded by a periodic extension of the signal itself. The total symbol duration is $T_{total}=T_g+T_s$, where T_g is the guard interval. Figure 2.19 shows a typical guard

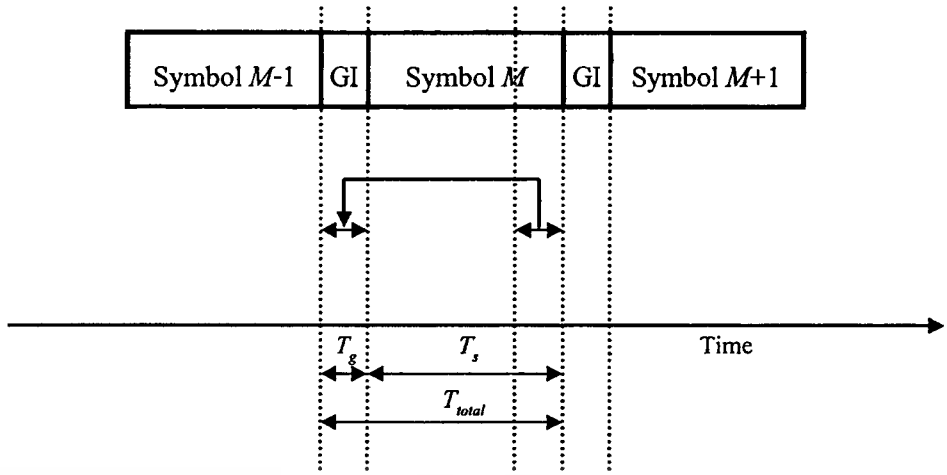

Figure 2.19 Guard interval insertion

interval. Each symbol is made of two parts. The whole signal is contained in the active symbol, the last past of which is also repeated at the start of the symbol and is called a guard interval. When the guard interval is longer than the channel impulse response, or the multi-path delay, the effect of ISI can be eliminated. However, the ICI still exists. The ratio of the guard interval to the useful symbol duration is application-dependent. Because the insertion of a guard interval will reduce the data throughput, T_g is usually smaller than $T_s/4$.

After the insertion of a guard interval, the OFDM signal is given by

$$s'(t) = \sum_{k=-\infty}^{\infty} \sum_{i=0}^{N-1} d_i(k) \exp(j2\pi f_i(t - kT_{total})) f'(t - kT_{total}) \tag{2.56}$$

where $f'(t)$ is the modified pulse waveform of each symbol defined as

$$f'(t) = \begin{cases} 1 & (-T_g \le t \le T_s) \\ 0 & (t < -T_g > T_s) \end{cases} \tag{2.57}$$

The OFDM signal is transmitted to the receiver. However, the transmitted data, $s'(t)$, is contaminated by multi-path fading and AWGN. At the receiver, the received signal is given by

$$r(t) = \int_0^{\infty} h(\tau, t) s(t - \tau) d\tau + n(t) \tag{2.58}$$

where $h(\tau, t)$ is the impulse response of the radio channel at time t, and $n(t)$ is the complex AWGN.

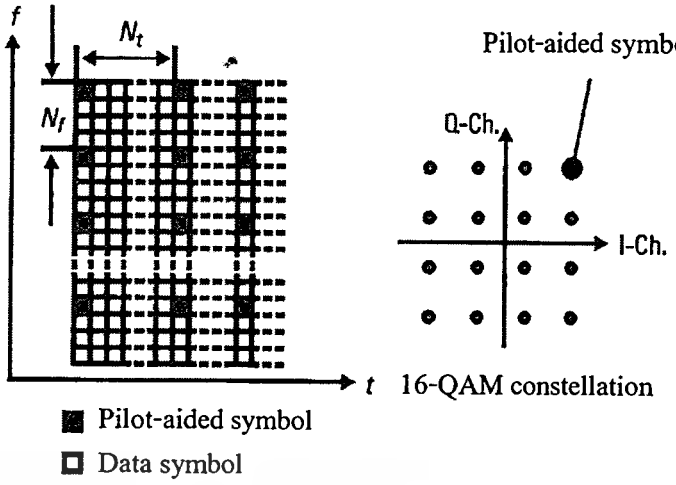

Figure 2.20 Frequency/time signal format

2.3.7 Channel Estimation

When applying receivers with coherent detection in fading channels, information about the channel state is required and has to be estimated by the receiver. The basic principle of pilot symbol aided channel estimation is to multiplex reference symbols, so-called pilot-aided symbols, into the data stream. The receiver estimates the channel state information based on the received, known pilot-aided symbols. The pilot-aided symbols can be scattered in time and/or frequency direction in OFDM frames as shown in Figure 2.20. Special cases are either pilot-aided tones which are sequences of pilot-aided symbols in time direction on certain sub-carriers, or OFDM reference symbols which are OFDM symbols consisting completely of pilot-aided symbols [26].

Figure 2.19 shows the frequency/time signal format. A pilot symbol is inserted in every N_f sub-carrier in the frequency-domain and in every N_t OFDM symbol in the time-domain. Figure 2.21 shows an interpolation method using pilot symbols to estimate frequency responses at data sub-carriers. In the time-domain, linear interpolation is also used to cope with time variation of channel [26].

In the case of time-varying channels the pilot-aided signal should be repeated frequently. The spacing between pilot-aided signals in time and frequency depends on coherence time and bandwidth of the channel. We can reduce the pilot-aided signal overhead by using a pilot-aided signal with a maximum distance of less than the time and coherence bandwidths. Then, by using time and frequency interpolation, the impulse response and frequency response of the channel can be calculated [30].

Channel estimation can be done in various ways. Training-based estimation techniques are common in most communication systems, where the sender emits some know signal, to achieve synchronization and channel estimation. For burst communication system, training symbols are used at the beginning of each burst. Since the burst is short, the channel is assumed static over a whole burst so that once the channel is estimated, and the inverse of the estimated channel response will be used to compensate the signal for the whole burst. Assuming the received signal after DFT is

$$R(k) = H(k)S(k) + N_0(k), \tag{2.59}$$

where k is sub-carrier index, H is the DFT of channel response, S is the pilot data, and N_0 is the noise. The simplest way to estimate the channel is then by

$$\tilde{H}(k) = \frac{R(k)}{S(k)}, \tag{2.60}$$

i.e. dividing the received signal by the known pilot-aided. Without noise, this gives the correct estimation. When noise is present, there could be error.

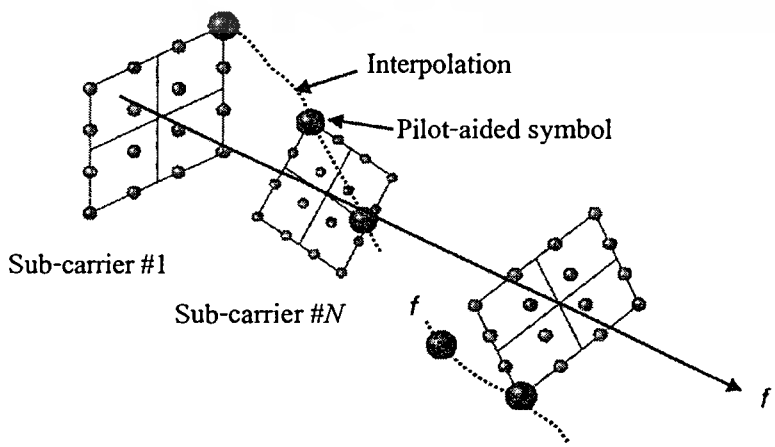

Figure 2.21 Interpolation in frequency-domain

2.4 Introduction to Harmonic Transform

Various transforms have been widely used in diverse applications of science, engineering and technology. New transforms are emerging to solve many problems, which may have left unsolved in the past, or newly created by modern science or technologies. Various methods have been continuously reported to improve the implementation of these transforms. Early developments of fast algorithms for discrete transforms have significantly stimulated the advance of digital signal processing technologies. In spite of the tremendous increase in the speed of computers or processors, that demands for higher processing throughout seemingly never ends [29].

Some discrete transforms are not suitable for signals that have time-varying frequency components. Although several approaches are available for such applications, various inherent problems still remain unsolved. Methods of time-frequency signal analysis have been actively researched for many years. The use of existing and new transforms has been studied and reported in the literature.

The other direction of development is to find new transforms that have some special capabilities to meet new requirements for current and future applications. The harmonic transform has been proposed in [13]. The harmonic transform is made to achieve improvements for harmonic signals (e.g., voice speech and music), which are composed of the fundamental and harmonics. We know that the Fourier transform decomposes the signals into the sum of a number of sinusoidal components and can be loosely interpreted as the integral of the signal in the time-frequency domain along the time axis. The difference between the harmonic transform and Fourier transform is the harmonic kernel $e^{j\omega\phi_u(t)}$, which can be loosely interpreted as the integration of the signal along the curves $\omega\phi_u'(t)$, where $\phi_u'(t)$ is the derivative of $\phi_u(t)$. When $\phi_u(t) = t$, the harmonic transform becomes the Fourier transform.

The Fourier transform, a pervasive and versatile method, is used in many fields of science to map a problem into the frequency-domain in which it can be more easily solved. The Fourier transform is effective for signals consisting of elements with fixed frequencies. The resultant representation in the frequency-domain exhibits a number of sharp peaks that succinctly describe the intensities and the associated phases in terms of frequencies. The original signal can be reconstructed from these peaks. These characteristics show that the Fourier transform effectively captures the essence of this class of signals. The analytical power of the Fourier transform, however, drops quickly when the frequencies of signal components

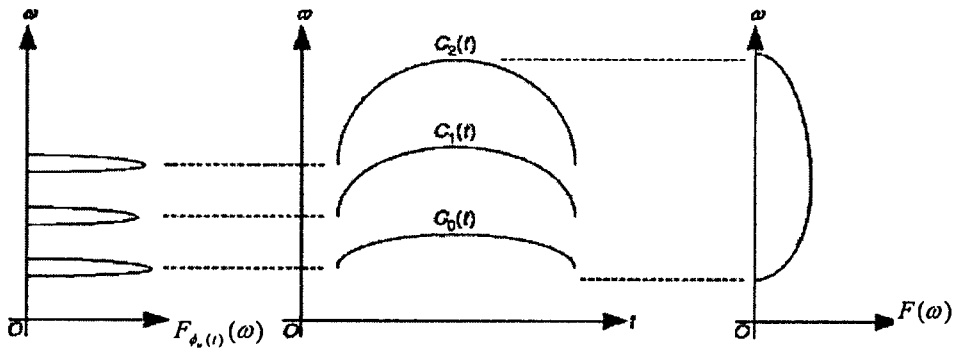

(a) Harmonic transform (b) Time-frequency representation (c) Fourier transform

Figure 2.22 The concept of the Harmonic transform

become time variant. The resultant Fourier spectrum will contain overlapping lumps that reveal little useful information about the signals.

The harmonic transform can make substantial improvements on the performance of the Fourier transform for signals containing variable frequencies, such as voiced speech and music. In the time-frequency plane, the harmonic transform is interpreted as the integrals of the signal along the nominal frequencies of the fundamental and harmonics. This interpretation is illustrated in Figure 2.22. The harmonic transform is also equivalent to transforming the fundamental and harmonics to constant frequency components and then calculating the Fourier transform of the processed signal. The most concise way to describe the spectrum of the signal is to follow its pattern, calculating the sum of the fundamental and its harmonic separately.

The time-varying harmonic signal generally contains harmonics whose nominal instantaneous frequencies are expressed by [13]

$$c_k(t) = (k+1)c_0(t), \quad k = 1,2,3,\ldots \tag{2.61}$$

where $c_0(t)$ is the frequency of the fundamental and $c_k(t)$ is the frequency of the kth harmonic component. The nominal instantaneous frequency of the fundamental, defined as the instantaneous frequency of the pulse sequence, varies in time.

Now let us consider a time-varying harmonic signal in the time–frequency plane. For simplicity, only the nominal instantaneous frequency of the fundamental and the first two harmonics are given in Figure 2.22(b). The Fourier transform of the signal, as illustrated in Figure 2.22(c), can be treated as the linear integration of the signal along the time axis in the time–frequency plane, which fails to distinguish the harmonic components. A better solution is

to integrate the signal along the nominal instantaneous frequency of every component, rather than along the time axis, to obtain an impulse-train spectrum, as shown in Figure 2.22(a). This is the basic concept of the harmonic transform (HT).

The harmonic transform of a signal $f(t)$ is defined as

$$F_{\phi_u(t)}(\omega) = \int_{-\infty}^{+\infty} f(t)\phi_u'(t)e^{-j\omega\phi_u(t)}dt, \tag{2.62}$$

where $\phi_u(t)$ is known as the unit phase function and $\phi_u'(t)$ is the derivative of $\phi_u(t)$. The unit phase function is the phase function of the fundamental at time $t = 0$. The constant can be other values, for it only scales the harmonic transform and has no impact on its concentration. Note that the harmonic transform becomes the Fourier transform when $\phi_u(t) = t$. The inverse harmonic transform is

$$f(t) = \frac{1}{2\pi}\int_{-\infty}^{+\infty} F_{\phi_u(t)}(\omega)e^{j\omega\phi_u(t)}d\omega. \tag{2.63}$$

Now let we show the examples of using the Harmonic transform. Since speech is one of most popular time-varying harmonic signals, a short sentence of a male voice, 'Mailman, your mail', is used to show the merits of the harmonic transform [13]. The HT can be used for coding, enhancement and re-synthesis of voiced speech or other time-varying harmonic signals in which spectrum and time–frequency distribution are very important information. A more concentrated spectrum or time–frequency distribution always leads to a smaller bit rate on coding, higher signal/noise ratio on enhancement, and smaller distortion on re-synthesis. Compared with the Fourier transform, all simulation results provided to show the significant improvement obtained by HT and its application to time–frequency transformation.

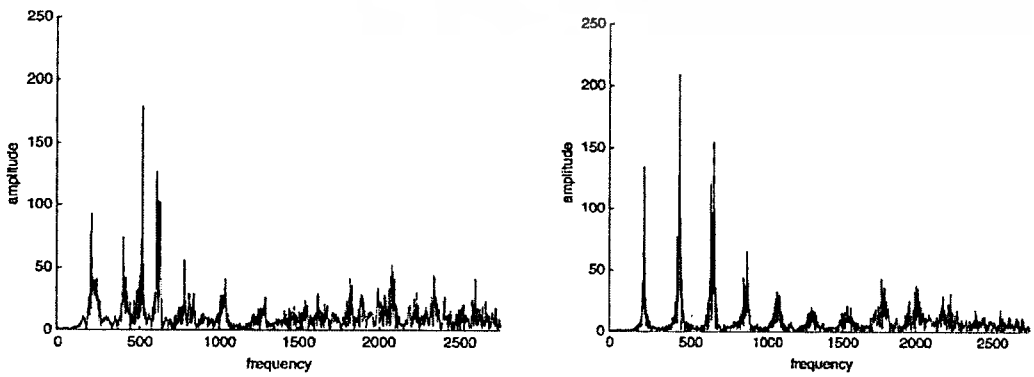

(a) The FT (b) The HT

Figure 2.23 The FT and HT of speech signal

The HT and FT of the speech sentence are compared to demonstrate the strength of the HT. The duration is about one second. The corresponding unit phase function $\phi_u(t)$ is proportional to the integral of the nominal instantaneous frequency of the fundamental, which can be extracted from the result of the harmonic transform. Figure 2.23 shows, respectively, the FT and HT of speech signals. Clear peaks representing the fundamental and harmonics are seen in the HT, while the same observation cannot be made from the FT.

Chapter 3

Adaptive Cyclic Prefix for OFDM Signal Transmission under Multi-path Fading Environments

In the Orthogonal Frequency Division Multiplexing (OFDM) system, the guard interval, i.e., Cyclic Prefix (CP) is added to the header of transmitted signal in order to avoid the interference between two adjacent signals. Under the multi-path fading environments, the fading of one signal will cause the interference to the next transmitted signal at the receiver. But, this interference can be avoided by adding the CP of the size equal to the maximum of Arrival Time Difference between a signal and its last arrival fading (ATD). However, the conventional OFDM of the standard IEEE 802.11a has fixed the value of CP as 0.8 μs, so that the channel utilization or throughput will be limited. In order to increase the throughput, therefore, the adaptation of CP in according to the transmission or multi-path fading environments is proposed in this chapter.

3.1 Introduction to Adaptive Cyclic Prefix Concept

In OFDM, the broadband signals are transmits by dividing into a large number of narrowband channels in order to achieve resistance to such a long delay spread. In addition, a guard interval that is equal or longer than the maximum of *Arrival Time Difference between a signal and its last arrival fading* (ATD) is added to the header of each signal, i.e., inserted between adjacent OFDM symbols (or signals). This guard interval is called *cyclic prefix* (CP). By using CP as the gap between any two adjacent symbols, the inter-symbol and inter-carrier interferences (ISI and ICI) are completely eliminated. By adding CP ($\geq$ATD) as a guard interval, the ISI of their data portion is avoided. In this situation, the orthogonality between sub-carriers will be maintained. If the CP is less than current ATD, the ISI between data portion of adjacent symbols will occur and orthogonality between sub-carriers is lost. Moreover, since the size of OFDM symbols is fixed, then as bigger as CP is assigned, the data portion will become smaller. Therefore, to assign the appropriate CP that closely equal to the current ATD is preferable. This will not only avoid ISI of data portion but also keep the data portion as large as possible. This is the main objective of our proposed idea which is shown in Figure 3.1.

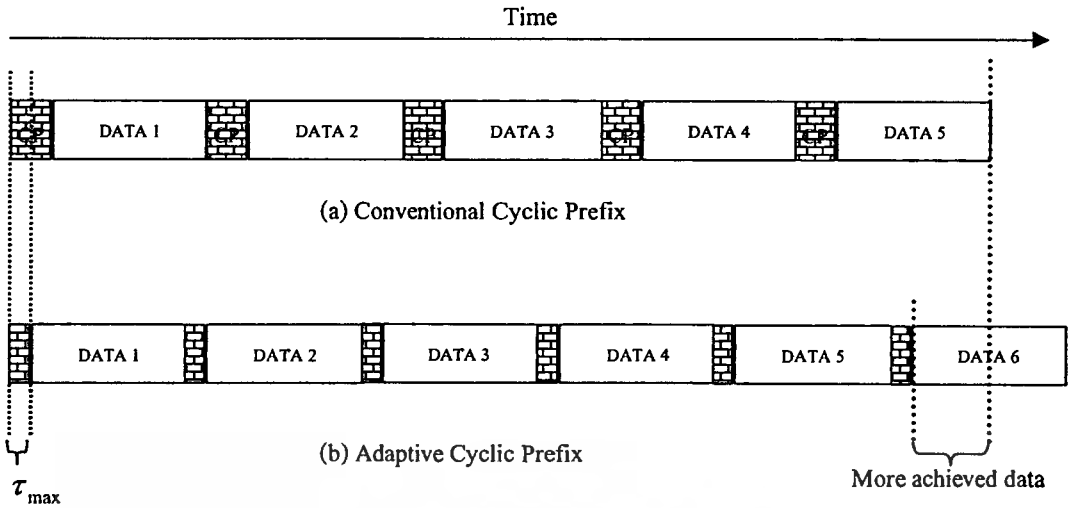

Figure 3.1 The concept idea of adaptive cyclic prefix

In this chapter, the adaptive cyclic prefix is proposed for OFDM transmission under multipath environment. Based on standard 802.11a, the cyclic prefix of the OFDM symbol is fixed. However, in mobile communications, the mobile unit is un-stationary, it move to the different environments. Therefore, the effect of multi-path is also difference. In order to achieve a better throughput, the cyclic prefix length should be adapted to the suitable values for each multi-path fading environment. Moreover, the adapted values should have long enough to avoid the ISI.

In order to support our concept idea, we would like show the character of the multi-path fading environments. In mobile radio communications, the RF signal from the transmitter may be reflected of objects such as hills, buildings, vehicles, walls, etc. Some of these reflections will arrive at the receiver, effectively creating multiple transmission paths, commonly referred to as a multi-path environment. The radio signal travels over a different distance for each of these paths, and thus takes a different amount of propagation time. If we were to transmit an RF pulse in a multi-path environment, we would receive a signal like the one shown in Figure 3.2(a). Each impulse corresponds to one path, with the strength of each impulse dependent on the path loss for that path. For a fixed frequency signal, (i.e. a sine wave) the propagation delay results in a phase rotation of the signal. The amount of phase rotation corresponds to 360° for each wavelength of path length travelled. Each of the multi-path signals will have a different propagation distance and thus a different phase rotation. These signals add at the receiver, resulting in constructive or destructive interference. Each of the multi-path signals can be represented as a phasor, which has vector length corresponding to signal power and the angle

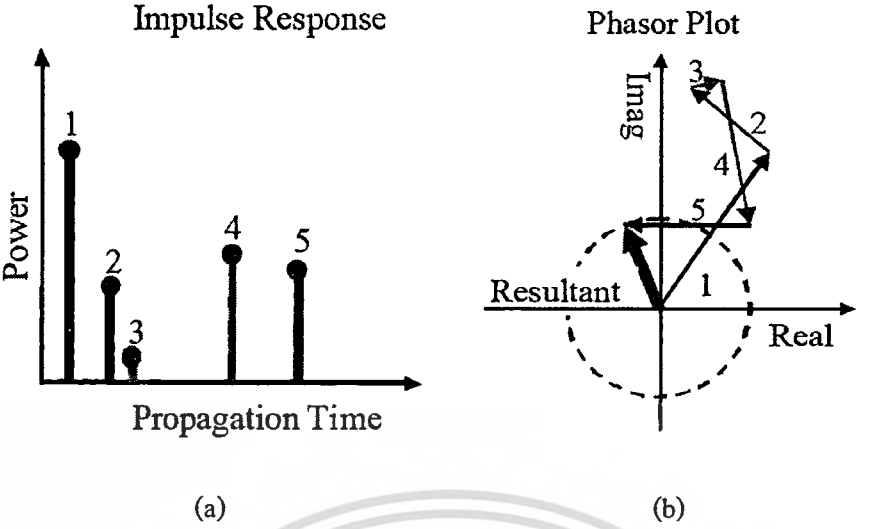

Figure 3.2 Impulse response and phasor plot for multi-path channel

corresponding to the phase. The received signal corresponds to the vector sum of the multi-path phasors as shown in Figure 3.2(b). Destructive interference occurs when the vector sum adds to zero. This is also referred to as a 'null'. Constructive interference occurs when all the signals have a similar phase, reinforcing each other.

The effect of multi-path propagation on a radio channel impulse response depends on the path-length difference(s) relatively to the wavelength. Consider the exemplary case study of 2 paths, each with their own delay, attenuation, and phase shift. In case the path length difference is an entire multiple of the wavelength, the paths add constructively.

Delay spread is a measure of the spread in the time over which the multi-path signals arrive. It is a measure of the time dispersion of a channel, and is very important in determining how fast the symbol rate can be in digital communications. A symbol is a period over which one or more groups of bits of information are sent. For a single carrier transmission, using Binary Phase Shift Keying (BPSK) as the modulation scheme, each symbol carries one bit of information. The symbol corresponds to the period required to send the phase information as 0° or 180°, which corresponds to the digital information of zero or one respectively. The faster the phase is varied the faster the symbol rate and the higher the data rate and bandwidth. For OFDM transmission, each symbol corresponds to a parallel transmission of many low bandwidth carriers. The symbol time in this case corresponds to the period over which the amplitude and phase of the data carriers is remained fixed corresponding to one data vector.

The impulse response of a multipath channel can be modeled by

$$H(t) = \sum_{p=1}^{P} A_p \cdot \delta(t - \tau_p), \tag{3.1}$$

where A_p is the complex amplitude and τ_p is the time delay of each impulse; P is the number of received multipath components, and δ is the dirac delta function. The RMS delay spread is one of the most widely used measurements for characterizing the delay spread of a multipath channel and was originally used by

$$T_{rms} = \sqrt{\frac{\sum_{p=1}^{P} (\tau_p - D)^2 \cdot Po_p}{\sum_{p=1}^{P} Po_p}}, \tag{3.2}$$

where T_{rms} is the RMS delay spread, and D is the average excess time delay, which is equivalent to the centre of energy for the impulse response.

$$D = \frac{\sum_{p=1}^{P} T_p \cdot Po_p}{\sum_{p=1}^{P} Po_p}, \tag{3.3}$$

where Po is the power of each impulse and is the magnitude of the complex impulse squared:

$$Po_p = |A|^2. \tag{3.4}$$

Delay spread results in time blurring, where energy from previous data symbols becomes mixed in with current symbols. This causes interference, known as ISI, because previous symbols are uncorrelated, effectively adding noise to the signal. Single carrier transmissions are particularly prone to problems caused by delay spread as it normally sets the upper limit on symbol rate. This is because the bit error rate (BER) increases as the delay spread time becomes a significant fraction of the symbol time.

Therefore, we have considered the situation of the transceiver as follows. First, the location detections are not included in the transmitter and receiver. Second, the transmitter and receiver cooperate with location detection.

Firstly, in the case of without location detection, the transmitter sends the echo test signal (ETS) to the receiver in order to estimate τ_{max} value or ATD. Then, the receiver will send ATD value to the transmitter in order to adapt the new CP value. The conditions of this situation are considered as follows.

- The ISI is detected by the system.
- If the system detects the ISI, the system requests to adjust the timeout for the next adjusting: *TNA* for $t_{TNA} = 0$ to T_{TNA}. The T_{TNA} is the timeout value which depends on the multi-path fading environments.

However, the T_{TNA} value relate to the multi-path fading environments. In the case of the good environment, the OFDM signals are not much affected by the multi-path fading, the T_{TNA} value may contain the large value. In contrast, in bad environment, the T_{TNA} value may contain small value in order to frequently update the parameters. Thus, the T_{TNA} value is varied depending on the conditions of the multi-path fading environments to be the suited T_{TNA} value for each environment. Moreover, if the system safely transmits the OFDM signals without any ISI occurrence, then the suited CP value will be considered. The system will calculate the ATD and then, the new CP is applied.

Secondly, we assume that the system can detect the location of the transmitter or the receiver. If the location is detected by transmitter or receiver, it means that the ISI may occur. Therefore, the transmitter will be stopped the transmitted OFDM signal, ETS will be applied to calculate the new parameters to be adjusted in the next transmission.

The next section, the suitable CP is explained which include the system that performs cooperative with the location detector and without location detector.

3.2 Appropriate Cyclic Prefix

In this section, we present the methodology for selecting the appropriate cyclic prefix under multi-path fading environment. The appropriate CP length is selected by considering the maximum delay $\tau_{\max}$ which is estimated by the channel estimation. We also model the maximum delay as the arrival time difference.

According to the IEEE 802.11a standard, the CP length is fixed as 16 points (800 ns). Therefore, the appropriate CP can be divided as 16 parts. Therefore, each point of appropriate CP is 50 ns. Thus, the appropriate CP is selected by cooperating with the $\tau_{\max}$ value as shown in Figure 3.3.

Channel Estimation (estimated τ_{max})

If $0 \leq \tau_{max} < 50$	Then CP = 1 Point
Else if $50 \leq \tau_{max} < 100$	Then CP = 2 Point
Else if $100 \leq \tau_{max} < 150$	Then CP = 3 Point
Else if $150 \leq \tau_{max} < 200$	Then CP = 4 Point
Else if $200 \leq \tau_{max} < 250$	Then CP = 5 Point
Else if $250 \leq \tau_{max} < 300$	Then CP = 6 Point
Else if $300 \leq \tau_{max} < 350$	Then CP = 7 Point
Else if $350 \leq \tau_{max} < 400$	Then CP = 8 Point
Else if $400 \leq \tau_{max} < 450$	Then CP = 9 Point
Else if $450 \leq \tau_{max} < 500$	Then CP = 10 Point
Else if $500 \leq \tau_{max} < 550$	Then CP = 11 Point
Else if $550 \leq \tau_{max} < 600$	Then CP = 12 Point
Else if $600 \leq \tau_{max} < 650$	Then CP = 13 Point
Else if $650 \leq \tau_{max} < 700$	Then CP = 14 Point
Else if $700 \leq \tau_{max} < 750$	Then CP = 15 Point
Else CP = 16 Point	

Figure 3.3 The selected CP point for appropriate CP for each range of the delay time

The estimated τ_{max} is estimated by the channel estimation which considers the maximum delay time. Any channel estimation technique that can estimate the delay time, it also can be applied in our proposed scheme. The appropriate CP is an integer in order to compatible with OFDM systems and convenient remove at the receiver. Moreover, the same appropriate CP will be inserted in the OFDM frame as shown in Figure 3.4. We can say that point number of CP is CP length. The appropriate CP length must be sent from transmitter to receiver as the information for operation. It will be stored in the head of the frame which is called "preamble". The appropriate CP length requests 4 bit data for storied information which covers 16 condition of the appropriate CP length.

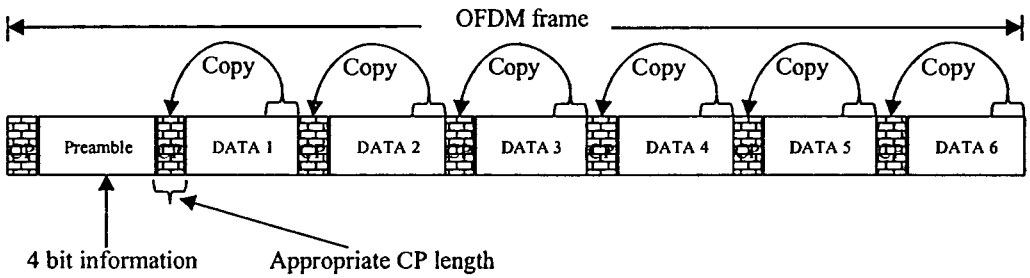

Figure 3.4 The structure of the appropriate CP in an OFDM frame

3.3 Adaptive Cyclic Prefix Methodology

The adaptive cyclic prefix is proposed method that the OFDM guard interval can be varied. This method is presented for improving the system data throughput by choosing the appropriate cyclic prefix. Therefore, the transmitter and receiver should exchange the information to the both of them. The next subsection, the system model and the cooperation of the transmitter and the receiver will be presented.

3.3.1 System Model and Channel Estimation

In order to support our proposed algorithm, we have modified the conventional OFDM system as shown in Figure 3.5 by adding the process of *ACP Information* in the transmitter and *Channel Estimator* in the receiver. The transmitter and receiver must exchange the information data in order to synchronize the cyclic prefix value of the both side. In order to measure the multi-path character, the channel estimation is applied that is performed at the receiver.

In the transmitter, the input data is formatted into the bit block size required for the modulation mapping and shifted in to a parallel format. The data on each symbol is then mapped to a complex symbol based on the modulation mapping scheme. After the required spectrum is worked out, an inverse fast Fourier transform (IFFT) is used to find the corresponding time waveform. The CP is then added to the start of each symbol by cooperating with ACP information. Its length is an appropriate CP which is selected the suitable value at the receiver, and is sent to store at the transmitter. After the guard has been added, the symbols are then converted back to a serial time wave form. This is then the baseband signal for the wireless OFDM transmission.

In the receiver, it basically does the reverse operation to the transmitter. The received signals are estimated by the channel estimation to find out the maximum delay in order to tell the information to the transmitter. The CP is then removed corresponding with the ACP information which is inserted in the received preamble. After that, the FFT of each symbol is then taken to find the original transmitted spectrum. The complex symbol of each transmission carrier is then evaluated and converted back to the data by demodulating the received symbol. The parallel data are then combined back to the same data size as the input data.

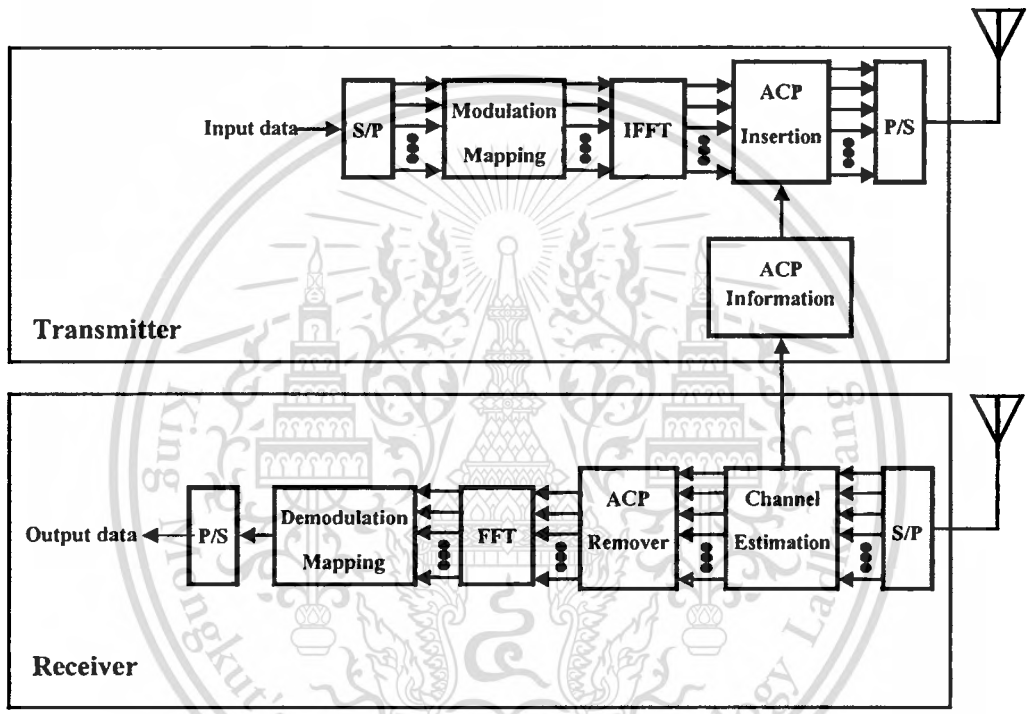

Figure 3.5 Modified OFDM transceiver for adaptive cyclic prefix

The channel estimation is based on autocorrelation function. It will estimate the maximum delay spread by considering the impulse response of the received signals that its value more than the thresholds value. The estimated maximum delay spread will be sent to the ACP information at the transmitter in order to adjust the new CP length that suitable for the currently multi-path fading environments. The new CP length will be added in the preamble of an OFDM frame, it requires 4 bit for cover the appropriate CP length information. At receiver, the ACP remover will remove the CP length according to the CP length value of this frame. Therefore, there are two cooperative units which are ACP information and channel estimator. They are performed in order to determine whenever the new CP should be applied. The *ACP Information* unit will take the duty of;

(a) Setting the new ACP whenever it receives the current ATD information from receiver. The new ACP will be sent to the transmitter when the ACP should be changed which is considered by the receiver.

(b) Stopping the transmission and send ETS to receiver whenever it receives the NAK signal from receiver or it changes location.

At receiver, the *Channel Estimator* unit will take the duty of;

(a) Computing the current ATD whenever it received the ETS from transmitter. The channel estimator will estimate the received ETS in order to measure the multi-path fading and, calculate the current ATD.

(b) Sending NAK to transmitter whenever it detects ISI or *timeout for the next adjusting* (TNA) is expired or it changes location. When the movement is detected, the transmitter should be stopped to transmit the signal for avoiding signal error. The new ACP should be applied. Therefore, the ETS is sent from transmitter to estimate the new ACP. In contrast, whenever the multi-path fading affects not much to the OFDM signal. Therefore, the decreasing ACP length should be applied, the timeout for the next adjusting is considered to determine the time interval to estimate the multi-path fading environment in order to apply the appropriate CP length.

Thus, in our proposed algorithm, the ACP for OFDM symbols will be readjusted under the following 3 conditions. First, when the ISI is detected at receiver. Second, whenever the transmitter or the receiver has changed its location. Third, when the *TNA* is expired. Initially, at the starting of operation, transmitter will send the first *echo test signal* (ETS: request for the information of current ATD) to receiver. Whenever receiver received ETS, receiver will detect and compute the ATD between ETS and its fading, and send this current ATD back to transmitter for setting new ACP, and TNA is reset. After all, the procedure for adjusting the new ACP is as follow. Again, here ATD is Arrival Time Difference between a signal and its last arrival fading that is the maximum value of all its time difference.

We have explained the overall system of the adaptive cyclic prefix that how and when it should be performed. Next, the details of the proposed algorithms will be presented. We derive our method as two parts as following section.

3.3.2 Adaptive Cyclic Prefix without Location Detection

In this subsection, the adaptive cyclic prefix without location detection is considered. In this case, the adaptive cyclic prefix can be applied in the wireless OFDM systems which do not

include the global positioning system (GPS). The system will use the received signals (ETS) which are transmitted from the transmitter, to estimate the multi-path fading characters. The receiver, then send the appropriate cyclic prefix information to the transmitter for adjusting the new CP in the next transmission. The proposed algorithms are shown as 2 parts which are at transmitter and receiver.

At transmitter, the ETS need to be sent to the receiver in order to estimate the multi-path fading characteristics. Then, it will look for two signals which are NAK and ATD. Otherwise, the conventional process is normally performed. The adaptive cyclic prefix process without the location detector of the transmitter is shown as the Fig.3.6, its algorithms are shown as follows.

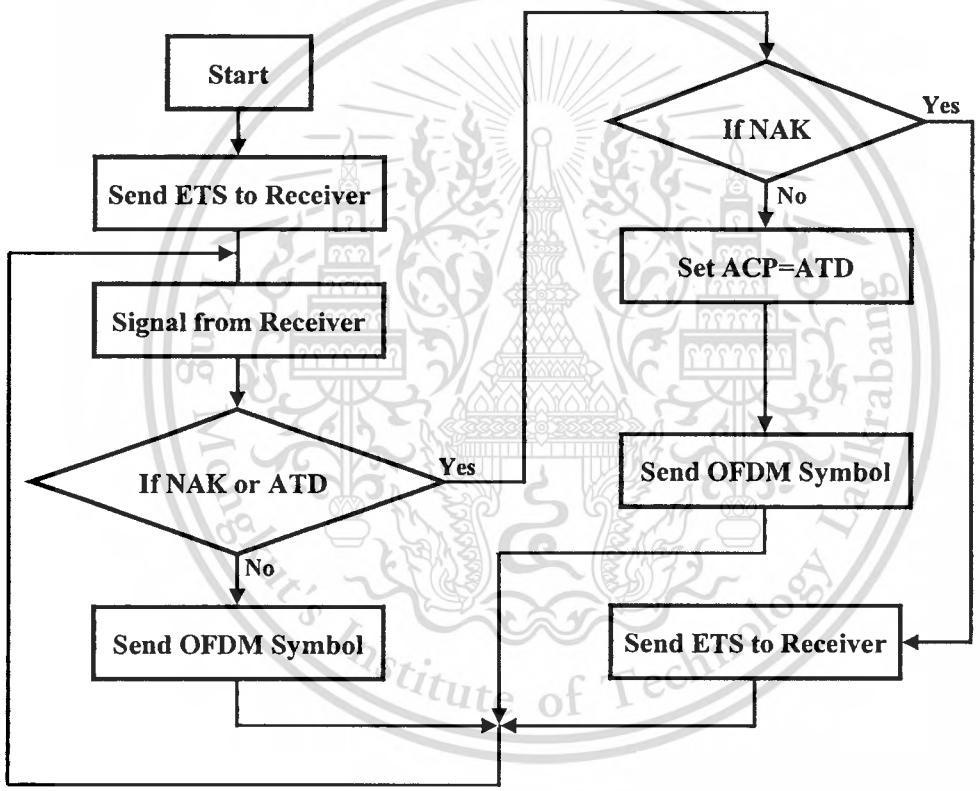

Figure 3.6 Adaptive cyclic prefix algorithm at the transmitter without location detector

Algorithm: Operation at Transmitter

1: Initially, send ETS to receiver and wait for current ATD.

2: If received current ATD, then adjust new ACP = current ATD to OFDM symbol for transmission.

3: Whenever received NAK (*Not-acknowledgement*) signal from receiver, stop the transmission and send ETS to receiver, then back to step 2.

4: If transmitter changes location, stop the transmission and send ETS to receiver, then back to step 2.

At the receiver, it will look for the received ETS. Whenever the ETS has been received, it means that the multi-path fading characteristics should be estimated. The channel estimation will estimate the ATD value in which will be sent as information to the transmitter. However, the channel estimation should be performed according to the multi-path fading environments. So that the timeout for next adjusting period is applied, it is the T_{TNA}. The counter time will increase in every transmission loop to store at the t_{TNA} variable. If the counter time t_{TNA} reaches the timeout for next adjusting period T_{TNA}, the receiver will send NAK to transmitter in order to require the ETS. While the counter time does not reach the T_{TNA} value yet, the ISI detector will be also performed. If the ISI is detected, the receiver will send NAK to transmitter in order to require the ETS as well. The adaptive cyclic prefix process without the location detector of the receiver is shown as the Fig.3.7, its algorithms are shown as follows.

Algorithm: Operation at Receiver

1: When receive ETS, detect and compute the current ATD between ETS and its fading, and send this current ATD back to transmitter, and reset t_{TNA} (i.e., $t_{TNA} = 0$, upper bound is T_{TNA})

2: If ISI is detected, send NAK back to transmitter, and wait for ETS, then back to step 1.

3: If $t_{TNA} = T_{TNA}$, send NAK back to transmitter, and wait for ETS, then back to step 1.

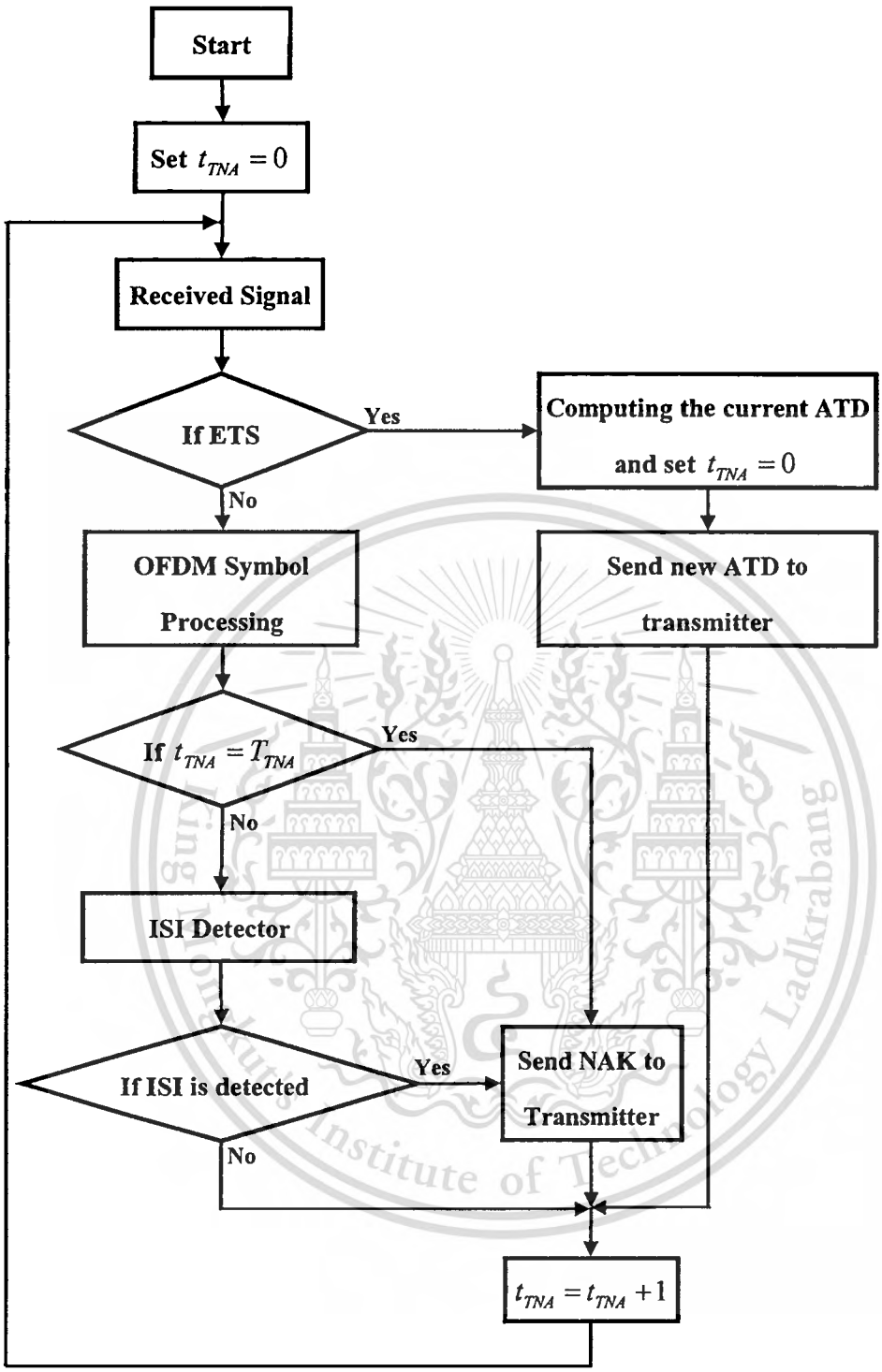

Figure 3.7 Adaptive cyclic prefix algorithm at the receiver without location detector

3.3.3 Adaptive Cyclic Prefix with Location Detection

In this subsection, the adaptive cyclic prefix with location detection is considered. The location detector is applied in order to avoid the ISI occurrence due to mobile movement. This system may apply the GPS for detecting the movement due to changed location. If changed location, it means the multi-path fading environment will be changed; therefore, the ISI may

occurs. Thus, in order to avoid the bit error due to occurrence of ISI cause of mobile movement, the location detection will be applied as a location detector. Whenever the transceiver moves, the system will use the received signals (ETS) which are transmitted from the transmitter, to estimate the multi-path fading characteristics. The receiver, then send the ACP information to the transmitter for adjusting the new CP in the next transmission. The proposed algorithms are shown as 2 parts which are at the transmitter and the receiver.

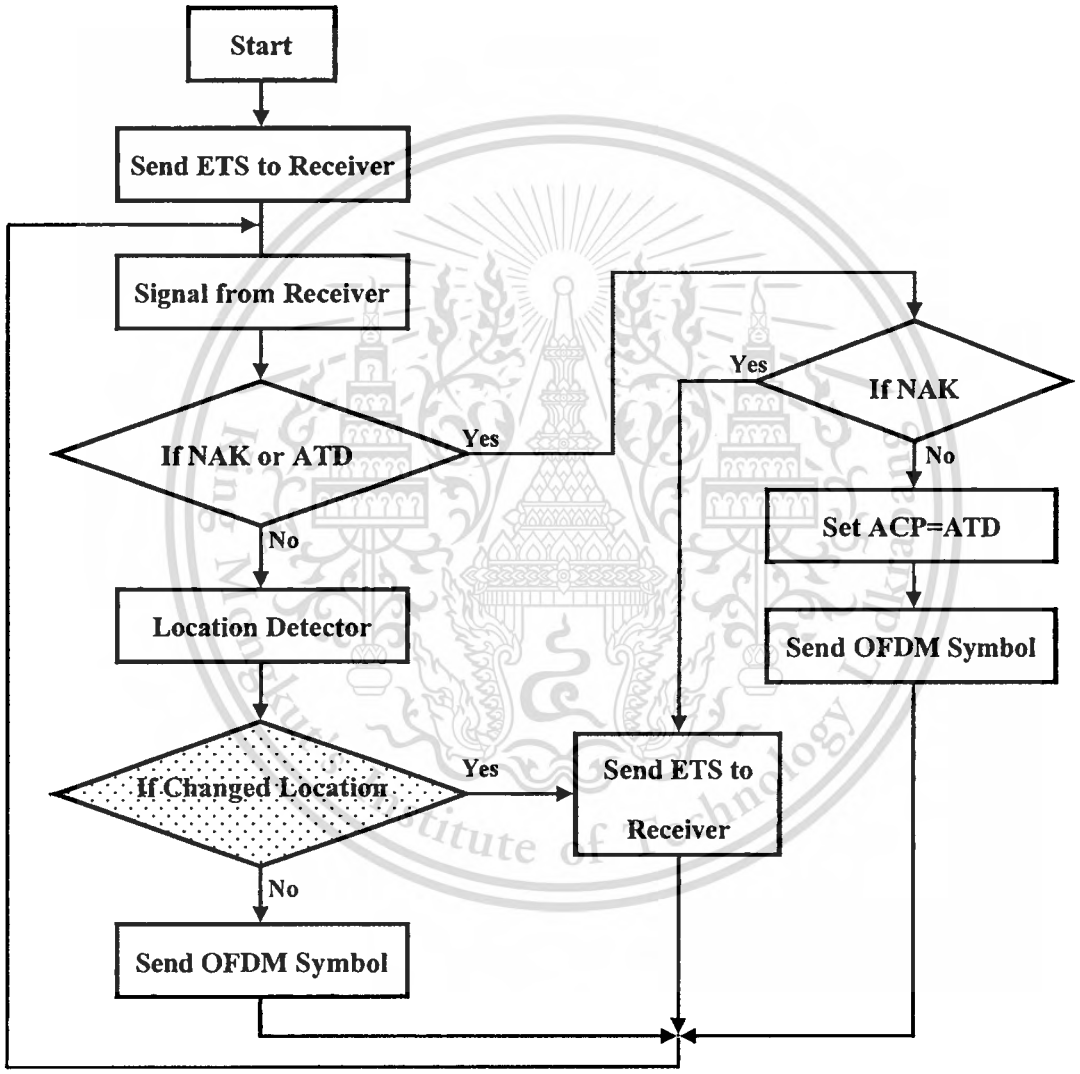

Figure 3.8 Adaptive cyclic prefix algorithm at the transmitter with location detector

At transmitter, the ETS need to be sent to the receiver in order to estimate the multi-path fading characteristics. Then, it will look for two signals which are NAK and ATD in order to listen the signals which are used to determine when the new CP should be set or when it should send the echo test signal (ETS) to the receiver. Otherwise, the location detector is performed. If the transmitter moves to another location, the transmitter will send the ETS to the

receiver for requiring new CP. Continuously, if the processes do not fall in any condition that mention above, the conventional process is normally performed. The adaptive cyclic prefix process cooperative with the location detector of the transmitter is shown as the Fig.3.8, its algorithms are shown as follows.

Algorithm: Operation at Transmitter

1: Initially, send ETS to receiver and wait for current ATD.

2: If received current ATD, then adjust new ACP = current ATD to OFDM symbol for transmission.

3: Whenever received NAK (*Not-acknowledgement*) signal from receiver, stop the transmission and send ETS to receiver, then back to step 2.

4: If transmitter changes location, stop the transmission and send ETS to receiver, then back to step 2.

5: Else if the signals do not fall in any condition, the normally OFDM processes will be performed.

However, the receiver will look for the received ETS. Whenever the ETS has been received, it means that the multi-path fading characteristics should be estimated. The channel estimation will estimate the ATD value which will be sent as the information to the transmitter. However, the channel estimation should be performed according to the multi-path fading environments. So that the T_{TNA} is applied. The counter time is increased in every transmission loop, and store to t_{TNA} . If the counter time t_{TNA} reaches to T_{TNA}, the receiver will send NAK to transmitter in order to require the ETS. While the counter time does not reach the T_{TNA} value yet, then the ISI detector is also performed. If the ISI is detected, the receiver will send NAK to the transmitter in order to require the ETS as well. However, else if the ISI is not detected, the location detector will be performed. If the movement is detected, the receiver will send NAK to the transmitter for requiring the ETS to estimate new cyclic prefix. The adaptive cyclic prefix process cooperative with the location of the receiver is shown as the Figure 3.9, its algorithms are shown as follows.

Algorithm: Operation at Receiver

1: When receive ETS, detect and compute the current ATD between ETS and its fading, and send this current ATD back to transmitter, and reset t_{TNA} (i.e., $t_{TNA} = 0$, upper bound is T_{TNA})

2: If ISI is detected, send NAK to transmitter, and wait for ETS, then back to step 1.

3: If $t_{TNA} = T_{TNA}$, send NAK back to transmitter, and wait for ETS, then back to step 1.

4: If receiver changes location, send NAK back to transmitter, then back to step 1.

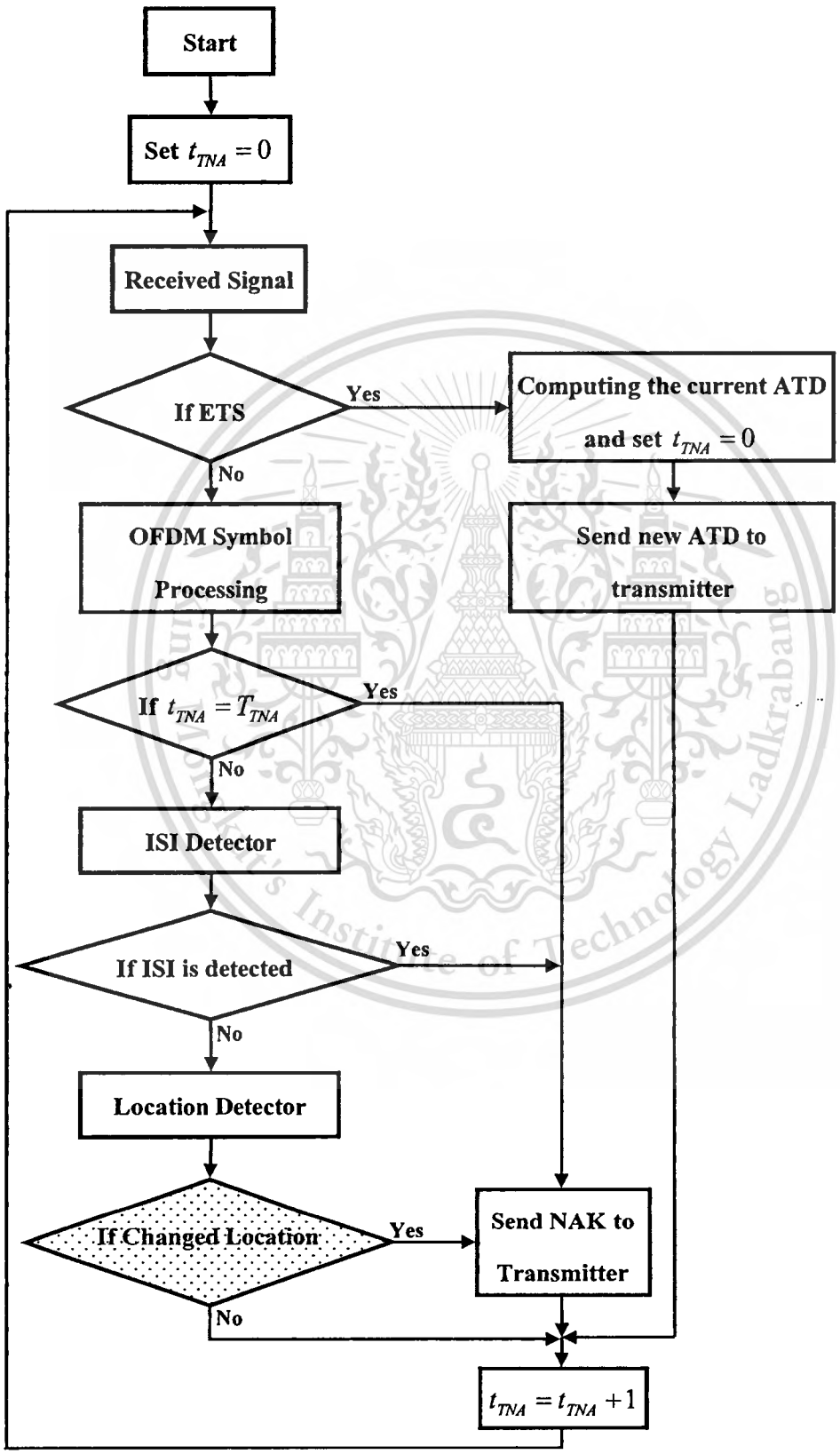

Figure 3.9 Adaptive cyclic prefix algorithm at the receiver with location detector

3.4 Numerical Analysis

Here, we will discuss the methodology for throughput calculation. Let X (bits) and Y (bits) be the length of OFDM symbol and its CP portion respectively as shown in Figure 3.10. The normalized throughput can be considered in term of channel utilization. As the assumption of fixed size for all OFDM symbols, the normalized throughput in term of bits (ρ) can be formulated as shown in Eq.(3.5).

$$\rho = \frac{X - Y}{X}. \tag{3.5}$$

If the data transmission rate is known as a bit/sec, then the normalized throughput in term of time (ρ) can be formulated as shown in Eq. (3.6).

$$\rho = \frac{\frac{X}{a} - y_t}{\frac{X}{a}}, \tag{3.6}$$

where $y_t = \frac{Y}{a}$ is the CP in term of time length. From Eq.(3.5) and Eq.(3.6), it is clear that ρ of Eq.(3.5) is equal to ρ of Eq.(3.6).

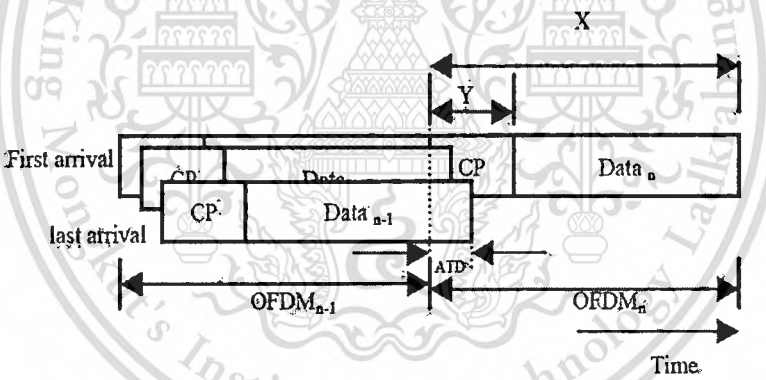

Fig.3.10 Relation of CP and data in OFDM symbol

In according to the standardization (IEEE802.11a), $y_t = 0.8\mu s$, and total length of OFDM symbol in term of time is equal to $4\mu s$. Under this standardization, it is guaranteed that there is no ISI will occur. Therefore, the upper bound of CP is $0.8\mu s$ in this paper. That is $0 \le y_t \le 0.8\mu s$.

As mentioned before that conventional OFDM uses the fixed or constant value of $y_t = 0.8\mu s$, and not change. Therefore, if Y, i.e., CP is fixed, then ρ will be limited to a constant value as shown in Figure 3.11. That is, when $X/a = 4\mu s$ and $y_t = 0.8\mu s$, then $\rho =$ 0.8 as the result. But if the value of Y or CP can be adjustable, then ρ can be obtained in

various values as shown in Figure 3.11. That is the reason of this research to adjust the ACP in according to current ATD that will result in the increasing of normalized throughput.

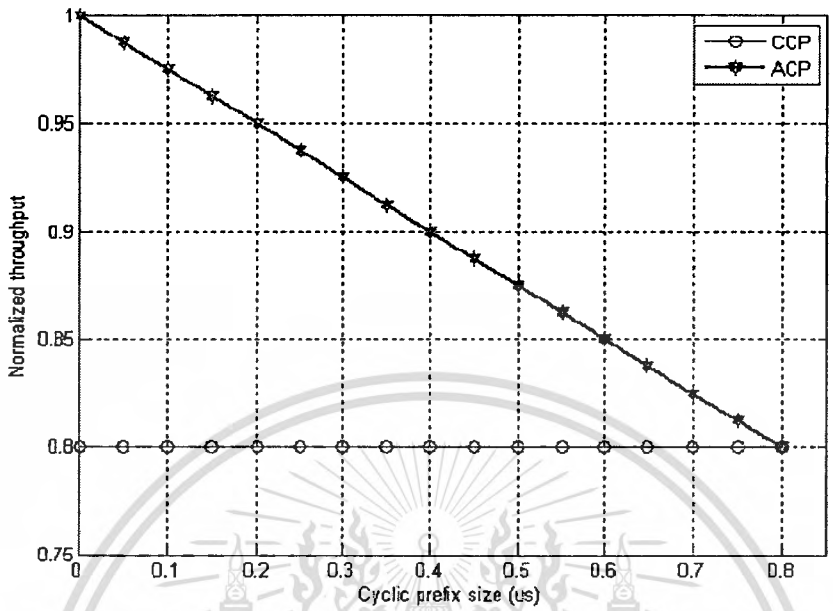

Figure 3.11 Normalized throughput versus the length CP

Chapter 4

Doppler Spread Mitigation Using Harmonic Transform

Doppler spread is one of the serious problems in mobile communications due to mobile unit movement. In this chapter, we focus on the Doppler spread mitigation using harmonic transform. The harmonic transform will be derived to the modified discrete harmonic transform which suits for wireless OFDM systems in mobile communications. The channel estimations are also proposed for cooperative with the proposed transformation. The proposed scheme will be compared the conventional wireless OFDM scheme.

4.1 Introduction

Orthogonal Frequency Division Multiplexing (OFDM) has become a prime candidate for future high-data-rate wireless systems because of its strong resistance to the inter-symbol interference (ISI), inserted by multi-path propagation effects in the real world indoor and outdoor channels. However, the wireless OFDM systems vary their sensitive to frequency offset and symbol timing offset due to the Doppler effect of the mobile communications.

The conventional OFDM systems employ the inverse discrete Fourier transform (IDFT) and discrete Fourier transform (DFT). However, the practical implementation involves the inverse fast Fourier transform (IFFT) and the fast Fourier transform (FFT) at the transmitter and receiver respectively using the fast algorithms of the IDFT and DFT. Therefore, applying the DFT for transformation from time-domain into frequency-domain is worse performance, when the channel is the time-varying channel. Therefore, the time scales of the received signals change the wavelength. This result induces the loss of orthogonal among OFDM sub-carriers due to the DFT performance.

However, in order to cope with the Doppler spread in the conventional DFT-OFDM scheme, compensation and equalization techniques are needed. The channel estimation (CE) and pilot-aided, are used for those techniques. The accuracy of the system depends on the performance of the channel estimation, amount and pattern of pilot-aided. The pilot-aided are inserted in the OFDM symbol in order to put the reference data in the OFDM symbol. Thus, the use of pilot-aided lowers the achievable data rate. Moreover, the channel estimation of conventional OFDM is performed after transformation. Thereby, the accuracy of the estimated values is affected by additive white Gaussian noise (AWGN).

In this research, we have considered that the transformation of wireless OFDM systems should be improved. We derive the appropriate equations that more suitable for the mobility situation in the mobile communication systems which is the one of our contribution.

However, in order to apply the harmonic transform for wireless OFDM systems, a modification of the discrete harmonic transform is needed. We combine the good characteristics of the harmonic transform and the concept of instantaneous frequency together. Moreover, the proposed scheme is called the MDHT-OFDM scheme [21]. Furthermore, the MDHT is performed as an adaptive transformation which cooperates with the parameters. Thus, adaptation requires a form of accurate parameter measurement. One key parameter in adaptation of mobile communications is f_D. Therefore, we propose a novel channel estimation technique that can cooperate to provide the suitable parameters for the MDHT-OFDM scheme.

The proposed channel estimation is performed in both the time-domain and the frequency-domain. In the time-domain estimation, the self-correlation function is performed to get the OFDM Framing Duration ($T_{estimated}$) in order to calculate the Doppler scaling factor ($\alpha_{estimated}$) and the symbol timing offset ($\varepsilon_{estimated}$). We use $\alpha_{estimated}$ by means of f_D. On the other hand, the frequency-domain estimation is performed in order to get the root mean square error of the preamble symbol (θ_{RMSE}) in order to select a suitable modulation mapping scheme.

The advantages of the proposed scheme are less pilot-aided, strong resistance to AWGN, and adaptability. However, the different characteristics between the conventional DFT-OFDM scheme and the proposed MDHT-OFDM scheme are shown in Table 4.1.

Table 4.1 The characteristics comparison of the conventional DFT-OFDM scheme and the proposed MDHT-OFDM scheme

Characteristics	Conventional OFDM	Proposed MDHT-OFDM
Transformation	DFT, FFT	MDHT
Transformation performing	Fixed	Adaptive
Channel estimation	Frequency domain	Time domain and frequency domain
Position of channel estimation	After transformation	Before and after transformation
Pilot-Aided	Needed	Compatible
Transformation complexity	N^2 (DFT) $N\log_2 N$ (FFT)	N^2 (MDHT)

4.2 Problem Definition and Conventional Wireless OFDM systems

In wireless OFDM systems, one serious problem is the frequency offset and symbol timing offset caused by the Doppler effect, which severely degrades the system performance. When the transmitter or receiver is moving, the received signal will have the maximum Doppler frequency of $f_D = v/\lambda$ associated with it, where v is the mobile velocity, and λ is the signal wavelength. The time variations of the channel change over the OFDM symbol duration, and the wavelength is scaled. Thus, the time coherence is concerned. We define the coherence time T_C to be the range of Δt values over the OFDM symbol. The maximum Doppler frequency value is called the Doppler spread of the channel. The coherence time is the time-domain dual of Doppler spread and is used to characterize the time-varying channel. The Doppler spread and coherence time are inversely proportional to one another. That is $f_D \approx 1/T_C$ [25].

Conventional wireless OFDM systems employ the DFT in order to transform the signals. For signals consisting of fixed frequency components, the DFT effectively provides their frequency contents. But, this capability deteriorates when the frequency components are time-varying. Since the Doppler effect occurs in the time-domain which is impacted on the wavelength of each OFDM sub-carrier. Moreover, the frequency-domain channel estimation of the conventional DFT-OFDM scheme is affected by AWGN which has been reported in [9].

According to the problems that mention above, the novel transformation and novel channel estimation should be considered to be suitable for wireless OFDM systems. Before discussing the proposed scheme, we would like to describe the conventional wireless OFDM systems.

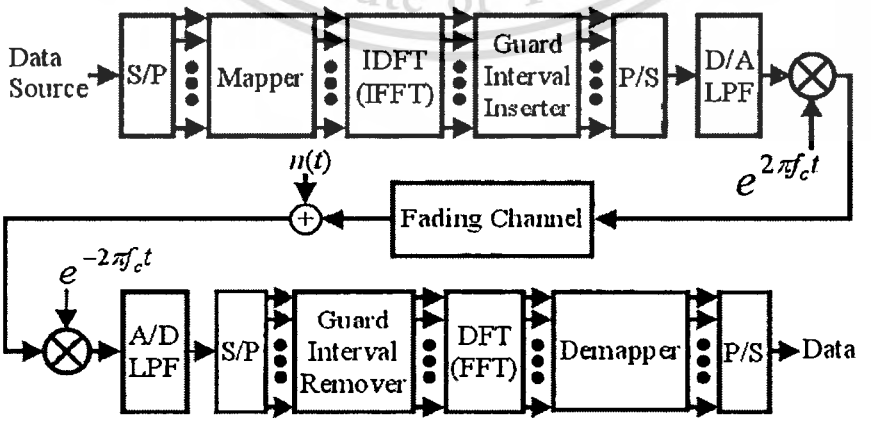

Figure 4.1 The block diagram of the conventional DFT-OFDM scheme

The conventional DFT-OFDM scheme block diagram is shown in Figure 4.1. The data is transformed into time-domain using inverse discrete Fourier transform (IDFT) or inverse fast Fourier transform (IFFT) at the transmitter. The definition of the *N*-point of IDFT is given by

$$x_f(n) = \frac{1}{N}\sum_{k=0}^{N-1} X_f(k) e^{\frac{2j\pi kn}{N}} . \tag{4.1}$$

On the conventional DFT-OFDM receiver side, the data is transformed back to the frequency-domain by performing DFT or fast Fourier transform (FFT) on the received signals. The definition of the *N*-point DFT is given by

$$X_f(k) = \sum_{n=0}^{N-1} x_f(n) e^{-\frac{2j\pi kn}{N}}, \tag{4.2}$$

where x_f is the time-domain OFDM signals, X_f is the data symbol of frequency-domain, N is the number of sub-carriers, and n is the sampling instant.

DFT is most commonly used for signal transformation. Unfortunately, it has a poor performance in the case of time-varying channels. In order to mitigate the Doppler spread in the conventional DFT-OFDM, pilot-aided symbols are inserted at the transmitter at the fix time interval and at the receiver, the channel characteristics are estimated by using the pilot-aided symbol. Then, the received data can be recovered. The channel estimation is performed after transformation which is affected by AWGN. Thereby, the system performance is strongly dependant on the amount and patterns of pilot-aided which are needed as space on an OFDM symbol.

In wireless OFDM systems channel estimation is popularly performed in frequency-domain. Channel frequency response estimates are affected by AWGN. Due to the additive noise will be combined in transformation process. Therefore, the recovery symbols will be destroyed. As a result, Doppler estimates based on frequency-domain channel estimates will be affected significantly. In contrast, the time-domain channel estimation is robust to AWGN, works well for low SNR, regardless of the variation of channel environment. Furthermore, channel estimation in the time-domain turns out to be more efficient since the number of the unknown parameters is greatly decreased compared to that in the frequency-domain.

4.3 Proposed MDHT-OFDM Scheme for Wireless OFDM systems

The proposed MDHT-OFDM scheme is shown in Figure 4.2. The contributions of the proposed MDHT-OFDM scheme are as follows. Firstly, we investigate the novel transformation which can adapt itself to the condition of the channels. Secondly, we fined out the novel channel estimation to cooperate with the novel transformation.

4.3.1 A Novel Transformation for Wireless OFDM Systems

Harmonic transform has been proposed in [12], but it has been proposed for signal analysis, especially speech signals. We have found that the harmonic transform has a good property for signals that contain time-varying signals. The difference between the harmonic transform and the Fourier transform is the harmonic kernel $e^{j\omega\phi_u(t)}$, where $\phi_u(t)$ is the unit phase function. The harmonic kernel can be loosely interpreted as the integration of the signal along the curves $\omega\phi_u'(t)$, where $\phi_u'(t)$ is the derivative of $\phi_u(t)$. In the case of $\phi_u(t)=t$, the harmonic transform is equivalent to the Fourier transform. The discrete form of harmonic transform was proposed in [12]. Unfortunately, it is not suitable for wireless OFDM systems. Because the traditional harmonic transform is designed for speech signal analysis, the unit phase function ($\phi_u(t)$) of its depends on the scaling property which is determined by the relation between $\phi_u(t)$ and $\phi_u(t/a)$, where a is a constant. Scaling and phase shifting operation are defined before calculation in order that the suitable parameters are set as constant. Moreover, only real numbers are required by speech signal analysis. In contrast, the transformations of wireless OFDM systems require the complex numbers. In mobile communications, the mobile station may often change its position during the communication as we call the mobility of mobile unit. In this situation, the constant parameter may be not suitable. This means that it should be varied according to the mobility of mobile unit. Therefore, the traditional harmonic transform may be not suitable for the mobile communications. For this reason, the traditional harmonic transform should be modified. In this chapter, we derive the appropriate equations that more suitable for the mobility situation in the mobile communication systems which is the one of our contribution.

In order to apply to wireless OFDM systems, we have to modify the harmonic transform which is shown in the following step. Let us start from the continuous form of the harmonic transform which has been proposed in [12]. The harmonic transform of a time-domain signal $f(t)$ can be defined by

$$F_{\phi_u(t)}(\omega) = \int_{-\infty}^{+\infty} f(t)\phi_u'(t)e^{-j\omega\phi_u(t)}dt. \tag{4.3}$$

The inverse harmonic transform is given by

$$f(t) = \frac{1}{2\pi}\int_{-\infty}^{+\infty} F_{\phi_u(t)}(\omega)e^{j\omega\phi_u(t)}d\omega, \tag{4.4}$$

where $\phi_u(t)$ is the unit phase function of fundamental of $f(t)$. $\phi_u'(t)$ is the first-order derivative of $\phi_u(t)$.

We now start to modify the harmonic transform to be used in wireless OFDM systems. A discrete calculation is required to compute the discrete form of $F_{\phi_u(t)}$ when $f(t)$ and $\phi_u(t)$ are in a discrete form. The discrete harmonic transform is defined as the sampled version of the harmonic transform, $f(t) \Rightarrow f(n)$ and $\phi_u(t) \Rightarrow \phi_u(n)$, where Δt is the sample period, $t = n\Delta t$ and $n \in [0, N-1]$, the variable t of $f(t)$ and $\phi_u(t)$ is limited to the range $[0, T]$, where $T = N\Delta t$. Note that the relationship between ω and f is $\omega = 2\pi f$. Due to the traditional harmonic transform is proposed for speech signal analysis, it provides only real numbers. But, in the case of wireless OFDM systems, the transformations of the OFDM signals are formed in terms of complex numbers. Thus, we have to modify the discrete form of the

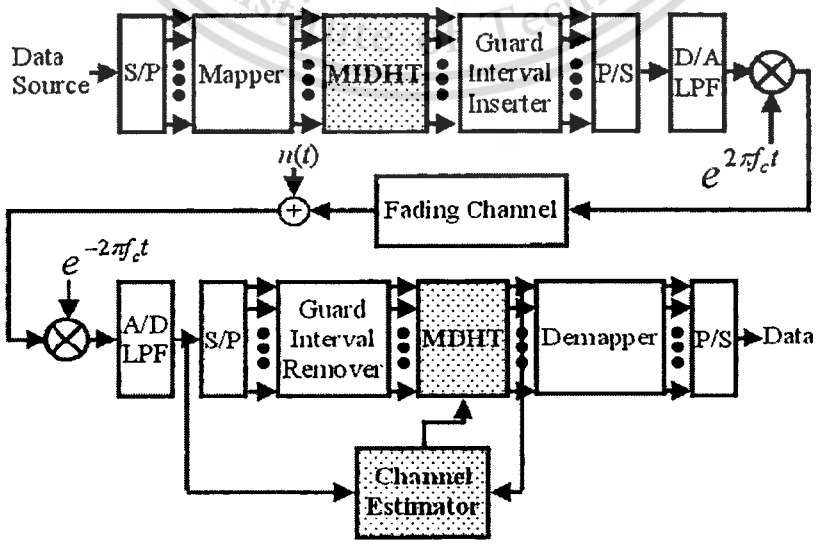

Figure 4.2 The propose MDHT-OFDM scheme for wireless OFDM systems

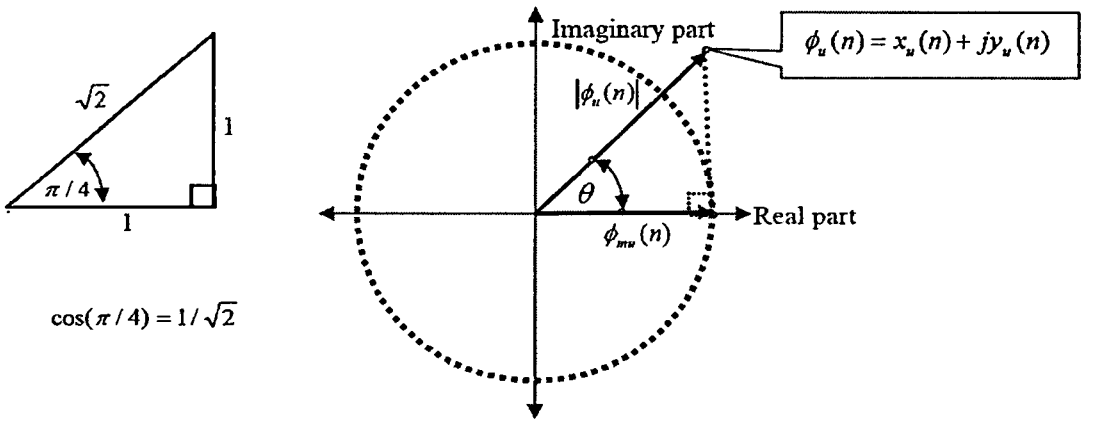

Figure 4.3 The complex plane of the modified unit phase function

traditional harmonic transform. For this reason, we have to define the unit phase function as a complex number. So that, the unit phase function in the exponential function has to be modified because we need the real number. Thus, we have to define the unit phase function as a complex number as shown in the following equation

$$\phi_u(n) = x_u(n) + jy_u(n), \tag{4.5}$$

where $x_u(n)$ and $y_u(n)$ are real and imaginary components of the linear function, respectively, and j is equal to $\sqrt{-1}$.

Therefore, the unit phase function in the exponential function has to be modified as well, it must be a real number. Regarding to the complex plane as shown in Figure 4.3, the modified unit phase function can be derived as follows

$$\phi_{mu}(n) = |\phi_u(n)|\cos(\theta). \tag{4.6}$$

The angle θ of the $x_u(n) = y_u(n)$ is $\pi/4$. Thus, $\cos(\pi/4) = 1/\sqrt{2}$. Therefore, the modified unit phase function can be expressed as follows

$$\phi_{mu}(n) = \frac{|\phi_u(n)|}{\sqrt{2}}, \tag{4.7}$$

where: $\phi_{mu}(n)$ is the modified unit phase function, and $|\phi_u(n)|$ is the magnitude of unit phase function. Thus, we can rewrite as the modified inverse discrete harmonic transform (MIDHT) as shown in the following equation

$$x_h(n) = \frac{1}{N}\sum_{k=0}^{N-1} X_h(k) e^{j\frac{2\pi k \phi_{mu}(n)}{N}} . \quad (4.8)$$

The modified discrete harmonic transform (MDHT) can be rewritten as shown in the following equation

$$X_h(k) = \sum_{n=0}^{N-1} x_h(n)\phi'_u(n) e^{-j\frac{2\pi k \phi_{mu}(n)}{N}} , \quad (4.9)$$

where $x_h(n)$ is the time-domain OFDM signals, $X_h(k)$ is the frequency-domain OFDM signals, $\phi_u(n)$ is the unit phase function, $\phi'_u(n)$ is the first-order derivative of $\phi_u(n)$, $\phi_{mu}(n)$ is the modified unit phase function, k and n are the integer $[0, N-1]$. The first-order derivative of $\phi_u(n)$ can be represented in terms of an instantaneous frequency.

However, the idea of frequency is very clear when applied to periodic signals. It represents the number of times a signal is identically reproduced during a unit of time. By convention the term "frequency" is associated with the Fourier transform defined as an infinite integral over the time-domain. Thus, the time variable is removed, implying that the Fourier frequency is not a descriptor of a signal at a specific instant in time. On the other hand, Instantaneous frequency is a function of time and thus represents a different concept than Fourier frequency. The instantaneous frequency of a signal is often used as an aid to time-frequency analysis of non-stationary signals, it taken as the derivative of the phase of the signal, is interpreted in the time–frequency as the average frequency of the signal at each time. To process non-stationary signals, the time-frequency representation which takes into account the time and frequency variations of the signal. The instantaneous frequency is defined as the phase derivative with respect to time. The definition for the instantaneous frequency of a real continuous-time signal is shown as follows,

$$f_{IF}(t) = \frac{d\phi(t)}{dt} , \quad (4.10)$$

where $f_{IF}(t)$ is the instantaneous frequency function of time t, and $\phi(t)$ is the phase function of t. Note that, the instantaneous frequency can be written in form of $f_{IF}(t) = \phi'(t)$ [13].

For a discrete-time signal, the two-point symmetric phase difference has been defined as a discrete instantaneous frequency. The two-point discrete instantaneous frequency is a good approximation to samples of the continuous-time instantaneous frequency. The discrete-time instantaneous frequency is a function of time. its mean must be evaluated in the time-domain.

Good approximations to the differentiation operation in discrete-time can be obtained by using a phase differencing operation. Specifically, the cases where the discrete-time instantaneous frequency is defined as the backward, central, and forward differences, respectively, are shown as following equation [19]

$$\phi(n) = \phi(n) - \phi(n-1), \tag{4.11}$$

$$\phi'(n) = \phi(n) - \phi(n-1), \tag{4.12}$$

$$\phi'(n) = \phi(n) - \phi(n-1). \tag{4.13}$$

However, the unit phase function of the modified harmonic transform is a complex signal; it is defined as the derivative of the phase. Thereby, the first-order derivative of $\phi_u(n)$ can be defined by

$$\phi'_u(n) = \frac{d\phi_u(n)}{dn}. \tag{4.14}$$

Therefore, we define the discrete-time instantaneous frequency to be the backward difference of $\phi_u(n)$. Thus, the first-order derivative of $\phi_u(n)$ can be defined by

$$\phi'_u(n) = \phi_u(n) - \phi_u(n-1), \tag{4.15}$$

where $\phi_u(n)$ is a complex number and $n \in [0, N-1]$.

Equation (4.8) and equation (4.9) are the proposed equations which are applied in the proposed MDHT-OFDM scheme according to Figure 4.2. We investigate the MIDHT and MDHT by replacement of the IDFT and DFT, respectively.

4.3.2 Transceiver Design of MDHT-OFDM Scheme

The proposed MDHT-OFDM scheme applies the novel signal transformation in order to mitigate the Doppler spread in mobile communications. It can perform adaptively depending on the condition of channels. Figure 4.2 shows the proposed MDHT-OFDM scheme which includes our proposed channel estimation that estimates the MDHT-Parameters.

The MDHT-Parameters consist of three values, which are the mode, the Doppler scaling factor ($\alpha_{estimated}$), and the symbol timing offset ($\varepsilon_{estimated}$). The mode is selected in

channel estimation to be DFT-Mode or MDHT-Mode. If the DFT-Mode is selected, then the unit phase function is defined by

$$\phi_u(n) = n + jn, \tag{4.16}$$

where n is an integer, $n \in [0, N-1]$, and j is equal to $\sqrt{-1}$.

On the other hand, if the MDHT-Mode is selected, then the unit phase function is defined by

$$\phi_u(n) = (n\alpha_{estimated} + \varepsilon_{estimated}) + j(n\alpha_{estimated} + \varepsilon_{estimated}), \tag{4.17}$$

where n is an integer and $n \in [0, N-1]$, j is equal to $\sqrt{-1}$, $\alpha_{estimated}$ is the Doppler scaling factor, and $\varepsilon_{estimated}$ is the symbol timing offset.

4.3.2.1 MDHT-OFDM Scheme Transmitter

At the MDHT-OFDM scheme transmitter, the N complex data sequences are modulated by using modulation mapping schemes onto each sub-carrier independently. Then, the mapped data is taken by the MIDHT-OFDM process. According to the fundamental concept of OFDM, the OFDM signal is the orthogonal of sub-carriers in the frequency-domain. Hence, the MDHT-OFDM transmitter requires only the DFT-Mode, which is enough to generate the orthogonal signal. According to Eq.(4.8), the computational step of the MIDHT-OFDM algorithm at the transmitter is shown in Figure 4.4.

```
for n=0 to N − 1
begin
        φu(n) = n + jn
        for k=0 to N − 1
        begin
                xh(n) = xh(n) + Xh(k)exp(j2πkφmu(n)/N)
        end
        xh(n) = xh(n)/N
end
```

Figure 4.4 The algorithm of N-point MIDHT-OFDM

Setup $\phi_u(n)$
for $k = 0$ to $N - 1$
begin
    for n=0 to $N - 1$
    begin
        $X_h(k) = X_h(k) + x_h(n)\phi'_u(n)\exp(-\frac{j2\pi k\phi_{mu}(n)}{N})$
    end
end

Figure 4.5 The algorithm of N-point MDHT-OFDM

4.3.2.2 MDHT-OFDM Scheme Receiver

At the MDHT-OFDM scheme receiver, the received signal is estimated by the channel estimator. Then, the MDHT-Parameters will be sent to transformation which is the MDHT. For the DFT-Mode, The unit phase function is set as Eq.(4.16), otherwise, the unit phase function as Eq.(4.17) is set for the MDHT-Mode. Then, the MDHT is performed according to the MDHT-Parameters. However, after the received signal is transformed to the frequency-domain, the transformed data of the preamble symbol will be sent to the channel estimator again to estimate the root mean square error of the preamble symbol (θ_{RMSE}) in order to select a suitable modulation mapping scheme for the next transmission, while, the transformed data of OFDM symbol will be sent to the demapper according to the modulation mapping scheme. The computational step of the MDHT-OFDM algorithm at the receiver is shown in Figure 4.5 which is corresponding to Eq.(4.9).

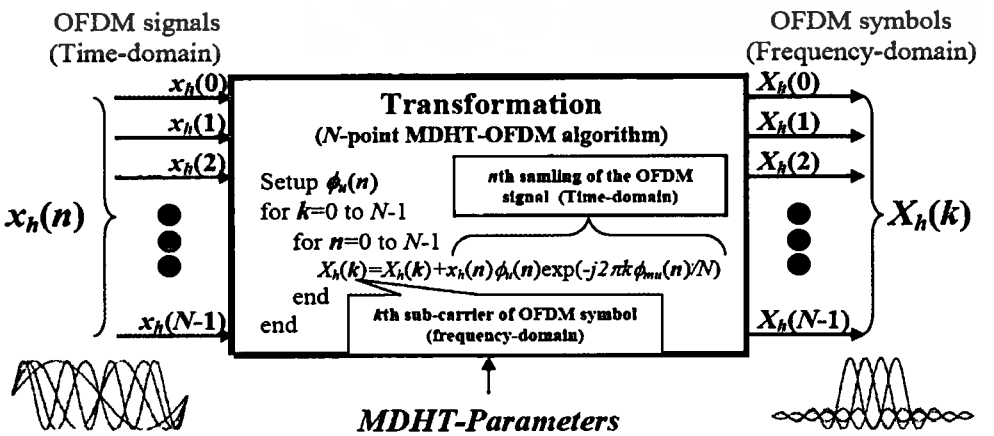

Figure 4.6 The input and output of N-point MDHT-OFDM algorithm

The Equation (4.17) is the unit phase function of the MDHT-Mode. It will be used in the MDHT-OFDM algorithm. The unit phase function $(\phi_u(n))$ is still in the time-domain. The Doppler scaling factor is the time-domain as well. So that, the unit phase function and the Doppler scaling factor are not in form of the frequency-domain, but after the MDHT-OFDM algorithm has done, the OFDM signals become OFDM symbol. The MDHT-OFDM algorithm is warp transform which the OFDM signals (time-domain) are warped in time-domain before calculation to the frequency-domain as shown in Figure 4.6.

4.3.2.3 Complexity Analysis

We now compare the computational complexity between the MDHT-OFDM algorithms and DFT-OFDM algorithms. In order to compare the computational complexity, the *BigO* notation is used. Let N be the number of sub-carriers of the OFDM system. The computational complexity of the MDHT-OFDM algorithm has the order of $O(N^2)$, which is equivalent to the DFT algorithm, but the MDHT-OFDM algorithm requires more computational processes for addition and multiplication of the complex number.

However, the DFT algorithms have been developed for many years ago. Several fast algorithms of DFT have been reported for the computational complexity of the DFT. The fast Fourier transform (FFT) algorithms were derived to significantly reduce the computational complexity from the order of $O(N^2)$ to the order of $O(N\log_2 N)$.

4.3.2.4 Transformation Performance Results

We evaluated the transformation performance of the MDHT by computer simulation. The compuater simulation focuses on the effect of the frequency offset and Doppler spread to compare the proposed MDHT-OFDM with the conventional DFT-OFDM for comparing the transformation performance.

In the computer simulation, we disregard the effect of noise and multi-path fading, assuming ideal fading channel. Table 4.2 lists the simulation parameters. Becase we would like to aviod the bias of other factor.

Table 4.2 Simulation parameters

Parameter Name	Value
Number of N points	64
Length of guard interval	16
Modulation	QPSK
Transformation	DFT, MDHT
Type of testing	Frequency offset: Δt =3.125% of OFDM symbol duration. Doppler spread: Doppler scaling factor = 0.9968.

We consider an OFDM symbol in which N complex data symbols an, n=0...N-1, T_s is an OFDM symbol duration. We indicate with T_c the sampling period, T_s=NT_c. The frequency offset can e expressed in terms of the sub-carrier bandwidth $1/NT_c$. Since OFDM systems use DFTs, a time shift is equivalent to a cyclic shift of the input data. This is valid since the DFT input is seen as periodic due to the cyclic prefix. A cyclic shift can be used to influence the channel characteristics. In the presence of a static channel the cyclic shift might be used to counteract the effect of the time shift on the useful part of the receive signal. The cyclic shift (Δt) of 3.125% of OFDM symbol duration is 2 point of N, it corresponds to frequency offset about 625 KHz.

We can calculate the Doppler spread by means of Doppler scaling factor. The Doppler scaling factor relates to the coherence time. Corresponding to the coherence time 0.9986*T_s, the maximum Doppler spread can be calculated by $f_{max} \approx 1/T_c$. If we consider 802.11a with carrier frequency of 5 GH, sub-carrier spacing 312.5 KHz, so that, maximum Doppler spread is approximately 1 kHz, the normalized Doppler spread is approximately 0.0032, it corresponds to a mobile speed about 216 Km/hr.

For the testing, we used the reference data of frequency-domain OFDM symbols, i.e., reference sub-carrier data, are 0, 1+j, 1-j, -1+j and -1-j, as shown in Figure 4.7, the left and right figures in which indicates real part and imaginary part, respectively. At the transmitter, the transmitted frequency-domain OFDM symbols are converted to time-domain OFDM signals by IDFT. The OFDM signals are passed through the channel. At the receiver, the time-domain OFDM signals having complex values are taken by either transformation to the signal into in-phase, and quadrature sequences, i.e., real and imaginary parts, respectively. These results were

used for the comparison in term of accuracy between the proposed MDHT-OFDM with conventional DFT-OFDM.

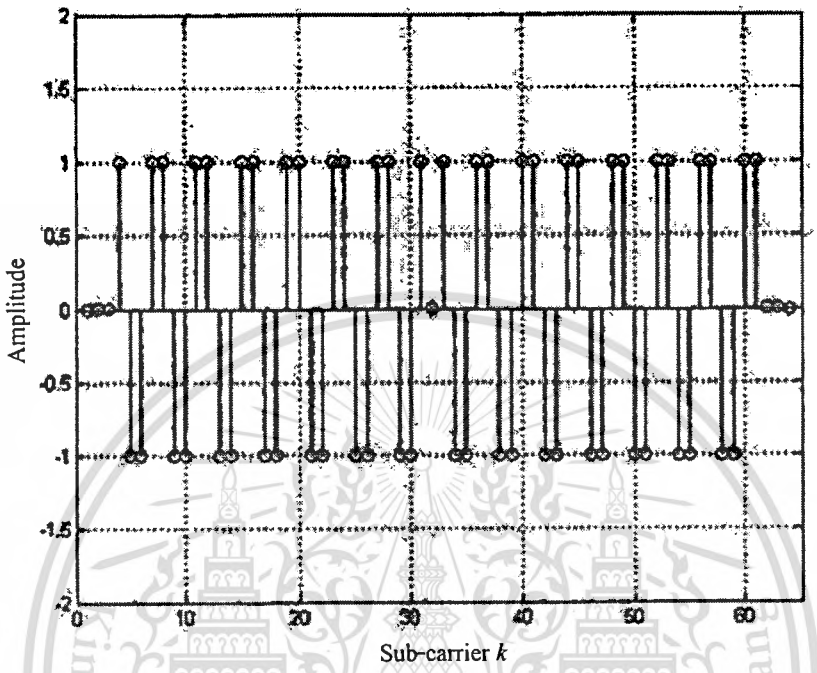

(a) Real part (In-phase)

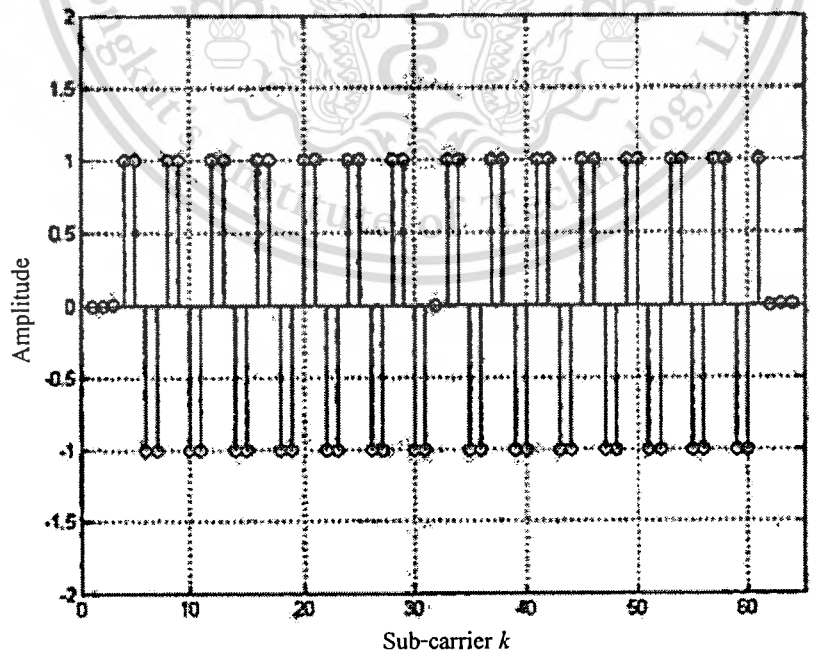

(b) Imaginary part (Quadrature)

Figure 4.7 Reference data of OFDM symbol

First, we considered the effect of the frequency offset error caused by the time offset error. In order to evaluate the time offset error, 3.125% of OFDM symbols duration, which amounts to 2 samples, is shifted. Then, the 64-point DFT or the 64-point MDHT is taken. The results for both are shown in Figure 4.8 to Figure 4.10.

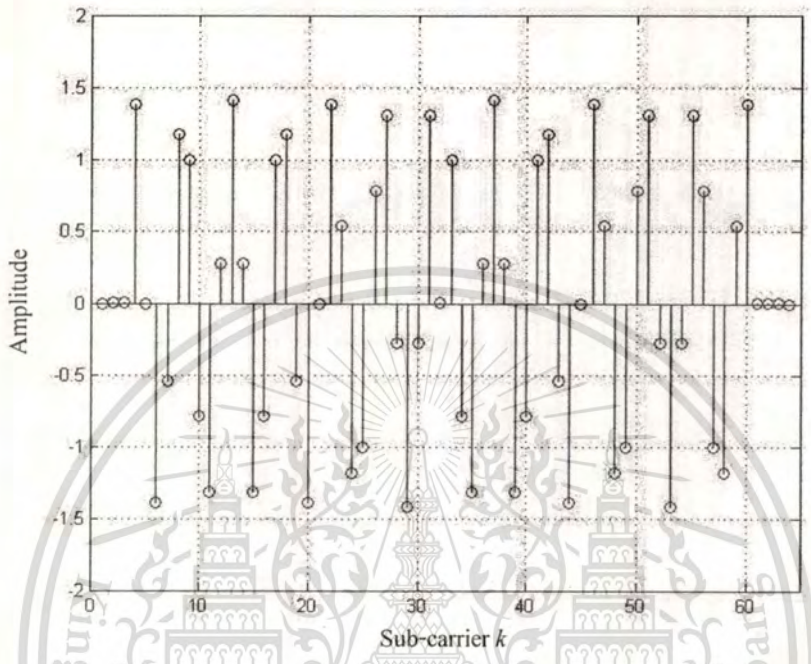

(a) DFT

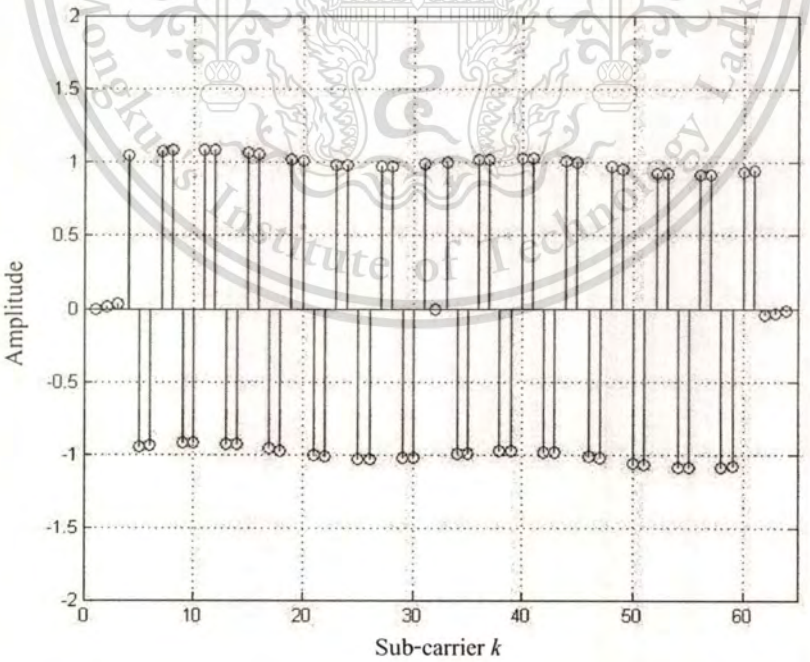

(b) MDHT

Figure 4.8 Real part of OFDM symbol effect from frequency offset

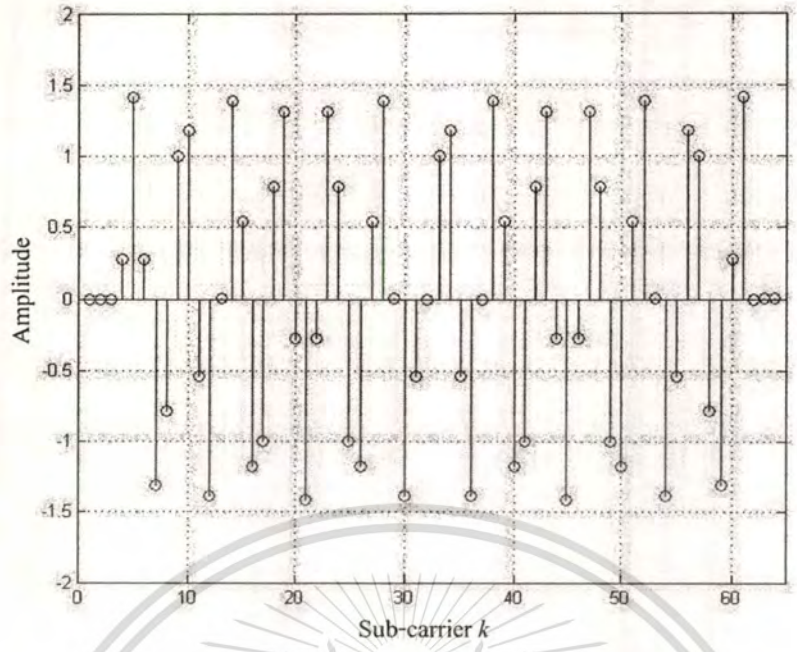

(a) DFT

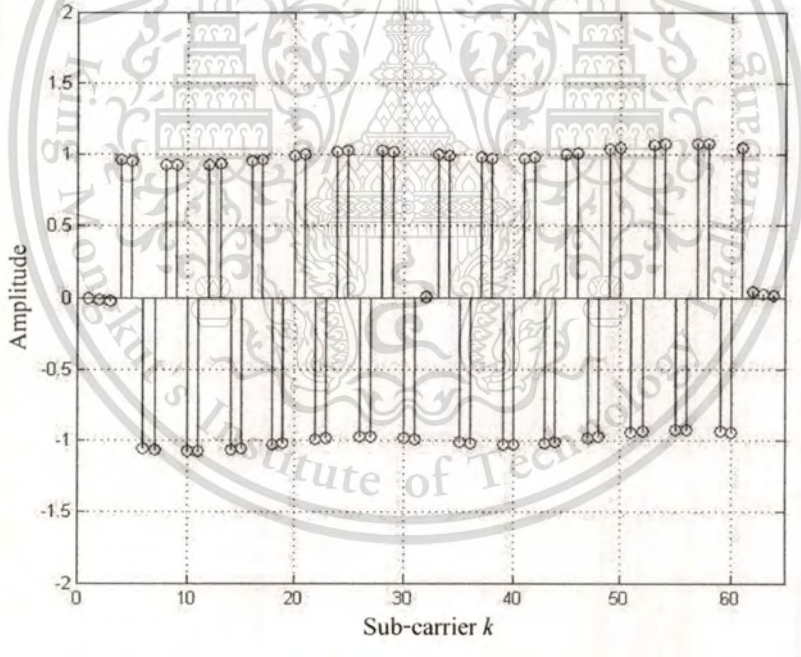

(b) MDHT

Figure 4.9 Imaginary part of OFDM symbol effect from frequency offset

Figures 4.8 and 4.9 show the amplitudes of the received sub-carriers for DFT and MDHT transformations, respectively, in the presence of the frequency offset error. These figures suggest recovery accuracy of each sub-carrier. From these figure, the constellation diagram can be shown in Figure 4.10. It is observed that the phase rotation of the DFT is shifted

in comparison with that of the MDHT. The MDHT provides time offset error at least $3\pi/8$ radians of each sub-carrier when the time offset of OFDM symbols is shifted about 3.125% of OFDM symbol duration.

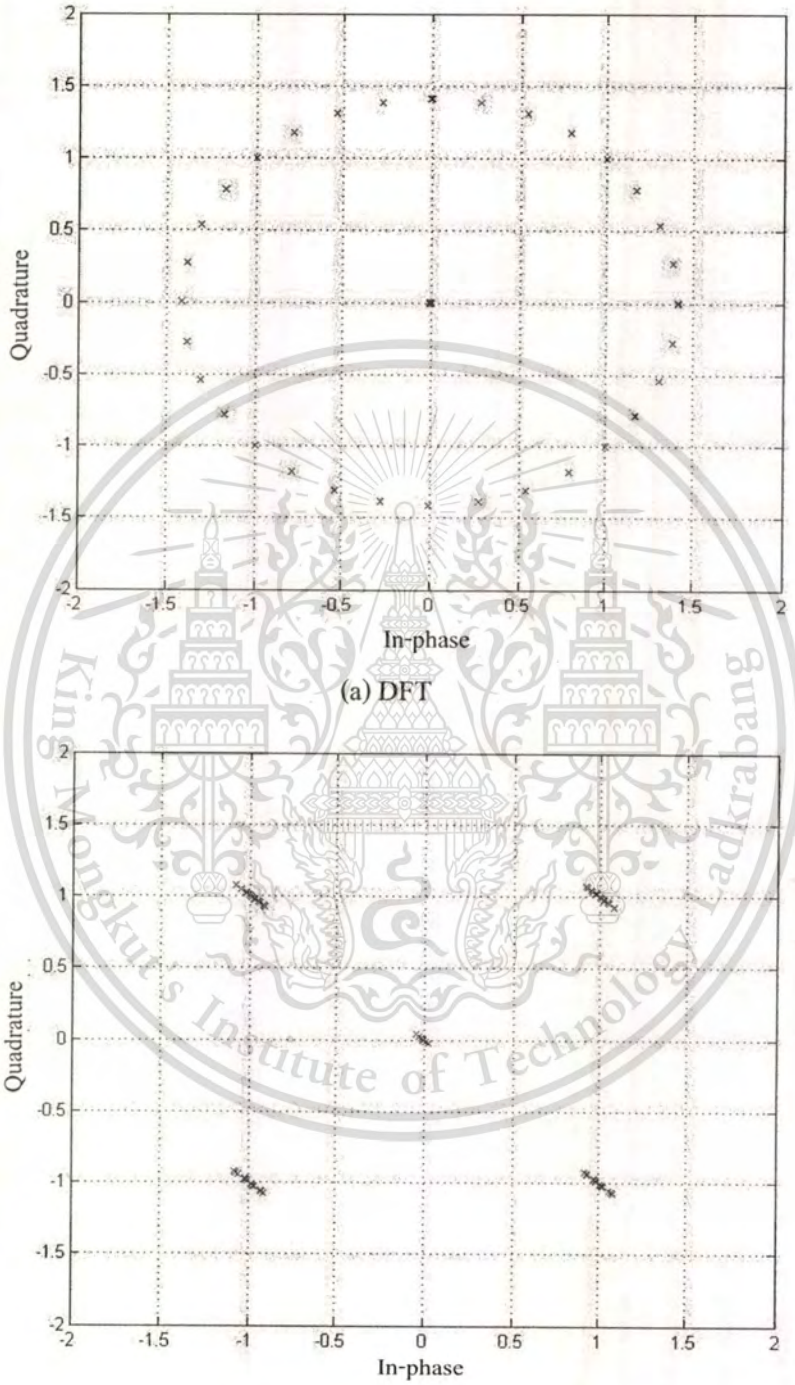

(a) DFT

(b) MDHT

Figure 4.10 The QPSK signal constellation effect from frequency offset

Then, we considered the effect of the Doppler spread. The Doppler spread is affected over the duration of OFDM symbols. We assumed the duration of the received OFDM signal is less than 0.32% of that of original OFDM signal. This means that the scale factor can be calculated as 0.9968. After adopting the Doppler shift for the received OFDM signal, the 64-point DFT or the 64-point MDHT is applied. The results are shown in Figure 4.11 to Figure 4.13.

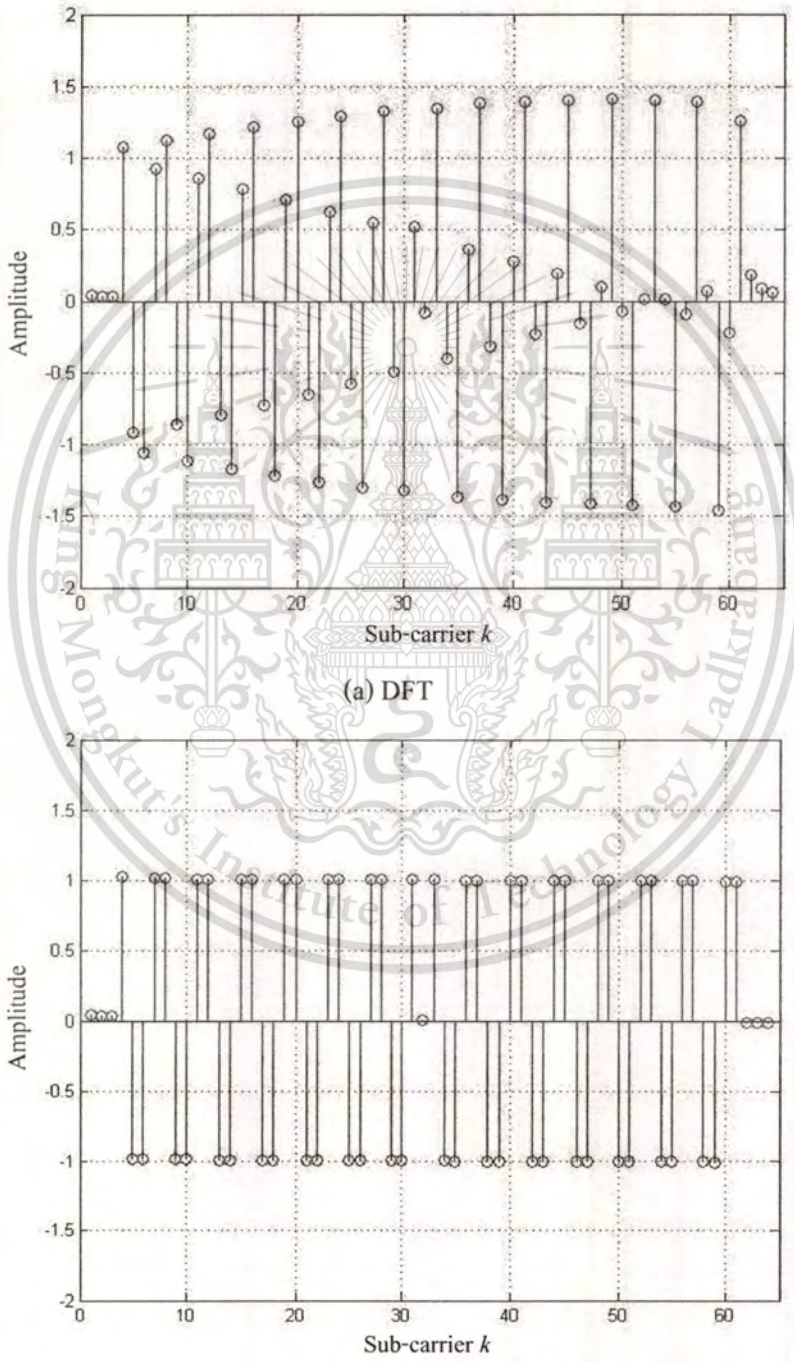

Figure 4.11 Real part of OFDM symbol effect from Doppler spread

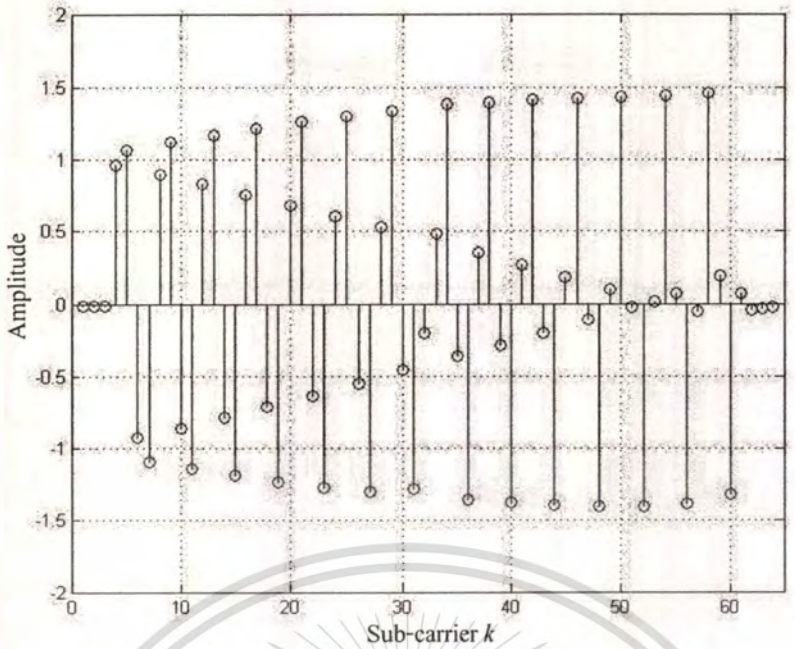

(a) DFT

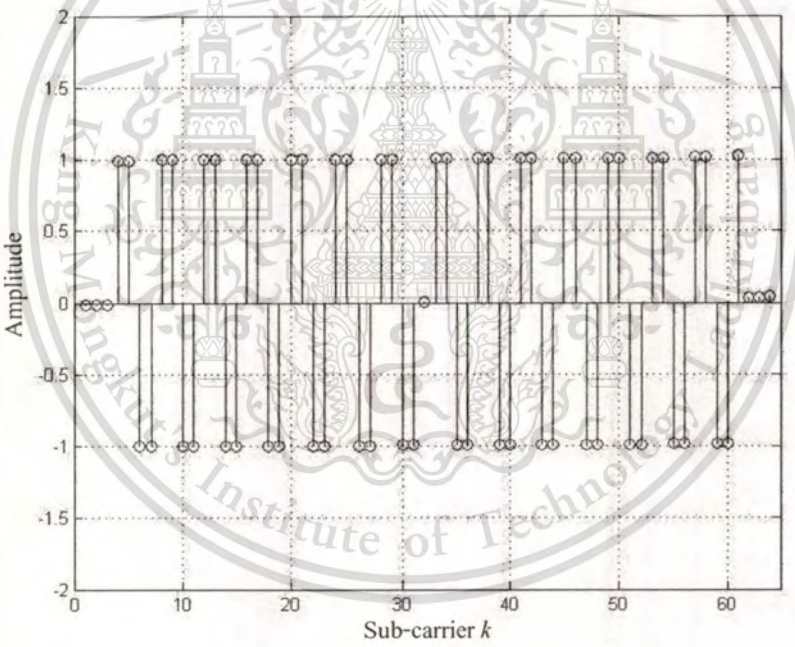

(b) MDHT

Figure 4.12 Imaginary part of OFDM symbol effect from Doppler spread

Figures 4.11 and Figure 4.12 show the amplitudes of the received sub-carriers for both transformations in the presence of the Doppler shift. Note that Doppler spread was set to $\pi/4$ radians, and the scale factor was set to 0.9968 accordingly. The signal constellations of the sub-carriers of both transformations are in Figure 4.13. In Figure 4.13(b), we can see that the phase rotation can of the MDHT be explicitly resolved unlike that of DFT shown in Figure 4.13(a). Hence, the scale factor is necessary to mitigate the Doppler spread. It can be seen that the

MDHT can reduce the effect of phase rotation caused by Doppler spread successfully by approximately $\pi/4$ radians.

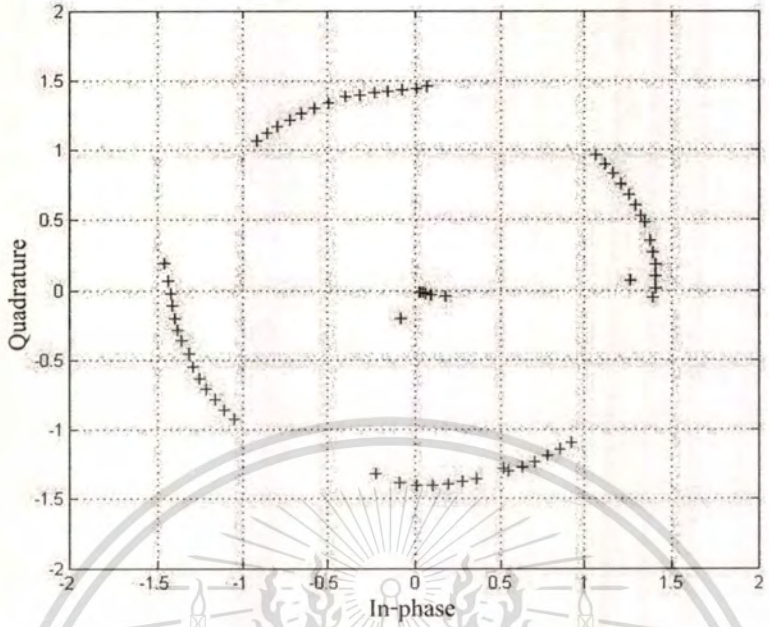

(a) DFT

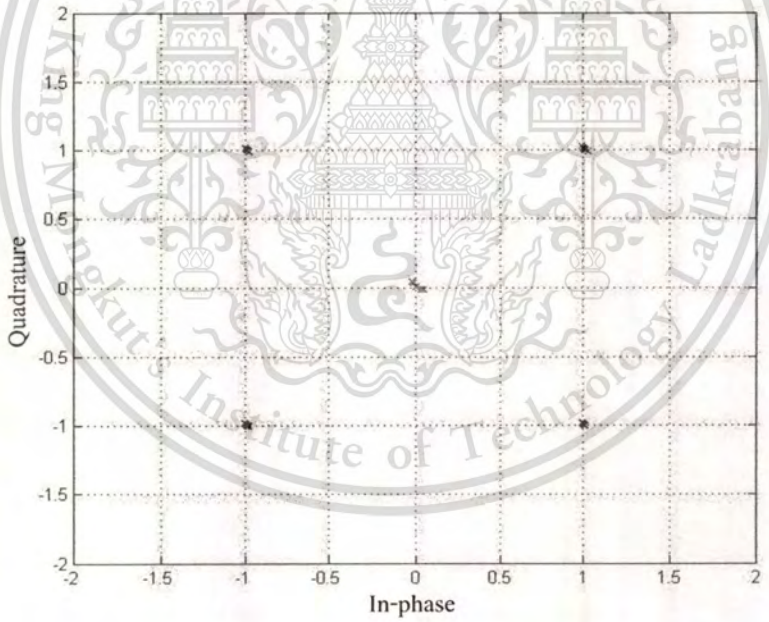

(b) MDHT

Figure 4.13 The QPSK signal constellation effect from Doppler spread

Based on the simulation results, the MDHT can improve the accuracy of recovery of the phase rotation caused by the Doppler spread and frequency offset in comparison with the DFT. The MDHT-OFDM scheme requires the channel estimation to cooperative. The proposed channel estimation will be presented in the next subsection.

4.4 Channel Estimation for MDHT-OFDM Scheme

There are two main problems in designing channel estimators for wireless OFDM systems. The first problem is the arrangement of pilot-aided information, where pilot-aided means the reference signal used by both transmitters and receivers. The second problem is the design of an estimator with both low complexity and good channel tracking ability. The combination of high data rates and low bit error rates in OFDM systems necessitates the use of estimators that have both low complexity and high accuracy, where the two constraints work against each other and a good trade-off is needed. The two basic pilot-aided channel estimations are block-type pilot-aided channel estimation and comb-type pilot-aided channel estimation, in which the pilots are inserted in the frequency direction and in the time direction, respectively. The two basic types of pilot-aided channel estimations in wireless OFDM systems are illustrated in Figure 4.14.

In OFDM systems, channel estimation is usually done in the frequency-domain either by sending pilot-aided to capture channel variations. But, it is affected by additional noise. Hence, the proposed channel estimation is preformed in both the time-domain and frequency-domain. It consists of three parts which are the OFDM framing duration estimator, the preamble symbol error estimator, and the MDHT-Rules. It estimates the MDHT-Parameters, which are to cooperate with MDHT-OFDM at the receiver. Figure 4.15 depicts the burst frame for the

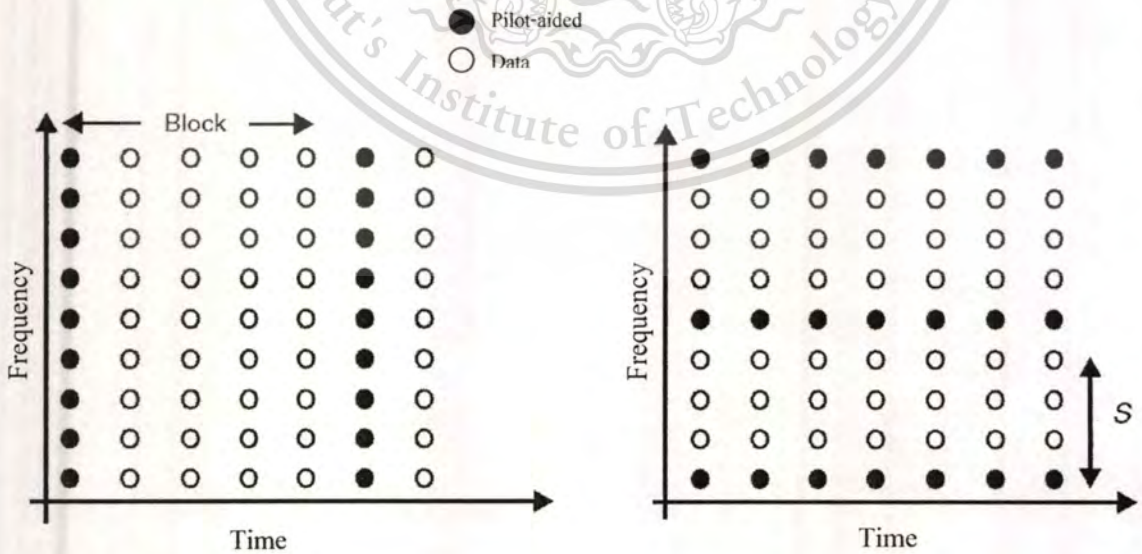

(a) Block-type pilot-aided channel estimation (b) Comb-type pilot-aided channel estimation

Figure 4.14 Two basic types of pilot-aided arrangement for OFDM channel estimations

MDHT-OFDM scheme which is required by the OFDM framing duration estimator. The cooperative processes are illustrated in Figure 4.16. The OFDM framing duration estimator and the preamble symbol error estimator estimate the channel characteristics which are sent to the MDHT-Rules. Then, the MDHT-Parameters are determined by the MDHT-Rules for the transformation process. In addition, the conventional channel estimation also can be applied in our proposed scheme.

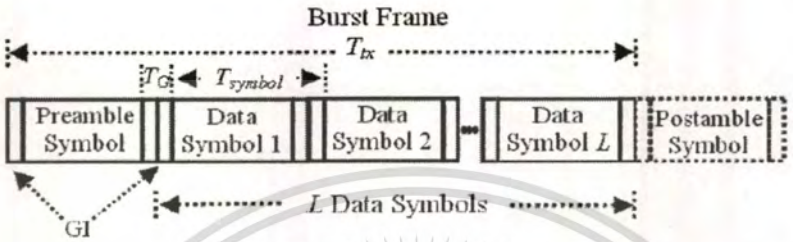

Figure 4.15 The burst frame structure for the MDHT-OFDM scheme

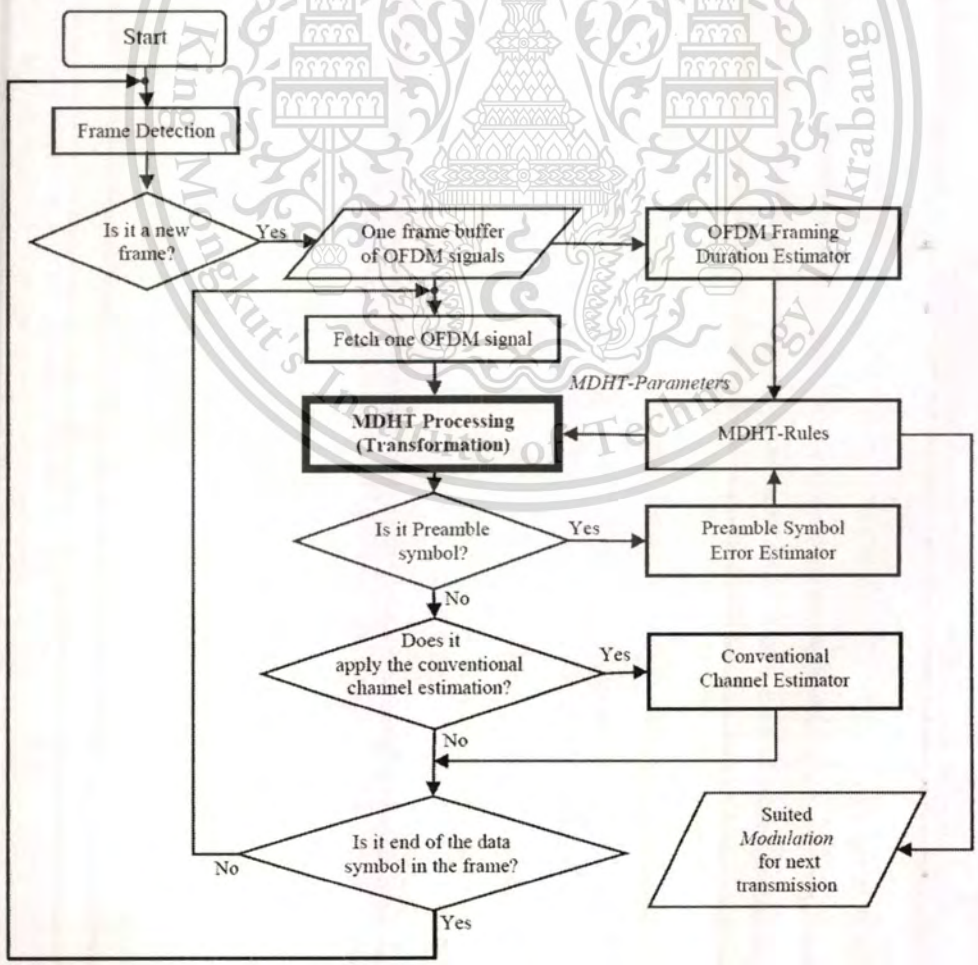

Figure 4.16 The cooperative processes of proposed MDHT-OFDM scheme at receiver

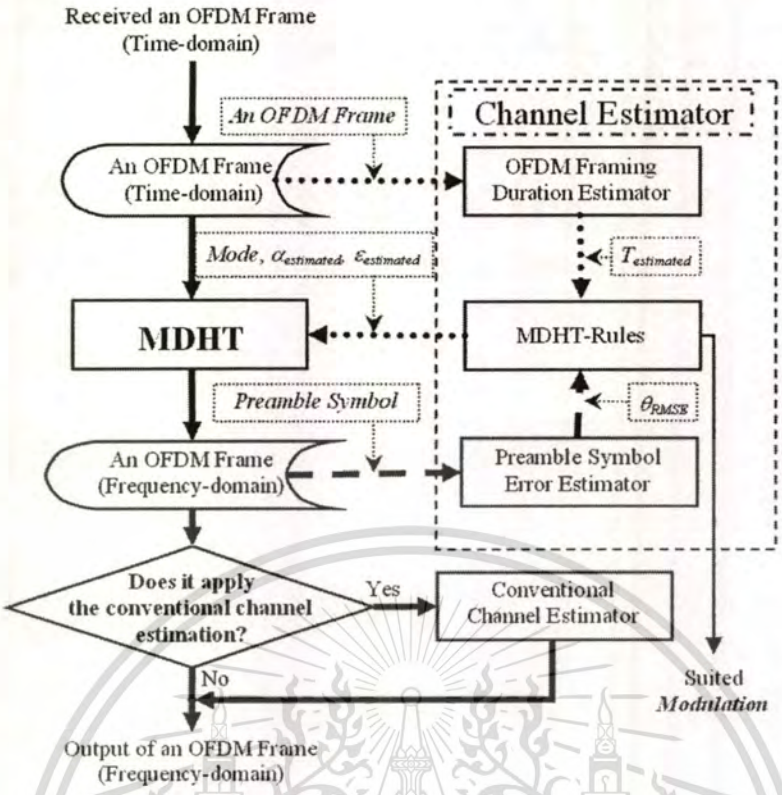

Figure 4.17 Data flow diagram of the proposed channel estimation for the MDHT-OFDM scheme at receiver

The Doppler scaling factor and the symbol timing offset should be known at receiver before the transformation. Our channel estimator can be performed in both time-domain and frequency-domain. The input time-domain OFDM signal will be sent to the channel estimator (OFDM Framing Duration Estimator) before the transformation. However, the input frequency-domain preamble symbol will be sent to the channel estimator (Preamble Symbol Error Estimator) after the transformation. For more detail, the brief flowchart of our proposed MDHT-OFDM scheme is shown in Figure 4.17.

4.4.1 OFDM Framing Duration Estimator

The OFDM framing duration estimator performs in the time-domain. Its function is to estimate the OFDM Framing Duration ($T_{estimated}$) in order to calculate the Doppler scaling factor ($\alpha_{estimated}$) and the symbol timing offset ($\varepsilon_{estimated}$). We use the $\alpha_{estimated}$ by means of f_D. The OFDM burst frame structure, containing L OFDM symbols, is used as shown in Figure 4.15. The postamble of our method is the preamble of the next frame. By correlating the received signal with the known preamble, the OFDM framing duration estimator estimates $T_{estimated}$ value. So, we call self-correlation. The computation step is shown as follows.

4.4.1.1 Self-Correlation

The correlating of the received signal and the known preamble is computed by the self-correlation function. Only the preamble and postamble of the received signals are considered. The self-correlation function is defined as follows

$$R_{AB}(lag) = xcorr(R_A, R_B), \tag{4.18}$$

where lag is the index of the self-correlation function, $\in [0, 2T_{tx} - 1]$. The $xcorr()$ is the cross-correlation function. The received signal of preamble and postamble is R_A. We define R_B as the known preamble which is in the time-domain. The result of the self-correlation function is shown in Figure 4.18(a).

4.4.1.2 The Desired Peak Signal

The desired peak *lag* search for $lag_{estimated}$ estimation. We consider the desired peak *lag* which can be searched by finding the peak magnitude. The range between the start peak *lag*

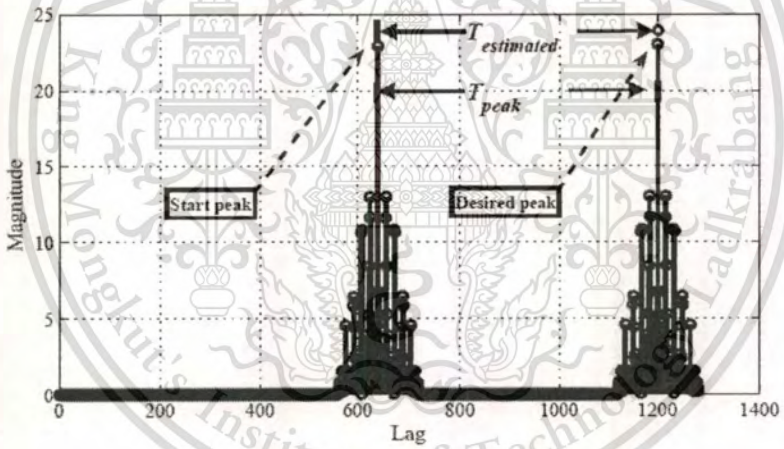

(a) Full scale in a frame.

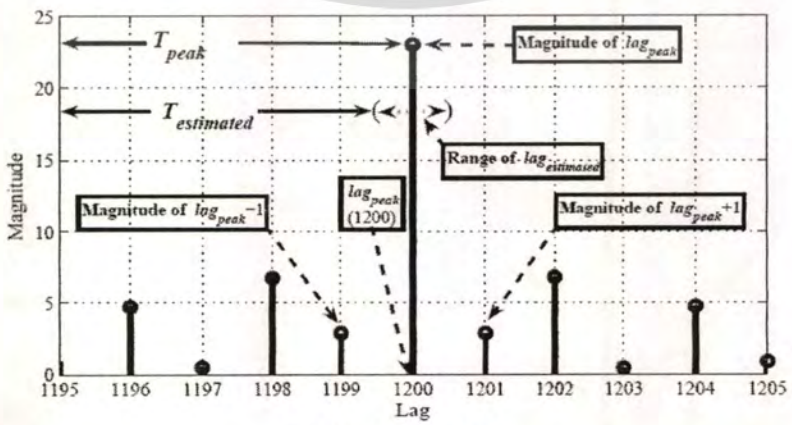

(b) Desired peak lag.

Figure 4.18 Self-Correlation of the OFDM frame

and the desired peak *lag* is T_{peak} as shown in Figure 4.18(a). We are interested in only two neighbor *lags* around the desired peak *lag* as shown in Figure 4.18(b). Then, the weight function is calculated. The weight function is applied by using the mass center concept. There are two parameters which are weights and positions. We define the weights as the magnitude of the interested *lags*, $\left|R_{AB}(lag_{peak}-1)\right|$, $\left|R_{AB}(lag_{peak})\right|$, and $\left|R_{AB}(lag_{peak}+1)\right|$. However, we consider the position of lag_{peak} which is defined as a center position, and the x_1 value is equal to 1. Then, the positions of two neighbor *lags* around lag_{peak} are defined as $x_0 \to 0\ (x_0 \neq 0)$, and $x_2 \to 2$. Therefore, if the value of x_0 and the value of x_2 are defined as tenths decimal point, then the positions of x_0 and x_2 are $x_0 = 0.1$ and $x_2 = 1.9$, respectively. Therefore, $lag_{estimated}$ can be estimated as follows

$$lag_{estimated} = \frac{\left(0.1\left|R_{AB}(lag_{peak}-1)\right| + \left|R_{AB}(lag_{peak})\right| + 1.9\left|R_{AB}(lag_{peak}+1)\right|\right)}{\left|R_{AB}(lag_{peak}-1)\right| + \left|R_{AB}(lag_{peak})\right| + \left|R_{AB}(lag_{peak}+1)\right|}, \qquad (4.19)$$

where $lag_{estimated}$ is $\Re^+$ and $0.5 \le lag_{estimated} \le 1.5$. Therefore, $T_{estimated}$ can be obtained by the different value between T_{peak} and $T_{estimated}$ where $T_{estimated}$ is $\Re^+$, T_{peak} is an integer as shown in the next step.

The Equation (4.19) is adopted for modifying the estimated peak *lag* obtained in step self correlation step because we would like to improve the accuracy of the OFDM framing duration($T_{estimated}$). We considered that the T_{peak} can be estimated by searching duration of two peak *lag* where T_{peak} is an integer, it can be improved by considering the relation of two neighbor *lag* magnitudes. Therefore, this can be obtained by employing the weight function. In this section we explain about how to estimate the OFDM framing duration ($T_{estimated}$). Basically, we can estimate the $T_{estimated}$ value by searching the T_{peak} value. In the case of without the effect of Doppler spread, the $T_{estimated}$ value is equal to the T_{peak} value which is the integer as shown in Figure 4.19.

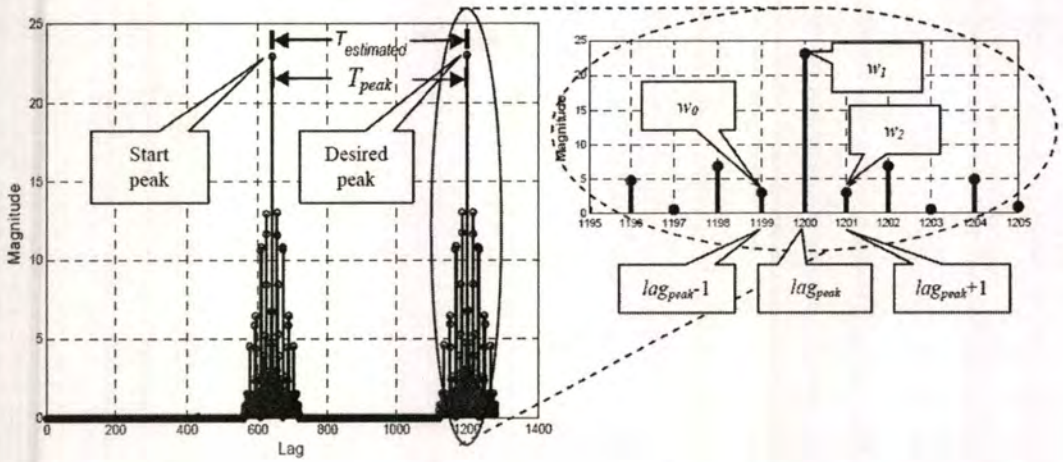

Figure 4.19 Self-Correlation of the OFDM frame without the effect of Doppler spread

In Figure 4.20, we show the self-correlation of the OFDM frame which is effected by the Doppler spread. The lag_{peak} is moved to another *lag*. The magnitude of neighbor *lags* around lag_{peak} is not the same value. Therefore, we considered that the $T_{estimated}$ can be improved by applying the weight function that we have proposed in this research. We consider only two neighbor *lags* around lag_{peak}, where lag_{peak} is *lag* index that obtained peak magnitude value.

The weight function is applied by using the mass center concept as shown in the left hand side of Figures 4.21 and 4.22, respectively. The weight function is a positive function, with weights w_0, w_1, and w_2 and the position x_0, x_1, and x_2. The position of w_1 is located at the center if the value of w_0 is equal to the value of w_2 as shown in Figure 4.21.

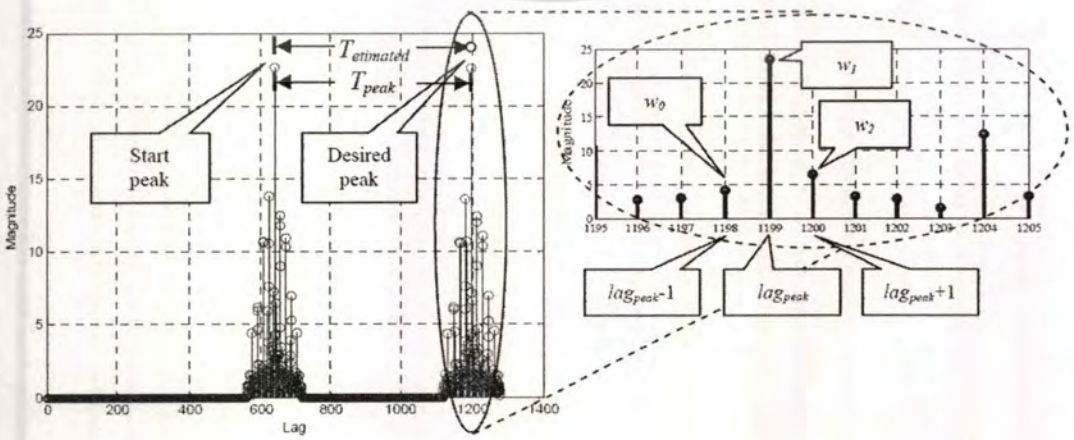

Figure 4.20 Self-Correlation of the OFDM frame cased by the Doppler spread

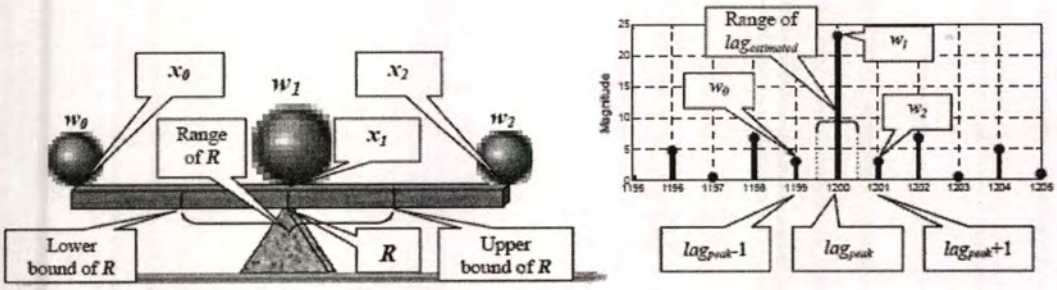

Figure 4.21 The concept of mass center using in weight function in the case of without the effect of Doppler spread

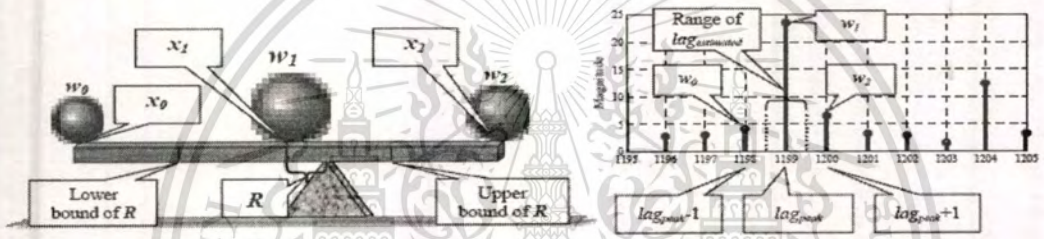

Figure 4.22 The concept of mass center using in weight function in the case of the effect of Doppler spread

According to Figures 4.21 and 4.22, the center of mass R of a system is defined as the average of their positions, x_i, weighted by their masses, w_i as shown in the following equation:

$$R = \frac{\sum_{i=0}^{I-1} w_i x_i}{\sum_{i=0}^{I-1} w_i}, \tag{4.20}$$

where I is the number of mass objects. We defined the position x_0, x_1, and x_2 are the constant, where $x_0 = 0.1\ (x_0 \to 0)$, $x_1 = 1$, and $x_2 = 1.9\ (x_2 \to 1.9)$. The weights are defined as magnitude of the self-correlation function.

Where $w_0 = \left|R_{AB}(lag_{peak}-1)\right| = \sqrt{\mathrm{Re}\left(R_{AB}\left(lag_{peak}-1\right)\right)^2 + \mathrm{Im}\left(R_{AB}\left(lag_{peak}-1\right)\right)^2}$,

$w_1 = \left|R_{AB}(lag_{peak})\right| = \sqrt{\mathrm{Re}\left(R_{AB}\left(lag_{peak}\right)\right)^2 + \mathrm{Im}\left(R_{AB}\left(lag_{peak}\right)\right)^2}$,

$w_2 = \left|R_{AB}(lag_{peak}+1)\right| = \sqrt{\mathrm{Re}\left(R_{AB}\left(lag_{peak}+1\right)\right)^2 + \mathrm{Im}\left(R_{AB}\left(lag_{peak}+1\right)\right)^2}$,

$R_{AB}(*)$ is the self-correlation function, and lag_{peak} is the desired peak *lag*.

Thus, we can estimate the position around lag_{peak} by using the weight function. Where R means the $lag_{estimated}$.

4.4.1.3 OFDM Framing Duration Estimation

In this step, $T_{estimated}$ is estimated. Due to the start peak *lag* is not changed to another *lag*, it will be stationed at the center position of self-correlation results. This *lag* position can be a constant which depends on signal samples. Therefore, $lag_{estimated}$ can be calculated by following equation

$$T_{estimated} = T_{peak} - (1 - lag_{estimated}), \tag{4.21}$$

where T_{peak} is the length of two peak *lag*, note that T_{peak} is equal to $T_{estimated}$ when two neighbor *lags* are equality values. The $T_{estimated}$ is then sent to the MDHT-Rules.

It is true that our channel estimation depends on two peak *lags*, but the first peak *lag* (start peak *lag*) is not changed to another *lag*, it will be stationed at the center position of the self-correlation results. This *lag* position can be a constant which depends on signal samples. So that, we consider only the second peak *lag* which called desire peak *lag*. The range between the first peak lag and the second peak *lag* is T_{peak}. Therefore, the value of $T_{estimated}$ can be calculated by Eq.(4.21) which uses T_{peak} as a reference values.

In the case of without effect of the Doppler spread as shown in Figure 4.21, the $lag_{estimated}$ value is equal to 1. So that, $T_{estimated}$ is equal to T_{peak}. In contrast, the self-correlation of the OFDM frame cased by the Doppler spread as shown in Figure 4.22, the magnitude of $lag_{peak}+1$ is heavier than $lag_{peak}-1$. Therefore, the $lag_{estimated}$ is moved to $lag_{peak}+1$ side, where the range value of the $lag_{estimated}$ is in the range of $1 < lag_{estimated} < 1.5$.

Equation 4.19 is adopted for modifying the estimated peak lag in order to improve the accuracy of $T_{estimated}$ by considering the relation of two neighbor *lags* magnitude. The magnitude of two neighbor *lags* and peak *lag* are weighed by using weight function which

applies center mass concept. Therefore, the relation between $T_{estimated}$ and T_{peak} is $T_{peak} - 0.5 < T_{estimated} < T_{peak} + 0.5$.

4.4.2 Preamble Symbol Error Estimator

The preamble symbol error estimator is the frequency-domain estimation, which is performed after taking MDHTOFDM. In this estimation, the root mean square error is estimated. This method requires the known preamble symbol as reference data.

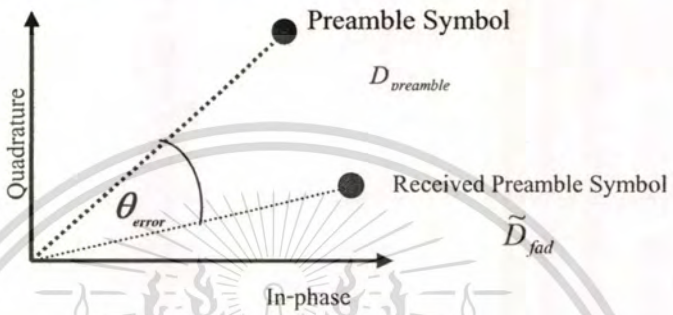

Figure 4.23 The idea of recovery data in the frequency-domain

Let $D_{preamble}$ denotes the known preamble symbol, $\widetilde{D}_{fad}$ and $\widetilde{D}_{error}$ is the received preamble symbol which is affected by fading. The error vector of the complex data can be expressed as

$$\widetilde{D}_{error} = \widetilde{D}_{fad} - D_{preamble}, \tag{4.22}$$

This equation indicates that we can estimate the angle error (θ_{error}). Therefore, we estimate the θ_{error} of the preamble symbol sequence as the root mean square error (RMSE) as shown in the following equation

$$\theta_{RMSE} = \sqrt{\frac{1}{P}\sum_{p=1}^{P}\left(\angle\left(\widetilde{D}_{fad}(p)\right) - \angle\left(D_{preamble}(p)\right)\right)^2}, \tag{4.23}$$

where θ_{RMSE} is the root mean square error of the angle error of the received preamble symbol sequence, $\widetilde{D}_{fad}$ denotes the received preamble symbols, $D_{preamble}$ is the known preamble symbol, p is the order of preamble symbols, and P is the number of preamble symbols, $\angle(\bullet)$ is the angle function of a complex number.

Therefore, the θ_{RMSE} is estimated for the modulation mapping scheme selection. The details of procedure will be described in the next subsection.

4.4.3 MDHT-Rules

The MDHT-Rules are the method to determine the MDHT-Parameters values which are suitable parameters for the MDHT-OFDM. The input values of the MDHT-Rules are obtained by the OFDM framing duration estimator and preamble symbol error estimator, which are $T_{estimated}$ and θ_{RMSE}, respectively. There are two situations that are needed to be considered. Firstly, when should the DFT-Mode or MDHT-Mode, be performed? Secondly, what kind of the modulation mapping scheme is suitable for the channel currently?

The mode of the MDHT-OFDM is selected by considering the channel characteristics.

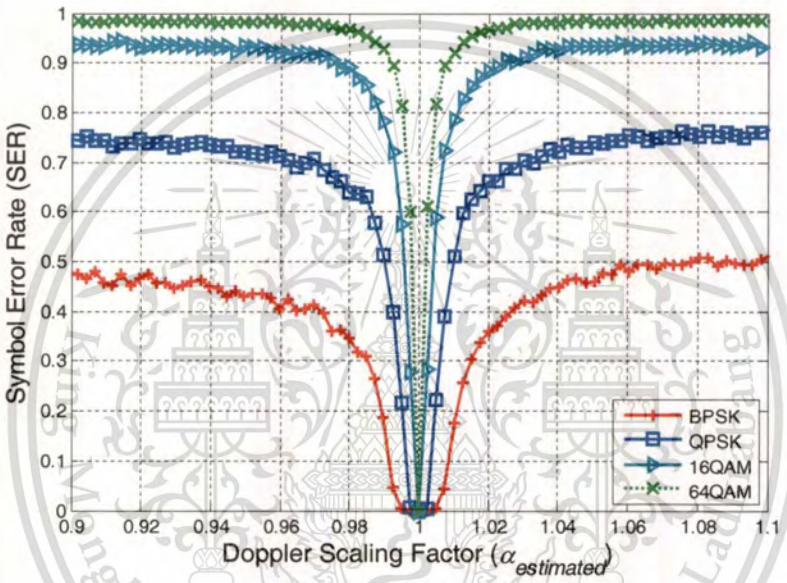

(a) DFT-Mode.

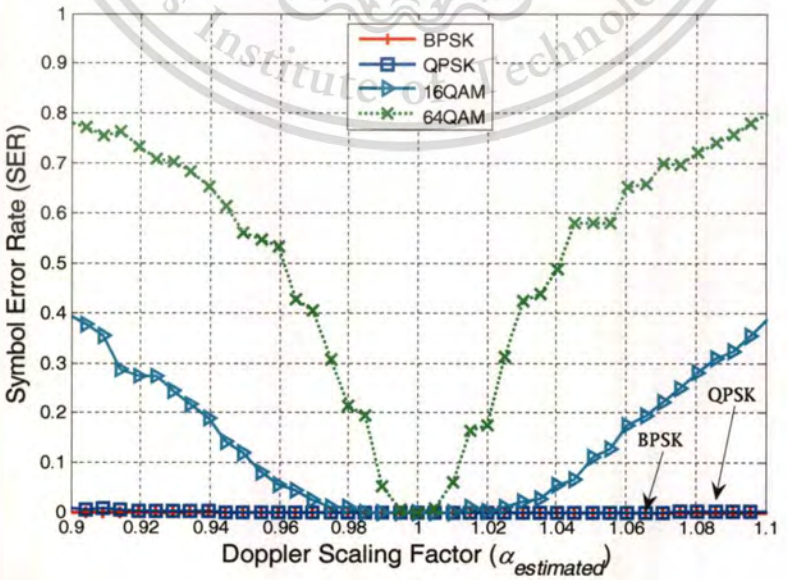

(b) MDHT-Mode.

Figure 4.24 The effective range of each mode for each modulation mapping scheme

According to the effect of the Doppler spread due to mobile unit movement, the waveform of the received signal is scaled in time. We consider the Doppler spread by means of the Doppler scaling factor ($\alpha_{estimated}$), which corresponds to the mobile movement speed. The Doppler scaling factor can be obtained by

$$\alpha_{estimated} = \frac{T_{estimated}}{T_{tx}}, \tag{4.24}$$

where $\alpha_{estimated}$ is the Doppler scaling factor, $T_{estimated}$ is the estimated timing duration of the received frame, and T_{tx} is the known timing duration of an OFDM frame. The $\alpha_{estimated}$ is employed to decide the mode of MDHT-OFDM and, used as the parameter of the MDHT-OFDM. Moreover, the mode of the MDHT-OFDM is also dependant on the modulation mapping scheme. Because each of modulation mapping scheme combats differently to the Doppler spread. Due to the proposed MDHT-OFDM transformation is a warped transformation which the OFDM signal is warped in time-domain before calculation to the frequency-domain. Therefore, the time-domain estimation can be applied as the parameters for the transformation. Those parameters allow the Doppler scaling factor can be implied in the time-domain sub-carriers manner. Thus, Eq.(4.16) and Eq.(4.17) are used as the warped function of the transformation for the DFT-Mode and the MDHT-Mode, respectively. Therefore, the OFDM signals can be compensated in time-domain by the mechanism of DMHT-OFDM transformation before transforming to the frequency-domain. Our time-domain channel estimation requires a long preamble symbol which is always used for frame synchronization in conventional OFDM systems. Thus, the pilot-aided in data symbol is not required for our proposed MDHT-OFDM scheme.

Based on simulation, we consider only the effect of Doppler spread to determine the threshold values so that the AWGN and multipath are ignored. The simulation parameters are

Table 4.3 The threshold values for the MDHT-Rules

Modulation Mapping scheme	**Doppler scaling factor ($\alpha_{estimated}$)**	
	Lower bound	**Upper bound**
BPSK	0.994	1.006
QPSK	0.9976	1.0024
16QAM	0.9992	1.0008
64QAM	0.9997	1.0003

set as follows. The number of sub-carriers is chosen to be N=64, and the length of cyclic prefix is 16. The BPSK, QPSK, 16QAM, and 64QAM modulation mapping schemes are adopted in each condition. The MDHT-OFDM transform is taken by each mode. In case of the MDHT-Mode, the perfect channel estimation is applied. The variation of Doppler spread is used by means of the Doppler scaling factor. In the simulation results, the SER of each modulation mapping scheme in the DFT-Mode and MDHT-Mode of the MDHT-OFDM scheme versus the Doppler scaling factor are shown in Figure 4.24 which demonstrate the effective range of each mode. According to Figure 4.24, we can achieve the threshold values as shown in Table 4.3 which are applied in the algorithm as shown in Figure 4.25. Due to the MDHT-Mode requires more computational complexity than the DFT-Mode. Therefore, in case of small Doppler effect, the DFT-Mode is performed in order to save mobile resource. Otherwise, the MDHT-Mode is performed. Figure 4.24(a) is used to determine when the MDHT-Mode should be performed. The threshold values of each modulation mapping scheme are chosen by considering the last

```
Call Doppler scaling factor estimator
if Modulation = BPSK then
    if α_lowBPSK ≤ α_estimated ≤ α_upBPSK then
        CurrentMode =DFT-Mode
    else
        CurrentMode =MDHT-Mode
    end if
else if Modulation = QPSK then
    If α_lowQPSK ≤ α_estimated ≤ α_upQPSK then
        CurrentMode =DFT-Mode
    else
        CurrentMode =MDHT-Mode
    end if
else if Modulation = 16QAM then
    if α_low16QAM ≤ α_estimated ≤ α_up16QAM then
        CurrentMode =DFT-Mode
    else
        CurrentMode =MDHT-Mode
    end if
else if Modulation = 64QAM then
    if α_low64QAM ≤ α_estimated ≤ α_up64QAM then
        CurrentMode =DFT-Mode
    else
        CurrentMode =MDHT-Mode
    end if
end if
if CurrentMode=MDHT-Mode then
    Call symbol timing offset estimator
else
    Set symbol timing offset to default values
end if
```


Figure 4.25 The mode decision algorithm of the MDHT-Rules

point of the Doppler scaling factor where the symbol error rate is still the zero value. The Doppler scaling factor is estimated according to Eq.(4.24). We define $\alpha_{lowBPSK}$, $\alpha_{lowQPSK}$, $\alpha_{low16QAM}$, and $\alpha_{low64QAM}$ as the lower bound values, define α_{upBPSK}, α_{upQPSK}, $\alpha_{up16QAM}$, and $\alpha_{up64QAM}$ as the upper bound values of BPSK, QPSK, 16QAM, and 64QAM, respectively. *Modulation* is the variable which is stored by the type of the modulation mapping scheme.

Each OFDM symbol in the OFDM frame is also affected by the Doppler spread. For that reason, the symbol timing offset of each OFDM symbol is also shifted so we call that "symbol timing offset" which can be express by the linear function as shown in the following equation

$$\varepsilon_{estimated}(l) = l\alpha_{estimated} - l, \tag{4.25}$$

where $\varepsilon_{estimated}(l)$ is the symbol timing offset of the $l-$th OFDM symbol, l is sequence of the OFDM symbol in a frame, which are [0, 1, 2, ..., L], and L is number of the symbol in a frame including a preamble symbol. According to Figure 4.25, the symbol timing offset estimator is estimated by using Eq.(4.25).

However, the suited modulation mapping scheme is selected by considering the θ_{RMSE}. The Doppler spread directly effects to the shifty angle of the received OFDM symbols. Hence, the algorithm in Figure 4.26 is employed for selecting the modulation mapping scheme. The preamble symbol error estimator is estimated by using Eq.(4.23). Selecting the modulation mapping scheme will be used in the next transmission. Finally, the MDHT-Parameters are sent to MDMTOFDM process which is performed adaptively.

```
Call Preamble symbol error estimator
if 0 ≤ θ_RMSE < π/22 then
    Modulation=64QAM
else if π/22 ≤ θ_RMSE < π/9 then
    Modulation=16QAM
else if π/9 ≤ θ_RMSE < π/4
    Modulation=QPSK
else
    Modulation=BPSK
end if
```

Figure 4.26 The modulation mapping scheme decision algorithm of the MDHT-Rules

Chapter 5

Performance Evaluations

This chapter presents the results of the computer simulation described in Chapter 3 and Chapter 4. Firstly, the performance evaluations by means of throughput on proposed adaptive cyclic prefix are presented. Secondly, the performance evaluations by means of symbol error rate on proposed Doppler spread mitigation are presented. The performance comparisons are done by comparing the proposed scheme and conventional scheme with several cases of each condition. We have employed MATLAB 6.0 to develop the simulator.

5.1 Performance Evaluations on Adaptive Cyclic Prefix under Multi-path Fading Environments

In this section, the throughput performance by means of computer simulation is evaluated, and compared them with that of conventional OFDM scheme. The performance evaluations of proposed adaptive cyclic prefix are separated as two considerations. First, we consider the throughput performance when the transceiver does not apply the location detector. Second parts, in contrast, we consider the throughput performance when the transceiver applies the location detector.

In these simulations, we use the parameters in the IEEE 802.11a standard. Table 5.1 shows the parameter values for the simulation. The channel estimation is assumed to be perfect channel estimation which knows at the receiver. Regarding the multi-path fading environments, the maximum delay spread will be varied in the range of 0 to 0.8 μs (0 to 16 point). The

Table 5.1 OFDM symbol parameters according to IEEE 802.11a

Parameter	Value
Channel Spacing	20 MHz
Number of FFT point	64
Number of Sub-carriers	52
Effective Symbol Duration	3.2 μs
Guard Interval	0.8 μs
Modulation	BPSK, QPSK, 16QAM, 64QAM

64QAM is applied in order to achieve the highest data rate. We assume that, if ISI occurs in a OFDM symbol, then the data will be lost or error all of this OFDM symbol.

Here, let us call the conventional OFDM that used fixed CP as "CCP". Let us call the adaptive cyclic prefix algorithms without location detector as shown in Figure 3.6 and Figure 3.7, and with location detector as shown in Figure 3.8 and Figure 3.9 as "ACP-1" and "ACP-2", respectively.

In simulation, all schemes are performed in the same channel conditions. The same multi-path fading channel will be used. The maximum delay spread randomly assigned ranged form 0 to 0.8 μs on each duration time. The Doppler spread and AWGN will be disregarded due to avoid another biased factor. The 64QAM is used for achieving the maximum data rate due to noise free. In the case of ISI occurs, the received data will be considered as zero in that OFDM symbol.

Let we now consider the simulation results in each comparison. In the first comparison, the CCP and ACP-1 are compared by means of normalized throughput. The simulation result is shown in Figure 5.1. We can realize that the normalized throughput of CCP is equal to 0.8, and not change. Sometime the normalized throughput of ACP-1 decreased lower than CCP due to the loss of data portion caused by ISI. But for overall, ACP-1 shows the better performance than CCP in term of average normalized throughput.

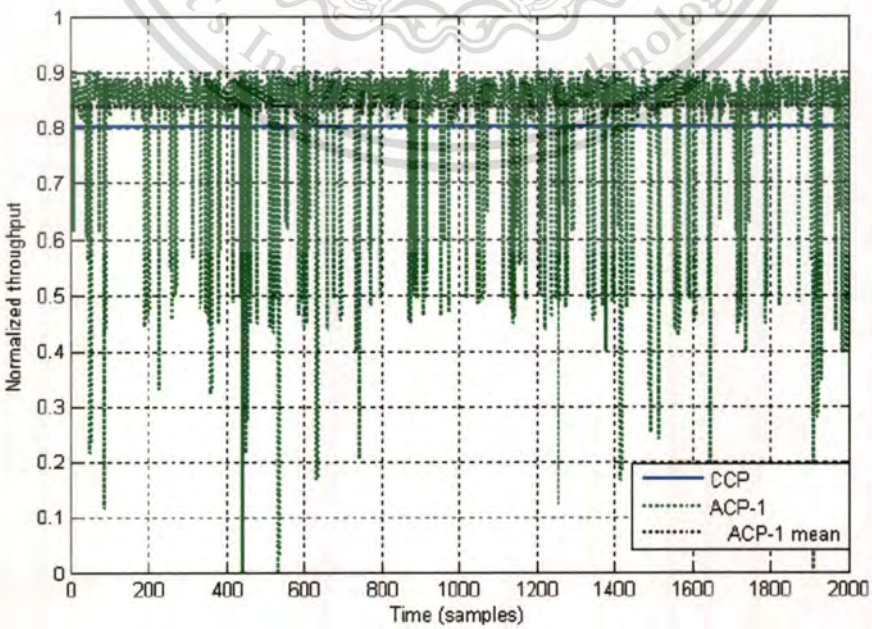

Figure 5.1 Normalized throughput without location detector

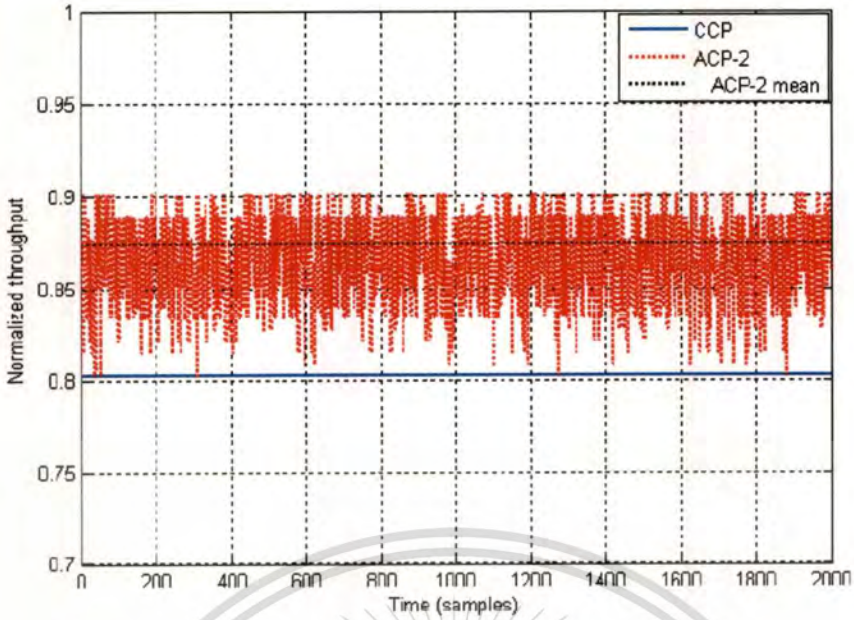

Figure 5.2 Normalized throughput with location detector

In the second comparison, the CCP and ACP-2 are also compared by means of normalized throughput. In this simulation, we would like to know that if the transceiver knows the situation that may cause the ISI beforehand, and then avoid it, how much the throughput can be achieved. The simulation result is shown in Figure 5.2. It shows that when the location detector is provided, the normalized throughput of ACP-2 increased obviously in comparing with CCP. This is due to the early informing of the location detector information that can avoid ISI beforehand. Moreover, in ACP-2, the transmitter stop its transmission when it changes the location, or the receiver immediately send NAK signal to transmission, then the new current ATD will be applied so that the loss of data due to ISI is avoided.

In the third comparison, we compare the throughput performance of ACP-1 and ACP-2. It is obvious that the performance of ACP-2 is better than ACP-1 as shown in Figure 5.3. In order to see how much performance difference among ACP-1, ACP-2 and CCP, we have illustrated their cumulative normalized throughputs by using Eq.(5.1) as shown in Figure 5.4.

Let $f_\rho(i)$ the density function of normalized throughput of OFDM symbol at time sample i, and n represents the consecutive integer value of time sample (where n =0, 1, 2, 3,….). Then the cumulative normalized throughput of OFDM symbols up to time sample n, i.e., $F_\rho(n)$ can be formulated as shown as follows

$$F_\rho(n) = \sum_{i=0}^{n} f_\rho(i). \tag{5.1}$$

Regarding Figure 5.4, we can see that, performances of ACP-1 and ACP-2 are about 5% and 9.4% better than CCP, respectively.

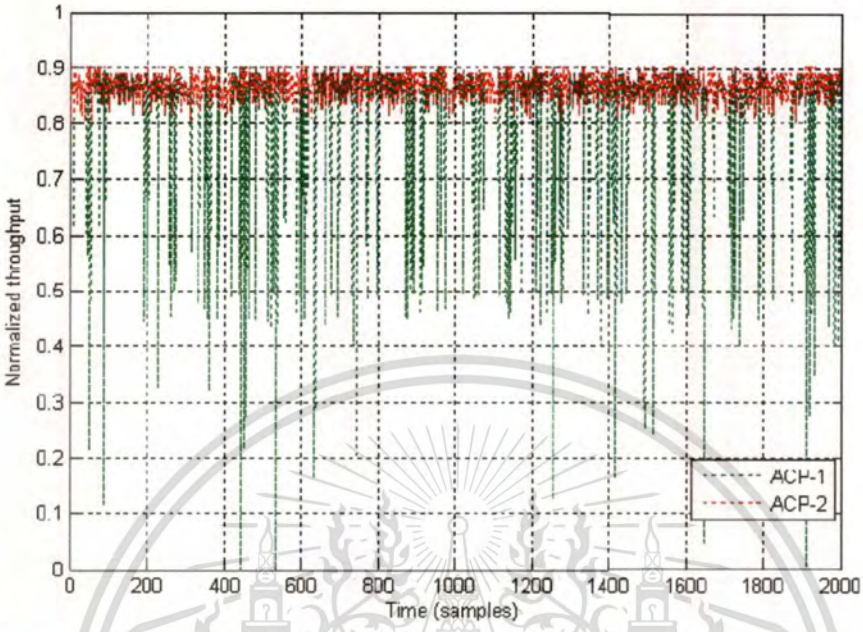

Figure 5.3 Normalized throughput comparison between ACP-1 and ACP-2

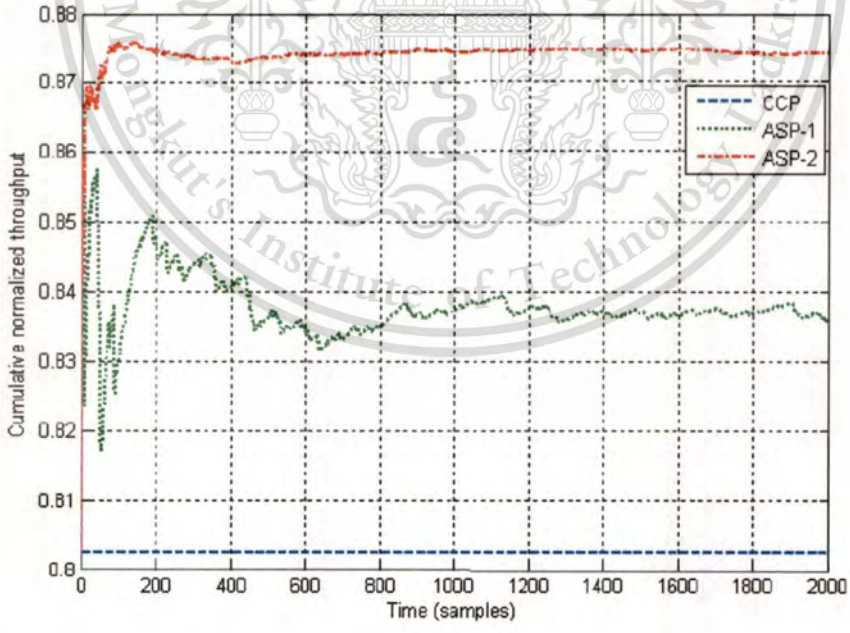

Figure 5.4 Cumulative normalized throughput of CCP, ACP-1, and ACP-2

5.2 Performance Evaluations on Doppler Spread Mitigation

We evaluated the performance of the proposed MDHTOFDM scheme by means of simulation. We focused on the effect of the Doppler spread according to mobile movement. We evaluated the performance of the MDHT-OFDM scheme in terms of the symbol error rate (SER) by comparing those of the conventional DFT-OFDM scheme. As for the channel model, we considered the COST 207 models. The simulation parameters are set as shown in Table 5.2.

Table 5.2 Simulation parameters

Parameter Name	Value
Number of *N* points	64
Length of Guard Interval	16
Modulation Mapping Scheme	BPSK, QPSK, 16QAM, 64QAM
Transformation	DFT, MDHT
Channel	COST 207 Model (rural area), AWGN channel

The OFDM frame is generated in the simulations as shown in Fig.5 which consist of 6 OFDM symbols and one preamble symbol. The long preamble symbol in standard 802.11a is applied for the preamble symbol in these simulations. In each OFDM symbol is generated by the channel model according to COST 207 rural area with 6-path channel model which is presented in [22]. The frequency-selective deterministic channel models are considered. The method of equal distance is used for the computation of the discrete Doppler frequencies and Doppler coefficients [22]. The carrier frequency is set to 5 GHz and the available channel bandwidth is 20 MHz. Sub-carrier spacing is 312.5 KHz. For Doppler spreads are approximate to -236 and 236 Hz, they correspond to mobile unit speed approximately 50 Km/hr and Doppler spreads are approximate to -474 and 474 Hz, they correspond to mobile unit speed approximately 100 Km/hr, respectively. The additive white Gaussian noise (AWGN) is included. The OFDM symbol interval and a guard interval are defined by 3.2 μs and 0.8 μs, respectively.

We separated the performance evaluation into four parts which are demonstrated by the SER performance comparison in each case as illustrated in the following subsections.

5.2.1 The Performance Comparisons for the Doppler Spread of Each Modulation Mapping Scheme

In order to compare the performance of the proposed MDHT-OFDM scheme with the conventional DFT-OFDM scheme in each modulation mapping scheme, in this simulation, we assume the perfect channel estimation that means the receiver knows the exact value of $T_{estimated}$. In this case, we would like to avoid the error of our time-domain channel estimation and compare our proposed MDHT-OFDM transformation with the traditional DFT-OFDM transformation without any the biased factor of channel estimation. The pilot-aided channel estimation is ignored. We consider three maximum Doppler frequency (f_D) values which are set at approximately -236, 0, and 236 Hz, respectively. The symbol error rate (SER) performances of each modulation mapping scheme versus the SNR are shown in Figure 5.5 to Figure 5.8. The simulation results show that the SER performances of the proposed MDHT-OFDM scheme and DFT-OFDM scheme have the same performance in the case of f_D is equal to 0. It means that the performance is the same when the Doppler effect is free. However, in these figures, it can be seen that comparing Figure 5.5, Figure 5.6, Figure 5.7 and Figure 5.8, the sensitiveness of the Doppler effect is 64QAM, 16QAM, QPSK, and BPSK, respectively.

However, in the conventional DFT-OFDM scheme, and the whole modulation mapping schemes, the SER performances are greatly degraded when increasing f_D. For small values of SNR, channel noise is the dominant factor that degrades the system performance. But, if the noise power reduces rapidly, the Doppler spread becomes the dominant degrading factor. Even when the SNR increases dramatically, the SER performances change slightly.

In contrast, the proposed MDHT-OFDM scheme, the SER performances degradation in 64QAM are more severe than that in 16QAM, QPSK, and BPSK, respectively, which can be improved by increasing the SNR values. In this case, the main dominant factors are the effects of multipath and AWGN.

Therefore, the perfect channel estimation is the time-domain channel estimation. Because of our proposed channel estimation performs in time-domain. In this point, we want to compare our time-domain channel estimation with the perfect one. The perfect channel estimation, the receiver knows exactly $T_{estimated}$. In this simulation, we apply the perfect channel estimation because we would like to compare our proposed MDHT-OFDM transformation with the traditional DFT-OFDM transformation without the biased factor of channel estimation to mitigate the Doppler spread as shown in Figure 5.5.

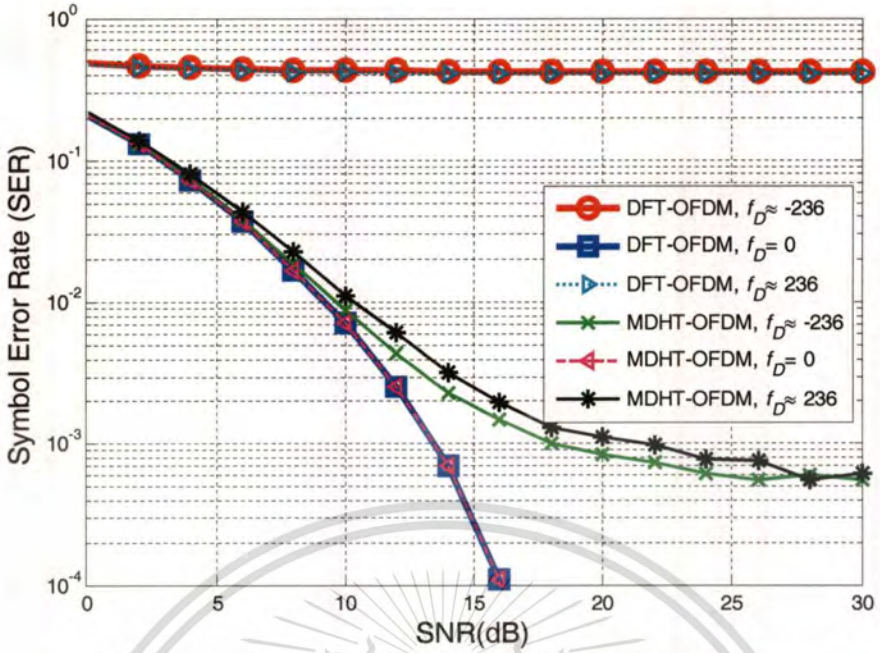

Figure 5.5 The performance comparisons of BPSK for the Doppler spread

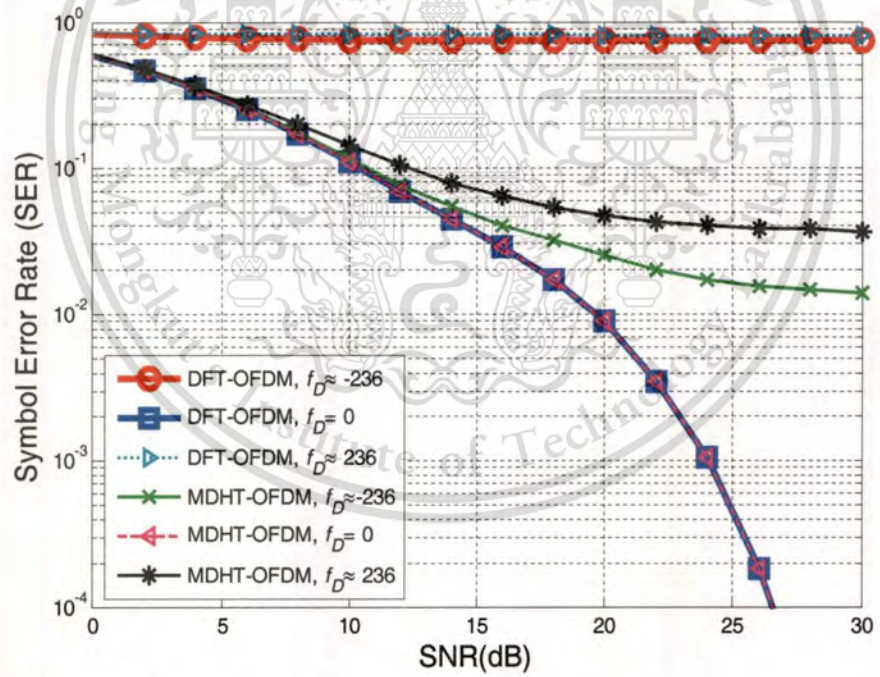

Figure 5.6 The performance comparisons of QPSK for the Doppler spread

In the simulation, the performance without pilot-aided channel estimation is shown. We would like to explain how to compensate data symbols without any channel knowledge. However, the conventional channel estimation performs in the frequency-domain which is affected from AWGN. We avoid the frequency-domain channel estimation, so that the proposed channel estimation is performed in time-domain. In order to compensate the data symbol,

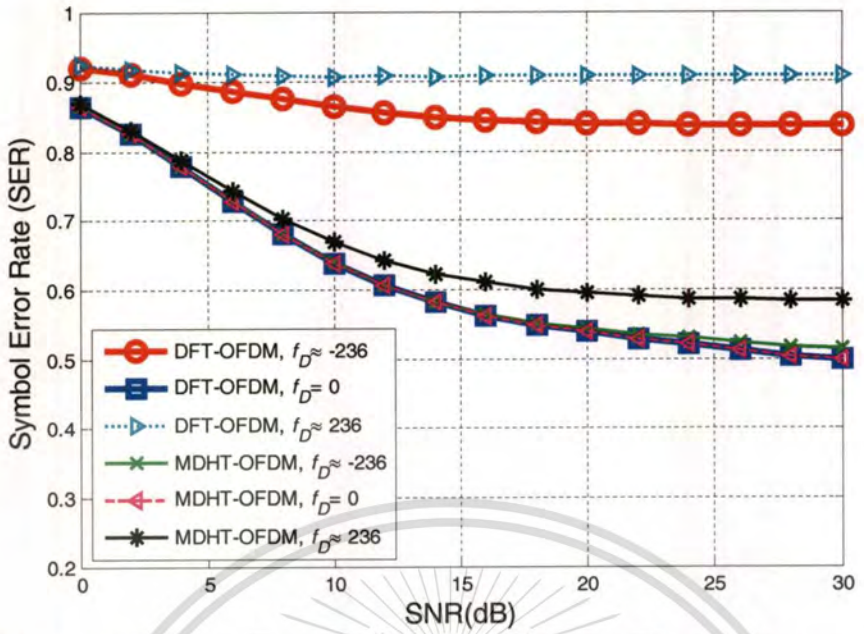

Figure 5.7 The performance comparisons of 16QAM for the Doppler spread

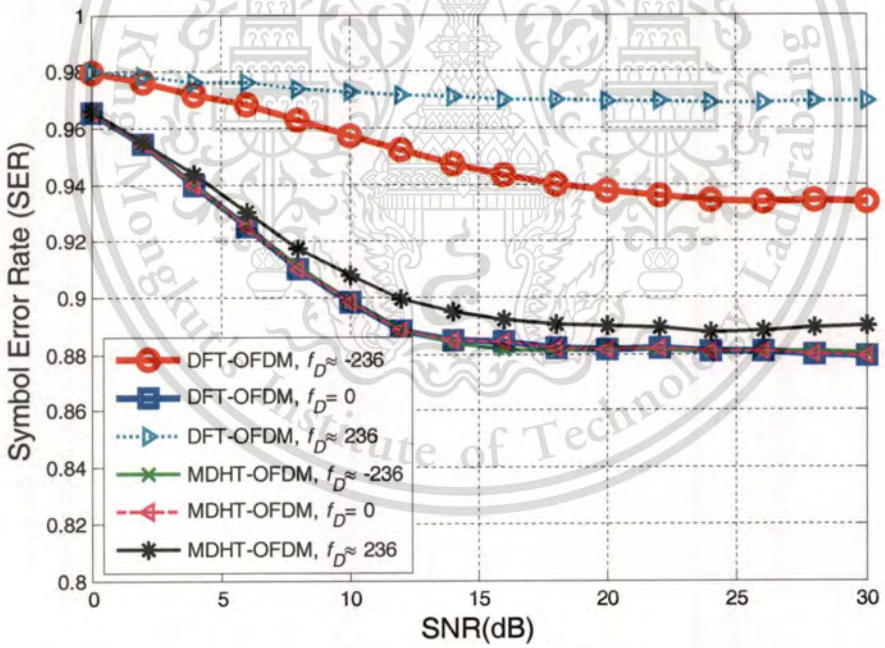

Figure 5.8 The performance comparisons of 64QAM for the Doppler spread

MDHT-OFDM transformation and time-domain channel estimation are performed as the cooperative process. Moreover, Doppler Effect can occur due to the movement of the mobile station. Therefore, each wavelength of sub-carrier is scaled because of the Doppler Effect. All wavelength of sub-carrier are scaled in the same scale in time-domain. Thus, the Doppler scaling factor is considered. The symbol timing offset is estimated in time-domain as well. Then, the Doppler scaling factor and symbol timing offset are sent to MDHT-OFDM

transformation as the MDHT-Parameters. The OFDM signal will be compensated in time-domain before transfer to the frequency-domain.

5.2.2 The Performance Comparisons of Channel Estimation for the Doppler Spread

In this simulation, we investigate the performances of the proposed channel estimation cooperating with MDHTOFDM. We compare the proposed channel estimation with the pilot-aided channel estimation of the conventional DFTOFDM scheme. The QPSK modulation mapping scheme is selected. We apply the block-type pilot-aided channel estimation for the conventional channel estimator as shown in Figure 5.9.

In this section, we would like to compare the proposed channel estimation (time-domain) and the conventional channel estimation (frequency-domain). First of all, we would like to note that the conventional channel estimation can be applied in our proposed MDHT-OFDM scheme as shown in Figure 4.17. If the conventional channel estimation is applied, the pilot-aided must be configured at the transceiver beforehand.

For the conventional channel estimation, we apply the block-type pilot-aided channel estimation as shown in Figure 5.9. The pilot-aided is classified into two types as follows:

· Type I: The pilot-aided are inserted to all sub-carrier in the OFDM symbol number 1 ($L = 1$) as shown in Figure 5.9(a).

• Type II: The pilot-aided are inserted to all sub-carrier in the OFDM symbol number 1 and 4 ($L = 1$ and $L = 4$) Figure 5.9(b).

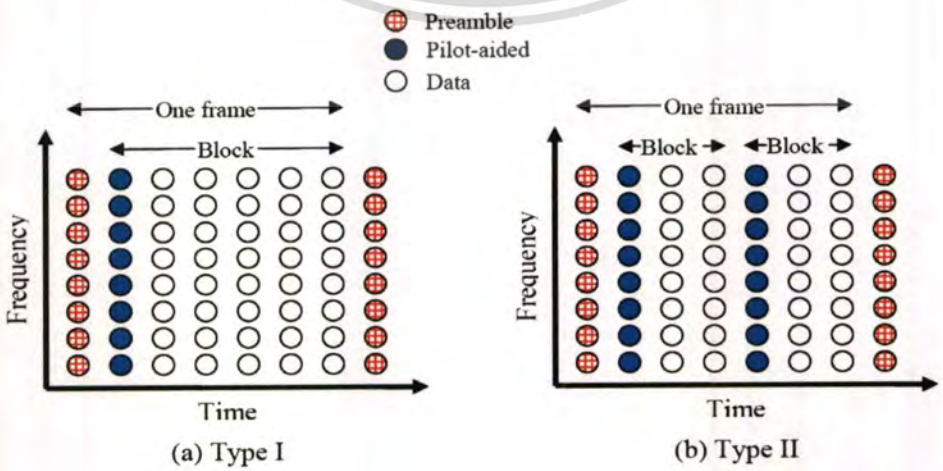

Figure 5.9 Block-type pilot-aided channel estimation of pilot-aided arrangement for conventional channel estimation

Table 5.3 The condition of the channel estimation

Condition	Scheme	Channel Estimation			
		Time-domain (Proposed Channel Estimation)		Frequency-domain (Conventional Channel Estimation)	
		Perfect CE	Proposed CE	Pilot-aided Type I	Pilot-aided Type II
Modulation QPSK $f_D \approx$ -236 Hz	DFT-OFDM				
	DFT-OFDM			✓	
	DFT-OFDM				✓
	MDHT-OFDM	✓			
	MDHT-OFDM	✓		✓	
	MDHT-OFDM	✓			✓
Modulation QPSK $f_D \approx$ -474 Hz	MDHT-OFDM	✓			
	MDHT-OFDM	✓		✓	
	MDHT-OFDM	✓			✓
	MDHT-OFDM		✓		
	MDHT-OFDM		✓	✓	
	MDHT-OFDM		✓		✓

The pilot-aided channel estimation is applied as the conventional channel estimation. So that, two pilot symbols are not used for generating $T_{estimated}$. But it is performed separately with our channel estimation. It performs independence. Because of the domain is difference. On the other hand, the preamble symbols are used for generating $T_{estimated}$.

However, we apply the pilot-aided channel estimation for only comparing with our proposed channel estimation as the following condition as shown in Table 5.3.

Figure 5.10 compares the SER performance of the proposed MDHT-OFDM scheme cooperating with the perfect channel estimation of the conventional DFT-OFDM scheme cooperated by pilot-aided channel estimation in the case of f_D approximately -236 Hz. The results show that the conventional DFT-OFDM scheme, the SER performance degradation is more severe than the proposed MDHT-OFDM scheme even when increasing the SNR values. The proposed MDHT-OFDM scheme can achieve better SER performance even the conventional DFT-OFDM scheme applies the pilot-aided channel estimation type II compared with those without applying any pilot- aided channel estimation.

We next carried out a comparison on the SER performance of the proposed MDHT-OFDM scheme cooperating with the proposed channel estimation and perfect channel estimation. In this simulation, the proposed MDHT-OFDM scheme is considered. We also apply the pilot-aided channel estimation to each channel estimation. We set the value of f_D too approximately -474 Hz. Figure 5.11 shows that the SER performances of the perfect channel and proposed channel estimation without any pilot-aided have slightly difference performances. Moreover, in the case of applying pilot-aided channel estimation Type I and Type II, the

performances are also slightly different, but it achieves better performance than those without pilot-aided.

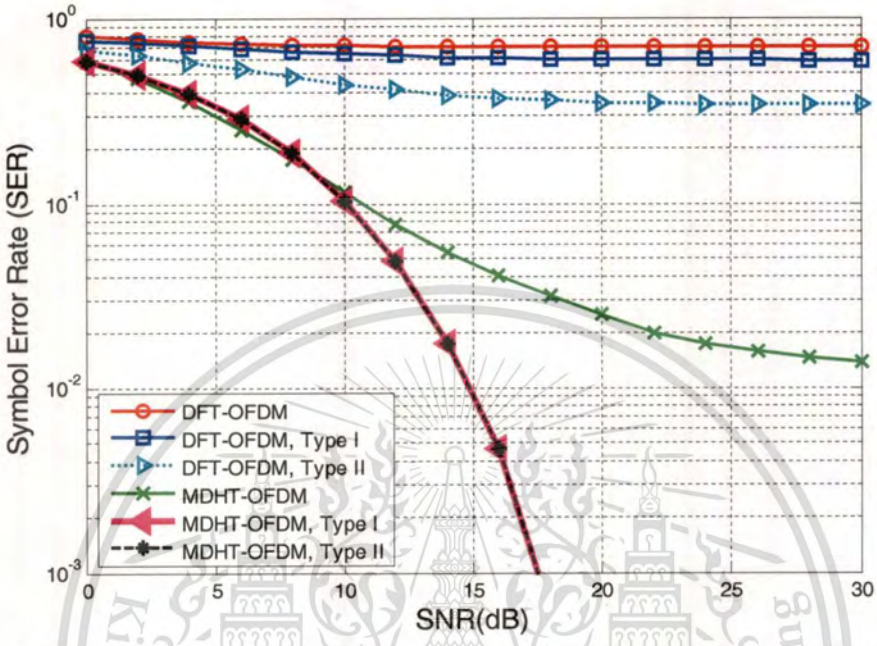

Figure 5.10 The performance comparisons for DFT-OFDM scheme and the MDHT-OFDM scheme cooperated with the perfect channel estimation, $f_D \approx -236$ Hz

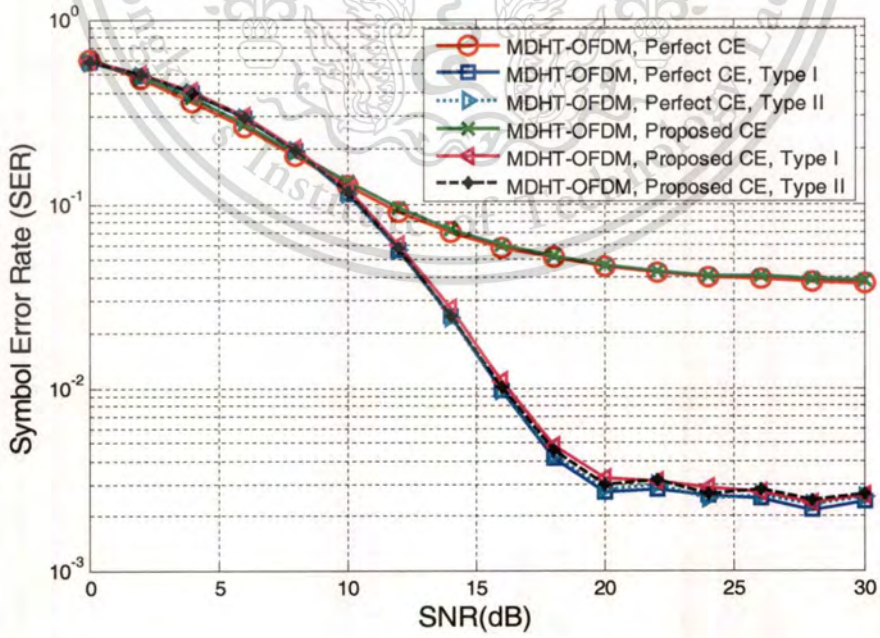

Figure 5.11 The performance comparisons for the MDHT-OFDM scheme cooperated with the proposed channel estimation and perfect channel estimation $f_D \approx -474$ Hz

5.2.3 The Performance Comparisons for the Variation of Doppler Spread

In this simulation, the variation of f_D is considered. The influence of the Doppler spread in the 6-path COST 207 model is investigated for each of channel estimation. We consider the average SNR at 20 dB and the modulation mapping scheme is QPSK. For comparison, first we investigated the SER performance of the conventional DFT-OFDM scheme and the proposed MDHT-OFDM scheme cooperating with perfect channel estimation, as shown in Figure 5.12. Second, we investigate the proposed MDHT-OFDM scheme cooperated with perfect channel estimation or propose channel estimation, as shown in Figure 5.13. Moreover, the pilot-aided is also applied.

Figure 5.12 shows that the SER performances of the DFT-OFDM and MDHT-OFDM are the same in the case of f_D equal to 0, this cause of the MDHT-OFDM performs in DFT-Mode, its performance is equivalent to the DFT-OFDM. However, the SER performances are improved in the case of applying the pilot-aided channel estimation as Type I or Type II, because the effected of multi-path fading is reduced by pilot-aided channel estimation. On the other hand, when f_D is not equal to zero, the SER performance of the DFT-OFDM scheme degrade even when pilot-aided channel estimation Type I and Type II are applied. In the case of the proposed MDHT-OFDM, it can greatly improve the SER performance, although the f_D is gathered, the proposed MDHT-OFDM can still achieve the SER performance better than the conventional DFT-OFDM scheme. However, the SER performances are slight changed in the case of the proposed MHT-OFDM applying the pilot-aided channel estimation as Type I or Type II. However, in cases of $f_D >$ zero (the mobile unit moves to the base station), the recovery processes of pilot-aided channel estimation Type I and Type II fail to recover the corrected data, maybe the effected of multi-path fading becomes random noise in which recovery data is not achievable.

Figure 5.13, The SER performance of the prefect channel estimation and proposed channel estimation are compared. As expected, the SER performances of the perfect channel estimation are slightly better than those of the proposed channel estimation. However, when the pilot-aided channel estimation as Type I and Type II are applied, the SER performances of those are slightly difference. However, in cases of $f_D >$ zero (the mobile unit moves to the base station), the proposed channel estimation is affected by multi-path fading, its performance is worse than the perfect channel estimation. The multi-path fading affects to the pilot-aided channel estimation as well.

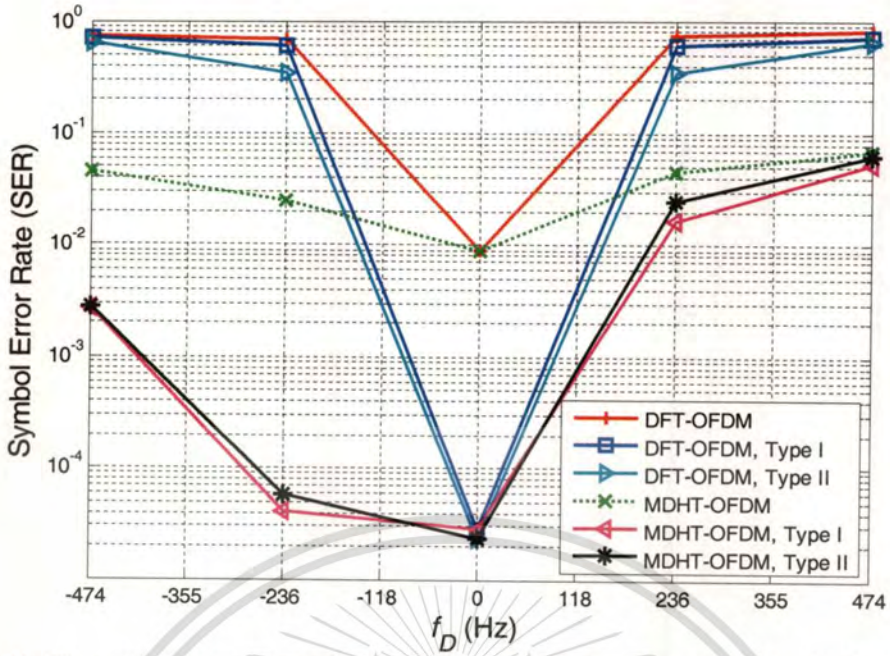

Figure 5.12 The performance comparisons of the DFT-OFDM scheme and the MDHT-OFDM scheme cooperated with the perfect channel estimation for the variation of Doppler spread

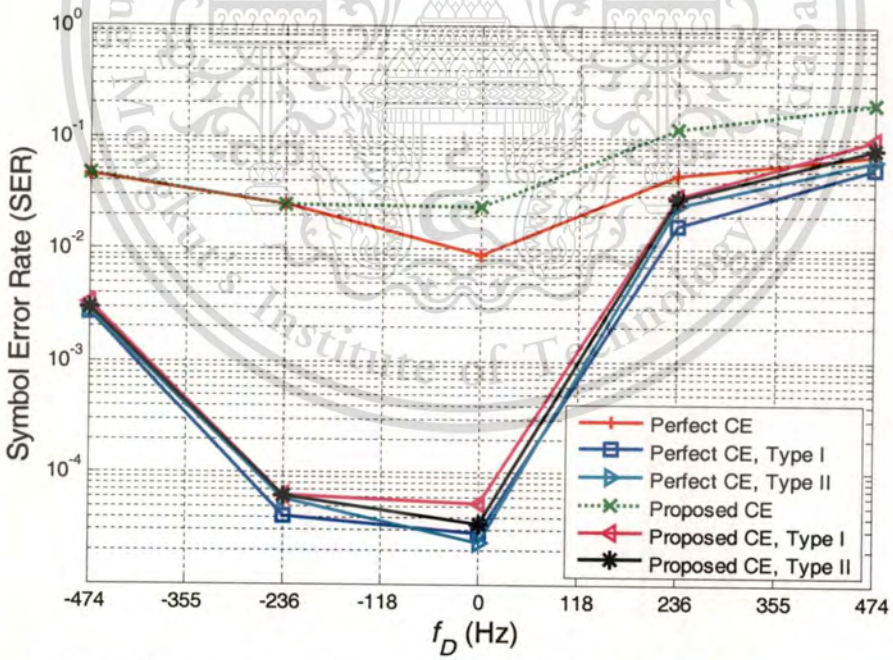

Figure 5.13 The performance comparisons of the MDHT- OFDM scheme cooperated with the proposed channel estimation and perfect channel estimation for the variation of Doppler spread

5.2.4 The Performance Comparisons for the Ordering of the OFDM Symbol in the Frame

In this simulation, we investigated the Doppler effect to the symbol timing offset of the OFDM symbol in the frame in each of channel estimation. We assume the frame synchronization is perfect, the f_D is approximately -236 Hz, and the modulation mapping scheme is QPSK. But, the synchronizations of each OFDM symbol are fixed to the values of the OFDM symbol interval. We consider the ordering of the OFDM symbol number 2 and 5.

In Figure 5.14 to Figure 5.16, we compare the conventional DFT-OFDM scheme, the proposed MDHT-OFDM scheme with perfect channel estimation, and the proposed MDHT-OFDM scheme with proposed channel estimation which are shown in Figure 5.14, Figure 5.15, and Figure 5.16, respectively.

In the conventional DFT-OFDM scheme as shown in Figure 5.14, we can see that when the ordering of the OFDM symbol is far away from the frame starting point, the SER performance is more degraded due to symbol timing offset errors. However, the SER performance can be improved by applying a higher level of the pilot-aided channel.

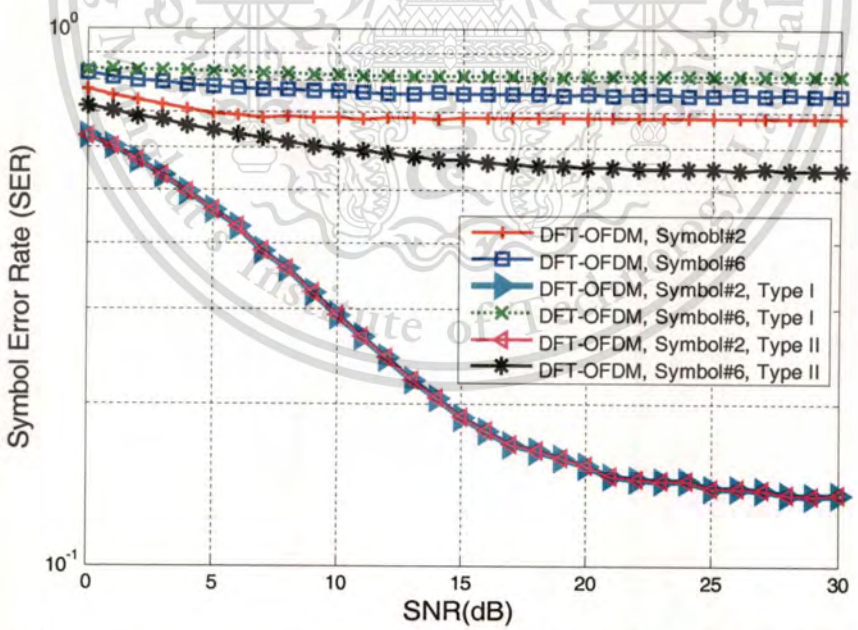

Figure 5.14 The performance comparisons of the DFT-OFDM scheme for the various ordering OFDM symbols

On the other hand, the proposed MDHT-OFDM scheme as shown in Figure 5.15 and Figure 5.16, the SER performances do not change much in the case of the ordering of the OFDM symbol. Moreover, the SER performances improve more after applying the pilot-aided channel. Furthermore, the SER performances of the proposed channel estimation are a bit lower than those of the perfect channel estimation.

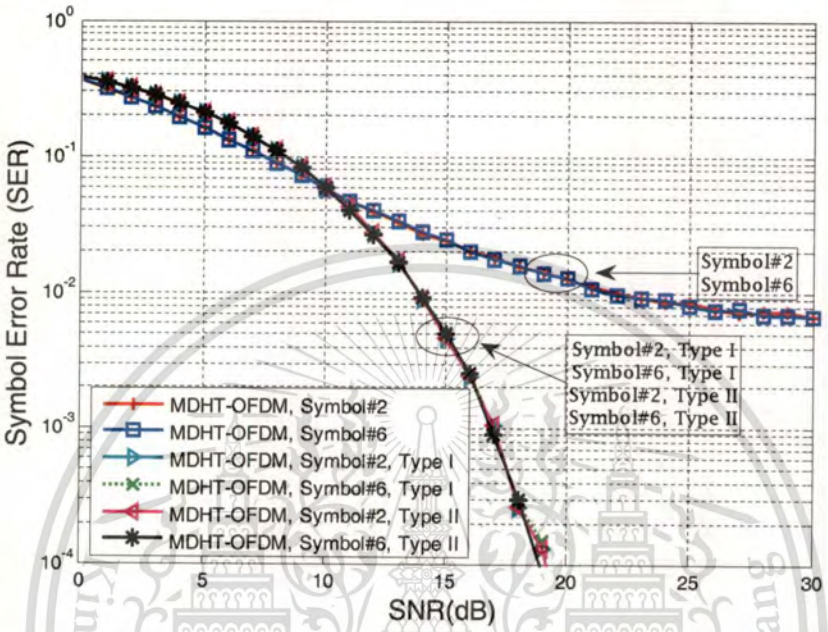

Figure 5.15 The performance comparisons of the MDHT-OFDM scheme cooperated with the perfect channel estimation for various ordering OFDM symbols

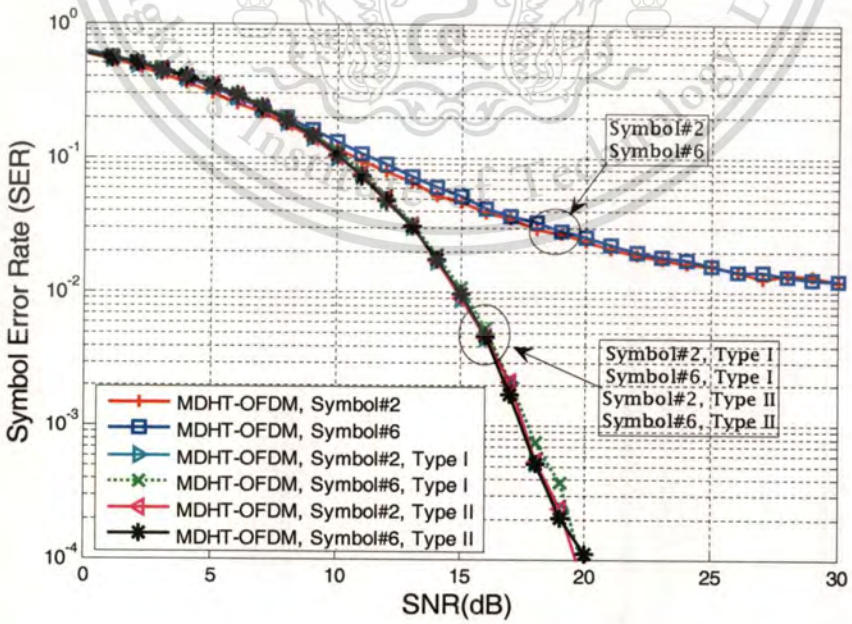

Figure 5.16 The performance comparisons of the MDHT-OFDM scheme cooperated with the proposed channel estimation for various ordering OFDM symbols

Chapter 6

Conclusions

Mobile communications is one of the fastest growing sectors of the telecommunication industry. In a mobile radio channel, the signal is disturbed by multi-path fading and Doppler effect. Due to the enormous growth of wireless services during the last decade, the need of a modulation technique that can transmit reliably high data rates at high bandwidth efficiency arises. OFDM has a bright future; it promises to emerge as the technology of choice in many next-generation wireless communication systems because it is very effective in combating multi-path fading. But one of its disadvantages is its sensitiveness to frequency offset. The sub-carriers orthogonality will be spoiled when the frequency offset exists. Frequency offset will be also cause inter-carrier interference (ICI) due to the Doppler effect caused by mobile movements, leading to the system performance to deteriorate drastically.

This thesis has proposed two schemes for wireless OFDM systems in mobile communications. Firstly, we have proposed the adaptive cyclic prefix for OFDM transmission under multi-path fading environments in order to improve the throughput performances. Secondly, we have proposed the Doppler spread mitigation using harmonic transform in order to mitigate Doppler effect caused by mobile movement. The conclusions of each scheme will be concluded as follows.

6.1 Adaptive Cyclic prefix under Multi-path Fading Environments

One of the enabling techniques for OFDM is the insertion of cyclic prefix. The cyclic prefix is used to mitigate the effects of inter-symbol interference (ISI) between OFDM symbols caused by multi-path fading. In conventional OFDM system, the cyclic prefix is fixed as constant values in which some unnecessary cyclic prefix portions are inserted. Due to the motion of mobile unit in mobile communication, the multi-path fading is varied depending on the environments. Therefore, if unnecessary cyclic prefix portions are removed, then, the throughput performance of the OFDM system will improve.

We have proposed a new algorithm to adjust the appropriate cyclic prefix for OFDM symbols which has been described in Chapter 3. The appropriate cyclic prefix is decided by considering with the real arrival time difference between OFDM symbol and its last arrival

fading at the receiver. The proposed method is performed cooperative with channel estimator in which to estimate the maximum delay time of multi-path fading environments. The appropriate cyclic prefix is adaptively adjusted corresponding the maximum delay time. We have considered that if we know beforehand the situations which cause ISI, we can avoid the ISI. Therefore, the movement of transceiver is considered. We separated as two parts. Firstly, the adaptive cyclic prefix method without the movement detector is proposed, in this case the transceiver does not know beforehand the ISI. Secondly, the movement detector is applied for the adaptive cyclic prefix method. The transceiver predicts the ISI, and then, avoidance of ISI.

With these approaches, the performance of OFDM signal transmission system in term of throughput is improved. That is because of the appropriate cyclic prefix can increase the data portion of OFDM symbol and decrease the number of loss that may be caused by the inter-symbol interference. The simulation results shown that the both of proposed adaptive cyclic prefix can achieve the throughput performances greater than or equal to the conventional cyclic prefix under multi-path fading environments.

6.2 Doppler Spread Mitigation Using Harmonic Transform

Due to mobile movement, the Doppler spread plays a significant problem in mobile communications. It introduces the frequency offset and symbol timing offset in which severely degrade the system performance. However, Conventional wireless OFDM systems employ the DFT in order to transform the signals which deteriorates the performance when the frequency components are time- varying. Therefore, we have considered that the transformation of wireless OFDM systems should be improved. Thus, the suited transformation for wireless OFDM systems in mobile communication is proposed.

We have proposed the modified discrete harmonic transform to perform in wireless OFDM systems in the presence of symbol error rate (SER) caused by the Doppler effect. The main objective of this research is to improve the performance of the transformation. We have also proposed the novel channel estimation which cooperates with the proposed transformation. Our channel estimation performs in time-domain in which achieve better estimated accuracy. We have shown the derivation of new equations for discrete harmonic transform and the new channel estimation which are suitable when we apply the harmonic transform for the signal transformation in the wireless OFDM systems. The MDHT-OFDM scheme strongly reduces the SER caused by the frequency offset and symbol timing offset due to Doppler effect. We have

presented the SER performances by means of a simulation for the comparison between the conventional DFT-OFDM scheme and the proposed MDHT-OFDM scheme. The results have shown that the proposed MDHT-OFDM scheme outperforms the DFT-OFDM scheme. Performance-wise, it can be concluded that MDHT-OFDM scheme is more suitable for mobile OFDM systems.

6.3 Discussion

The channel estimation for adaptive cyclic prefix can use any techniques that can be estimated the maximum delay. Moreover, if the bit error rate is still high in any case, the appropriate cyclic prefix length should be increased by the ratio of estimated maximum delay because its length is not long enough to combat the ISI. However, by removing the appropriate cyclic prefix at the receiver, the channel is converted to a circular convolution so that simple frequency-domain equalization can be adopted.

A key issue of adopting the MDHT-OFDM scheme is challenging computation, which is more complex than the conventional DFT-OFDM scheme. For the future work, the simpler implementation should be considered. However, the accuracy of channel estimation is very essential for the MDHT-OFDM scheme. To achieve the better system performance, the channel estimation and transformation can be operate. Hence, the channel estimation is one of the challenging issues.

In practical, our two proposed scheme, adaptive cyclic prefix and MDHT-OFDM scheme, can be worked together in OFDM system. The combination of both schemes is effortless. The most important factor is the time-domain parameters in which can be estimated by time-domain channel estimation. Since, the proposed channel estimations of both schemes can be performed in time-domain. Moreover, they perform based on correlation function, so that it comes naturally to jumble function as shown in Figure 6.1.

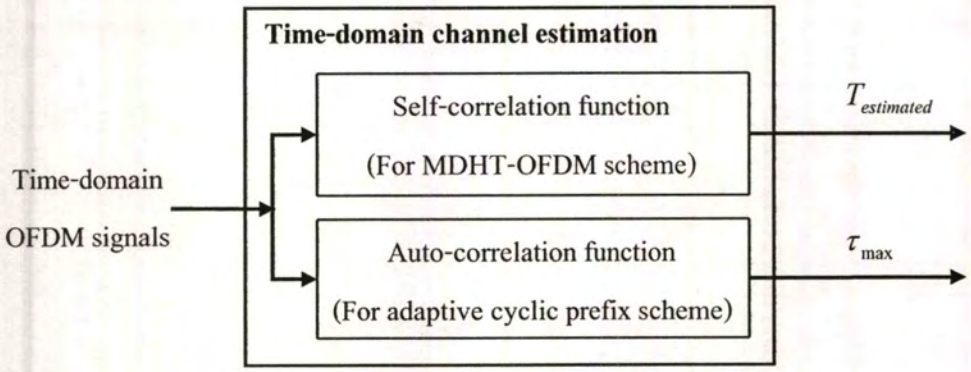

Figure 6.1 The time-domain channel estimation for the combination of the adaptive cyclic prefix scheme and the MDHT-OFDM scheme

REFERENCE

[1] RW. Chang,"**Synthesis of band-limited orthogonal signals for multichannel data transmission**," Bell Sys Tech J, pp 1775-1796.1966.

[2] RW. Chang,"**Orthogonal frequency division multiplexing,**" U.S. Patent no. 3488445, 1970.

[3] W. Shieh and I. Djordjevic,"**OFDM for Optical Communications**," California: Elsevier, 2010.

[4] S. Weinsten and P. Ebert,"**Data transmission by frequency-division multiplexing using the discrete Fourier transform**," IEEE Trans Commun., Vol.com.19, no.5, p 698-634, Octorber 1971.

[5] A. Peled and A. Ruiz,"**Frequency-Domain Data Transmission using Reduced Coputational Complexity algorithms**," IEEE Int Conf. on ICASSP 08, vol.5, pp.964-967, 1980.

[6] Radio broadcasting system,"**Digital Audio Broadcasting (DAB) to mobile portable and fixed receiver,**" ETS 300 401, ETSI-European Telecommunications Standards Institute, Valbonne, France, Feb, 1995.

[7] S. Saiyod, T. Chontong, R. Varakulsiripunth, and S. Thipchaksurate,"**Adaptive Cyclic Prefix under Multi-path fading environments**," Int. Conf. ICEAST 2007, Bangkok, Thailand, November 2007.

[8] T. Pollet, M.V. Bladel, and M. Moeneclaey,"**BER sensitiviy of ofdm systems to carrier frequency offset and wiener phase noise**," IEEE Trans. Commun.,vol.43,no.2/3/4, pp.191-193. Feb./March/April 1995.

[9] G. Mkrtchyan, K. Mori, and H. Kobayashi,"**Correction of ofdm signal form in time domain to reduce ici due to the Doppler spread and carrier frequency offset,**" IEICE Trans. Commun., vol.E88-B, no.1, pp. 122-133, Jan. 2005.

[10] S. Chen and T.Yao,"**Intercarrier interference suppression and channel estimation for ofdm system in time-varying frequency-selective fading channels**," IEEE Trans. Consum. Electron., vol.50, no.2, pp.429-435, May 2004.

[11] J. Van De Beek, M. Sandell, and P. Borjesson,"**ML estimation of time and frequency offset in ofdm system,**" IEEE Trans. Signal Process., vol.45, no.7, pp.1800-1805, July 1997.

[12] F. Zhang, G. Bi, and Y. Chen,"**Harmonic transform,**" IEE Proc. Vis., Image Process., vol.151, no.4, pp.257-263, Aug. 2004.

[13] R. Venkataramanan and K. Prabhu, "**Estimation of frequency offset using warped dft**," European J. Signal Processing, vol.86, pp.250-256, Feb. 2006.

[14] A. Makur and S. Mitra,"**Warped discrete-Fourier transform: Theory and applications**," IEEE Trans. Circuits Syst. I Fundam. Theory Appl., vol.48, no.9, pp.1086-1093, Sept. 2001.

[15] S. Saiyod, S. Thipchaksurat, and R. Varakulsiripunth, "**Signal Transformation using Hormonic transform based on OFDM**," Proc. ECTI-CON 2007, pp.911-914, Chiang Rai, Thailand, May 2007.

[16] S. Ghofrani, D. McLernon, and A. Ayatollahi, "**Weighted average instantaneous frequency based on adaptive signal decomposion**" 13th European Signal Processing Conf.(EUSIPCO2005), Antalya, Turkey, Sept. 2005.

[17] B. Boashash, "**Estimationg and interpreting the instantaneous frequency of a signal. II. Algorithms and applications**," Proc. IEEE, vol.80, no.4, pp.540-568, April 1992.

[18] L. Qu, A. Kot, and S.H. Lum, "**Comparative study of some discrete instantaueous frequency estimators**," Proc. IEEE Information Engineering, pp.608-612, July 1995.

[19] W. Nho and P. Loughlin, "**When is instantaneous frequency the average frequency at each time?**," IEEE Trans. Signal Process. Lett., vol.6, no.4, pp.78-80, April 1999.

[20] M. Sum and R. Scalbassi, "**Discrete-time instantaneous frequency and its computation**," IEEE Trans. Signal Process., vol.41, no.5, pp.1867-1880, May 1993.

[21] S. Saiyod, S. Thipchaksurat, and R. Varakulsiripunth,"**Doppler spread mitigation using harmonic transform for wireless OFDM systems in mobile communications**," IEICE Tran. Fundam, Vol.E93A, No.12, December 2010, pp.2634-2645.

[22] M. Patzold,"**Mobile Fading Channel**," John Wiley, Chichester, 2003.

[23] H. Schulze and C. Luders,"**Theory and Applications of OFDM and CDMA Wideband Wireless Communications**," John Wiley & Sons, Chichester, 2005.

[24] H. Harada and R. Prasad,"**Simulation and Software Radio for Mobile Communications**," Artech House, Boston, 2002.

[25] A. Goldsmith,"**Wireless Communications**," Cambridge University Press, New York, 2005.

[26] S. Hara and R. Prasad,"**Multicarrier Techniques for 4G Mobile Communications**," Boston: Artech House, 2003.

[27] Jr. Cimini,"**Analysis and simulation of ta Digital Mobile Channel Using Orthogonal Frequency Division Multiplexing**," IEEE Trans. Commun., Vol. COM-33, No,7, pp. 665-675, July 1985.

[28] M.J. Roberts,"**Signal and Systems: analysis using transform methods and MATLAB**," Mc Graw Hill, Singapore, 2003.

[29] G. Bi and Y. Zeng, "**Transforms and Fast Algorithms for Siganl Analysis and Representations**," Birkhauser, Boston, 2004.

[30] A. Bahai, B. Saltzerg, and M. Ergen,"**Multi-Carrier Digital Communications Theory and Application of OFDM**," Springer NewYork, 2004.

APPENDIX A.

ABBREVIATIONS

ABBREVIATIONS

OFDM	Orthogonal Frequency Division Multiplexing
LOS	Line-of-Sight
3G	Third Generations
4G	Fourth Generations
ISI	Inter-symbol Interference
GI	Guard Interval
CP	Cyclic Prefix
$\tau_{\max}$	Maximum Delay Spread
ACP	Appropriate Cyclic Prefix
ICI	Inter-Carrier Interference
SNR	Signal-to-Noise Ratio
MCM	Multi-Carrier Modulation
T_{FFT}	Time Duration of FFT
DFT	Discrete Fourier Transform
IDFT	Inverse Discrete Fourier Transform
IFFT	Inverse Fast Fourier Transform
FFT	Fast Fourier Transform
VLSI	Very large-scale integrated
DAB	Digital Audio Broadcasting
DVB	Digital Video Broadcasting
WiMax	Wireless Metropolitan Area Networks
ADSL	Asymmetric Digital Subscribe Line
ITU	International Telecommunication Union
LTE	Long-Term Evolution
f_D	Doppler Spread
CE	Channel Estimation
AWGN	Additive White Gaussian Noise
$\phi_u(*)$	Unit Phase Function of *
$\phi'_u(*)$	Derivative of Unit Phase Function of *
MDHT	Modified Discrete Harmonic Transform

IMDHT	Inverse Modified Discrete Harmonic Transform
$T_{estimated}$	OFDM Framing Duration
$\alpha_{estimated}$	Doppler Scalling Factor
$\varepsilon_{estimated}$	Symbol Timing Offset
θ_{RMSE}	Root Mean Square Error of Preamble Symbol
DSC	Digital Cellular System
UMTS	Universal Mobile Telecommunications System
MBS	Mobile Broadband System
IMT	International Mobile Telecommunications
α_n	Angle of Arrival
$f_{\max}$	Maximum Doppler Frequency
f_0	Carrier Frequency
f_n	Doppler Frequency of n Arrival
v	Speed of Mobile Unit
c_0	Speed of Light
WGN	White Gaussian Noise
$v_i(t)$	Linear Time-Invariant Filter
$H_i(f)$	Transfer Function
$\mu(t)$	Zero-Mean Complex Gaussin Random Process
$\mu_i(t)$	Stochastic Gaussian Random Process
$\hat{\mu}_i(t)$	Stochastic Process
$\tilde{\mu}_i(t)$	Real Deterministic Process or Deterministic Function
MED	Methods of Equal Distances
$S_{\mu_i\mu_i}(f)$	Power Spectral Density
$c_{i,n}$	Doppler Coefficients
$f_{i,n}$	Discrete Doppler Frequencies
$\theta_{i,n}$	Discrete Phases
Gcd	Greatest Common Divisor
COST	European Cooperation in the Field of Scientific and Technical Research
CEPT	Conference of European Posts and Telecommunications Administrations
GSM	Global System for Mobile
RA	Rural Area
TU	Typical Urban

BU	Bad Urban
HT	Hill Terrain
WSSUS	Wide-Sense Stationary Uncorrelated Scattering
$S_{\tau'\tau'}(\tau')$	Delay Power Spectral Density Function
$p_{\tau'}(\tau')$	Probability Density Function
$S_{\mu\mu}(f)$	Doppler Power Spectral Densities of Stochastic
$\widetilde{S}_{\mu_i\mu_i}(f)$	Dopper Power Spectral Density of Deterministic
τ'	Propagation Delays
$\widetilde{h}(\tau',t)$	Time-Variant Impulse Response
$\widetilde{a}_\ell$	Delay Coefficients
$\widetilde{\tau}'_\ell$	Discrete Propagation Delays
$\widetilde{\mu}_\ell(t)$	Deterministic Gaussian Processes
ℓ th	Discrete Propagation Path
$N_{i,\ell}$	Number of Harmonic Function
US	Uncorrelated Scattering
DGUS	Deterministric Gaussian Uncorrelated Scattering
f_{corr}	Coherence Bandwidth
PDF	Probability Density Function
$s(t)$	Transmitted Signal
$r(t)$	Received Signal
$w(t)$	Additive White Guasian Noise Function
PSD	Power Spectrum Density
s_k	Complex Transmit Symbols
ϕ_k	Phase Value
d_k	Information Data Sequence
TDM	Time Division Multiplexing
FDM	Frequency Division Multiplexing
f_c	Center Frequency
T_c	Carrier Signal Period
N_{NC}	Number of Carrier
T_{symbol}	Symbol Period
T_s	OFDM symbol Period
T_g	Guard Interval

T_{total}	Combination of OFDM Symbol Period and Guard Interval
$c_t(t)$	Frequency of Fundamental
$c_k(t)$	Frequency of kth Harmonic Component
HT	Harmonic Transform
FT	Fourier Transform
ATD	Arriveal Time Difference
I	In-phase Part
Q	Quadrature Part
BPSK	Binary Phase Shift Keyiing
QAM	Qudrature Amplitude Modulation
ASK	Amplitude Shift Keying
AM	Amplutude Modulation
A	Amplitude
A_p	Complex Amplitude
τ_p	Propagation Delays
P	Number of Received Multipath
δ	Dirac Delta Function.
BER	Bit Error Rate
ETS	Echo Test Signal
T_{rms}	RMS Delay Spread
Po	Power of Each Impulse
TNA	Timeout for the Next Adjusting
T_{TNA}	Timeout of the Next Adjustiong Period
GPS	Global Positioning System
$T_{estimated}$	Estimated OFDM Framing Duration
$\alpha_{estimated}$	Estimated Doppler Scaling Factor
$\varepsilon_{estimated}$	Estimated Symbol Timing Offset
λ	Signal Wavelength
T_C	Coherence Time
$\phi_{mu}(*)$	Modified Unit Phase Function of *
$f_{IF}(t)$	Instantaneous Frequency Function of Time t
lag	Index of Self-Correlation Function,
$xcorr(*)$	Cross-Correlation Function of *

R_A	Received Signal of Preamble and Postamble
R_B	Known Preamble in Time-Domain
$lag_{estimated}$	Desired Peak *lag*
T_{peak}	Range between the Start Peak *lag* and the $lag_{estimated}$
$T_{estimated}$	Estimated OFDM Framing Duration
w_0	Weight Function of Left Side
w_1	Weight Function of Center
w_2	Weight Function of Right Side
x_0	Position of w_0
x_1	Position of w_1
x_2	Position of w_2
$D_{preamble}$	Known Preamble Symbol
$\tilde{D}_{fad}$	Received Preamble Symbol
$\tilde{D}_{error}$	Error Vector of Complex Data
T_{tx}	Known Timing Duration of an OFDM Frame
SER	Symbol Error Rate
$\alpha_{lowBPSK}$	Lower Bound Value of Doppler Scaling Factor of BPSK
$\alpha_{lowQPSK}$	Lower Bound Value of Doppler Scaling Factor of QPSK
$\alpha_{low16QAM}$	Lower Bound Value of Doppler Scaling Factor of 16QAM
$\alpha_{low64QAM}$	Lower Bound Value of Doppler Scaling Factor of 64QAM
α_{upBPSK}	Upper Bound Value of Doppler Scaling Factor of BPSK
α_{upQPSK}	Upper Bound Value of Doppler Scaling Factor of QPSK
$\alpha_{up16QAM}$	Upper Bound Value of Doppler Scaling Factor of 16QAM
$\alpha_{up64QAM}$	Upper Bound Value of Doppler Scaling Factor of 64QAM

APPENDIX B.

List of Publications

International Conference

[1] S. Saiyod, S. Thipchaksurat, and R. Varakulsiripunth,"Signal Transformation using Hormonic transform based on OFDM," Proc. ECTI-CON 2007, pp.911-914, Chiang Rai, Thailand, May 2007.

[2] S. Saiyod, T. Chontong, R. Varakulsiripunth, and S. Thipchaksurate,"Adaptive Cyclic Prefix under Multi-path fading environments," Int. Conf. ICEAST 2007, Bangkok, Thailand, November 2007.

International Journal

[1] S. Saiyod, S. Thipchaksurat, and R. Varakulsiripunth,"Doppler spread mitigation using harmonic transform for wireless OFDM systems in mobile communications," IEICE Tran. Fundam, Vol.E93A, No.12, December 2010, pp.2634-2645.

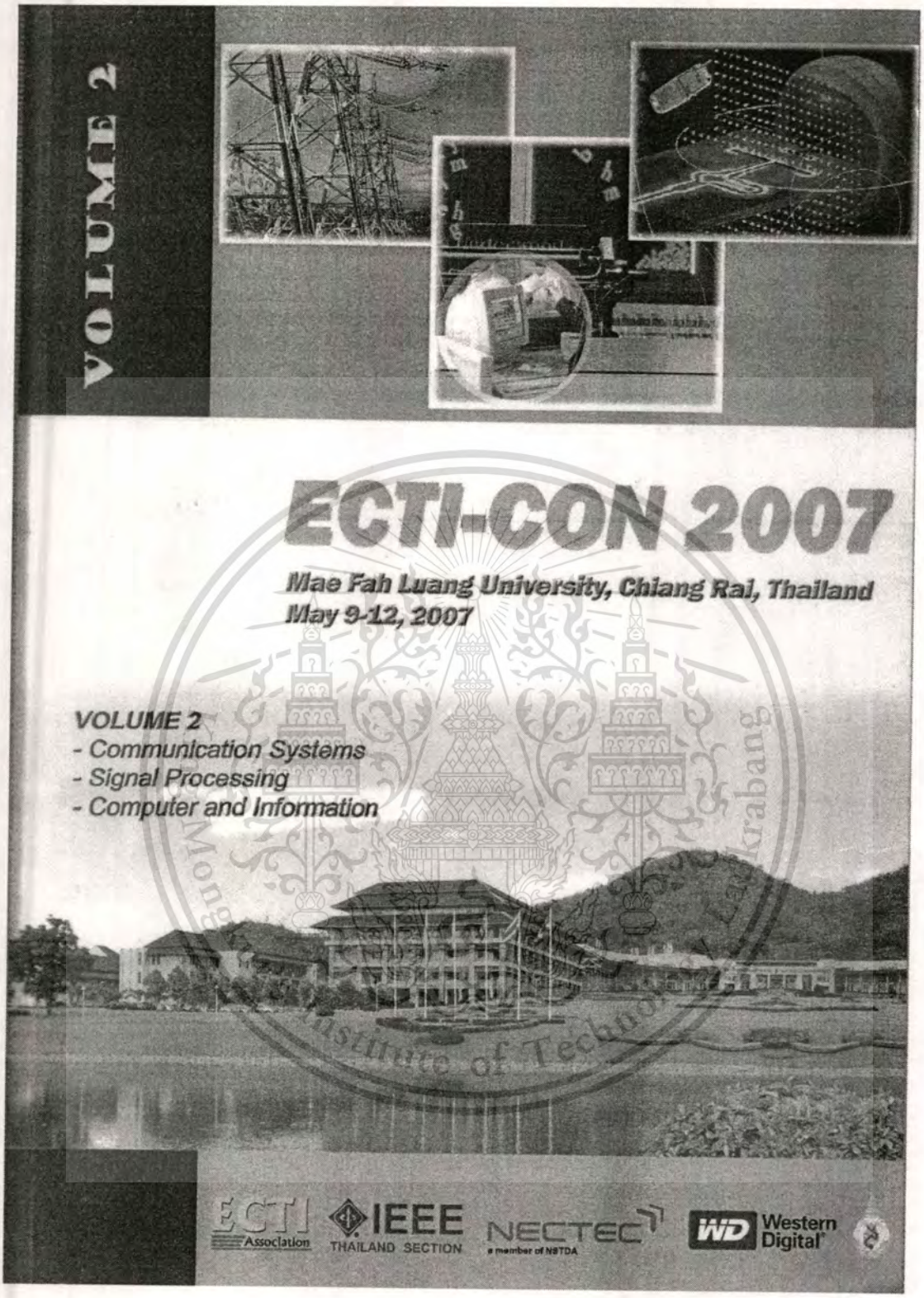

Signal Transformation Using Harmonic Transform Based on OFDM

Saiyan SAIYOD, Sakchai THIPCHAKSURAT, and Ruttikorn VARAKULSIRIPUNTH
Faculty of Engineering and Research Center for Communication and Information Technology (ReCCIT)
King Mongkut's Institute of Technology Ladkrabang (KMITL), Bangkok, Thailand
Email: {s8060055, ktsakcha, kvruttik}@kmitl.ac.th

***Abstract*- In this paper, we propose a new transformation for orthogonal frequency division multiplexing (OFDM) systems with Harmonic transform. The main idea of our research is to improve performance of estimating a small frequency offset in a signal with a large carrier frequency. The most appealing feature of OFDM is the simplicity of the receiver design due to the efficiency of frequency offset. OFDM can cope with the effects of frequency-selective multipath channels. OFDM is more sensitive to carrier frequency offset than the one of single-carrier systems. To solve those problems, the Harmonic transform can be applied. In this paper, we evaluate the performance of our proposed system in the terms of the accuracy of estimation and computational complexity. Finally, we show the improvement of our purposed system comparing with the conventional fast-Fourier transform (FFT).**

***Keywords*-OFDM, Fourier transform, Harmonic transform**

I. INTRODUCTION

Use of wireless access to the Internet has exploded in recent years with appearance of mobile Internet access services such as wireless LAN (WLAN) systems. In the near future people will demand much higher data rate in wide coverage to transfer large data files or enjoy high quality video streaming anytime anywhere.

OFDM is well known for its sensitivity to the time and frequency offset [1], [2]. There have been several papers on the subject of synchronization for OFDM in recent year. Moose gives the maximum likelihood estimator for the carrier frequency offset which is calculated in the frequency domain after taking the FFT [3], [4], [5], [6].

In the problem of frequency offset estimation, there have been proposed in [7], [8], [9] for warped discrete Fourier transform (WDFT). It is efficient to resolve closely spaced sinusoids. Harmonic transform (HT) [10] is a new method of spectrum analysis. This paper, we use this method to transform the signal.

The rest of the paper is organized as follows. We consider the OFDM system model and problem definition in section II, while section III illustrates main idea of Harmonic transform. We develop the Harmonic transform based on OFDM in section IV. In selection V, we discuss on results for computation complexity of proposed receivers, with Fourier transform and Harmonic transform. Finally, in section VI, some conclusions are drawn.

II. OFDM SYTEM MODEL AND PROBLEM DEFINITION

A. *OFDM System Model*

Firstly, we introduce some basic of OFDM : Orthogonal Frequency Division Multiplexing). The "orthogonal" part of the OFDM name indicates that there is a precise mathematical relationship between the frequencies of the carriers in the system. Fig. 1 shows the spectrum of an OFDM. The conventional OFDM signal is generated at baseband by taking the inverse fast Fourier transform (IFFT) of quadrature amplitude modulated (QAM) or phase-shift keyed (PSK). In the fig. 2, an OFDM symbol has a useful period T and proceeding each symbol is a cyclic prefix of length T_g, which is longer than the channel impulse response so that there will be no intersymbol interference (ISI) [11]. The frequencies of the complex exponentials are $f_k = k/T$,and the useful part for $2N+1$ subcarriers is given by

$$u(t) = \sum_{k=-N}^{N} c_k e^{j2\pi f_k t}, \quad 0 \le t \le T \qquad (1)$$

A carrier frequency offset of Δf causes a phase rotation of $2\pi t\Delta f$. The carrier frequency offset is not correct a rotation of the constellation and a spread of the constellation points similar to additive white Gaussian noise (AWGN) [2].

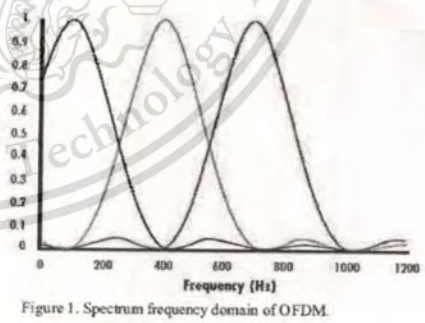

Figure 1. Spectrum frequency domain of OFDM.

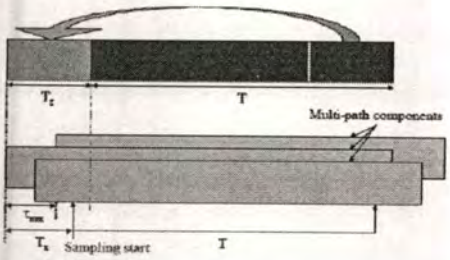

Figure 2. Multipath fading of OFDM

Figure 3 illustrates a general system overview of OFDM. At the transmitter, the signal is defined in the frequency domain. It is a sampled digital signal, and it is defined such that the discrete Fourier spectrum exists only at discrete frequencies. Each OFDM carrier corresponds to one element of discrete Fourier spectrum. The amplitudes and phases of the carriers depend on the data that is transmitted. The data transmissions are synchronized at the carriers, and can be processed together, symbol by symbol.

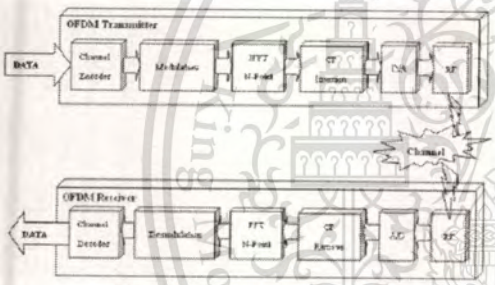

Figure 3. General system overview of OFDM.

B. Problem definition.

The main problem with reception of radio signals is fading caused by multipath propagation. Also, there are intersymbol interference (ISI), shadowing, interference. This makes link vary. As a result of the multipath propagation, there are many reflected signals, which arrive at the receiver at different time. Delayed signals are the result of reflections from terrain features such as trees, hills or mountains, or objects such as people, vehicles or buildings as shown in Fig. 2. These echoes cause ISI. The time delay of each OFDM symbol is the time-shifting property in signals, which indicates that a shift of a function in time corresponds to multiplication of the harmonic function by a complex function of harmonic number k [12]. Therefore, we use Harmonic transform to analysis the signals in OFDM symbol caused by multipath propagation.

III. HARMONIC TRANSFORM

Harmonic is a new method of spectrum analysis, which is proposed to provide an impulse-train spectrum for signals that are comprised of time-varying harmonics.

The Fourier transform (FT) represents signal $f(t)$ in term of sinusoids of various frequencies, that is defined as

$$F(\Omega) = \int_{-\infty}^{+\infty} f(t) e^{-j\Omega t} dt \qquad (2)$$

The original signal is recovered by the inverse Fourier transform (IFT)

$$f(t) = \frac{1}{2\pi} \int_{-\infty}^{+\infty} F(\omega) e^{-j\omega t} d\omega \qquad (3)$$

For signals consisting of fixed frequency components, the FT effectively reveals their frequency contents and is generally able to represent the signals with an acceptable resolution within a narrow band of spectra. However, this capability deteriorates quickly when the frequency components are time-varying as shown in Fig. 4

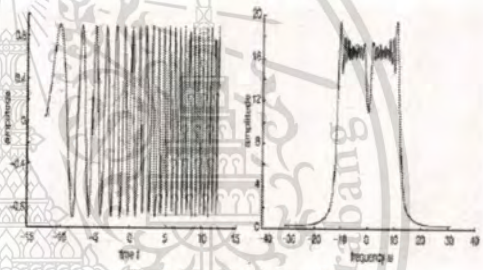

Figure 4. Fourier transforms of signals
Left: Waveforms Right: Corresponding spectra

One solution to avoid the deterioration is the warped Fourier transform, in which the signal is warped in time before calculation of the spectrum. Harmonic transform has a built-in warping function.

The time-varying harmonic signal generally contains harmonics whose nominal instantaneous frequencies are expressed by

$$c_k(t) = (k+1)c_0(t), \quad k = 1, 2, 3, \ldots \qquad (4)$$

where $c_0(t)$ is the frequency of the fundamental and $c_k(t)$ is the frequency of the kth harmonic component.

Now let us consider a time-varying harmonic signal in the time-frequency plane. For simplicity, only the nominal instantaneous frequency of the fundamental and the first two harmonics are given in Fig. 5(b). The Fourier transform of the signal, as shown in Fig. 5(c), can be treated as the linear

integration of the signal along the time axis in the time-frequency plane, which fails to distinguish the harmonic components. A better solution is to integrate the signal along the nominal instantaneous frequency of every component, rather than along the time axis, to obtain an impulse-train spectrum, as shown in Fig. 5(a). This is the basic concept of the harmonic transform (HT).

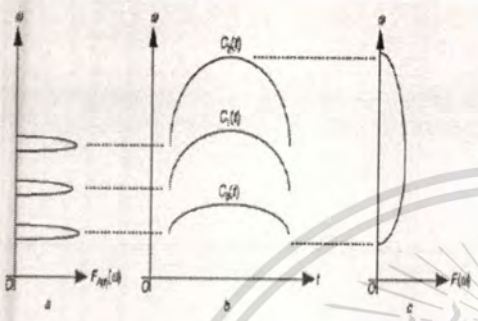

Figure 5. Concept of harmonic transform
a: Harmonic transform
b: Time-frequency representation
c: Fourier transform

The Harmonic transform of $f(t)$ is defined by

$$F_{\varphi_n(t)}(\Omega) = \int_{-\infty}^{+\infty} f(t)\phi_n(t)e^{-j\Omega\varphi_n(t)}dt \qquad (5)$$

where $\phi_n(t)$ is the unit phase function, which is the phase function of the fundamental divided by its nominal instantaneous frequency and $\phi'_n(t)$ is the first-order derivative of $\phi_n(t)$. The requirement for $\phi_n(t)$ is that it should be differentiable and invertible on $(-\infty, +\infty)$. HT of the signal will be scaled if the nominal instantaneous frequency of any harmonic is used. The inverse harmonic transform (IHT) is

$$F(t) = \frac{1}{2\pi}\int_{-\infty}^{+\infty} F_{\varphi_n(t)}(\omega)e^{-j\omega\varphi_n(t)}d\omega \qquad (6)$$

It is noted that the Harmonic transform becomes the Fourier transform when $\phi_n(t) = t$. Fig. 6 shows FT and HT of speech. Clear peaks representing the fundamental and harmonics are seen in the HT, while the same observation cannot be made from the FT.

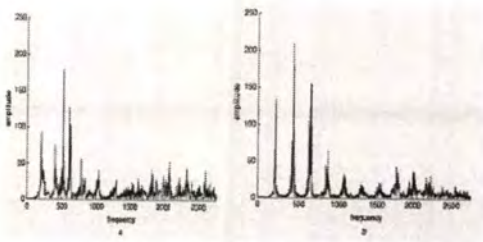

Figure 6. Transform of speech.

IV. HARMONIC TRANSFORM BASED ON OFDM

A basic diagram of an OFDM system under proposed scheme is shown in Fig.7. We consider the transformation of an OFDM system. We substitute IHT and HT into IFFT and FFT, respectively.

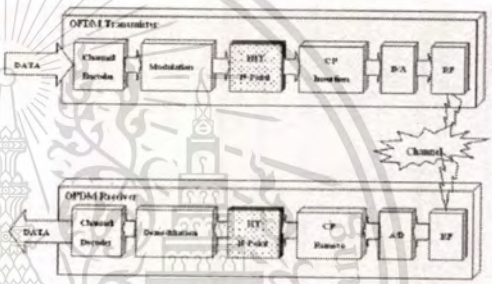

Figure 7. OFDM system based on HT.

In figure 8, we present the block diagram of channel estimation based on Harmonic transform using same pilot sequences [13] that to measure the number of multipath (NoM). While signal to interference plus noise power ratio (SINR) is used to calculate interference plus noise level (I+N level). The most important issue is that the receiver should know the number of multipath and interference plus noise level for each subcarrier to setup parameter of Harmonic transform.

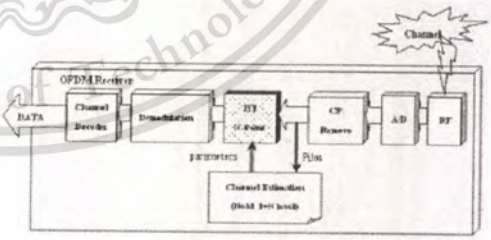

Figure 8. Block diagram of channel estimation based on HT.

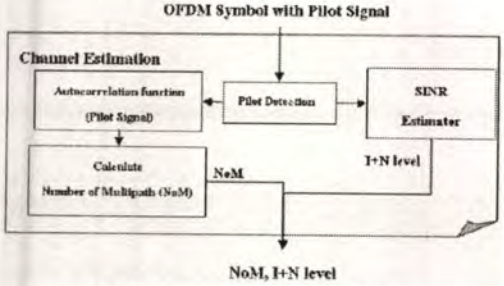

Figure 9. Procedure of channel estimation for HT.

The I+N level for each subcarrier is estimated by calculating vector error of the received symbols from the reference symbols. SINR estimator takes the average values of vector error over adjacent sub carriers.

In order to estimate channel multipath delay desired locations and interfering channels, same pilot symbols are received OFDM symbol signals from the transmitters. The Pilot detection will prepare pilot signals for next function.

First part of the algorithm is estimating number of multipath. In this method, Autocorrelation function will be used. We can calculate number of multipath by peak of pilot signals counting. The NoM will be used in Harmonic transform as a number of harmonic.

Second part of the algorithm is SINR Estimator, which estimate SINR for calculate I+N level of each subcarrier. The I+N level will be used in Harmonic transform for setup parameter of each subcarrier.

V. Discussions

We now compare the performance of the HT with FT based on OFDM systems. The use of Fourier transform in conventional OFDM is not flexible and very sensitive to carrier frequency offset, which is much more affected by carrier frequency errors. A small frequency offset at the receiver compromises the orthogonally between the sub channels, causes a degradation in a system performance. The channel estimation after taking FFT has been researched and more complexity cause of no more information from FFT.

In the case of HT based on OFDM is the best way to achieve flexibility. It can adapt on condition of environments, when signals are very strong echoes. In bad environments, the HT will be adapted and have more efficiency. But it has more computational complexity. In other hand, good environments, the computational complexity of our proposed system similar as the conventional OFDM. Therefore, the conventional transmitter can use for our proposed scheme. It does not design any more for transmitter. However, we can reduce design and computational complexity of channel estimation after taking FFT in the conventional OFDM.

Harmonic transform based on OFDM especially in the multipath propagation, interference and fading environment is a promising technique for digital communications including mobile multimedia.

VI. Conclusions

We propose a new signal transformation using Harmonic transform based on OFDM. The main idea of our research is to improve performance of frequency offset estimation. Therefore, the receiver can reduce computational complexity after take FFT. Our proposed system is flexibility and computes on condition of environments. However, transmitter can process with the conventional OFDM. The computational complexities of transformation in receiver depend on environments. But it still has an accuracy frequency offset.

References

[1] Bruce McNair, Leonard J.,and Nelson S.,"A Robust Timing and Frequency Offset Estimation Scheme for Orthogonal Frequency Division Multiplexing (OFDM) Systems",*Vehicular Technology Conference, 1999 IEEE 49th*, Vol.1, 16-20 May 1999, pp. 690 – 694.

[2] Timothy M. Schmidl and Donald C. Cox, "Robust Frequency and Timing Synchronization for OFDM", *IEEE Transaction on communications*, Vol.45, No. 12, December 1997. p.1613-1621

[3] Van De Beek, Sandell M. and Borjesson P.O., "ML estimation of time and frequency offset in OFDM systems", *IEEE Trans. Signal Process.*, 1997, Vol.45, No.7, pp. 1800-1805.

[4] Jing Lei and Tung-Sang Ng, "Pilot-Tone-Based Maximum Likelihood Estimator for Carrier Frequency Offset in OFDM Systems", *IEEE International Conference*, 2003, p.2046-2050.

[5] Lee J., Lou H. and Toumpakaris D., "Maximum likelihood estimation of time and frequency offset for OFDM systems", *Electronics Letters 28th*, October 2004, Vol.40 No.22. p.

[6] Lee J., Lou H. and Toumpakaris, "Approximate Maximum Likelihood Estimation of Integer Carrier Frequency Offset in OFDM Systems", *Communications IEEE International Conference on Volume 4*, 2005, pp. 2543-2547

[7] Makur A. and Mitra K., "Warped Discrete-Fourier Transform: Theory and Application", *IEEE Transaction on Circuits and System*, Vol 48, No.9 , September 2001, p. 1086-1093.

[8] Franz S., Mitra K., Schmidt J.C. and Doblinger G., ,"Warped Discrete Fourier Transform: A New Concept in Digital Singal Processing", *(ICASSP '02).IEEE International Conference*, Vol 2, 2002, p.1205-1208.

[9] Venkataramanan R. and Prabhu K.M.M. "Estimation of Frequency Offset using Warped DFT", *Signal Processing*, Vol. 86, Feb. 2006, p. 250-256.

[10] Zhang F., Bi G. and Chen Y.Q.,"Harmonic Transform", *IEE Proc.-Vis Image Signal process.*, Vol.151, No. 4, August 2004, p. 257-263.

[11] Batariere M., Baum K. and Krauss T.P., "Cyclic Prefix Length Analysis for 4G OFDM System", *Vehicular Technology Conference, 2004. VTC2004-Fall. 2004 IEEE 60th*, 2004, pp.543-547.

[12] Roberts M.J. , *Signals and Systems : analysis using transform methods and MATLAB*. Mcgraw Hill, Singapore, 2004.

[13] Simeone O., Bar-Ness Y., "Pilot-Based Channel Estimation for OFDM Systems by Tracking the Delay Subspace", *IEEE Transactions on Wireless Communications*, Vol.3, No.1 January 2004. p.315-325.

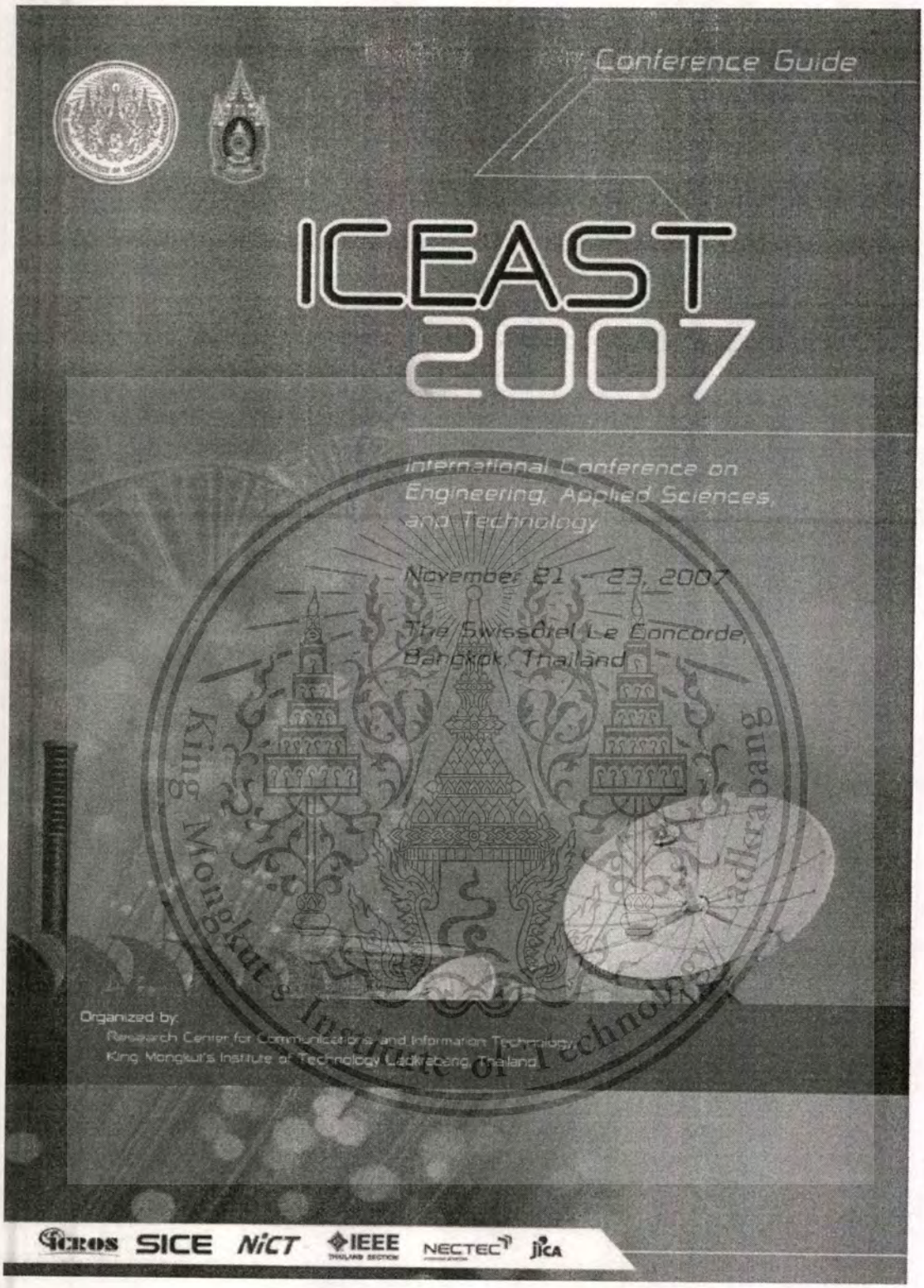

Adaptive Cyclic Prefix for OFDM Signal Transmission Under Multipath Fading Environments

Saiyan SAIYOD, Tawatchai CHONTONG, Ruttikorn VARAKULSIRIPUNTH and Sakchai THIPCHAKSURAT
Faculty of Engineering and Research Center for Communications and Information Technology (ReCCIT)
King Mongkut's Institute of Technology Ladkrabang (KMITL), Bangkok, Thailand
Email: s8060055@kmitl.ac.th, Tawatchai.c@gmail.com
kvruttik@kmitl.ac.th, ktsakcha@kmitl.ac.th

Abstract—**In the Orthogonal Frequency Division Multiplexing (OFDM) system, the guard interval, i.e., Cyclic Prefix (CP) is added to the header of transmitted signal in order to avoid the interference between two adjacent signals. Under the multipath fading environments, the fading of one signal will cause the interference to the next transmitted signal at the receiver. But, this interference can be avoided by adding the CP of the size equal to the maximum of Arrival Time Difference between a signal and its last arrival fading (ATD). However, the conventional OFDM has fixed the value of CP as 0.8 μs, so the channel utilization or throughput will be limited. In order to increase the throughput, therefore, the adaptation of CP in according to the transmission or mutipath fading environments is proposed in this paper. The length of CP is adjusted as fit as the current value ATD. Whenever, the transmitter or receiver changed its location, or whenever the interference is detected at the receiver, the proposed algorithm will be introduced to calculate new current ATD and use it for adjusting the new CP. The simulation results have shown that the proposed algorithm has a good performance than the conventional OFDM one in term of throughput.**

Keywords— **OFDM (Orthogonal Frequency Division Multiplexing), Cyclic Prefix, Inter-Symbol Interference**

I. INTRODUCTION

Orthogonal Frequency Division Multiplexing (OFDM) [1] has become a prime candidate for future high-data-rate wireless communication systems. It has been adopted for digital broadcasting, xDSL, and wireless LAN applications [2, 3]. OFDM is also known as multi-carrier modulation that incorporates a large number of orthogonally selected sub-carriers for transmitting a high-data-rate parallel bit stream in the frequency domain. In OFDM, the broadband signals are transmits by dividing into a large number of narrowband channels in order to achieve resistance to such a long delay spread. In addition, a guard interval that is equal or longer than the maximum of *Arrival Time Difference between a signal and its last arrival fading* (ATD) is added to the header of each signal, i.e., inserted between adjacent OFDM symbols (or signals). This guard interval is called *cyclic prefix* (CP). By using CP as the gap between any two adjacent symbols, the *inter-symbol and inter-carrier interferences* (ISI and ICI) are completely eliminated [4, 5, 6, 7]. Since, the occurring of ICI depends on ISI, therefore, only ISI solving problem is considered in this paper.

Figure 1 (a) shows the ISI of data portion between two adjacent OFDM symbols when there is no CP. But by adding CP (≥ATD) as a guard interval, the ISI of their data portion is avoided as shown in Figure 1 (b). In this situation, the orthogonality between sub-carriers will be maintained. If the CP is less than current ATD, the ISI between data portion of adjacent symbols will occur and orthogonality between sub-carriers is lost. Moreover, since the size of OFDM symbols is fixed, then as bigger as CP is assigned, the data portion will become smaller. Therefore, to assign the appropriate CP that closely equal to the current ATD is preferable. This will not only avoid ISI of data portion but also keep the data portion as large as possible. This is the main objective of our proposed algorithm.

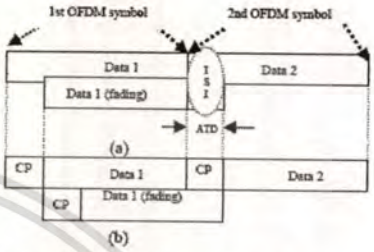

Fig.1 OFDM symbols without and with CP.

Practically, up on arrival of OFDM symbols at receiver, CP is removed before the symbols are decomposed into the sub-carriers by using a Fourier transform.

The rest of paper is organized as follow. In Section II, the modified OFDM system and channel estimation scheme are introduced. Our proposed algorithm is described in details in Section III. The numerical and simulation results are discussed Section IV. The conclusion of this research is described in Section V.

II. MODIFIED OFDM SYSTEM AND CHANNEL ESTIMATION SCHEME

In order to support our proposed algorithm, we have modified the conventional OFDM system as shown in Fig. 2 by adding the process of *Information Processing* in transmitter and *Channel Estimator* in receiver. In the transmitter, a high-speed serial data stream is digitally quadrature modulated and converted to parallel low-speed modulated data streams, and fed to several traffic sub-carrier channels.

978-974-8308-56-2 ©2007 KMITL

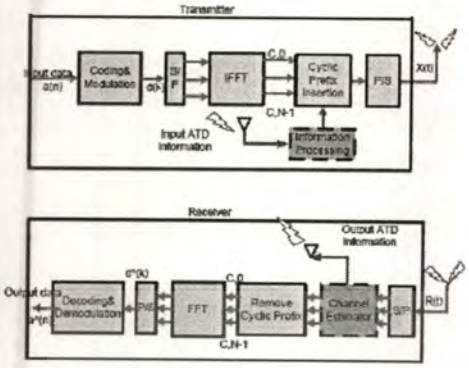

Fig. 2 Modified OFDM transmission system.

The modulated signals are multiplex orthogonally by an Inverse Fast Fourier transformation (IFFT) circuit to perform OFDM symbols. A cyclic prefix is inserted in front of each OFDM symbol before converted to serial for transmission as an analog wave signal. Here, the *Information Processing* unit will take the duty of;

(a) setting the new ACP whenever it receives the current ATD information from receiver, or

(b) stopping the transmission and send ETS to receiver whenever it receives the NAK signal from receiver or it changes location.

At receiver, arrival signal is down-converted to lower frequency. After the CP is removed, it is fed into an FFT circuit and de-multiplexed as sub-carrier channel data and then demodulated by digital quadrature demodulator. Here, the *Channel Estimator* unit will take the duty of;

(a) computing the current ATD whenever it received the ETS from transmitter, or

(b) sending NAK to transmitter whenever it detects ISI or *timeout for the next adjusting* (TNA) is expired or it changes location.

III. ADJUSTING APPROPRIATE CYCLIC PREFIX

In our proposed algorithm, the *appropriate CP* (ACP) for OFDM symbols will be readjusted under the following 3 conditions. First, when the ISI is detected at receiver. Second, when transmitter or receiver has changed its location. Third, when the TNA is expired. Initially, at the starting of operation, transmitter will send the first *echo test signal* (ETS: request for the information of current ATD) to receiver. Whenever receiver received ETS, receiver will detect and compute the ATD between ETS and its fading, and send this current ATD back to transmitter for setting new ACP, and TNA is reset. After all, the procedure for adjusting the new ACP is as follow. Again, here ATD is *Arrival Time Difference between a signal and its last arrival fading*, that is the maximum value of all its time difference.

Algorithm 1: Operation at Transmitter (Fig. 3)

1: Initially, send ETS to receiver and wait for current ATD.
2: If received current ATD, then adjust new ACP = current ATD to OFDM symbol for transmission.
3: Whenever received NAK (*Not-acknowledgement*) signal from receiver, stop the transmission and send ETS to receiver, then back to step 2.
4: If transmitter changes location, stop the transmission and send ETS to receiver, then back to step 2.

The process of Algorithm 1 is shown in Fig. 3.

Transmitter

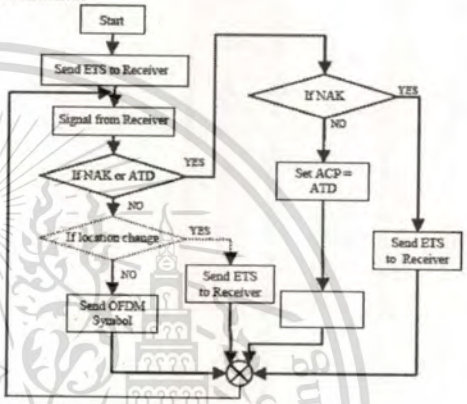

Fig. 3 Algorithm 1: at Transmitter.

Receiver

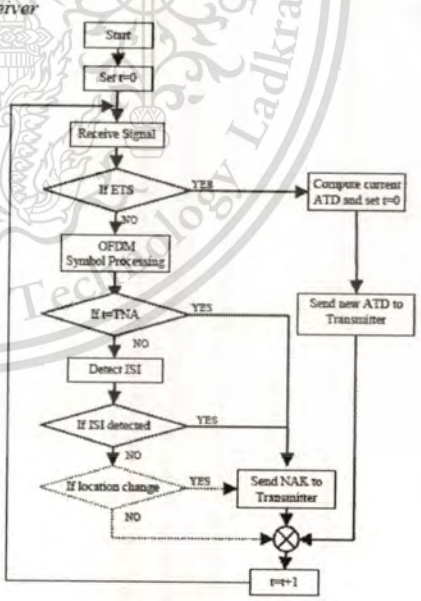

Fig. 4 Algorithm 2: at Receiver.

Algorithm 2: Operation at Receiver (Fig. 4)

1: When receive ETS, detect and compute the current ATD between ETS and its fading, and send this current ATD back to transmitter, and reset TNA (i.e., t = 0, upper bound is TNA)
2: If detects ISI, send NAK back to transmitter, and wait for ETS, then back to step 1.
3: If t = TNA, send NAK back to transmitter, and wait for ETS, then back to step 1.
4: If receiver changes location, send NAK back to transmitter, and wait for ETS, then back to step 1.

The process of Algorithm 2 is shown in Fig. 4.

IV. NUMERICAL ANLYSIS

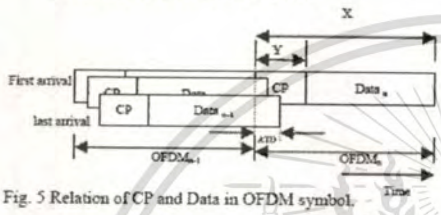

Fig. 5 Relation of CP and Data in OFDM symbol.

Here, we will discuss the methodology for throughput calculation. Let X (bits) and Y (bits) be the length of OFDM symbol and its CP portion respectively as shown in Fig. 5. The normalized throughput can be considered in term of channel utilization. As the assumption of fixed size for all OFDM symbols, the normalized throughput in term of bits (ρ) can be formulated as shown in Eq. (1).

$$\rho = \frac{X - Y}{X} \quad (1)$$

If the data transmission rate is known as a bit/sec, then the normalized throughput in term of time (ρ) can be formulated as shown in Eq. (2).

$$\rho = \frac{\frac{X}{a} - y_t}{\frac{X}{a}} \quad (2)$$

Where, $y_t = \frac{Y}{a}$ is the CP in term of time length.

From Eq. (1) and Eq. (2), it is clear that $\rho = \rho$

In according to the standardization (IEEE802.11a), $y_t = 0.8\mu s$, and total length of OFDM symbol in term of time is equal to $4\ \mu s$. Under this standardization, it is guaranteed that there is no ISI will occur. Therefore, the upper bound of CP is $0.8\mu s$ in this paper. That is $0 \le y_t \le 0.8\mu s$.

As mentioned before that conventional OFDM uses the fixed or constant value of $y_t = 0.8\mu s$, and not change. Therefore, if Y, i.e., CP is fixed, then ρ will be limited to a constant value as shown in Fig. 6. That is, when $X/a = 4\ \mu s$ and $y_t = 0.8\mu s$, then $\rho = 0.8$ as the result. But if the value of Y or CP can be adjustable, then ρ can be obtained in various values as shown in Fig. 6. That is the reason of this research to adjust the ACP in according to current ATD that will result in the increasing of normalized throughput.

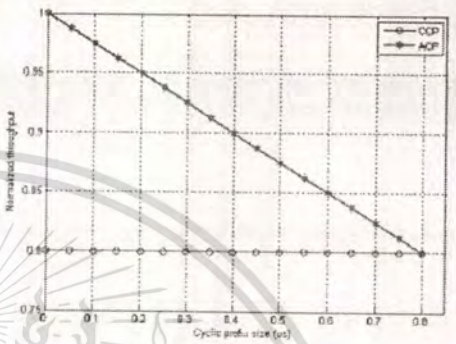

Fig. 6 Normalized throughput versus the length CP.

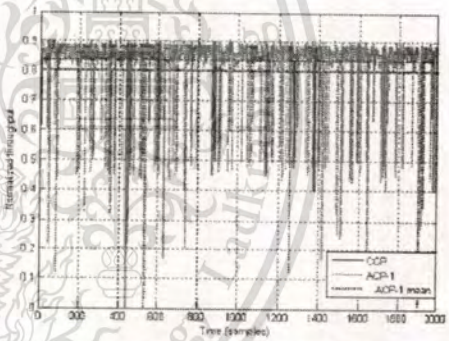

Fig. 7 Normalized throughput without location changing information

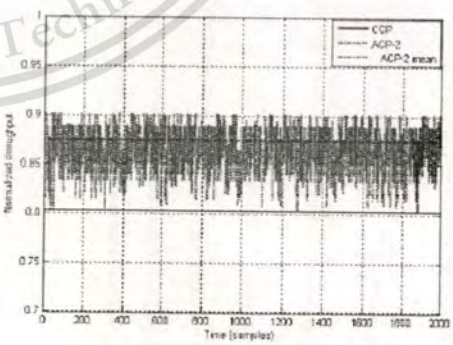

Fig. 8 Normalized throughput with location changing information

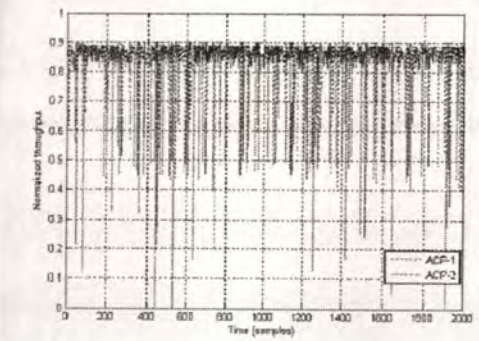

Fig. 9 Comparison between ACP-1 and ACP-2

V. SIMULATION RESULTS

Here, let us call the conventional OFDM that used fixed CP as "CCP". We will consider our proposed algorithm in two categories. These are the procedures without and with location changing information, i.e., when the operation of step 4 in algorithm 1 and algorithm 2 is not provided and is provided, respectively. Let us call the first one as "ACP-1" and the second one as "ACP-2", respectively.

The simulation results are shown in Figs.7-10. The normalized throughputs for each time sample of OFDM symbols are illustrated in Figs.7-9. The comparison between CCP and ACP-1 under the multipath environment is shown in Fig. 7. We can realize that the normalized throughput of CCP is equal to 0.8, and not change. Sometime the normalized throughput of ACP-1 decreased lower than CCP due to the loss of data portion caused by ISI. But for overall, ACP-1 shows the better performance than CCP in term of average normalized throughput.

When the location changing information is provided, the normalized throughput of ACP-2 increased obviously in comparing with CCP as shown in Fig. 8. This is due to the early informing of the location change that can avoid ISI beforehand. Moreover, in ACP-2, the transmitter stop its transmission when it changes the location, or the receiver immediately send NAK signal to transmission, then the new current ATD will be applied so that the loss of data due to ISI is avoided. Finally, it is obvious that the performance of ACP-2 is better than ACP-1 as shown in Fig. 9. In order to see how much performance difference among ACP-1, ACP-2 and CCP, we have illustrated their cumulative normalized throughputs by using Eq. (3) as shown in Fig. 10.

Let $f_\rho(i)$ is the density function of normalized throughput of OFDM symbol at time sample i, and n represents the consecutive integer value of time sample (where n =0, 1, 2, 3,….). Then the cumulative normalized throughput of OFDM symbols up to time sample n, i.e., $F_\rho(n)$ can be formulated as shown in Eq. (3).

From Fig. 10, we can see that, performances of ACP-1 and ACP-2 are about 5% and 9.4% better than CCP, respectively.

$$F_\rho(n) = \sum_{i=0}^{n} f_\rho(i) \qquad (3)$$

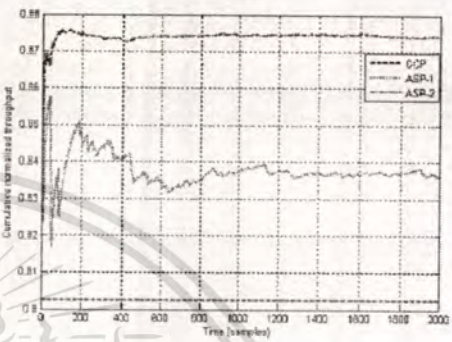

Fig. 10 Cumulative normalized throughput of CCP, ACP-1, ACP-2.

VI. CONCLUSION

In this paper, we have proposed a new algorithm to adjust the appropriate cyclic prefix for OFDM symbols. The appropriate cyclic prefix is decided by considering with the real arrival time difference between OFDM symbol and its last arrival fading at the receiver. With this approach, the performance of OFDM signal transmission system in term of throughput is improved. That is because of the appropriate cyclic prefix can increase the data portion of OFDM symbol and decrease the number of loss that may be caused by the inter-symbol interference.

REFERENCES

[1] R.W. Chang and R.A. Gibby, "A theoretical study of performance of an scheme", IEEE Trans. Commun., vol. COM-16, no.4, pp.529-540, Aug. 1968.

[2] Nee, R., and Prasad, R.: "OFDM for wireless multimedia communications" (Artech House, Norwell, MA, USA, 2000).

[3] Keleer, T., and Hanzo, L.: "Adaptive modulation: A convenient Framework for time-frequency processing in wireless communications", Proc. IEEE, 2000, 88, pp. 611-642.

[4] J. A. C. Bingham, "Multicarrier modulation for data Transmission: An idea whose time has come," IEEE Commun. Mag., vol. 28, no. 5, pp. 5–14, May 1990.

[5] W.G. Jeon, K.H. Chang, and Y.S. Cho, "An equalization technique for orthogonal frequency-division multiplexing systems in time-variant multipath channels," IEEE Tran. Commun., vol.47, no.1, pp.27-32, Jan 1999.

[6] D. Li and K. Yamashita, "An equalization technique for high-speed-mobile OFDM systems in Rayleigh multipath channels," IEICE Tran. Commun, vol.E87-B, no.1, pp.158-160, Jan 2004.

[7] A. Peled and A. Ruiz, "Frequency domain data transmission using reduced computational complexity algorithms," Proc. IEEE Int. Conf. Acoustics, Speech, Signal Proc. (ICASSP'80), pp.964-967, 1980.

IEICE
TRANSACTIONS

on Fundamentals of Electronics,
Communications
and Computer Sciences

VOL.E93-A
NO.12
DECEMBER 2010

A PUBLICATION OF THE ENGINEERING SCIENCES SOCIETY
The Institute of Electronics, Information and Communication Engineers
Kikai-Shinko-Kaikan Bldg., 5-8, Shibakoen 3-chome, Minato-ku, TOKYO, 105-0011 JAPAN

2634 IEICE TRANS. FUNDAMENTALS, VOL.E93–A, NO.12 DECEMBER 2010

PAPER Special Section on Wideband Systems

Doppler Spread Mitigation Using Harmonic Transform for Wireless OFDM Systems in Mobile Communications

Saiyan SAIYOD[†a)], *Student Member*, Sakchai THIPCHAKSURAT[†b)], *and* Ruttikorn VARAKULSIRIPUNTH[†c)], *Nonmembers*

SUMMARY In wireless OFDM systems, the system performance is suffered from frequency offset and symbol timing offset due to the Doppler effect. Using the discrete Fourier transform (DFT) and inverse discrete Fourier transform (IDFT) for traditional signal transformation from the time-domain into frequency-domain, and vice versa, the system performance may be severely degraded. To make the OFDM system that can tolerate the above problems, we have considered that the harmonic transform can be applicable to the traditional signal transformation, thereby improving the system performance. In this paper, we combine the good characteristics of harmonic transform and instantaneous frequency to be a novel transformation for wireless OFDM systems. We propose a modified discrete harmonic transform (MDHT) which can be performed adaptively. Our proposed scheme called the modified discrete harmonic transform OFDM (MDHT-OFDM scheme). We derive the equations of the novel discrete harmonic transform which are suitable for wireless OFDM systems and the novel channel estimation cooperated with the novel transformation. The proposed channel estimation is performed in both time-domain and frequency-domain. The performance of a MDHT-OFDM scheme is evaluated by means of a simulation. We compare the performance of a MDHT-OFDM scheme with one of the conventional DFT-OFDM scheme in the term of symbol error rate (SER). MDHT-OFDM scheme can achieve better performance than that of the conventional DFT-OFDM scheme in mitigating the Doppler spread.

key words: *OFDM, channel estimation, DFT, Doppler spread, harmonic transform*

1. Introduction

Orthogonal Frequency Division Multiplexing (OFDM) has become a prime candidate for future high-data-rate wireless systems because of its strong resistance to the Inter-Symbol Interference (ISI), inserted by multi-path propagation effects in the real world indoor and outdoor channels. However, the wireless OFDM systems vary their sensitive to frequency offset and symbol timing offset due to the Doppler effect of the mobile communications [1]. Therefore, the Doppler spread (f_D) is a measure of the spectral broadening caused by the Doppler effect. Thus, the orthogonal among sub-carriers is destroyed, which results in inter-carrier interference (ICI) thereby degrading the systems performance severely. Moreover, in mobile communications, the channel is time-variant during one OFDM symbol period.

Manuscript received March 27, 2010.
Manuscript revised July 12, 2010.

[†]The author are with the Faculty of Engineering, King Mongkut's Institute of Technology Ladkrabang, Bangkok, 10520, Thailand.
a) E-mail: s8060055@kmitl.ac.th
b) E-mail: ktsakcha@kmitl.ac.th
c) E-mail: kvruttik@kmitl.ac.th

DOI: 10.1587/transfun.E93.A.2634

The conventional OFDM systems employ the inverse discrete Fourier transform (IDFT) and discrete Fourier transform (DFT). However, the practical implementation involves the inverse fast Fourier transform (IFFT) and the fast Fourier transform (FFT) at the transmitter and receiver respectively using the fast algorithms of the IDFT and DFT. Therefore, we agree with [2] that the occurrence of the ICI is due to the use of the DFT for transformation from time-domain into frequency-domain, when the channel is the time-varying channel. Therefore, the time scales of the received signals change the wavelength. This result induces the loss of orthogonal among OFDM sub-carriers due to the DFT performance.

However, in order to cope with the Doppler spread in the conventional DFT-OFDM scheme, compensation and equalization techniques are needed. The channel estimation (CE) and pilot-aided, are used for those techniques. The accuracy of the system depends on the performance of the channel estimation, amount and pattern of pilot-aided. The pilot-aided are inserted in the OFDM symbol in order to put the reference data in the OFDM symbol. Thus, the use of pilot-aided lowers the achievable data rate. Moreover, the channel estimation of conventional OFDM is performed after transformation. Thereby, the accuracy of the estimated values are affected by additive white Gaussian noise (AWGN).

Most of the previous algorithms to mitigate the Doppler spread are to deal with ICI cancellation, and simply focus on mitigating the irreducible error floor [3]. However, many approaches estimate the frequency offset first then correct it, but usually required considerable computational complexity [4]. Another common approach is to apply various signal processing techniques to reduce the sensitivity of the OFDM system to the frequency offset; hence many windowing methods have been presented.

In this paper, we have considered that the transformation of wireless OFDM systems should be improved. A solution to avoid deterioration of DFT is the warped Fourier transform [5]–[7], in which the signal is warped in time before the calculation of the spectrum. The harmonic transform is a good alternative way. The harmonic transform has been proposed in [5], but it has been proposed for signal analysis, especially speech signals. Moreover, the proposal in [8] is a good attractive choice for OFDM systems. The main idea of the proposal is to improve the efficiency of the transformation for the OFDM systems using a harmonic

transform. We have found that the harmonic transform has good properties for signals that contain a time-varying signal. Unfortunately, the discrete form of harmonic transform was proposed in [5], is not suitable for wireless OFDM systems. Because the traditional harmonic transform is designed for speech signal analysis, the unit phase function ($\phi_u(t)$) of its depends on the scaling property which is determined by the relation between $\phi_u(t)$ and $\phi_u(t/a)$, where a is a constant. Scaling and phase shifting operation are defined before calculation in order that the suitable parameters are set as constant. Moreover, only real numbers are required by speech signal analysis. In contrast, the transformations of wireless OFDM systems require the complex numbers. In mobile communications, the mobile station may often change its position during the communication as we call the mobility of mobile station. In this situation, the constant parameter may be not suitable. This means that it should be varied according to the mobility of mobile station. Therefore, the traditional harmonic transform may be not suitable for the mobile communications. For this reason, the traditional harmonic transform should be modified. In this paper, we derive the appropriate equations that more suitable for the mobility situation in the mobile communication systems which is the one of our contribution.

However, in order to apply the harmonic transform for wireless OFDM systems, a modification of the discrete harmonic transform is needed. We combine the good characteristics of the harmonic transform and the concept of instantaneous frequency [9]–[13] together. The proposed transformation is called Modified Discrete Harmonic Transform (MDHT). Moreover, the proposed scheme is called the MDHT-OFDM scheme. Furthermore, the MDHT is performed as an adaptive transformation which cooperates with the parameters. Thus, adaptation requires a form of accurate parameter measurement. One key parameter in adaptation of mobile communications is f_D. Therefore, we propose a novel channel estimation technique that can cooperate to provide the suitable parameters for the MDHT-OFDM scheme. The proposed channel estimation is performed in both the time-domain and the frequency-domain. In the time-domain estimation, the self-correlation function is performed to get the OFDM Framing Duration ($T_{estimated}$) in order to calculate the Doppler scaling factor ($\alpha_{estimated}$) and the symbol timing offset ($\epsilon_{estimated}$). We use $\alpha_{estimated}$ by means of f_D. On the other hand, the frequency-domain estimation is performed in order to get the root mean square error of the preamble symbol (θ_{RMSE}) in order to select a suitable modulation mapping scheme.

The advantages of the proposed scheme are less pilot-aided, strong resistance to AWGN, and adaptability. However, the different characteristics between the conventional DFT-OFDM scheme and the proposed MDHT-OFDM scheme are shown in Table 1. The rest of the paper is organized as follows. In Sect. 2, we describe the problem definition and the conventional wireless OFDM systems. Section 3, the proposed MDHT-OFDM scheme for wireless OFDM systems will be described. Novel channel estimation for MDHT-OFDM scheme is proposed in Sect. 4. Section 5 provides the simulation results to demonstrate the performance of the proposed scheme. Finally, Sect. 6 concludes this paper.

Table 1 The characteristics comparison of the conventional DFT-OFDM scheme and the proposed MDHT-OFDM scheme.

Characteristics	Conventional OFDM	Proposed MDHT-OFDM
Transformation	DFT, FFT	MDHT
Transformation performing	Fixed	Adaptive
Channel estimation	Frequency domain	Time domain and frequency domain
Position of channel estimation	After Transformation	Before and after transformation
Pilot-Aided	Needed	Compatible
Transformation complexity	N^2 (DFT) $N \log_2 N$ (FFT)	N^2 (MDHT)

2. Problem Definition and Conventional Wireless OFDM Systems

2.1 Problem Definition

In wireless OFDM systems, one serious problem is the frequency offset and symbol timing offset caused by the Doppler effect, which severely degrades the system performance. When the transmitter or receiver is moving, the received signal will have the maximum Doppler frequency of $f_D = v/\lambda$ associated with it, where v is the mobile velocity, and λ is the signal wavelength. The time variations of the channel change over the OFDM symbol duration, and the wavelength is scaled. Thus, the time coherence is concerned. We define the coherence time T_C to be the range of Δt values over the OFDM symbol. The maximum Doppler frequency value is called the Doppler spread of the channel. The coherence time is the time-domain dual of Doppler spread and is used to characterize the time-varying channel. The Doppler spread and coherence time are inversely proportional to one another. That is $f_D \approx 1/T_C$ [14].

Conventional wireless OFDM systems employ the DFT in order to transform the signals. For signals consisting of fixed frequency components, the DFT effectively provides their frequency contents. But, this capability deteriorates when the frequency components are time-varying. Since the Doppler effect occurs in the time-domain which is impacted on the wavelength of each OFDM sub-carrier. Moreover, the frequency-domain channel estimation of the conventional DFT-OFDM scheme is affected by AWGN which has been reported in [2].

According to the problems that mention above, the novel transformation and novel channel estimation should be considered to be suitable for wireless OFDM systems. Before discussing the proposed scheme, we would like to describe the conventional wireless OFDM systems.

2.2 Conventional Wireless OFDM Systems

The conventional DFT-OFDM scheme block diagram is shown in Fig. 1. The data is transformed into time-domain using inverse discrete Fourier transform (IDFT) or inverse fast Fourier transform (IFFT) at the transmitter. The definition of the N-point of IDFT is given by

$$x_f(n) = \frac{1}{N}\sum_{k=0}^{N-1} X_f(k) e^{\frac{2\pi jkn}{N}} \tag{1}$$

On the conventional DFT-OFDM receiver side, the data is transformed back to the frequency-domain by performing DFT or fast Fourier transform (FFT) on the received signals. The definition of the N-point DFT is given by

$$X_f(k) = \sum_{n=0}^{N-1} x_f(n) e^{-\frac{2\pi jkn}{N}} \tag{2}$$

where x_f is the time-domain OFDM signals, X_f is the data symbol of frequency-domain, N is the number of subcarriers, and n is the sampling instant.

DFT is most commonly used for signal transformation. Unfortunately, it has a poor performance in the case of time-varying channels. In order to mitigate the Doppler spread in the conventional DFT-OFDM, pilot-aided symbols are inserted at the transmitter at the fix time interval and at the receiver, the channel characteristics are estimated by using the pilot-aided symbol. Then, the received data can be recovered. The channel estimation is performed after transformation which is affected by AWGN. Thereby, the system performance is strongly dependant on the amount and patterns of pilot-aided which are needed as space on an OFDM symbol.

In wireless OFDM systems channel estimation is popularly performed in frequency-domain. Channel frequency response estimates are affected by AWGN. Due to the additive noise will be combined in transformation process. Therefore, the recovery symbols will be destroyed. As a result, Doppler estimates based on frequency-domain channel estimates will be affected significantly. In contrast, the time-domain channel estimation is robust to AWGN, works well for low SNR, regardless of the variation of channel environment. Furthermore, channel estimation in the time-domain turns out to be more efficient since the number of the unknown parameters is greatly decreased compared to that in the frequency-domain.

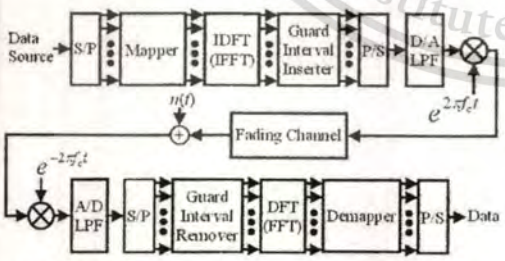

Fig. 1 The block diagram of the conventional DFT-OFDM scheme.

3. Proposed MDHT-OFDM Scheme for Wireless OFDM Systems

The proposed MDHT-OFDM scheme is shown in Fig. 2. The contributions of the proposed MDHT-OFDM scheme are as follows. Firstly, we investigate the novel transformation which can adapt itself to the condition of the channel. Secondly, we fined out the novel channel estimation to cooperate with the novel transformation.

3.1 A Novel Transformation for Wireless OFDM Systems

Harmonic transform has been proposed in [5], but it has been proposed for signal analysis, especially speech signals. We have found that the harmonic transform has a good property for signals that contain time-varying signals. The difference between the harmonic transform and the Fourier transform is the harmonic kernel $e^{j\omega\phi_u(t)}$, where $\phi_u(t)$ is the unit phase function. The harmonic kernel can be loosely interpreted as the integration of the signal along the curves $\omega\phi_u'(t)$, where $\phi_u'(t)$ is the derivative of $\phi_u(t)$. In the case of $\phi_u(t) = t$, the harmonic transform is equivalent to the Fourier transform. The discrete form of harmonic transform was proposed in [5]. Unfortunately, it is not suitable for wireless OFDM systems.

In order to apply to wireless OFDM systems, we have to modify the harmonic transform which is shown in the following step. Let us start from the continuous form of the harmonic transform which has been proposed in [5]. The harmonic transform of a time-domain signal $f(t)$ can be defined by

$$F_{\phi_u(t)}(\omega) = \int_{-\infty}^{+\infty} f(t)\phi_u'(t) e^{-j\omega\phi_u(t)} dt \tag{3}$$

The inverse harmonic transform is given by

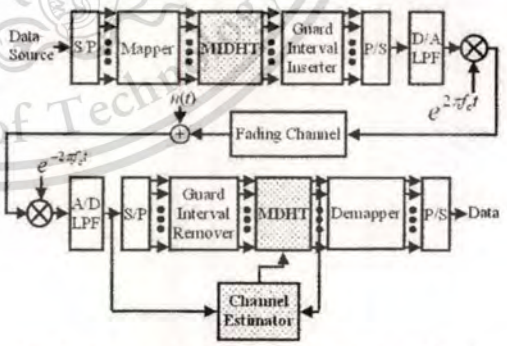

Fig. 2 The proposed MDHT-OFDM scheme for wireless OFDM systems.

$$f(t) = \frac{1}{2\pi}\int_{-\infty}^{+\infty} F_{\phi_u(t)}(\omega)e^{j\omega\phi_u(t)}d\omega \quad (4)$$

where $\phi_u(t)$ is the unit phase function of fundamental of $f(t)$. $\phi'_u(t)$ is the first-order derivative of $\phi_u(t)$.

We now start to modify the harmonic transform to be used in wireless OFDM systems. A discrete calculation is required to compute the discrete form of $F_{\phi_u(t)}$ when $f(t)$ and $\phi_u(t)$ are in a discrete form. The discrete harmonic transform is defined as the sampled version of the harmonic transform, $f(t) \Rightarrow f(n)$ and $\phi_u(t) \Rightarrow \phi_u(n)$, where Δt is the sample period, $t = n\Delta t$ and $n \in [0, N-1]$, the variable t of $f(t)$ and $\phi_u(t)$ is limited to the range $[0, T]$, where $T = N\Delta t$. Note that the relationship between ω and f is $\omega = 2\pi f$. Due to the traditional harmonic transform is proposed for speech signal analysis, it provides only real numbers. In the case of wireless OFDM systems, the transformations of the OFDM signals are formed in terms of complex numbers. Thus, we have to define the unit phase function as a complex number as shown in the following equation

$$\phi_u(n) = x_u(n) + jy_u(n) \quad (5)$$

where $x_u(n)$ and $y_u(n)$ are real and imaginary components of the linear function, respectively, and j is equal to $\sqrt{-1}$.

Therefore, the unit phase function in the exponential function has to be modified as well, it must be a real number. Regarding to the complex plane, the modified unit phase function can be derived as $\phi_{mu}(n) = \mid \phi_u(n) \mid \cos(\pi/4)$, where $\pi/4$ is the angle of $x_u(n) = y_u(n)$. Thus, the modified unit phase function can be expressed as follows

$$\phi_{mu}(n) = \frac{\mid \phi_u(n) \mid}{\sqrt{2}} \quad (6)$$

where: $\phi_{mu}(n)$ is the modified unit phase function, and $\mid \phi_u(n) \mid$ is the magnitude of unit phase function. Thus, we can rewrite as the modified inverse discrete harmonic transform (MIDHT) as shown in the following equation

$$x_h(n) = \frac{1}{N}\sum_{k=0}^{N-1} X_h(k)e^{j\frac{2\pi k\phi_{mu}(n)}{N}} \quad (7)$$

The modified discrete harmonic transform (MDHT) can be rewritten as shown in the following equation

$$X_h(k) = \sum_{n=0}^{N-1} x_h(n)\phi'_u(n)e^{-j\frac{2\pi k\phi_{mu}(n)}{N}} \quad (8)$$

where $x_h(n)$ is the time-domain OFDM signals, $X_h(k)$ is the frequency-domain OFDM signals, $\phi_u(n)$ is the unit phase function, $\phi'_u(n)$ is the first-order derivative of $\phi_u(n)$, $\phi_{mu}(n)$ is the modified unit phase function, k and n are the integer $[0, N-1]$. The first-order derivative of $\phi_u(n)$ can be represented in terms of an instantaneous frequency. The instantaneous frequency of a complex signal is defined as the derivative of the phase [12]. The derivative of phase can be approximated by the forward, backward and central differences [13]. Therefore, The first-order derivative of $\phi_u(n)$ can be defined by

$$\phi'_u(n) = \frac{d\phi_u(n)}{dn} \quad (9)$$

Therefore, we define the discrete-time instantaneous frequency to be the backward difference of $\phi_u(n)$. Thus, the first-order derivative of $\phi_u(n)$ can be defined by

$$\phi'_u(n) = \phi_u(n) - \phi_u(n-1) \quad (10)$$

where $\phi_u(n)$ is a complex number and $n \in [0, N-1]$.

Equation (7) and Eq. (8) are the proposed equation which are applied in the proposed MDHT-OFDM scheme according to Fig. 2. We investigate the MIDHT and MDHT by replacement of the IDFT and DFT, respectively.

3.2 Transceiver Design of MDHT-OFDM Scheme

The proposed MDHT-OFDM scheme applies the novel signal transformation in order to mitigate the Doppler spread in mobile communications. It can perform adaptively depending on the condition of channel. Figure 2 shows the proposed MDHT-OFDM scheme which includes our proposed channel estimation that estimates the MDHT-Parameters.

The MDHT-Parameters consist of three values, which are the mode, the Doppler scaling factor ($\alpha_{estimated}$), and the symbol timing offset ($\epsilon_{estimated}$). The mode is selected in channel estimation to be DFT-Mode or MDHT-Mode. If the DFT-Mode is selected, then the unit phase function is defined by

$$\phi_u(n) = n + jn \quad (11)$$

where n is an integer, $n \in [0, N-1]$, and j is equal to $\sqrt{-1}$.

On the other hand, if the MDHT-Mode is selected, then the unit phase function is defined by

$$\phi_u(n) = (n\alpha_{estimated} + \epsilon_{estimated}) + j(n\alpha_{estimated} + \epsilon_{estimated}) \quad (12)$$

where n is an integer and $n \in [0, N-1]$, j is equal to $\sqrt{-1}$, $\alpha_{estimated}$ is the Doppler scaling factor, and $\epsilon_{estimated}$ is the symbol timing offset.

3.2.1 MDHT-OFDM Scheme Transmitter

At the MDHT-OFDM scheme transmitter, the N complex data sequences are modulated by using modulation mapping schemes onto each sub-carrier independently. Then, the mapped data is taken by the MIDHT-OFDM process. According to the fundamental concept of OFDM, the OFDM signal is the orthogonal of sub-carriers in the frequency-domain. Hence, the MDHT-OFDM transmitter requires only the DFT-Mode, which is enough to generate the orthogonal signal. According to Eq. (7), the computational step of the MIDHT-OFDM algorithm at the transmitter is shown in Fig. 3.

3.2.2 MDHT-OFDM Scheme Receiver

At the MDHT-OFDM scheme receiver, the received signal

is estimated by the channel estimator. Then, the MDHT-Parameters will be sent to transformation which is the MDHT. For the DFT-Mode, The unit phase function is set as Eq. (11), otherwise, the unit phase function as Eq. (12) is set for the MDHT-Mode. Then, the MDHT is performed according to the MDHT-Parameters. However, after the received signal is transformed to the frequency-domain, the transformed data of the preamble symbol will be sent to the channel estimator again to estimate the root mean square error of the preamble symbol (θ_{RMSE}) in order to select a suitable modulation mapping scheme for the next transmission, while, the transformed data of OFDM symbol will be sent to the demapper according to the modulation mapping scheme. The computational step of the MDHT-OFDM algorithm at the receiver is shown in Fig. 4 which is corresponding to Eq. (8).

3.2.3 Complexity Analysis

We now compare the computational complexity between the MDHT-OFDM algorithms and DFT-OFDM algorithms. In order to compare the computational complexity, the *BigO* notation is used. Let N be the number of sub-carriers of the OFDM system. The computational complexity of the MDHT-OFDM algorithm has the order of $O(N^2)$, which is equivalent to the DFT algorithm, but the MDHT-OFDM algorithm requires more computational processes for addition and multiplication of the complex number.

However, the DFT algorithms has been developed for many years ago. Several fast algorithms of DFT have been reported for the computational complexity of the DFT. The fast Fourier transform (FFT) algorithms were derived to significantly reduce the computational complexity from the order of $O(N^2)$ to the order of $O(N \log_2 N)$.

for n=0 to $N-1$
begin
$\phi_w(n) = n + jn$
for k=0 to $N-1$
begin
$x_h(n) = x_h(n) + X_h(k)\exp(\frac{j2\pi k\phi_{mw}(n)}{N})$
end
$x_h(n) = \frac{x_h(n)}{N}$
end

Fig. 3 The algorithm of N-point MIDHT-OFDM.

Setup $\phi_w(n)$
for $k = 0$ to $N-1$
begin
for n=0 to $N-1$
begin
$X_h(k) = X_h(k) + x_h(n)\phi'_n(n)\exp(-\frac{j2\pi k\phi_{mw}(n)}{N})$
end
end

Fig. 4 The algorithm of N-point MDHT-OFDM.

4. Channel Estimation for MDHT-OFDM Scheme

In OFDM systems, channel estimation is usually done in the frequency-domain either by sending pilot-aided to capture channel variations. But, it is affected by additional noise. Hence, the proposed channel estimation is preformed in both the time-domain and frequency-domain. It consists of three parts which are the OFDM framing duration estimator, the preamble symbol error estimator, and the MDHT-Rules. It estimates the MDHT-Parameters, which are to cooperate with MDHT-OFDM at the receiver. Figure 5 depicts the burst frame for the MDHT-OFDM scheme which is required by the OFDM framing duration estimator. The cooperative processes are illustrated in Fig. 6. The OFDM framing duration estimator and the preamble symbol error estimator estimate the channel characteristics which are sent to the MDHT-Rules. Then, the MDHT-Parameters are determined by the MDHT-Rules for the transformation process. In addition, the conventional channel estimation also can be applied in our proposed scheme. The following subsections describe the channel estimation method for the MDHT-OFDM scheme.

4.1 OFDM Framing Duration Estimator

The OFDM framing duration estimator performs in the time-domain. Its function is to estimate the OFDM Framing Duration ($T_{estimated}$) in order to calculate the Doppler scaling factor ($\alpha_{estimated}$) and the symbol timing offset ($\epsilon_{estimated}$). We use the $\alpha_{estimated}$ by means of f_D. The OFDM burst frame structure, containing L OFDM symbols, is used as shown in Fig. 5. The postamble of our method is the preamble of the next frame. By correlating the received signal with the known preamble, the OFDM framing duration estimator estimates $T_{estimated}$ value. So, we call self-correlation. The computation step is shown as follows.

- Step 1: The correlating of the received signal and the known preamble is computed by the self-correlation functions. Only the preamble and postamble of the received signals are considered. The self-correlation function is defined as follows

$$R_{AB}(lag) = xcorr(R_A, R_B) \tag{13}$$

where lag is the index of the self-correlation function, $\in [0, 2T_{ix} - 1]$. The $xcorr()$ is the cross-correlation

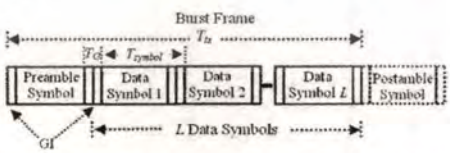

Fig. 5 The burst frame structure for the MDHT-OFDM scheme.

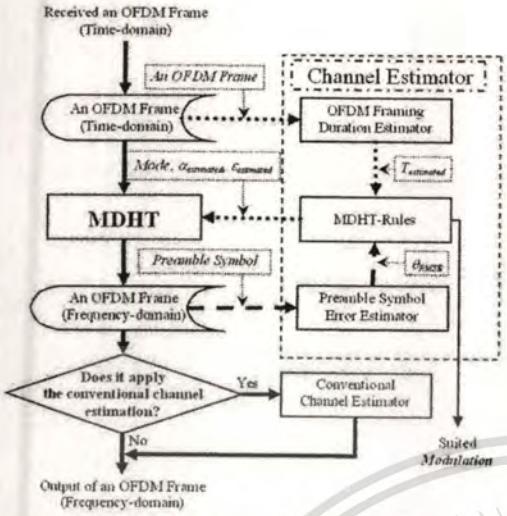

Fig. 6 Data flow diagram of the proposed channel estimation for the MDHT-OFDM scheme at receiver.

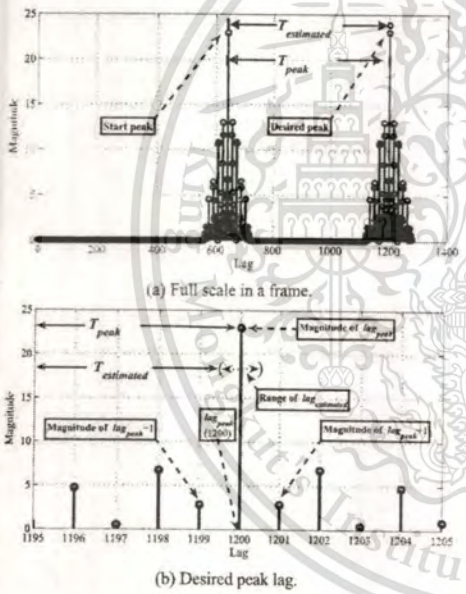

(a) Full scale in a frame.

(b) Desired peak lag.

Fig. 7 Self-Correlation of the OFDM frame.

function. The received signal of preamble and postamble is R_A. We define R_B as the known preamble which is in the time-domain. The result of the self-correlation function is shown in Fig. 7(a).

- Step 2: The desired peak *lag* search for $lag_{estimated}$ estimation. We consider the desired peak *lag* which can be searched by finding the peak magnitude. The range between the start peak *lag* and the desired peak *lag* is T_{peak} as shown in Fig. 7(a). We are interested in only two neighbor *lags* around the desired peak *lag* as shown in Fig. 7(b). Then, the weight function is calculated. The weight function is applied by using the mass center concept. There are two parameters which are weights and positions. We define the weights as the magnitude of the interested *lags*, $|R_{AB}(lag_{peak}-1)|$, $|R_{AB}(lag_{peak})|$, and $|R_{AB}(lag_{peak}+1)|$. However, we consider the position of lag_{peak} which is defined as a center position, and the x_1 value is equal to 1. Then, the positions of two neighbor *lags* around lag_{peak} are defined as $x_0 \rightarrow 0 (x_0 \neq 0)$, and $x2 \rightarrow 2$. Therefore, if the value of x_0 and the value of x_2 are defined as tenths decimal point, then the positions of x_0 and x_2 are x_0=0.1 and x_2=1.9, respectively. Therefore, $lag_{estimated}$ can be estimated as follows

$$lag_{estimated} = (0.1|R_{AB}(lag_{peak}-1)| + |R_{AB}(lag_{peak})| + 1.9|R_{AB}(lag_{peak}+1)|) / (|R_{AB}(lag_{peak}-1)| + |R_{AB}(lag_{peak})| + |R_{AB}(lag_{peak}+1)|) \quad (14)$$

where $lag_{estimated}$ is $\Re^+$ and $0.5 < lag_{estimated} < 1.5$. Therefore, $T_{estimated}$ can be obtained by the different value between T_{peak} and $T_{estimated}$ where $T_{estimated}$ is $\Re^+$, T_{peak} is an integer as shown in the next step.

- Step 3: $T_{estimated}$ is estimated. Due to the start peak *lag* is not changed to another *lag*, it will be stationed at the center position of self-correlation results. This *lag* position can be a constant which depends on signal samples. Therefore, $lag_{estimated}$ can be calculated by following equation

$$T_{estimated} = T_{peak} - (1 - lag_{estimated}) \quad (15)$$

where T_{peak} is the length of two peak *lag*, note that T_{peak} is equal to $T_{estimated}$ when two neighbor *lags* are equality values. The $T_{estimated}$ is then sent to the MDHT-Rules.

Equation (14) is adopted for modifying the estimated peak lag in order to improve the accuracy of $T_{estimated}$ by considering the relation of two neighbor *lags* magnitude. The magnitude of two neighbor *lags* and peak *lag* are weighed by using weight function which applies center mass concept. Therefore, the relation between $T_{estimated}$ and T_{peak} is $T_{peak} - 0.5 < T_{estimated} < T_{peak} + 0.5$.

4.2 Preamble Symbol Error Estimator

The preamble symbol error estimator is the frequency-domain estimation, which is performed after taking MDHT-OFDM. In this estimation, the root mean square error is estimated. This method requires the known preamble symbol as reference data.

Let $D_{preamble}$ denotes the known preamble symbol,

$\widetilde{D}_{fad}$ and $\widetilde{D}_{error}$ is the received preamble symbol which is affected by fading. The error vector of the complex data can be expressed as

$$\widetilde{D}_{error} = \widetilde{D}_{fad} - D_{preamble} \tag{16}$$

This equation indicates that we can estimate the angle error (θ_{error}). Therefore, we estimate the θ_{error} of the preamble symbol sequence as the root mean square error (RMSE) as shown in the following equation

$$\theta_{RMSE} = \sqrt{\frac{1}{P}\sum_{p=1}^{P}\left(\angle(\widetilde{D}_{fad}(p)) - \angle(D_{preamble}(p))\right)^2} \tag{17}$$

where θ_{RMSE} is the root mean square error of the angle error of the received preamble symbol sequence, $\widetilde{D}_{fad}$ denotes the received preamble symbols, $D_{preamble}$ is the known preamble symbol, p is the order of preamble symbols, and P is the number of preamble symbols, $\angle(\bullet)$ is the angle function of a complex number.

Therefore, the θ_{RMSE} is estimated for the modulation mapping scheme selection. The details of procedure will be described in the next subsection.

4.3 MDHT-Rules

The MDHT-Rules are the method to determine the MDHT-Parameters values which are suitable parameters for the MDHT-OFDM. The input values of the MDHT-Rules are obtained by the OFDM framing duration estimator and preamble symbol error estimator, which are $T_{estimated}$ and θ_{RMSE}, respectively. There are two situations that are needed to be considered. Firstly, when should the DFT-Mode or MDHT-Mode, be performed? Secondly, what kind of the modulation mapping scheme is suitable for the channel currently?

The mode of the MDHT-OFDM is selected by considering the channel characteristics. According to the effect of the Doppler spread due to mobile movement, the waveform of the received signal is scaled in time. We consider the Doppler spread by means of the Doppler scaling factor ($\alpha_{estimated}$), which corresponds to the mobile movement speed. The Doppler scaling factor can be obtained by

$$\alpha_{estimated} = \frac{T_{estimated}}{T_{tx}} \tag{18}$$

where $\alpha_{estimated}$ is the Doppler scaling factor, $T_{estimated}$ is the estimated timing duration of the received frame, and T_{tx} is the known timing duration of an OFDM frame. The $\alpha_{estimated}$ is employed to decide the mode of MDHT-OFDM and, used as the parameter of the MDHT-OFDM. Moreover, the mode of the MDHT-OFDM is also dependant on the modulation mapping scheme. Because each of modulation mapping scheme combats differently to the Doppler spread. Due to the proposed MDHT-OFDM transformation is a warped transformation which the OFDM signal is warped in time-domain before calculation to the frequency-domain. Therefore, the time-domain estimation can be applied as the parameters for the transformation. Those parameters allow the Doppler scaling factor can be implied in the time-domain sub-carriers manner. Thus, Eq. (11) and Eq. (12) are used as the warped function of the transformation for the DFT-Mode and the MDHT-Mode, respectively. Therefore, the OFDM signals can be compensated in time-domain by the mechanism of DMHT-OFDM transformation before transforming to the frequency-domain. Our time-domain channel estimation requires a long preamble symbol which is always used for frame synchronization in conventional OFDM systems. Thus, the pilot-aided in data symbol is not required for our proposed MDHT-OFDM scheme.

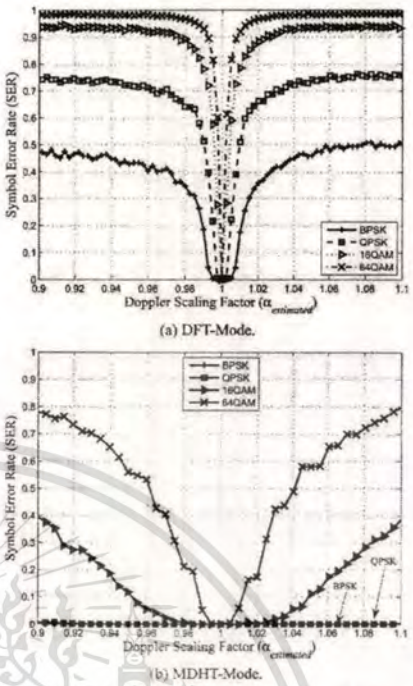

(a) DFT-Mode.

(b) MDHT-Mode.

Fig. 8 The effective range of each mode for each modulation mapping scheme.

Based on simulation, we consider only the effect of Doppler spread to determine the threshold values so that the AWGN and multipath are ignored. In the simulation results, the SER of each modulation mapping scheme in the DFT-Mode and MDHT-Mode of the MDHT-OFDM scheme versus the Doppler scaling factor are shown in Fig. 8 which demonstrate the effective range of each mode. According to Fig. 8, we can achieve the threshold values as shown in Table 2 which are applied in the algorithm as shown in Fig. 9. Due to the MDHT-Mode requires more computational complexity than the DFT-Mode. Therefore, in case of small Doppler effect, the DFT-Mode is performed in order to save mobile resource. Otherwise, the MDHT-Mode is performed.

Figure 8(a) is used to determine when the MDHT-Mode should be performed. The threshold values of each modulation mapping scheme are chosen by considering the last point of the Doppler scaling factor where the symbol error rate is still the zero value. The Doppler scaling factor is estimated according to Eq. (18). We define $\alpha_{lowBPSK}$, $\alpha_{lowQPSK}$, $\alpha_{low16QAM}$, and $\alpha_{low64QAM}$ as the lower bound values, define α_{upBPSK}, α_{upQPSK}, $\alpha_{up16QAM}$, and $\alpha_{up64QAM}$ as the upper bound values of BPSK, QPSK, 16QAM, and 64QAM, respectively. *Modulation* is the variable which is stored by the type of the modulation mapping scheme.

Table 2 The threshold values for the MDHT-Rules.

Modulation mapping scheme	Doppler scaling factor($\alpha_{estimated}$)	
	Lower bound	Upper bound
BPSK	0.994	1.006
QPSK	0.9976	1.0024
16QAM	0.9992	1.0008
64QAM	0.9997	1.0003

```
Call Doppler scaling factor estimator
if Modulation = BPSK then
    if α_lowBPSK ≤ α_estimated ≤ α_upBPSK then
        CurrentMode =DFT-Mode
    else
        CurrentMode =MDHT-Mode
    end if
else if Modulation = QPSK then
    If α_lowQPSK ≤ α_estimated ≤ α_upQPSK then
        CurrentMode =DFT-Mode
    else
        CurrentMode =MDHT-Mode
    end if
else if Modulation = 16QAM then
    if α_low16QAM ≤ α_estimated ≤ α_up16QAM then
        CurrentMode =DFT-Mode
    else
        CurrentMode =MDHT-Mode
    end if
else if Modulation = 64QAM then
    if α_low64QAM ≤ α_estimated ≤ α_up64QAM then
        CurrentMode =DFT-Mode
    else
        CurrentMode =MDHT-Mode
    end if
end if
if CurrentMode=MDHT-Mode then
    Call symbol timing offset estimator
else
    Set symbol timing offset to default values
end if
```

Fig. 9 The mode decision algorithm of the MDHT-Rules.

```
Call Preamble symbol error estimator
if 0 ≤ θ_RMSE < π/22 then
    Modulation=64QAM
else if π/22 ≤ θ_RMSE < π/9 then
    Modulation=16QAM
else if π/9 ≤ θ_RMSE < π/4
    Modulation=QPSK
else
    Modulation=BPSK
end if
```

Fig. 10 The modulation mapping scheme decision algorithm of the MDHT-Rules.

Each OFDM symbol in the OFDM frame is also affected by the Doppler spread. For that reason, the symbol timing offset of each OFDM symbol is also shifted so we call that "symbol timing offset" which can be express by the linear function as shown in the following equation

$$\epsilon_{estimated}(l) = l\alpha_{estimated} - l \tag{19}$$

where $\epsilon_{estimated}(l)$ is the symbol timing offset of the l-th OFDM symbol, l is sequence of the OFDM symbol in a frame, which are $[0, 1, 2, ..., L]$, and L is number of the symbol in a frame including a preamble symbol. According to Fig. 9, the symbol timing offset estimator is estimated by using Eq. (19).

However, the suited modulation mapping scheme is selected by considering the θ_{RMSE}. The Doppler spread directly effects to the shifty angle of the received OFDM symbols. Hence, the algorithm in Fig. 10 is employed for selecting the modulation mapping scheme. The preamble symbol error estimator is estimated by using Eq. (17). Selecting the modulation mapping scheme will be used in the next transmission. Finally, the MDHT-Parameters are sent to MDMT-OFDM process which is performed adaptively.

5. Simulation Results

We evaluated the performance of the proposed MDHT-OFDM scheme by means of simulation. We focused on the effect of the Doppler spread according to mobile movement. We evaluated the performance of the MDHT-OFDM scheme in terms of the symbol error rate (SER) by comparing those of the conventional DFT-OFDM scheme. As for the channel model, we considered the COST 207 models. The simulation parameters are set as shown in Table 3.

The OFDM frame is generated in the simulations as shown in Fig. 5 which consist of 6 OFDM symbols and one preamble symbol. The long preamble symbol in standard 802.11a is applied for the preamble symbol in these simulations. In each OFDM symbol is generated by the channel model according to COST 207 rural area with 6-path channel model which is presented in [15]. The frequency-selective deterministic channel models are considered. The

Table 3 Simulation parameters.

Parameter Name	Value
Number of N points	64
Length of Guard Interval	16
Modulation Mapping Scheme	BPSK, QPSK, 16QAM,64QAM
Transformation	DFT, MDHT
Channel	COST 207 Model (rural area), AWGN channel

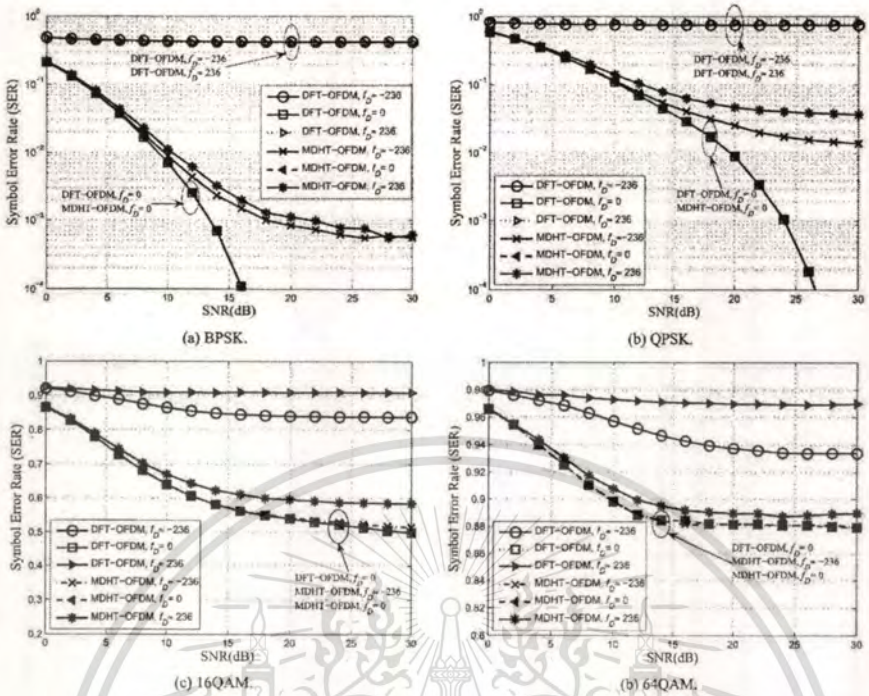

(a) BPSK. (b) QPSK.

(c) 16QAM. (d) 64QAM.

Fig. 11 The performance comparisons of each modulation mapping scheme for the Doppler spread.

method of equal distance is used for the computation of the discrete Doppler frequencies and Doppler coefficients [15]. The additive white Gaussian noise (AWGN) is included. The OFDM symbol interval and a guard interval are defined by 3.2 μs and 0.8 μs, respectively.

We separated the performance evaluation into four parts which are demonstrated by the SER performance comparison in each case as illustrated in the following subsections.

5.1 The Performance Comparisons for the Doppler Spread of Each Modulation Mapping Scheme

In order to compare the performance of the proposed MDHT-OFDM scheme with the conventional DFT-OFDM scheme in each modulation mapping scheme. In this simulation, we assume the perfect channel estimation that means the receiver knows the exact value of $T_{estimated}$. In this case, we would like to avoid the error of our time-domain channel estimation and compare our proposed MDHT-OFDM transformation with the traditional DFT-OFDM transformation without any the biased factor of channel estimation. The pilot-aided channel estimation is ignored. We consider three maximum Doppler frequency (f_D) values which are set at approximately −236, 0, and 236 Hz, respectively. The symbol error rate (SER) performances of each modulation mapping scheme versus the SNR are shown in Fig. 11. The simulation results show that the SER performance of the proposed MDHT-OFDM scheme and DFT-OFDM scheme have the same performance in the case of f_D is equal to 0. It means that the performance is the same when the Doppler effect is free. However, in Fig. 11, it can be seen that comparing Fig. 11(a), Fig. 11(b), Fig. 11(c) and Fig. 11(d), the sensitiveness of the Doppler effect is 64QAM, 16QAM, QPSK, and BPSK, respectively.

However, in the conventional DFT-OFDM scheme, and the whole modulation mapping schemes, the SER performances are greatly degraded when increasing f_D. For small values of SNR, channel noise is the dominant factor that degrades the system performance. But, if the noise power reduces rapidly, the Doppler spread becomes the dominant degrading factor. Even when the SNR increases dramaticly, the SER performances change slightly.

In contrast, the proposed MDHT-OFDM scheme, the SER performances degradation in 64QAM are more severe than that in 16QAM, QPSK, and BPSK, respectively, which can be improved by increasing the SNR values. In this case, the main dominant factors are the effects of multipath and AWGN.

5.2 The Performance Comparisons of Channel Estimation for the Doppler Spread

In this simulation, we investigate the performances of

the proposed channel estimation cooperating with MDHT-OFDM. We compare the proposed channel estimation with the pilot-aided channel estimation of the conventional DFT-OFDM scheme. The QPSK modulation mapping scheme is selected. We apply the block-type pilot-aided channel estimation for the conventional channel estimator as shown in Fig. 6. We define the pilot-aided channel estimation as follows.

- Type I: The pilot-aided are inserted to all sub-carrier in the OFDM symbol number 1 ($L = 1$).
- Type II: The pilot-aided are inserted to all sub-carrier in the OFDM symbol number 1 and 4 ($L = 1$ and $L = 4$).

Moreover, we also compare the proposed channel estimation with the perfect channel estimation with the condition of including pilot-aided in our proposed scheme.

Figure 12(a) compares the SER performance of the proposed MDHT-OFDM scheme cooperating with the perfect channel estimation of the conventional DFT-OFDM scheme cooperated by pilot-aided channel estimation in the case of f_D approximately −236 Hz. The results show that the conventional DFT-OFDM scheme, the SER performance degradation is more severe than the proposed MDHT-OFDM scheme even when increasing the SNR values. The proposed MDHT-OFDM scheme can achieve better SER performance even the conventional DFT-OFDM scheme applies the pilot-aided channel estimation type II compared with those without applying any pilot-aided channel estimation.

We next carried out a comparison on the SER performance of the proposed MDHT-OFDM scheme cooperating with the proposed channel estimation and perfect channel estimation. In this simulation, the proposed MDHT-OFDM scheme is considered. We also apply the pilot-aided channel estimation to each channel estimation. We set the value of f_D too approximately −474 Hz. Figure 12(b) shows that the SER performances of the perfect channel and proposed channel estimation without any pilot-aided have slightly difference performances. Moreover, in the case of applying pilot-aided channel estimation Type I and Type II, the performances are also slightly different, but it achieves better performance than those without pilot-aided.

5.3 Performance Comparisons of the Doppler Spread Variation

In this simulation, the variation of f_D is considered. The influence of the Doppler spread in the 6-path COST 207 model is investigated for each channel estimation. We consider the average SNR at 20 dB and the modulation mapping scheme is QPSK. For comparison, first we investigated the SER performance of the conventional DFT-OFDM scheme and the proposed MDHT-OFDM scheme cooperating with perfect channel estimation, as shown in Fig. 13(a). Second, we investigate the proposed MDHT-OFDM scheme cooperated with perfect channel estimation or propose channel estimation, as shown in Fig. 13(b). Moreover, the pilot-aided is also applied.

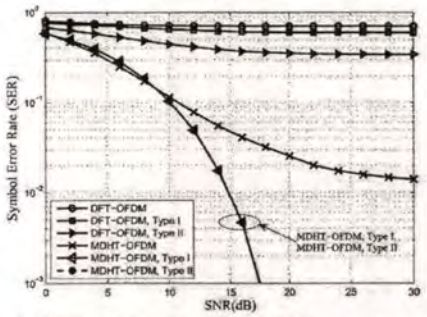

(a) The DFT-OFDM scheme and the MDHT-OFDM scheme cooperated with the perfect channel estimation, $f_D \approx$ -236 Hz.

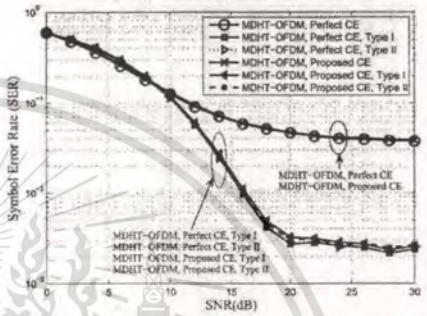

(b) The MDHT-OFDM scheme cooperated with the proposed channel estimation and perfect channel estimation, $f_D \approx$ -474 Hz.

Fig. 12 The performance comparisons for each of the channel estimation (CE).

Figure 13(a) shows that the SER performances of the DFT-OFDM and MDHT-OFDM are the same in the case of f_D equal to 0. However, the SER performances are improved in the case of applying the pilot-aided channel estimation as Type I or Type II. On the other hand, when f_D is not equal to zero, the SER performance of the DFT-OFDM scheme degrade even when pilot-aided channel estimation Type I and Type II are applied. In the case of the proposed MDHT-OFDM, it can greatly improve the SER performance, although the f_D is gathered, the proposed MDHT-OFDM can still achieve the SER performance better than the conventional DFT-OFDM scheme. However, the SER performances are slight changed in the case of the proposed MHT-OFDM applying the pilot-aided channel estimation as Type I or Type II.

Figure 13(b), The SER performance of the prefect channel estimation and proposed channel estimation are compared. As expected, the SER performances of the perfect channel estimation are slightly better than those of the proposed channel estimation. However, when the pilot-aided channel estimation as Type I and Type II are applied, the SER performances of those are slightly deferent.

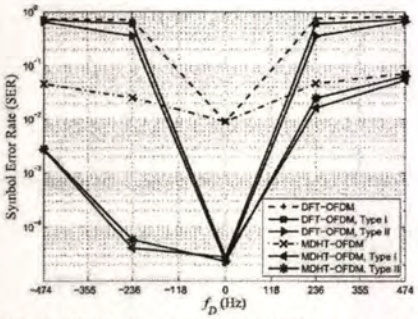

(a) The DFT-OFDM scheme and the MDHT-OFDM scheme cooperated with the perfect channel estimation.

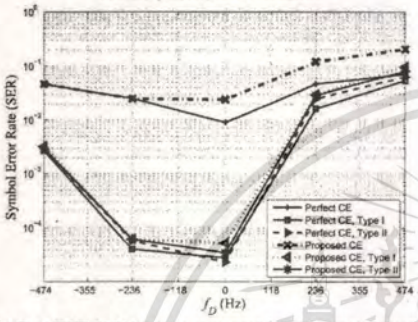

(b) The MDHT-OFDM scheme cooperated with the proposed channel estimation and the perfect channel estimation.

Fig. 13 The performance comparisons of the Doppler spread variation.

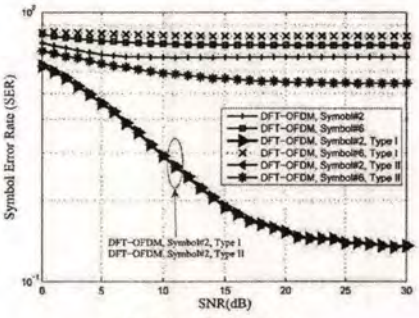

(a) The DFT-OFDM scheme.

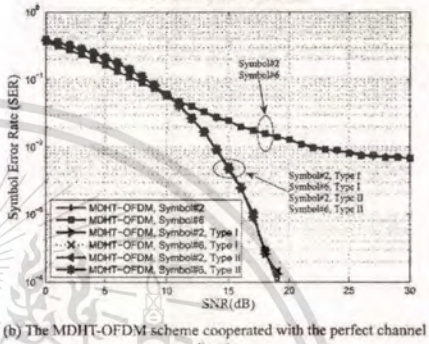

(b) The MDHT-OFDM scheme cooperated with the perfect channel estimation.

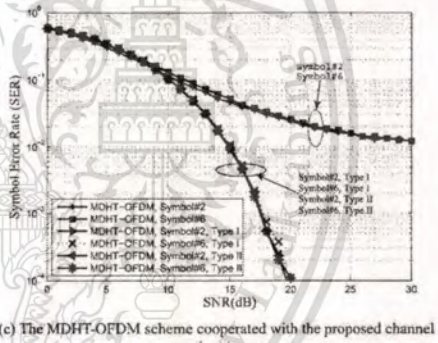

(c) The MDHT-OFDM scheme cooperated with the proposed channel estimation.

Fig. 14 The performance comparisons of the ordering of the OFDM symbol.

5.4 The Performance Comparisons for the Ordering of the OFDM Symbol in the Frame

In this simulation, we investigated the Doppler effect to the symbol timing offset of the OFDM symbol in the frame in each of channel estimation. We assume the frame synchronization is perfect, the f_D is approximately -236 Hz, and the modulation mapping scheme is QPSK. But, the synchronizations of each OFDM symbol are fixed to the values of the OFDM symbol interval. We consider the ordering of the OFDM symbol number 2 and 5.

In Fig. 14, we compare the conventional DFT-OFDM scheme, the proposed MDHT-OFDM scheme with perfect channel estimation, and the proposed MDHT-OFDM scheme with proposed channel estimation which are shown in Fig. 14(a), Fig. 14(b), and Fig. 14(c), respectively.

In the conventional DFT-OFDM scheme as shown in Fig. 14(a), we can see that when the ordering of the OFDM symbol is far away from the frame starting point, the SER performance is more degraded due to symbol timing offset errors. However, the SER performance can be improved by applying a higher level of the pilot-aided channel.

On the other hand, the proposed MDHT-OFDM scheme as shown in Fig. 14(b) and Fig. 14(c), the SER performances do not change much in the case of the ordering of the OFDM symbol. Moreover, the SER performances improve more after applying the pilot-aided channel. Furthermore, the SER performances of the proposed channel estimation are a bit lower than those of the perfect channel estimation.

6. Conclusions

We have proposed the modified discrete harmonic transform to perform in wireless OFDM systems in the presence

of symbol error rate (SER) caused by the Doppler effect. The main objective of our research is to improve the performance of the transformation. We have shown the derivation of new equations for discrete harmonic transform and the new channel estimation which are suitable when we apply the harmonic transform for the signal transformation in the wireless OFDM systems. The MDHT-OFDM scheme strongly reduces the SER caused by the frequency offset and symbol timing offset due to Doppler effect. We have presented the SER performances by means of a simulation for the comparison between the conventional DFT-OFDM scheme and the proposed MDHT-OFDM scheme. The results have shown that the proposed MDHT-OFDM scheme outperforms the DFT-OFDM scheme. Performance-wise, it can be concluded that MDHT-OFDM scheme is more suitable for mobile OFDM systems. A key issue of adopting the MDHT-OFDM scheme is challenging computation, which is complex rather than the conventional DFT-OFDM scheme. In future, simpler implementation will be studied.

Acknowledgments

The authors would like to express their gratitude to Dr. Ryuhei FUNADA and Dr. Hiroshi HARADA of the National Institute of Information and Communications Technology (NICT) Japan for their valuable suggestions. The authors also would like to acknowledge the constructive suggestions and comments of Prof.Dr. Yoshikuni ONOZATO of Gunma University, Japan.

The authors would like to express their gratitude to the reviewers for the helpful comments and suggestions to improve the quality of the paper.

References

[1] T. Pollet, M.V. Bladel, and M. Moeneclaey, "Ber sensitivity of ofdm systems to carrier frequency offset and wiener phase noise," IEEE Trans. Commun., vol.43, no.2/3/4, pp.191–193, Feb./March/April 1995.

[2] G. Mkrtchyan, K. Mori, and H. Kobayashi, "Correction of ofdm signal form in time domain to reduce ici due to the doppler spread and carrier frequency offset," IEICE Trans. Commun., vol.E88-B, no.1, pp.122–133, Jan. 2005.

[3] S. Chen and T. Yao, "Intercarrier interference suppression and channel estimation for ofdm system in time-varying frequency-selective fading channels," IEEE Trans. Consum. Electron., vol.50, no.2, pp.429–435, May 2004.

[4] J. Van De Beek, M. Sandell, and P. Borjesson, "Ml estimation of time and frequency offset in ofdm system," IEEE Trans. Signal Process., vol.45, no.7, pp.1800–1805, July 1997.

[5] F. Zhang, G. Bi, and Y. Chen, "Harmonic transform," IEE Proc. Vis., Image Process., vol.151, no.4, pp.257–263, Aug. 2004.

[6] R. Venkataramanan and K. Prabhu, "Estimation of frequency offset using warped dft," European J. Signal Processing, vol.86, pp.250–256, Feb. 2006.

[7] A. Makur and S. Mitra, "Warped discrete-fourier transform: Theory and applications," IEEE Trans. Circuits Syst. I, Fundam. Theory Appl., vol.48, no.9, pp.1086–1093, Sept. 2001.

[8] S. Saiyod, S. Thipchaksurat, and R. Varakulsiripunth, "Signal transformation using harmonic transform based on ofdm," Proc. ECTICON 2007, pp.911–914, Chiang Rai, Thailand, May 2007.

[9] S. Ghofrani, D. McLernon, and A. Ayatollahi, "Weighted average instantaneous frequency based on adaptive signal decomposition," 13th European Signal Processing Conf. (EUSIPCO2005), Antalya, Turkey, Sept. 2005.

[10] B. Boashash, "Estimating and interpreting the instantaneous frequency of a signal. ii. algorithms and applications," Proc. IEEE, vol.80, no.4, pp.540–568, April 1992.

[11] L. Qu, A. Kot, and S.H. Lum, "Comparative study of some discrete instantaneous frequency estimators," Proc. IEEE Information Engineering, pp.608–612, July 1995.

[12] W. Nho and P. Loughlin, "When is instantaneous frequency the average frequency at each time?," IEEE Trans. Signal Process. Lett., vol.6, no.4, pp.78–80, April 1999.

[13] M. Sun and R. Scalbassi, "Discrete-time instantaneous frequency and its computation," IEEE Trans. Signal Process., vol.41, no.5, pp.1867–1880, May 1993.

[14] A. Goldsmith, Wireless Communications, Cambridge University Press, New York, 2005.

[15] M. Patzold, Mobile Fading Channels, John Wiley, Chichester, 2002.

Saiyan Saiyod received the B.Sc. degree in Computer science from Mahasarakham University in 2000 and M.Eng. degrees in Computer Engineering from King Mongkut's Institute of Technology Ladkrabang, Thailand, in 2005. He is currently working toward the D.Eng. degree at the Department of Computer Engineering, Faculty of Engineering, King Mongkut's Institute of Technology Ladkrabang, Bangkok, Thailand. His current interests are in the area of performance evaluation on communication networks, digital-signal-processing, and mobile communication.

Sakchai Thipchaksurat received the B.Sc. degree in Statistics from Srinakaritwirot Prasarnmitr University in 1988, the M.Eng. degree in Electrical Engineering from King Mongkut's Institute of Technology Ladkrabang, Thailand, in 1996, and Ph.D. degree in Electronics Engineering and Computer Science from Gunma University, Japan in 2002. He is now an assistant professor in the Department of Computer Engineering, Faculty of Engineering, King Mongkut's Institute of Technology Ladkrabang, Bangkok, Thailand. His current research interests are in the area of performance evaluation of communication networks, wireless and mobile communications.

Ruttikorn Varakulsiripunth received the B.E. degree in Electrical and Electronics Engineering from Kyoto University, Kyoto, Japan in 1978. He obtained his M.E. and D.E. degrees in Electrical and Communication Engineering from Tohoku University, Sendai, Japan in 1983 and 1986, respectively. He is now an associate professor in the Department of Electronics, Faculty of Engineering, King Mongkut's Institute of Technology Ladkrabang, Bangkok, Thailand. His current research interests are concerned with computer communication network including switching system, queueing analysis, flow and congestion control, multimedia communication, wireless communication, image processing and natural language processing.

AUTHOR'S BIOGRAPHY

Mr. Saiyan Sayod was born on March 15, 1977 in Surin, Thailand. He received the B.Sc. degree in Computer science from Mahasarakham University in 2000 and M.Eng. degrees in Computer Engineering from King Mongkut's Institute of Technology Ladkrabang, Thailand, in 2005. He is currently working toward the D.Eng. degree at the Department of Computer Engineering, Faculty of Engineering, King Mongkut's Institute of Technology Ladkrabang, Bangkok, Thailand. From June to September 2008, he was a trainee of the National Institute of Information and Communications Technology (NICT), Kanagawa, Japan. His current interests are in the area of performance evaluation on communication networks, digital-signal-processing, and mobile communication.